

University of Warwick institutional repository: <http://go.warwick.ac.uk/wrap>

A Thesis Submitted for the Degree of PhD at the University of Warwick

<http://go.warwick.ac.uk/wrap/73131>

This thesis is made available online and is protected by original copyright.

Please scroll down to view the document itself.

Please refer to the repository record for this item for information to help you to cite it. Our policy information is available from the repository home page.

THE ELECTRICAL PROPERTIES AND STRUCTURE
OF HALO-BORATE GLASSES AND GLASS-CERAMICS

by

Phelim B. Daniels B.A.

A Thesis
Submitted for the Degree of
Doctor of Philosophy
of the
University of Warwick

Department of Physics

September 1984

IMAGING SERVICES NORTH

Boston Spa, Wetherby

West Yorkshire, LS23 7BQ

www.bl.uk

BEST COPY AVAILABLE.

VARIABLE PRINT QUALITY



IMAGING SERVICES NORTH

Boston Spa, Wetherby
West Yorkshire, LS23 7BQ
www.bl.uk

BEST COPY AVAILABLE.

**TEXT IN ORIGINAL IS
CLOSE TO THE EDGE OF
THE PAGE**

CONTENTS

	<u>Page</u>
CHAPTER 1: <u>Introduction</u>	
1.1 The Nature of Glass	1
1.2 Conversion to Glass-Ceramics	6
1.2.1 Nucleation	7
1.2.2 Crystal Growth	10
1.3 Origins of the Project and Possible Applications	11
1.4 Aims for Advancement	15
1.5 Thesis Plan	16
CHAPTER 2: <u>Electrical Conductivity Processes in Glasses, Glass-Ceramics and Ceramics</u>	
2.1 General Comments	17
2.2 Electronic Conductivity	18
2.3 Amorphous Semiconductors	20
2.4 Ionic Conductivity Theory	24
2.5 Ionic Conductivity Theory Applied to Glasses	29
2.6 The Nature of the Activation Energy	31
2.7 Ionically Conducting Glasses	32
2.7.1 Binary Alkali Silicates	32
2.7.2 Binary Alkali Borates	35
2.7.3 The Mixed Alkali Effect	37
2.7.4 Glasses Containing Halogens	39
1. Borates	39
2. Phosphates	41
3. Molybdates	41
2.7.5 Fluoride Ion Conducting Glasses	42
2.7.6 Alkali-Free Glasses	42

		<u>Page</u>
2.8	Ionically Conducting Glass-Ceramics	44
2.9	Ionically Conducting Ceramics	45
2.9.1	Alkali-Metal Ion Conducting Ceramics	46
2.9.2	Silver/Copper Ion Conducting Ceramics	48
2.9.3	Anion Conducting Ceramics	50
CHAPTER 3:	<u>Materials Preparation and Allied Topics</u>	
3.1	Choice of Compositions	52
3.2	Preparation of the Glasses	54
3.3	Thermal Analysis Techniques	59
3.3.1	Differential Scanning Calorimetry	59
3.3.2	Differential Thermal Analysis	61
3.4	Heat Treatments	61
3.4.1	Estimation of the Annealing Temperature	61
3.4.2	The Re-Crystallisation Process	62
CHAPTER 4:	<u>Experimental Techniques</u>	
4.1	Electrical Conductivity	65
4.1.1	Connections to the Specimen and Arrangement within the Furnace	65
4.1.2	D.C. Circuitry	66
4.1.3	A.C. Circuitry	67
4.1.4	Results for Standard Glasses	70
4.2	X-Ray Diffraction	71
4.3	Electron Microscopy	73
4.3.1	General Observations	73
4.3.2	The Use of E.D.A.X.	73
4.3.3	Determination of the Conducting Phase	74

		<u>Page</u>
4.4	Triple-Disc Experiments	75
4.5	Thermopower Experiments	76
4.6	Infra-Red Absorption	78
4.7	Nuclear Magnetic Resonance (N.M.R.)	81
	4.7.1 Aims	81
	4.7.2 Theory	82
	4.7.3 Boron Studies	83
	4.7.4 Sodium Studies	85
4.8	Density Measurements	86
CHAPTER 5:	<u>Results for Electrical Conductivity and Related Topics</u>	
5.1	Electrical Conductivity	88
	5.1.1 Glassy Materials Based on Anhydrous Borax	88
	5.1.2 Glass-Ceramics Based on Anhydrous Borax	95
	5.1.3 Alkali-free Borates	102
	5.1.4 Electronic Conductivity	106
	5.1.5 Further Comments	106
5.2	Determination of the Relative Resistivity of the Crystalline and Glassy Phases in the Glass-Ceramic Materials	108
5.3	Thermopower Experiments	109
5.4	Triple-Disc Experiments	110
CHAPTER 6:	<u>Results for Structural Investigational Techniques</u>	
6.1	X-Ray Diffraction	113
	6.1.1 Studies on Glassy Materials	113
	6.1.2 Studies on the Re-Crystallised Materials	114

		<u>Page</u>
6.2	Electron Microscopy	123
6.3	Infra-Red Absorption Measurements	126
6.4	N.M.R. Studies	136
	6.4.1 Studies on the Boron Nucleus	136
	6.4.2 Studies on the Sodium Nucleus	141
6.5	Density Measurements	145
CHAPTER 7:	<u>Discussion of the Results and of Possible Explanations</u>	
7.1	Initial Comment	148
7.2	Glassy Materials	148
7.3	Glass-Ceramics	162
CHAPTER 8:	<u>Final Overview</u>	
8.1	Achievements and Conclusions	179
8.2	Suggestions for Future Work	181
	<u>References</u>	184

List of Figures.

<u>Figure No.</u>		<u>Follows Page</u>
1.1	Variation of Nucleation Rate and Growth Rate with Temperature	11
2.1	Change of Potential with Position	25
2.2	Typical Conductivity vs. Temperature Relationship for a Crystal	29
3.1 - 3.4	Specimen Differential Scanning Calorimetry Curves	60
3.5	Specimen Differential Thermal Analysis Curve	61
3.6	Photograph illustrating the Effect of Heat Treatment Dwell Temperature on Crystallisation	63
3.7 - 3.10	Photographs illustrating the Dependence of Heat Treatment Dwell Time and Composition on Crystallisation for the system X NaCl + (100 - X) Borax	64
3.11	Photograph illustrating the Dependence of Grain Size on Composition	64
4.1	Electrode Arrangement for Connection to the Specimens	65
4.2	Furnace Arrangement for Resistivity Measurements	65
4.3	Resistivity Measuring Circuit for D.C. Mode	67
4.4	Block Diagram of the Resistivity Measuring Circuit for A.C. Mode	68
4.5	Circuit Diagram of the Filter used in the A.C. Resistivity Measuring Circuit	68
4.6	Resistivity Results for Pilkington's Float Glass together with Standard Data	70
4.7	Resistivity Results for Pure Borax Glass together with Standard Data	70
4.8	Schematic Diagram of the 'Triple-Disc' Apparatus	75

<u>Figure No.</u>		<u>Follows Page</u>
4.9	Diagram of the 'Triple-Disc' Apparatus	77
4.10, 4.11	Typical N.M.R. Spectra for a Nucleus with Spin $3/2$ in Crystalline and Glassy Materials	82
5.1	Resistivity Plots: (10%, 20%) CaCl_2 + (90%, 80%) Borax (Glasses)	89
5.2	Resistivity Plots: 10% (Ca, Mg) Cl_2 + 90% Borax (Glasses)	90
5.3	Resistivity Plots: 15% (Ba, Ca) Cl_2 + 85% Borax (Glasses)	91
5.4	Resistivity Plots: 10% $\text{Ca}(\text{Cl}_2, \text{Br}_2)$ + 90% Borax (Glasses)	91
5.5, 5.6	Resistivity Plots: 10% $\text{Ca}(\text{F}_2, \text{I}_2)$ + 90% Borax (Glasses)	92
5.7	Resistivity Plots: (10%, 20%, 30%) NaCl + (90%, 80%, 70%) Borax (Glasses)	93
5.8	Resistivity Plot: 8.77% NaCl + 7.89% B_2O_3 + 83.3% Borax (Glass)	93
5.9	Resistivity Plot: 10% $\text{Na}(\text{F}, \text{Cl}, \text{Br})$ + 90% Borax (Glasses)	94
5.10	Resistivity Plot: 10% ZnCl_2 + 90% Borax (Glass)	94
5.11	Resistivity Plots: 10% MgCl_2 + 90% Borax (Air and Nitrogen melts, Glasses)	95
5.12	Resistivity Plot: 10% ZnCl_2 + 90% Borax (Heat Treated) ²	97
5.13	Resistivity Plot: 10% CaCl_2 + 90% Borax (Heat Treated) ²	98
5.14	Resistivity Plot: 15% BaCl_2 + 85% Borax (Heat Treated) ²	99
5.15	Resistivity Plot: 10% NaCl + 90% Borax (Heat Treated)	99
5.16	Resistivity Plots: (10%, 20%, 30%) NaCl + (90%, 80%, 70%) Borax (Heat Treated)	100
5.17, 5.18	Resistivity Plots: 10% $\text{Na}(\text{F}, \text{Cl}, \text{Br})$ + 90% Borax (Heat Treated)	101

<u>Figure No.</u>		<u>Follows Page</u>
5.19	Resistivity Plot: 100% Borax (Heat Treated)	101
5.20	Resistivity Plots: (0%, 10%) CaCl_2 + (100%, 90%) CaB_4O_7 (Glass and Heat Treated)	104
5.21	Resistivity Plots: (0%, 10%) SrCl_2 + (100%, 90%) SrB_4O_7 (Glass and Heat Treated)	104
5.22	Resistivity Plots: (0%, 10%) BaCl_2 + (100%, 90%) BaB_4O_7 (Glass and Heat Treated)	104
5.23	Resistivity Plot: Repeated Tests on 20% NaCl + 80% Borax (Heat Treated)	107
5.24 - 5.27	Photographs concerned with determining the Relative Resistivity of the Glassy and Re-Crystallised phases in the Glass-Ceramics using the 'Charging-up' experiments	109
5.28 - 5.30	E.D.A.X. Analysis of 20% NaCl + 80% Borax (Heat Treated) used in the 'Triple-Disc' experiments	110
5.31 - 5.33	E.D.A.X. Analysis of 15% BaCl_2 + 85% Borax (Heat Treated) used in the 'Triple-Disc' experiments	111
6.1, 6.2	X-Ray Powder Diffraction patterns: 10% NaCl + 90% Borax (Glass and Crystalline)	113
6.3 - 6.5	Diffractometer Trace: 20% NaCl + 80% Borax (Glass, Semi-crystalline, Crystalline)	114
6.6	X-Ray Powder Diffraction Pattern: 10% ZnCl_2 + 90% Borax (Heat Treated)	114
6.7	Diffractometer Trace: 100% Borax (Heat Treated)	118
6.8, 6.9	Diffractometer Traces: (10%, 30%) NaCl + (90%, 70%) Borax (Heat Treated)	118
6.10	Diffractometer Trace: 10% CaCl_2 + 90% CaB_4O_7 (Heat Treated)	121
6.11, 6.12	Micrographs: 10% ZnCl_2 + 90% Borax (Heat Treated)	123

6.13	E.D.A.X. Analysis of 10% ZnCl ₂ + 90% Borax (Heat Treated)	124
6.14	Micrograph: 10% ZnCl ₂ + 90% Borax (Heat Treated)	125
6.15	Micrograph: 10% CaCl ₂ + 90% Borax (Heat Treated)	125
6.16, 6.17	E.D.A.X. Analysis of 10% CaCl ₂ + 90% Borax (Heat Treated)	125
6.18, 6.19	Infra-Red Absorption Spectra: 100% Borax (Glass and Wet Glass)	127
6.20	Infra-Red Absorption Spectrum: 10% ZnCl ₂ + 90% Borax (Glass)	129
6.21	Infra-Red Absorption Spectrum: 20% CaCl ₂ + 80% Borax (Glass)	129
6.22, 6.23	Infra-Red Absorption Spectra: (100%, 20%) MgF ₂ + (0%, 80%) Borax (Glass)	130
6.24	Infra-Red Absorption Spectrum: 100% Borax (Heat Treated)	131
6.25	Infra-Red Absorption Spectrum: 10% ZnCl ₂ + 90% Borax (Heat Treated)	131
6.26	Infra-Red Absorption Spectrum: 20% CaCl ₂ + 80% Borax (Heat Treated)	131
6.27	Infra-Red Absorption Spectrum: 20% MgF ₂ + 80% Borax (Heat Treated)	132
6.28 - 6.32	Infra-Red Absorption Spectra: (0%, 100%, 10%, 20%, 30%) NaCl + (100%, 0%, 90%, 80%, 70%) Borax (Glasses and Heat Treated)	133
6.33	Infra-Red Absorption Spectra: 3500cm ⁻¹ Water Band in (0%, 10%, 20%, 30%) NaCl + (100%, 90%, 80%, 70%) Borax (Glasses)	135
6.34, 6.35	Infra-Red Absorption Spectra: 100% CaB ₄ O ₇ (Glass and Heat Treated)	135
6.36, 6.37	Infra-Red Absorption Spectra: 10% CaCl ₂ + 90% CaB ₄ O ₇ (Glass and Heat Treated)	136
6.38	Boron Nuclear Resonance: 100% Borax (Glass)	137

Figure No.Follows Page

6.39	Boron Nuclear Resonance: 30% NaCl + 70% Borax (Glass)	138
6.40, 6.41	Boron Nuclear Resonances: (0%, 30%) NaCl + (100%, 70%) Borax (Heat Treated)	138
6.42 - 6.45	Boron Nuclear Resonances: (0%, 10%) NaCl + (100%, 90%)(20% Na ₂ O + 80% B ₂ O ₃) (Glass and Heat Treated)	138
6.46, 6.47	Sodium Nuclear Resonances: (0%, 30%) NaCl + (100%, 70%) Borax (Glasses)	141
6.48, 6.49	Sodium Nuclear Resonances: (0%, 30%) NaCl + (100%, 70%) Borax (Heat Treated)	142

Acknowledgements

I would like to record my gratitude to the late Prof. P. W. McMillan for his interest, encouragement and general supervision of this work. His knowledge and eminence within the general field of study has proved invaluable. I am also indebted to him for making the Physics departmental facilities available to me.

There are innumerable academic and technical staff members of the Physics department who have helped me during the course of the experimental work and deserve my thanks. In particular I would like to thank past and present members of the Glass-Ceramics Group including, among others, Dr. Diane Holland, Dr. Nigel Pratten and Dr. Ron Maddison for much advice and discussion, and Mr. R. Lamb, Mr. H. Mathers and Mr. J. Stanley for their technical assistance. The comradeship within the group was a tremendous asset throughout the whole period of the work.

I am also grateful to Prof. R. Thomson, Dr. J. Farmer, Mr. S. Badzioch, Dr. R. Biddulph and other members of staff of Borax Research Ltd. for many stimulating discussions, for their friendliness on the occasions of my visits to their laboratories and for their collaborative support of the project.

Finally, I am indebted to my wife, Barbara, who has shown great diligence and care in typing this manuscript and in other aspects of the final presentation of the thesis. She has also shown considerable patience and understanding during the period of writing and for this I owe her my thanks.

Memorandum

This dissertation is submitted to the University of Warwick in support of my application for admission to the degree of Doctor of Philosophy. It contains an account of my work carried out principally at the Department of Physics of the University of Warwick during the period October 1980 to September 1983 under the general supervision of the late Professor P. W. McMillan. No part of this dissertation has been used previously in a degree thesis submitted to this or any other university. The work described is the result of my own independent research except where specifically acknowledged in the text.

Phelim B. Daniels

September 1984

Phelim B. Daniels

Abstract

The effect on the electrical properties of doping simple borate materials with various halides has been investigated. Most of the work concentrates on sodium borate as a base material but an extension is made to also consider alkaline-earth borates. Initially, glassy products are examined but later in the project, because of significant and unexpected trends, attention is focussed on re-crystallised glass-ceramics formed from the original glassy specimens.

Results indicate that a wide range of halides can be used to reduce the inherent resistivity of the initial borate material. The effect occurs in both the glassy and glass-ceramic samples but is most dramatic in the latter case. The reduction is of such magnitude that, unusually, the glass-ceramic frequently has a lower resistivity than the parent glass, and some sodium borate based samples can almost be classed as fast-ion conductors.

Any accompanying structural changes were monitored using a range of techniques including X-ray diffraction, infra-red absorption, nuclear magnetic resonance and electron microscopy. These measurements met with varying success though the prominent finding of each investigation is that the added halide is absorbed into the base compound with remarkably little structural re-arrangement.

Because the resistivity reduction effect is so much greater for the glass-ceramics than for the glasses, investigations on the two types of specimen are discussed independently and differing theories put forward. These theories are thoroughly discussed and comparisons made with publications on analogous materials. For the glasses work on halide doped lithium borates and silver borates is the most similar yet reported, but it is believed that the study on re-crystallised specimens is the only work carried out on any halide doped borate glass-ceramics.

CHAPTER 1 : Introduction.

1.1 The Nature of Glass.

While glass is today one of the most widely used materials, having a host of applications, the nature of its structure is still not understood. Indeed, the first problem encountered is to define exactly what is meant by a 'glass'.

Early work on simple glasses, e.g. by Tammann (1), considered them simply to be 'super-cooled liquids'. The results of X-ray diffraction experiments on glasses in the early 1920's (2) showed a lack of long range order. To emphasise this finding the definition consequently changed to 'structureless solids' though the idea of the glassy state being a direct extension of the liquid state was not totally relinquished (3, 4, 5).

Later a commonly used definition of a glass was that it was "an inorganic product of fusion which has cooled to a rigid condition without crystallising", this definition was put forward by the American Society for Testing Materials in 1949. However, this definition is now thought to be unnecessarily restrictive. Firstly, various organic non-crystalline solids can be prepared which show similar characteristics to inorganic glasses, yet these would not be included in this definition. Secondly, amorphous materials showing glassy behaviour can be prepared by methods other than fusion e.g. vapour deposition or neutron bombardment.

In more modern definitions it is again the non-crystalline nature, or at least the lack of long range order, that is emphasised. Mackenzie (6) describes a glass as "any isotropic material, whether it be inorganic or organic, in which three-dimensional atomic periodicity is absent and the viscosity

of which is greater than about 10^{14} poise".

The fact that the definition of a glass has been subject to alteration indicates that considerable advances have been made in the level of understanding of glass structure. Originally efforts could only concentrate on observation of physical properties e.g. by Lebedev (7) in 1921, who expressed the opinion that glass consisted of highly dispersed small crystals whose presence could perhaps be investigated by X-rays. Some of the earliest X-ray structural analysis on glass was undertaken by Randall et al (8) on vitreous silica. The main conclusion arrived at in this work was that the observed diffraction pattern resulted from a structure of very small cristobalite crystals, of around 15 \AA in size.

However, Zachariasen (9) disagreed with this because of discrepancies in the expected and observed densities, the physical property behaviour and the failure of the model to account for the diffraction pattern of heat-treated samples. Instead, Zachariasen put forward a model which states that the linking of atoms is essentially the same for the glassy and crystalline form of a material and that both forms contain extended networks. However, the difference between the two systems is that the glassy network lacks periodicity and is not symmetric but is instead of a more random nature.

For oxide glasses Zachariasen, in the same reference, expanded the work of Goldschmidt (10) and put forward various criteria which have to be met if a material is to be capable of forming a glass. These concerned, for example, the anion radius / cation radius ratio, the number of cations available and the type of bonding between adjacent oxygen polyhedra.

For these oxide glasses it is postulated that two types of oxygen ion exists, those bonded to two polyhedra, bridging oxygens, and those bonded to only one polyhedron, non-bridging oxygens. The cations are then thought to exist in holes between the oxygen polyhedra where their charge neutralises the excess negative charge of the non-bridging oxygen ions. Oxides directly involved in the structural network are termed network formers, and those whose ions tend to fill an interstitial role are termed modifiers. Some oxides can not be directly classified and can play a dual role dependent on the circumstances and are therefore termed intermediate.

General support for these ideas came from the X-ray results of Warren and associated workers (11-19), though Warren pointed out that Zachariasen's model was not the only possible interpretation of his findings. Nevertheless the two sets of work are frequently combined as providing the 'random network model'.

An early criticism of Zachariasen's work came from Hagg (20) in 1935, who objected to the need for a continuous 3-dimensional network to be present. He thought that glass formation was due to the presence of large, complex anions in the melt, which are strongly bound. It was argued that these would be difficult to assimilate into a regular lattice and hence there would be a tendency towards supercooling and glass formation.

Solomin (21) in 1940, and Tarasov and co-workers in later years (22, 23), when considering the structure of vitreous silica suggest the presence of molecular chains or even 'linear branched net-like' regions. This, unlike the

Zachariasen model, accepts the possibility of silicon-oxygen tetrahedra being joined along their edges. Richter et al (24) come to a similar conclusion and these general ideas are supported by Stevels (25). An interesting observation, which can be considered to uphold this line of theory, comes from Bruckener (26). He finds an assymetry in the density of vitreous silica fibres, with the density in the radial direction being greater than that in the axial direction. He assumes this to be due to the orientation of the chains along the axis of the fibres. These general ideas of the presence of cross-linked chains are commonly referred to as the polymeric hypothesis.

Huggens, Sun and Silverman (27), again concentrating on silica, pointed to the fact that different molecular structures exist in the various crystalline silicate minerals. There are semi-infinite sheets in mica, semi-infinite chains in pyroxenes and rings in wollastonite. They considered that vitreous silica was made up of a mixture of these units, the fraction of each type being dependent on composition. Similarly, Van Wazer (28) believes in the presence of rings and chains in the structure of phosphate glasses.

In place of these units Bockris and co-workers (29, 30) and Fajans and Barber (31) consider a 'discrete ion' concept in which distinct, large but not infinite molecular groups are present in glass, with the physical properties being controlled by the type of ion that is predominating at a particular composition.

Kobeko (32), in a completely different approach, postulates the existence of a more 'orderly amorphous' structure

being present in the super-cooled liquid than in the more usual liquid. This new structure then becomes fixed on vitrification. This is often referred to as the 'hypothesis of short range order'.

Another theory to appear is the 'micro-homogeneity' theory, which is mostly the result of work by Porai-Koschitz and co-workers (33-35). Using mainly X-ray diffraction data attempts are made to illustrate the presence of micro-regions of varying composition. For example, binary silicates were thought to consist of regions with a sodium meta-silicate composition surrounded by vitreous silica. Notably, no attempt was made to explain the structure of the inherent vitreous silica.

Apart from direct structural theories various authors have put forward ideas regarding the nature of the chemical bonding necessary if glass formation is to take place. Sun (4) assumes that there is a greater tendency towards glass formation if the atomic bonds are very strong. Simplistically his line of thought is that on solidification it is more difficult for the atoms to rearrange into a crystalline form if the bonds in the liquid are strong.

Smekal (36) puts the emphasis on the actual type of bond. He believes that a mixed bond is desirable for glass formation, i.e. one which is neither purely covalent nor purely ionic. He argues that covalent bonds are too directional for the required random nature to be achieved, and that ionic bonds are so non-directional that it is easy for the atoms to align themselves on freezing, hence an intermediate bond is necessary. Stanworth (37) agrees with the need for intermediate bonds but

recognises the fact that the formation of such bonds is due to the particular difference in the electronegativities of the atoms concerned. Hence, it is his view that glass formation would be favoured if the difference in electronegativity of the constituent atoms lies within a certain range.

In general these bond theory predictions are in quite good agreement with what is found in practice. However, invariably there are exceptions to the general case and the predictions cannot be applied with a great deal of reliability. Similar comments can be made on the structural theories mentioned earlier; each theory can seem to be applicable in certain cases, but not to be applicable in certain other cases. Given the wide range of materials that form glasses it is highly probable that no one theory can apply universally. Indeed, even for a particular multicomponent system, the structure, and the theory pertaining to it, may change considerably as the composition within the overall system is varied.

1.2 Conversion to Glass-Ceramics.

The re-crystallisation of a glass into a glass-ceramic is somewhat analogous to the crystallisation of a melt on cooling. Crystallisation does not occur uniformly and simultaneously throughout the material, rather it occurs on certain sites, called nuclei, which tend to grow in size until much or all of the original material has become crystalline. It is thus possible to consider crystallisation as consisting of two processes. Firstly, there is the formation of the growth sites i.e. nucleation, and secondly there is the growth of these sites. The kinetics governing these two processes can be treated individually with the overall result being their

combined effect. Only a brief account of the processes is given here, since thorough, detailed accounts have been written by many other authors (e.g. 38-45).

1.2.1 Nucleation.

Nucleation can be of two types. If nucleation occurs in a pure phase, and the probability of it occurring is independent of position within that phase, then the phenomenon is called homogeneous nucleation. If nucleation occurs at the interface with a foreign particle, which would serve to catalyse the nucleation, then the phenomenon is called heterogeneous nucleation. Homogeneous nucleation will be discussed first.

Consider cooling a liquid to its 'melting point', T_m . At this temperature the free energy of the liquid is equal to that of the crystalline solid. On cooling below T_m the free energy of the liquid is higher than that of the solid and there is a tendency for nucleation to occur. However, the formation of nuclei necessitates the building of a solid/liquid interface which itself needs energy to achieve. Hence, it is generally the case that some degree of supercooling is necessary before it is favourable for nuclei to form.

It can be shown (40, 44, 46-49) that the rate of formation of nuclei per unit volume of liquid, I , is given by:

$$I = nf \cdot \exp\left(\frac{-16A\pi G_S^3 V^2}{3RTG_B^2}\right) \exp\left(\frac{-G_R}{RT}\right)$$

where:

n is the number of particles per unit volume,

f is the frequency of vibration of particles at the crystal/liquid interface,

A is Avogadro's number,

G_B is the bulk free energy of crystallisation,

G_S is the free energy per unit surface area of the crystal/liquid interface,

V is the molar volume,

G_R is the energy concerned with the re-arrangement of the liquid particles into the correct crystal structure.

In essence, the first exponential factor describes the 'thermodynamic barrier' to nucleation, while the second exponential factor is concerned with the 'kinetic barrier'.

Consider the case when the temperature is ΔT below the melting point. The entropy of fusion, ΔS , which is assumed to be independent of temperature, is related to the change in G_B with temperature by:

$$-\Delta S = \frac{d}{dT} (G_B)$$

However, the second law of thermodynamics shows (e.g. 50) that ΔS is equated to the latent heat of melting, L , by:

$$\Delta S = \frac{L}{T_m}$$

Hence

$$G_B = \frac{L}{T_m} \cdot \Delta T$$

It follows that the equation for the nucleation rate can be written as:

$$I = nf \cdot \exp\left(\frac{-16A\pi G_S^3 V^2 T_m^2}{3RTL^2 \Delta T^2}\right) \exp\left(\frac{-G_R}{RT}\right)$$

It will be noted that the nucleation rate is highly sensitive to the degree of supercooling due to the ΔT^2 term in the exponent.

The above treatment assumes that the steady state has

been reached and does not include initial transient effects.

If the melt is seeded then heterogeneous nucleation can take place, which will always tend to decrease the degree of supercooling that is necessary before nucleation begins. It must be recognised that pure homogeneous nucleation is rather difficult to achieve, there are always trace impurities available, or even the walls of the liquid container will suffice.

The effectiveness of such a seed, or nucleating agent, depends very much on the resemblance of the lattice spacings of the inhomogeneity with respect to those of the phase being crystallised. The smaller the degree of discrepancy then the greater the tendency to nucleate. It is for this reason that the best nucleating agent is an unmelted seed crystal of the liquid in question, or a similar isomorphous crystal.

The important factor in heterogeneous nucleation lies in the surface tension between the inhomogeneity and the nucleated phase. If this is low then heterogeneous nucleation is favoured. A manifestation of this surface tension lies in the contact angle, θ , at the junction of the inhomogeneity and the nucleated phase. It is possible to adjust the 'thermodynamic barrier' exponent by multiplying it by a function $f(\theta)$, in order to convert the resultant nucleation rate to be that concerned with heterogeneous nucleation. $f(\theta)$ is given by (see 45):

$$f(\theta) = (2 + \cos\theta)(1 - \cos\theta)^2/4$$

For any value of $(0^\circ < \theta < 180^\circ)$ the thermodynamic barrier is reduced and nucleation will occur more easily than in the homogeneous case.

1.2.2 Crystal Growth.

The following ideas regarding the subsequent growth of the nucleated crystals were first formulated by Turnbull in 1956 (43). Crystal growth is essentially the result of the difference between two kinetic processes; firstly the transfer of atoms from the liquid to the crystal, and secondly the reverse process. Two energy values are important. Firstly there is the diffusional energy, G_D , required for an atom to cross the interface between the liquid and the crystal, and secondly there is the free energy of crystallisation, G_B .

In transferring an atom from liquid to crystal the activation energy that has to be overcome is simply G_D , for G_B is in its favour. For the reverse process the activation energy becomes the sum of $G_D + G_B$. Hence the net rate of transfer of atoms to the crystal ΔN becomes:

$$\Delta N = nf \left[\exp\left(\frac{-G_D}{RT}\right) - \exp\left(-\frac{(G_D + G_B)}{RT}\right) \right]$$

$$\Delta N = nf \cdot \exp\left(\frac{-G_D}{RT}\right) \left(1 - \exp\left(\frac{-G_B}{RT}\right) \right)$$

The symbols used are as defined previously. As each particle is deposited on the crystal surface the effective increase in the crystal dimension is of the order of the particle separation a_0 . Consequently, the rate of crystal growth, U , is given by:

$$U = a_0 \cdot nf \cdot \exp\left(\frac{-G_D}{RT}\right) \left(1 - \exp\left(\frac{-G_B}{RT}\right) \right)$$

There is one further refinement to be made to this equation. Growth in general does not occur uniformly over the crystal surface, it is more energetically favourable for

atoms to be deposited on steps provided by screw dislocations present on the surface. Therefore only a fraction of the atomic sites are actually available for growth. The correction factor, by which the above growth rate has to be multiplied in order to allow for this effect, is given approximately by $\Delta T/2\pi T_m$ (45).

The decrease in the bulk free energy at the crystal surface results in the emission of heat. If the thermal conductivity of the material is not sufficient to conduct this away then there is a build up of temperature at the interface and the application of the above equation is affected (51). However, only in cases where extremely high growth rates occur does this become important (45).

Typical curves showing the relationship between the nucleation rate, the growth rate and the degree of undercooling are shown in Fig. 1.1 (45, 52). The crystallisation of a glass to form a glass-ceramic is analogous to these processes described above. Hence, depending on the crystallite size required, the conversion usually takes the form of a two stage heat treatment. The specimen is first held at a lower, nucleating temperature before being heated to the higher crystal growth temperature. It is then usually allowed to dwell at this temperature until crystallisation is complete.

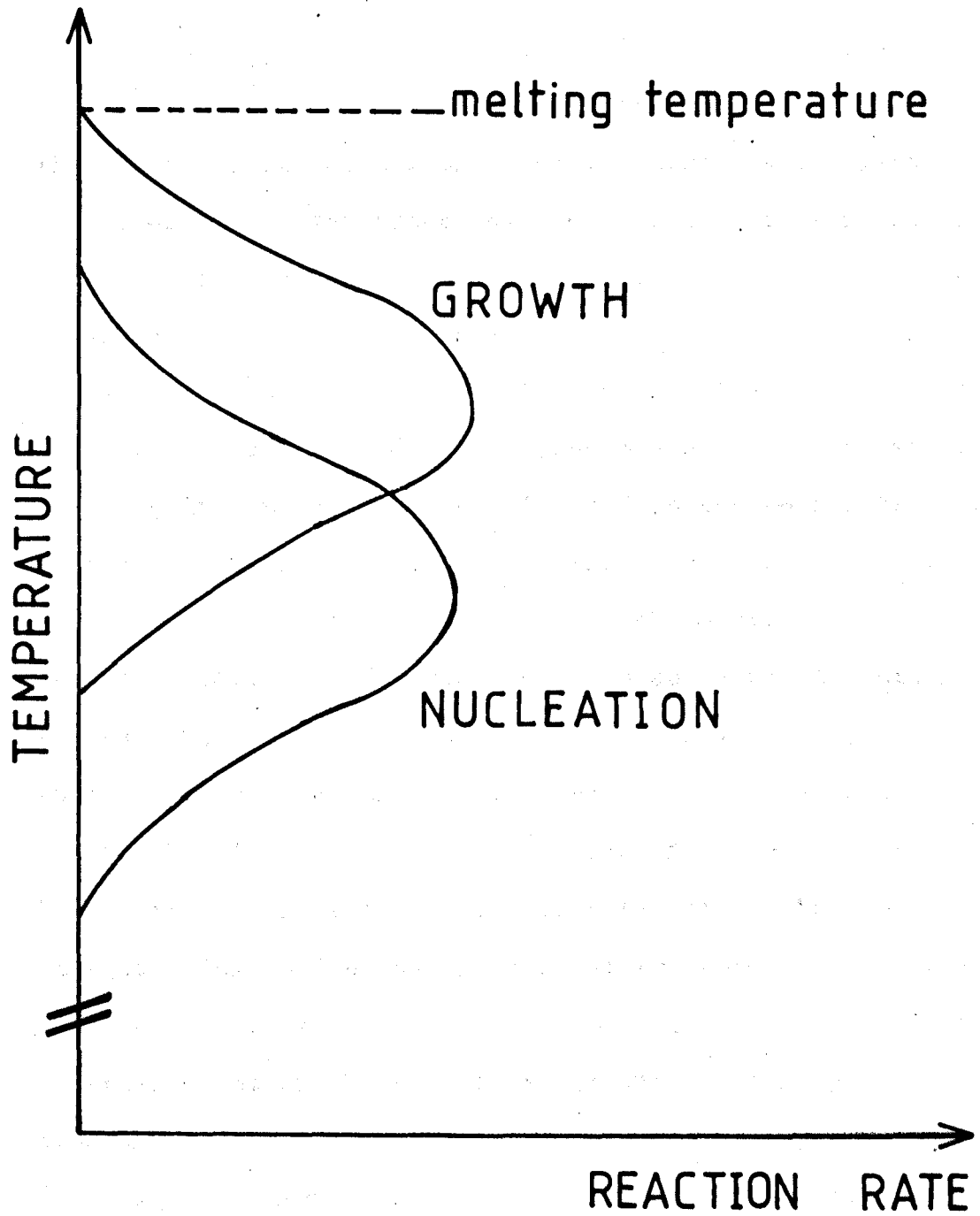
1.3 Origins of the Project and Possible Applications.

Initial ideas and enthusiasm for this project stemmed from communications with Borax Research Ltd. (B.R.L.). It had been discovered that a highly conducting glass or glass-ceramic could be formed by doping an anhydrous borax based glass ($\text{Na}_2\text{O}:2\text{B}_2\text{O}_3$) with certain halides (53).

There was obviously a great deal of scientific interest

FIGURE 1·1

VARIATION OF NUCLEATION RATE AND GROWTH RATE WITH TEMPERATURE



in these materials. The nature of the conducting species, the mechanism of conduction, the effects of heat treatment, and the inter-relation of conductivity and structure all had to be investigated. This type of work would involve the use of a wide range of experimental techniques and would form a very interesting project.

Furthermore, there is also a direct technological application associated with these materials. This application lies in the field of electrolytes for high power density batteries. Such batteries have been considered for use in various traction vehicles, such as railway engines, cars and other road vehicles (for example see 54-56), and for use as a load levelling facility by the electricity supply industry (for example see 57, 58). The possible use in such batteries of a highly conducting material based on sodium ion transport, will be illustrated in the following discussion.

The traditional battery in common use every day is the lead acid battery. However, this has an inherent problem in the fact that its associated energy density is very low; only approximately 30 Wh/kg. (58). Coupled with this is the relatively high cost of raw materials, i.e. lead. Hence, it is of little surprise that considerable effort has been made in attempting to find an alternative battery.

Several battery systems have been considered including nickel-iron at 40 Wh/kg., silver-cadmium at 80 Wh/kg., zinc-air at 150 Wh/kg. and lithium-sulphur at >300 Wh/kg., (all figures taken from 59). Despite its huge energy density the lithium-sulphur battery is not the most widely investigated battery. This is because of manufacturing problems and the

difficulty in obtaining an electrolyte. Rather, the battery most favoured is the sodium-sulphur battery, with an energy density of approximately 230 Wh/kg. (59). The basic principles of operation have been investigated by a host of workers and are well understood (e.g. 60-63) and the areas of possible application are constantly being reviewed (64-68).

The electrodes in this battery are liquid sulphur and liquid sodium, together with an electrolyte of beta-alumina. The battery is operated at 350°C in order to keep the electrodes molten. It was the discovery of beta-alumina that really made the possibility of manufacture of the battery a viable idea. The problem was not only that the material had to be highly conducting to sodium ions, but it also had to survive in a very harsh chemical environment, be mechanically strong, give long life, be easily formed to the necessary shape and the raw materials and manufacturing costs had to be as low as possible (see 69).

There are, however, considerable problems to be overcome when using beta-alumina as the electrolyte. Firstly, it is very difficult to machine and shape to the form needed, and secondly it is a difficult material on which to form seals. Despite these drawbacks beta-alumina has remained the first choice material because of its extremely high conductivity and chemical inertness.

Nevertheless, the idea arises of whether it would be possible to use a glassy material as the electrolyte instead of beta-alumina (e.g. 70). Glasses generally consist of low cost raw materials, the manufacturing process is usually easy, there is no problem in moulding a particular shape that may

be necessary, and the conduction is isotropic, so that there are no problems associated with grain boundaries or orientation. Furthermore, by adjusting the exact composition and/or changing the heat treatment procedure, the physical properties of the glass can be changed to some extent. Hence, the matching of thermal expansions for seals etc. can be achieved more easily. The seals themselves would still remain a problem, though the favourable possibility of direct glass-to-metal seals could be considered.

However, all of this speculation relies on the availability of a glass with high sodium ion conductivity. It is not absolutely necessary to emulate the extremely high conductivity of beta-alumina because the glass electrolyte could be made much thinner, nevertheless a very high conductivity is required. A number of highly ionically conducting glasses have been found, but in most cases the mobile ion is either lithium, silver or occasionally the fluoride ion. The glasses with highly mobile lithium ions include the systems $\text{Li}_2\text{O} + \text{LiF} + \text{Al}(\text{PO}_3)_3$ (71), $\text{Li}_2\text{O} + \text{B}_2\text{O}_3 + \text{LiX}$ ($\text{X} = \text{I}, \text{Br}, \text{Cl}, \text{F}$) (72-76), and $\text{Li}_2\text{O} + \text{B}_2\text{O}_3 + \text{LiF} + \text{Li}_2\text{SO}_4 + \text{Li}_2\text{SO}_3$ (77). Those with highly mobile silver ions include $\text{AgX} + \text{Ag}_2\text{O} + \text{P}_2\text{O}_5$ ($\text{X} = \text{I}, \text{Br}, \text{Cl}$) (78), $\text{AgI} + \text{Ag}_2\text{O} + \text{MoO}_3$ (79), $\text{AgX} + \text{Ag}_2\text{O} + \text{B}_2\text{O}_3$ ($\text{X} = \text{I}, \text{Br}$) (80) and $\text{Ag}_2\text{S} + \text{AgPO}_3$ (81). The fluoride ion conducting glasses are based on ZrF_4 (82).

Because of the direct comparison with highly conducting lithium halo-borate systems and silver halo-borate systems, mentioned above, in the first instance it is perhaps not surprising that the sodium halo-borates show high conductivity also. However, effects to be mentioned later give surprising

and interesting results.

It is usually the case that the electrical conductivity of the re-crystallised glass-ceramic is inferior to the parent glass (45, 79, 83). However, should the reverse be true in a particular case, then the material could still be considered as a possible electrolyte. Admittedly, a further heat treatment step would be introduced into the manufacturing process, but this could be contended with providing it brings about no great inherent deformation. Furthermore, the re-crystallised glass-ceramic is usually much stronger than the parent glass (45), which would be a favourable improvement.

Borates are quite resistant to attack by sodium and hence the possibility of using these materials as an electrolyte could be considered viable.

1.4 Aims for Advancement.

It must be remembered that throughout the period of this project there has been very close liason with an industrial research group at B.R.L., who have been working on similar materials. From the outset it was decided that the emphasis of the work in the respective laboratories should differ; while work at B.R.L. would concentrate on maximising the electrical conductivity of the materials and assessing their performance and viability as electrolytes, work at Warwick would concentrate on the understanding of the conduction process and its mechanism, on considering any structural effects, on the effect of heat treatments on conductivity, and on the possible extension to other analagous materials.

It is this latter area of work that is reported in this thesis.

1.5 Thesis Plan

The thesis is divided into eight chapters.

Chapter 2 reviews current knowledge and opinions regarding electrical conductivity in various glassy and crystalline materials. It includes a brief discussion of electronic conductivity but concentrates mainly on the theory of ionic conduction and on the various materials for which this process is important.

Chapter 3 describes the compositions used, the method of glass preparation and the heat treatment processes used in the conversion to glass-ceramics.

Chapter 4 discusses all the experimental apparatus used and the techniques employed in making the measurements, including forms of the samples used in each case. Also mentioned are possible sources of error that arise in each technique.

Chapter 5 contains the results pertaining to electrical conductivity and transport phenomena in general.

Chapter 6 gives an account of the results obtained from techniques that were used to investigate the structure of the glasses and glass-ceramics. Such results complement the results of Chapter 5.

Chapter 7 discusses the overall experimental findings and attempts are made to correlate the observed changes in conductivity with changes in the structure.

Chapter 8 summarises the salient features of the work and generally concludes the discussion. Suggestions for future work are made.

CHAPTER 2

Electrical Conductivity Processes in Glasses, Glass-Ceramics and Ceramics.

2.1 General Comments.

Electrical conductivity is one of the most important physical properties of any material and governs its possible use in a host of applications. The range of conductivity in glasses and ceramics is vast, some materials are highly insulating, others are semiconductors, while others are superionic conductors. Consequently, there is a great diversity of application, which serves to encourage further study into the understanding of electrical phenomena. Not only is there an interest in conductivity from a phenomenological viewpoint but it also provides a fascinating subject for workers in theoretical aspects of physics and materials science, and there is an increasing tendency to approach the subject from a modern quantum mechanical regime.

Charge can either be carried by electrons, holes or ions, hence the subject of electrical conductivity is generally split up into two branches, firstly electronic conductivity and secondly ionic conductivity. However there is a growing tendency to compare these two branches from a theoretical outlook and attempts have been made to unify theoretical ideas regarding the two subjects. (For a detailed discussion on this topic see (84)).

It should be remembered that both electronic and ionic conductivity occur in all materials. However it is usually the case that one of these mechanisms predominates over the other. Consequently materials tend to be classified as either

electronic conductors or ionic conductors. This project is mainly concerned with ionic conduction and hence a rather less detailed description of electronic conductivity processes will be given in comparison to the discussion on ionic conductivity.

2.2 Electronic Conductivity.

Theoretical ideas regarding electronic conduction have been developed from initial simple assumptions of electron movement in 'perfect', 'stationary', 'pure' crystalline lattices. The starting point is the 'Hartree-Fock one electron approximation'. This assumes that any electron interacts only with the time-averaged charge due to all the other electrons. Added to this is the adiabatic approximation which assumes that there is negligible coupling between the motion of the electrons and the relatively stationary ion cores; this means that the ions can be considered stationary on their lattice sites. Lastly boundary conditions inherent to the theory are set by the periodicity within the lattice.

Involved discussion of the calculations cannot be entered into here. (For a thorough discussion see (85-88)). However, the general results are threefold. Firstly the available energy states are sectioned into bands which lie only in certain energy regions. Secondly each electron becomes delocalised so that it can no longer be allotted to a given ion. Thirdly each electronic state can be described by a wave-vector which is restricted to lie in a given range called a Brillouin zone. The form of the Brillouin zone is governed only by the type of lattice concerned.

Implicit with this band theory is the concept of a density of states function, $N(E)$. This quantity denotes

the number of states per unit volume available for occupation at an energy E . It is possible to calculate the band structure of simple crystalline solids and hence to categorise the material. If $N(E)$ is non-zero at the Fermi energy then the material is a metal or metallic compound with a conductivity that tends to a finite value at low temperatures, (these materials will not be discussed further). If $N(E)$ is zero at the Fermi energy, i.e. the Fermi level is in the band gap, then the material is a semi-conductor or insulator.

For these pure intrinsic semi-conductors the number of charge carriers varies as $T^{3/2} \exp(-\Delta G/2kT)$ where ΔG is the energy gap (86 p.231, 87 p.198). The mobility of the carriers is governed by phonon scattering and varies with temperature as $T^{-3/2}$ (88 p.155, 89 p.15-16). The conductivity which is essentially the product of mobility and carrier density therefore varies as $\exp(-\Delta G/2kT)$.

Before considering amorphous semiconductors it is interesting to consider the results of doping or of including defects in crystalline materials. Such entities introduce localised states which lie within the energy gap. Depending on the type of defect or dopant that is present, two types of state can occur. Firstly occupied states can exist close to the conduction band (donor states), secondly unfilled states can exist just above the valence band (acceptor states). It then requires little energy to raise an electron from the donor level to the conduction band or from the valence band to a donor level (leaving a hole in the valence band). Consequently, the conductivity of the material is vastly increased even for relatively small amounts of impurities.

Such conductivity is termed extrinsic conductivity, in comparison to the intrinsic conductivity of the pure, perfect crystal. A thorough discussion of the doping of semiconductors can be found in any solid state physics text (e.g. 86-89).

2.3 Amorphous Semiconductors.

The whole theory of electron energy bands has been built up from ideas assuming lattice periodicity and that each electron can be described by a Bloch wavefunction with an associated wavenumber. Consequently, it may be thought that such bands could not exist in amorphous materials where there is no periodicity. However this is clearly not the case. One of the obvious features of most glasses is their transparency to visible or perhaps infra-red radiation. As the frequency of the radiation is increased a cut-off region is eventually reached; this is synonymous with an energy gap, i.e. bands still exist. It is assumed (85 p.1-2) that the band structure of the glass is not greatly different from that of the crystalline material, except that any structure in the bands is smoothed out and, more importantly, some localised states may appear in the energy gap. Consequently, it could therefore follow that $N(E_f)$ is not zero for an amorphous semiconductor. (E_f is the Fermi energy).

The origin of these bands is perhaps most easily explained by Anderson's tight binding approximation (85 p.43, 88 p.140). When atoms are well separated the equivalent energy levels on each atom will be exactly the same. However, as they are brought together the Pauli exclusion principle demands that the energy levels are slightly shifted relative to each other. Consequently, bands of energy states arise, the shape of the

bands (and whether they overlap or not) being determined by the final arrangement of the atoms and the particular type of energy state involved. From this qualitative viewpoint there is no inherent reason why the arrangement of the bands has to be periodic.

A difference between intrinsic crystalline semiconductor energy bands and those of an amorphous semiconductor lies in the respective tail regions of the conduction and valence bands. In the case of amorphous semiconductors, Gubanov (90) and Banyai (91) demonstrated that the states are localised and not extended, even though the wave functions of the states overlap (85 p.3 and p.46).

With this resulting band scheme for amorphous semiconductors three possible transport mechanisms for carrier conduction occur (85 p.47). Firstly, as in the case of intrinsic crystalline semiconductors, there is the possibility of promoting electrons to the conduction band, followed by their motion therein. In this case the conductivity varies as $\exp \frac{-(E_c - E_f)}{kT}$, where E_c is the lower edge of the extended state conduction band and E_f is the Fermi level. Here, the mobility has a value of approximately $0.1 \text{ cm}^2 \text{ V}^{-1} \text{ s}^{-1}$ (85 p.48). This expression should be compared to that above for intrinsic crystalline semiconductors where E_f lies in the centre of the gap so that $E_c - E_f = E_g/2$.

The second conductivity mechanism is hopping between the localised states in the band tail and the band gap. This type of hopping is thermally activated as it needs the interaction of phonons in order to succeed. The associated

mobility is given by (84 p.375):

$$\mu = \frac{ea^2}{kT} \cdot \nu_{\text{Ph}} \cdot \exp(-W/kT) \cdot \exp(-2\alpha a)$$

where W is the energy difference between the sites involved in the 'hop', ν_{Ph} is a phonon frequency, ' a ' is the hopping distance and the term $\exp(-2\alpha a)$ describes the overlap of the wavefunctions describing the two sites, with α indicating the rate of spacial decay of the localised wavefunction. The mobility in this case is typically an order of magnitude smaller than that in the former case.

Over most of the temperature range, dependent on the glass concerned, one of these two mechanisms, mentioned above, predominates. It is only at low temperatures that the third mechanism, variable range hopping, need be considered. This can only occur when $N(E_f)$ is non-zero and involves hopping to sites which are energetically, but not spacially, closer to the original site and foregoes nearest neighbour hopping. Conduction occurs only near the Fermi energy and varies as $\exp(-B/T^{1/4})$, (85 p.48).

Amorphous germanium and amorphous silicon are typical semiconductors and their conductivities are well documented. (As a general reference see 85 p.345 and p.362). It has proved possible to separate the conduction due to each of the above three mechanisms, and it is found that for germanium variable range hopping predominates almost up to room temperature, where localised electron hopping takes over. At higher temperatures localised hopping by holes becomes the most important factor. Similarly for silicon, over a large temperature range, variable range hopping proves to have first priority.

One further point must be mentioned in association with these two amorphous semiconductors. Their conductivity is not very sensitive to dopants which would form donor or acceptor states in the crystalline materials, (92). This is in marked contrast to the effect of such dopants on the crystalline materials, as was mentioned earlier. It is postulated (93, 94) that this difference is due to the fact that in the crystalline material the dopant, e.g. five valent phosphorus, is taken into the lattice directly in place of the four valent germanium or silicon atom. This allows its fifth valency electron to become loosely bound. In the case of amorphous germanium or silicon the network is able to rearrange so that all the valence electrons of the phosphorus atom are used in bonding. Consequently, there is no loosely bound electron able to contribute to conduction.

Chalcogenide glasses also form an interesting group of amorphous semiconductors. Their conductivities generally show an exponential dependency on temperature and the associated mechanism is thought to be thermally activated localised state hopping with holes being the main carriers (84 p.387, 85 p.535) though the precise nature of this hopping remains open to debate.

The value of the conductivity is very low, for amorphous selenium it is approximately $10^{-16} \Omega^{-1} \text{cm}^{-1}$ (95).

One other family of amorphous semiconductors must be discussed, and they provide rather a contrast to those mentioned previously as their conductivity mechanism does not involve band theory. These are the oxide glasses that contain transition metal ions. The electronic conduction

in these glasses arises from charge transfer between ions of variable valency. Historically the glass most frequently investigated is V_2O_5 in P_2O_5 , (96), but other transition metal oxides such as FeO, CoO, Cu_2O and NiO can easily be incorporated into a glass forming oxide base. (For a general review see 97 p.579). The conductivity of such glasses can be represented by the following typical equation:



i.e. inter-ion electron migration takes place. The conductivity is dependent on the overall concentration of the transition metal ions and also on the relative concentrations of the high- and low- valency ions, with a maximum in the conductivity occurring when the concentration ratio is unity (98).

Because the conductivity is governed by a migration rate the usual exponential dependence of conductivity on temperature is observed to hold (97 p.587).

2.4 Ionic Conductivity Theory.

Over the years an enormous amount of data has been published regarding the ionic conductivity of a wide range of both crystalline and glassy materials. Theoretical ideas describing these phenomena have remained rather simple, but nevertheless describe the experimental findings rather well.

As early as 1908 it had been established (99) that, for a large number of crystalline and glassy materials, the conductivity-temperature relationship could be described by:

$$\log \rho = A + \frac{B}{T}$$

where ρ is the resistivity and A and B are constants. However, the first person to determine experimentally that electrical

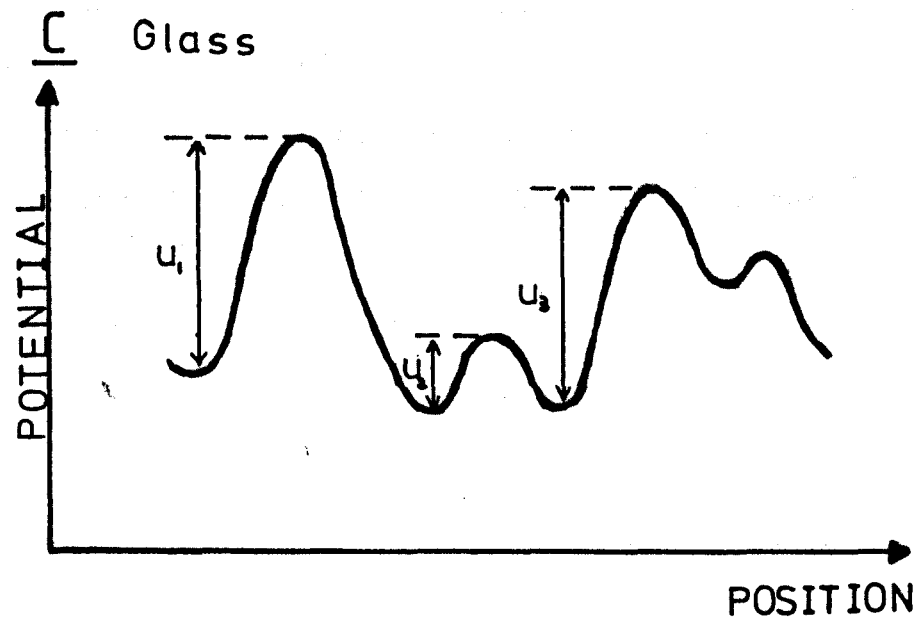
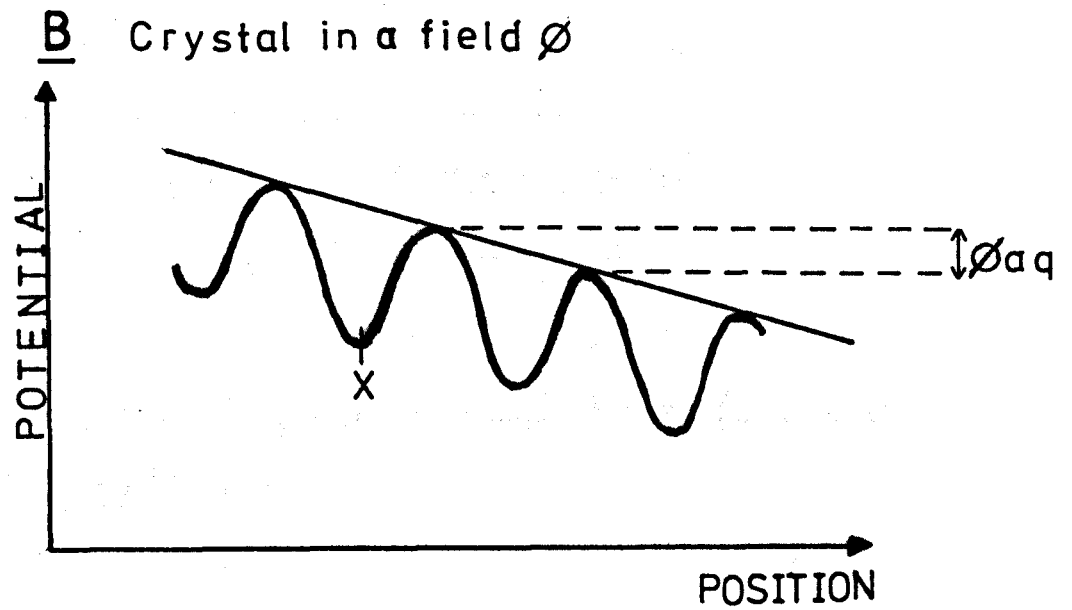
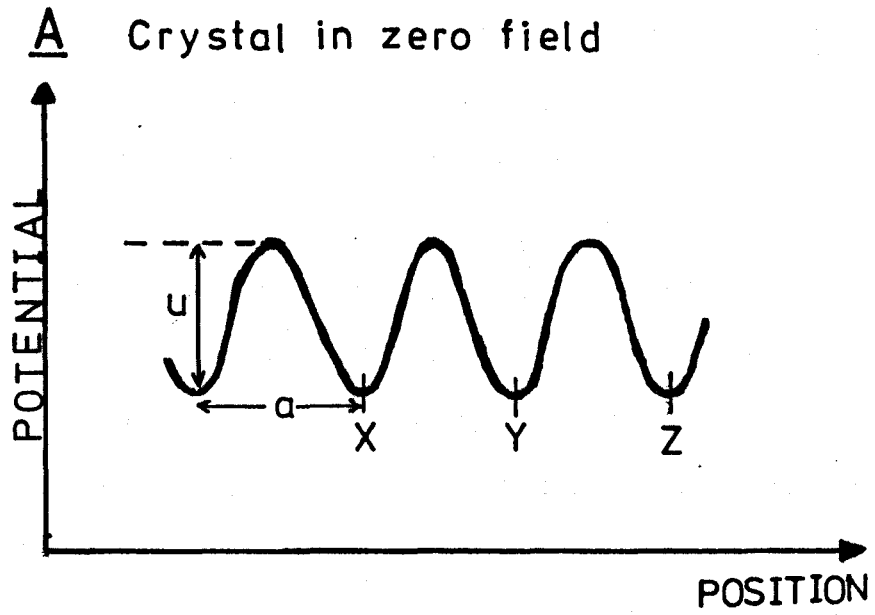
conduction could be due to the motion of ions was Joffe in 1931 (100), who was working on crystals of the rock-salt type. Even so, it was not until 1946 that Frenkel put forward ideas that related ionic motion to the above formula (101). He was working on crystalline materials at the time, though similar concepts for the glassy state soon followed from Stevels (102, a and b).

The diffusion process envisaged by Frenkel was of two types. Firstly there was the motion of interstitial ions between interstitial sites, and secondly there was the movement of lattice ions into neighbouring lattice site vacancies. Essentially this second process can be thought of as being the diffusion of lattice holes. In either case the ion is described as being in a potential well and the diffusion process is controlled by the activation energy needed to complete the inter-site 'jump'.

The following theory initially concerns periodic crystal lattices, but it will ultimately be extended to include glassy networks. In the case of these periodic lattices in zero applied field the varying atomic potential can be diagrammatically illustrated as in Fig. 2.1.A. The mobile ion will tend to rest at the minima of the potential well (i.e. at positions x, y, z) where they vibrate with thermal energy at a frequency f_0 . The probability that at any instant in time the ions have an energy E is governed by the Boltzmann factor $\exp(-E/kT)$.

It follows that the number of jumps per second that an ion makes either to the left or to the right, is given by $f_0 \cdot \exp(-U/kT)$ where U is the well height. In zero field

FIGURE 2.1



the probability of jumping to the left is equal to that of jumping to the right. Consequently if f_L corresponds to the frequency of jumps to the left, and f_R to the frequency of jumps to the right, then in zero field:

$$f_L = f_R = \frac{1}{2} f_0 \cdot \exp\left(-\frac{U}{kT}\right)$$

When an external electric field, ϕ , is applied, the potential diagram, while maintaining its well-like character, will acquire a constant slope, as in Fig. 2.1.B. The difference in potential energy of the ions in adjacent well troughs (or of adjacent peaks) is given by $\phi \cdot a \cdot q$, where q is the charge on the ion and a is the well separation. Consequently the barrier height for a jump to the left has been increased by $\frac{1}{2} \phi a q$, while that to the right has been decreased by the same amount, i.e. the situation becomes:

$$f_L = \frac{1}{2} \cdot f_0 \cdot \exp\left(-\frac{U + 1/2 \phi a q}{kT}\right)$$

$$f_R = \frac{1}{2} \cdot f_0 \cdot \exp\left(-\frac{U - 1/2 \phi a q}{kT}\right)$$

Thus the net flow of ions to the right, Δf , is given by:

$$\Delta f = f_R - f_L = \frac{1}{2} \cdot f_0 \cdot \exp\left(\frac{-U}{kT}\right) \left[\exp\left(\frac{1/2 \phi a q}{kT}\right) - \exp\left(\frac{-1/2 \phi a q}{kT}\right) \right]$$

$$\Delta f = f_0 \exp\left(\frac{-U}{kT}\right) \cdot \sinh\left(\frac{\phi a q}{2kT}\right)$$

It must be emphasised that the application of an external field does not 'force' or 'pull' ions out of the potential well, but rather serves only to preferentially direct what was otherwise random motion.

The distance moved with each jump is a , hence the drift velocity to the right, V , of each mobile ion is given by:

$$V = a \cdot \Delta f$$

The current density, j , is defined as:

$$j = n \cdot q \cdot V$$

where n is the number of mobile ions per unit volume.

Consequently:

$$j = n \cdot q \cdot f_0 \cdot a \cdot \exp\left(\frac{-U}{kT}\right) \cdot \sinh\left(\frac{\phi a q}{2kT}\right)$$

Except in cases of very high field, $\phi a q \ll 2kT$,

$$\text{i.e. } \sinh\left(\frac{\phi a q}{2kT}\right) \approx \frac{\phi a q}{2kT}$$

$$\text{and } j = \frac{n \phi q^2 a^2 f_0 \cdot \exp\left(\frac{-U}{kT}\right)}{2kT}$$

The resistivity, ρ , is defined as

$$\rho = \frac{E}{j}$$

$$\text{hence, } \rho = \frac{2kT}{n q^2 a^2 f_0} \cdot \exp\left(\frac{U}{kT}\right)$$

Note that this theory has described one dimensional behaviour. In a three dimensional crystal jumps will occur in directions that are not necessarily parallel to the applied field. This introduces a numerical multiplying constant, of the order of unity, into the pre-exponential part of the above equation.

The above relationship is the same as that deduced by Frenkel (101), Owen (103) and by Hench and Schakke (104). Other authors have put forward similar formulae which differ from this by only a numerical constant. For instance Stevels (102), when considering glassy materials, writes:

$$\rho = \frac{6kT}{b n q^2 a^2 f_0} \cdot \exp\left(\frac{U}{kT}\right)$$

where b is the number of adjacent wells that the mobile ion can jump into. Mazurin (105) supports the work of Skanavi (106) and defines the resistivity by:

$$\rho = \frac{3kT}{n q^2 a^2 f_0} \cdot \exp\left(\frac{U}{kT}\right)$$

In all cases the discrepancies are very minor. It is very

common to write the equation in the following form:

$$\log \rho = \log \left(\frac{2kT}{nq^2 a^2 f_0} \right) + \frac{U}{kT}$$

In most experiments, when measuring the resistivity as a function of temperature, the factor $\frac{U}{kT}$ varies very much more quickly than the logarithmic term in the expression. This logarithmic term is therefore frequently treated as a constant, and the equation can be written in the form:

$$\log \rho = A + \frac{B}{T}$$

$$\text{where } A = \log \left(\frac{2kT}{nq^2 a^2 f_0} \right)$$

$$\text{and } B = \frac{U}{k}$$

This is precisely the same form as that found empirically (mentioned above).

The equation needs one further refinement. The value of n has so far been taken to be constant; this is simply not the case. The number of vacancy pairs or interstitial ions per unit volume varies as:

$$n = n_0 \exp \left(\frac{-W}{2kT} \right)$$

where W is the energy needed to create a vacancy pair or to remove an ion from a lattice site to an interstitial position (86 p.539, 88 p.37). The resistivity equation then becomes:

$$\log \rho = \log \left(\frac{2kT}{n_0 q^2 a^2 f_0} \right) + \frac{U + 1/2W}{kT}$$

In principle this variation of n would only affect the gradient of a plot of $\log \rho$ versus $1/T$, the form of the relationship would be unaltered. However, in real crystals the situation is more complicated. In such a crystal there are some inherent defects such as interstitials and vacancies

which are due to the presence of impurity ions, grain boundaries etc., i.e. these defects are not thermally generated. At low temperatures the current is carried by these inherent defects, the thermally activated defects being negligible. The activation energy for the conduction is then simply U/k . It is only above a certain temperature that thermally activated defects need to be considered. At this stage the activation energy becomes $(U + W/2)/k$ and the conductivity increases more quickly with temperature (see 86 p.544 and 107 p.855 for further discussion on this topic). The overall conductivity/temperature relationship is shown in Fig. 2.2. The low temperature region is called the extrinsic region because it depends on impurities, while the high temperature region is called the intrinsic region. The situation is rather analagous to that of doped semi-conductors (see earlier).

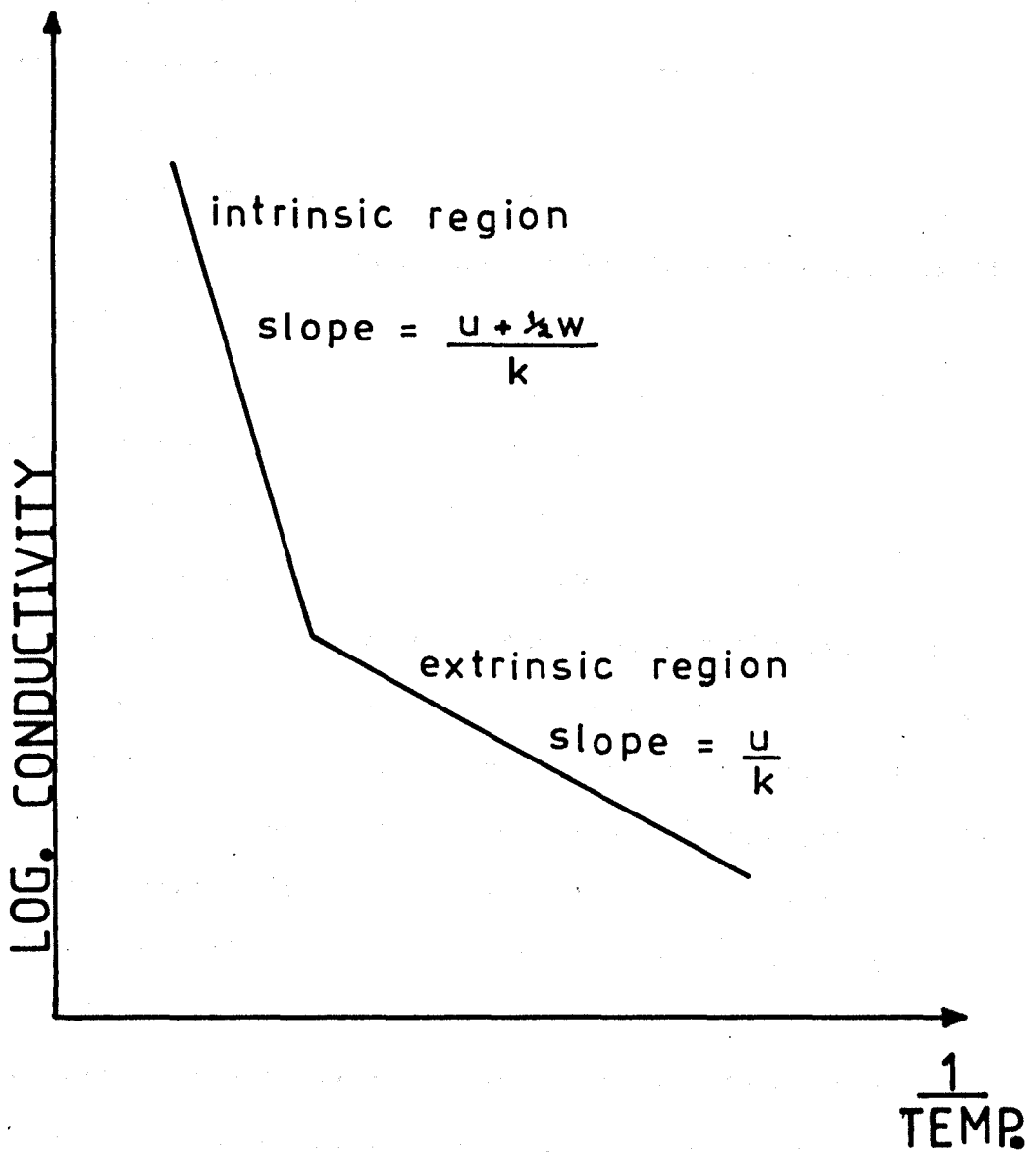
2.5 Ionic Conductivity Theory applied to Glasses.

The above theory and resultant equation for conductivity in crystalline materials requires only relatively minor adjustment in order to apply it to glasses. There are, however, a few points to be considered.

Firstly Fig. 2.1.A depicts a regular lattice with constant well depth and constant well separation. This is certainly not the case in a more randomly arranged glass. Instead, the situation is much more like that depicted in Fig. 2.1.C. Consequently it is more difficult to assign a single value to the well height. The best that can be done is to consider U as some complex average of the individual well heights, and it will be this average that is observed experimentally.

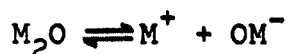
FIGURE 2.2

Typical conductivity — temperature relationship for a crystal



Secondly, the above theory concerns the movement of defects such as interstitial ions and vacancies, however, the more random nature of glass makes it very difficult to sensibly define such defects. Indeed in certain binary oxide glasses the alkali metal ions are thought to be almost entirely interstitial. In these circumstances it is certainly not necessary to have a vacancy formation energy as part of the overall activation energy. Consequently the activation energy reverts to being U/kT and a plot of $\log \rho$ versus $1/T$ results in a single straight line.

According to the above equation, the conductivity is directly proportional to n , the number density of mobile species. Hence assigning a numerical value to n is also an important issue. While it is thought that nearly all the alkali ions in binary glasses become interstitial, it does not necessarily follow that they are all mobile. The value of n is therefore not simply directly proportional to the concentration of alkali-oxide. For example, the conductivity of the system $\text{Na}_2\text{O}-\text{SiO}_2$ increases very quickly as more Na_2O is added (108), the rate of increase being far above the linear rate expected. One model which attempts to explain this effect is the 'weak electrolyte theory' (109, 110). In this theory it is postulated that only a small fraction of the available sodium ions are sufficiently loosely bound to be able to contribute to conduction. The remaining ions are held in the macro-molecular skeleton. The situation is then analogous to disassociation in an electrolytic solution illustrated by the following equation:



The rapid increase in conduction is then thought to be due to the degree of disassociation increasing rapidly on adding Na_2O , i.e. while the addition of a small amount of Na_2O may only slightly increase the number density of alkali ions, it drastically increases the number of mobile alkali ions. Ravaine and Souquet (109) have put forward conductivity data which they claim support this theory.

Models other than the weak electrolyte theory have been put forward which also claim to explain this variation of ionic conductivity with composition. For example, Glass and Nassau (111) suggest a random site model. They believe that a continuous energy distribution of alkali ion sites exists and that consequently a clear distinction between mobile and immobile ions is not meaningful. Instead, they believe that at low concentrations of alkali ions only the low lying energy states are filled. In this case a high activation energy barrier has to be overcome. At increased concentrations of alkali ions the less low lying states start to be populated with a consequent reduction in activation energy and a disproportionate increase in conduction.

It has not yet been discovered which of these models is correct.

2.6 The Nature of the Activation Energy.

Considerable effort has been made in attempting to calculate the activation energy U concerned with the ionic diffusion process (e.g. 112 - 115). Anderson and Stuart (112) have put forward a model which allows U to be calculated from other measurable physical phenomena concerned with the glass. In this model the activation energy is divided into two parts,

firstly an electrostatic energy contribution, and secondly a strain energy contribution. Hakin and Uhlmann (116) have applied the model to alkali silicate glasses with quite good results. The electrostatic contribution is calculated from the difference in potential between the situations when the alkali ions and oxygen ions are separated only by the sum of their radii, and when they are separated by half the distance between adjacent interstitial sites. The strain contribution is found from the work done in expanding a cavity of normal radius r_1 up to a radius r_2 , where r_2 is the radius of the alkali ion, the unexpanded void radius r_1 being estimated from data concerned with the diffusion of gases through the material.

2.7 Ionically Conducting Glasses.

Owing to the vast nature of this subject, and the enormous amount of data available, it is only possible to cover a few of the more simple or directly relevant glasses. The field is certainly still growing, with new and interesting glasses frequently being put forward.

2.7.1 Binary Alkali Silicates.

These glasses are perhaps the simplest ionically conducting glasses in existence. However, their useful application as ionic conductors is rather restricted because they are not particularly conducting. Vitreous silica itself is very resistive indeed ($\sim 10^{16} \Omega \cdot \text{cm}$. at room temperature, 104, p.594). It has been shown (117,118) that the conductivity of 'pure' silica is highly sensitive to the number of impurity ions, especially sodium ions. Consequently it becomes very difficult to assign a definite value to the

conductivity.

The addition of any alkali oxide to silica vastly increases the conductivity. The variation of conductivity, and its associated activation energy, with the mole fraction and type of added alkali oxide has proved to be a source of interest for many authors (e.g. 112,116,119 - 129). Owen (103 p.120) provides a neat review, as do Hench and Schaake (104 p.594 - 605) who also consider the glasses in the molten state.

Considerable scatter becomes apparent when the results of various authors are compared, this is particularly noticeable for the lithium and sodium silicates. However, at least up to approximately 25 mol.% alkali oxide, there is a clear trend that the smaller the alkali metal ion then the larger the increase in conduction.

The only disagreement with this general rule occurs when considering the sodium and lithium ions. At low percentages of alkali oxides both of these binary glasses tend to show some degree of phase separation with lithium silicate being particularly susceptible (126). Consequently, the conductivity that these materials exhibit will be very dependent on the precise glass forming conditions used. Presumably it is for this reason that such a large scatter of experimental results occur. The alkali ions with larger radius do not show this immiscibility phenomena.

At relatively low levels of alkali oxide Owen (103) argues that the silica network is still relatively compact. Consequently, the activation energy for conduction simply depends on the physical size of the ions. It is for this

reason that the smaller ions are more effective in increasing conduction than the larger ions.

At large percentages of alkali oxide (≥ 25 mol.%) many silicon-oxygen bonds are non-bridging and the network has a much more open structure. In this situation the physical size of the ion is not the only important factor. The Coulombic attraction the alkali ion has to its surroundings must also be taken into account. The smaller ions have a higher field strength than the larger ions, hence this electrostatic contribution to the activation energy will show an opposite effect, as far as ionic size is concerned, in comparison to the motional contribution. As a result, at large percentages of alkali metal oxide, the activation energies for the various types of alkali ions are much more similar than they are at low percentages of alkali oxide. Also, at large percentages of alkali metal oxide the overall rates of decrease of activation energy and resistivity on adding further oxide are much reduced (103 p.120, 116, 126). Typical results illustrating these overall effects are given in table 2.1 The values quoted are approximate averages taken from a review by Hakin and Uhlmann (116 p.134 - 135).

Table 2.1

Conductivity Data for Binary Alkali Silicates

Mol.% Alkali Oxide	Activation Energy kJ/mol.	Resistivity Ω .cm. (room temperature)
10% Na ₂ O	75	5×10^{11}
30% Na ₂ O	65	2×10^9
10% Cs ₂ O	93	6×10^{15}
30% Cs ₂ O	66	7×10^{10}

2.7.2 Binary Alkali Borates.

Like pure vitreous silica, pure vitreous boric oxide is very resistive. Consequently the resistivity that is measured for a particular sample is very dependent on impurity content (130). It is so resistive that measurements are usually made only at elevated temperatures ($> 200^{\circ}\text{C}$). Numerous workers (e.g. 130 - 136) have studied the conductivity of B_2O_3 , with some (130, 131, 133, 135, 136) extending the studies into the molten region. The conductivity is apparently continuous through the softening point and the activation energy stays constant. The activation energy for conduction that is reported by the various authors is reasonably consistent, with the stated values being in the range 102 ± 8 kJ/mol. Only Thomas (133) is outside this range with his results yielding a value of approximately 139 kJ/mol.

The results of the various authors can be extrapolated in order to calculate the room temperature resistivity. Typically this is of the order of $10^{20} \Omega\text{.cm}$, however there is some variation between authors. Arndt's results (131) yield $10^{18} \Omega\text{.cm}$ while those of Schtschukerew and Muller yield $10^{31} \Omega\text{.cm}$! The degree of purity of the samples may well be an important factor.

In general, the conductivity starts to increase as alkali metal oxide is added to the boric oxide base. However the situation is not the same as with silicate glasses. For silicate glasses, as was mentioned earlier, the conductivity drastically increases even on the addition of only small amounts of alkali metal oxide, the rate of increase then starts to decrease on further addition. In contrast to this behaviour, when small amounts of alkali metal oxide ($\leq 5\%$) are added to boric oxide the conductivity increases only

slightly. This is especially true for the alkali metals with large ionic radius (5 p.98, 97 p.567, 105 p.21, 132). Indeed Spaght and Clarke (134) find that the conductivity is at first decreased on adding alkali metal oxide. However, above approximately 8% alkali metal oxide the conductivity starts to increase dramatically, with it increasing at a faster rate than is found in the binary silicates over this region (97 p.566).

The alkali metal ions with smaller radius tend to increase the conductivity to a greater extent than those with larger radius (105 p.22), though this effect is not as pronounced as in the case of the binary silicates.

At higher percentages of alkali metal oxide the conductivity of the glasses reaches a reasonable level but is still far from high. For example considering a glass containing 36% Li_2O , Ravaine (70) finds a room temperature resistivity of $2 \times 10^{10} \Omega\text{.cm}$ with an activation energy of 70 kJ/mol. For a similar glass the results of Button et al (75) yield $4 \times 10^9 \Omega\text{.cm}$ and 69 kJ/mol. for the corresponding values.

Sample results for a glass containing 33% Na_2O are set out in Table 2.2. This glass is of extreme importance to this project as it forms the basis of most of the materials that have been investigated. See Chapter 3.

Table 2.2Conductivity Data for $\text{Na}_2\text{O} : 2\text{B}_2\text{O}_3$

Source reference	Room Temperature Resistivity ohm.cm.	Activation Energy kJ/mol.
Spaght (134)	2×10^{10}	68
Schtschukarew (132)	4×10^{10}	68
Namikawa (137)	1×10^{11}	73
Thomas (133)	2×10^{11}	77
Oka (138)* *	6×10^{11}	81

* For readings up to 440°C only.

2.7.3 The Mixed Alkali Effect.

If a second alkali metal oxide is added to a binary oxide glass, the resultant glass does not have a resistivity which is additive in the amounts of each alkali present (5 p.99). It is also true that if one alkali oxide is gradually replaced by another in a series of glasses then the resistivity does not vary linearly with composition. This effect is not limited to electrical conductivity, other physical properties show discrepancies with predicted behaviour, though electrical conductivity is one of the properties in which the effect is most pronounced. Nor is the phenomenon limited to a particular oxide base, similar trends are found in silicates, borates, borosilicates, germanates and other oxide glasses. This type of behaviour is called the 'mixed alkali effect'.

As far as resistivity is concerned, not only is there a departure from linearity as one alkali oxide is replaced by another, but a very pronounced maximum occurs, usually at a composition corresponding to equi-molar amounts of the two alkali oxides. The effect is most noticeable when

the radii of the two types of alkali ion differ considerably (105 p.22, 139).

Some of the effects can be quite startling. For example it has been found for the glass $\text{Na}_2\text{O} + 4\text{SiO}_2$ that the resistivity is increased more if half of the soda is replaced by potash, or by lithia, than if half of the soda is simply removed (123). Also if potash is added to a sodium silicate glass, the resistivity is increased, whereas the addition of further alkali oxide to a binary glass invariably leads to increased conduction (123, 140).

The dependence of this effect on the difference in ionic size between the two types of alkali ions is well illustrated by the fact that for the glass $X\text{Li}_2\text{O} + (1-X)\text{Cs}_2\text{O} + \text{SiO}_2$ the resistivity for $X = 0.5$ is a factor of approximately 10^4 higher than for the end members of the series, while for $X\text{Na}_2\text{O} + (1-X)\text{K}_2\text{O} + \text{SiO}_2$ the resistivity for $X = 0.5$ is only increased by a factor of approximately 70 over the end members (140, and for similar work see also 141 and 142).

Numerous theories have been put forward which attempt to explain the mixed alkali effect, some of which remain rather qualitative. Authors who have suggested theories include Lengyel in 1945 (141), Stevels in 1957 (102b), Markin in 1958 (143), Myuller in 1960 (114), Weyl in 1964 (144), Charles in 1965 (142), Day and co-workers (145 - 147), Hendrickson in 1972 (148), Hayami in 1972 (149), Sakka in 1978 (150) and Matusita in 1980 (151).

It is admitted and acknowledged that the mixed alkali effect is one of the most interesting and important phenomena in the subject of ionic conductivity, both from a technological

and fundamental point of view. However, it is not of direct relevance to the work contained in this thesis. Consequently these theories will not be elaborated on here, but most are discussed in a review article by Isard (152).

2.7.4 Glasses Containing Halogens.

2.7.4.1 Borates.

Most work in this category has concentrated mainly on the addition of halogens to lithium borates or silver borates. It has been consistently found that the addition of a halogen to the base glass has enhanced the ionic conductivity.

In a series of papers (73, 74, 153, 154) Levasseur, Hagenmuller and co-workers have studied the system $B_2O_3 + Li_2O + LiX$ ($X =$ a halogen). They have found that the resistivity can be reduced to only $3 \times 10^5 \Omega \cdot cm.$ at room temperature, the activation energy being approximately 44 kJ/mol. This occurs for the glass 41.1% $B_2O_3 + 23.4\% Li_2O + 35.4\% LiCl$ (see also Ravaine, 70).

Actually, for corresponding doping levels, it was found that the halides with larger anion radius (i.e. LiI) could enhance the conductivity to a greater extent than those with smaller anion radius (i.e. LiF). However, in the case of LiI , the glass-forming region is reduced because the glass tends to devitrify on the addition of only small quantities of it. Consequently, due to the fact that more $LiCl$ than LiI can be incorporated into the glass, maximum conductivity can be achieved by using the former halide.

Button et al (75, 155) have worked on similar materials. They found that the room temperature resistivity could be reduced to $7 \times 10^6 \Omega \cdot cm.$ for a glass of composition

22.6% LiCl + 21.0% Li₂O + 56.4% B₂O₃, the activation energy was approximately 55 kJ/mol.

Smedley, Angell and co-workers (72, 76, 77) have worked on the system Li₂O + B₂O₃ + LiF. The lowest resistivity achieved was approximately 10⁷ Ω.cm. at room temperature with an activation energy of 56 kJ/mol. This was for the glass 44% B₂O₃ + 36% Li₂O + 20% LiF. This group of workers also investigated the addition of Li₂SO₄ and Li₂SO₃ to the ternary glass. They found that the room temperature resistivity could be further reduced, for example down to 3 x 10⁶ Ω.cm. for 14.8% Li₂O + 25.5% LiF + 31.7% B₂O₃ + 15.7% Li₂SO₄ + 12.3% Li₂SO₃ (77, see also 72 for similar compositions).

Overall it appears that the addition of LiCl to the binary glass can increase the conductivity by up to 4 or 5 orders of magnitude if introduced in the correct proportions.

Minami and co-workers (80) have investigated the addition of silver halides (iodides and bromides) to silver borate glasses. The resulting glasses have proved to be very highly conducting indeed. The lowest resistivities were achieved using AgI and were of the order of 1.5 x 10² Ω.cm., the activation energy being approximately 25 kJ/mol. This occurred for the composition 50% AgI + 25% Ag₂O + 25% B₂O₃.

Apparently the only work carried out on sodium halo-borate materials was performed by Stalhane in 1930 (156) on the conductivity of molten specimens. Whilst this can not be directly related to work on glass, it is interesting to note that he found that the conductivity of Na₂O + 2B₂O₃ increased on the addition of NaF, and

increased to a greater extent on the addition of NaCl.

2.7.4.2 Phosphates.

As in the case of the halo-borate glasses mentioned above, the halo-phosphates that have been investigated most frequently are those of lithium and silver.

Doreau et al (157), in investigating the lithium chloro-borate system, found that the minimum room temperature resistivity occurred with the glass of composition 40.6% Li_2O + 29.4% P_2O_5 + 30% LiCl, and has a value of $2 \times 10^6 \Omega \cdot \text{cm}$. The corresponding activation energy was 51 kJ/mol.

Ravaine (70) quotes results for the glasses 56.3% Li_2O + 18.7% P_2O_5 + 25% LiX (X = F, Cl, Br). He finds that the room temperature resistivity decreases from $5 \times 10^7 \Omega \cdot \text{cm}$ for LiF, to $1.1 \times 10^7 \Omega \cdot \text{cm}$ for LiCl and to $1.3 \times 10^6 \Omega \cdot \text{cm}$ for LiBr. Thus for conductivity enhancement purposes the effect of the various halides is in the order $\text{LiBr} > \text{LiCl} > \text{LiF}$.

The silver halo-phosphate glasses are reported to be more conducting than the lithium based materials. Minami and Tanaka (78) investigated the glasses $\text{Ag}_2\text{O} + \text{P}_2\text{O}_5 + \text{AgX}$ (X = I, Br, Cl). It was found that the iodide glasses were more conducting than the bromide glasses which were in turn more conducting than the chloride glasses. The minimum room temperature resistivity that was achieved was approximately $60 \Omega \cdot \text{cm}$ for 65% AgI + 23.3% Ag_2O + 11.7% P_2O_5 . The activation energy was 23 kJ/mol. The minimum room temperature resistivity that could be achieved with a chloride based glass was $1.3 \times 10^5 \Omega \cdot \text{cm}$.

2.7.4.3 Molybdates.

Silver iodo-molybdate glasses have also proved to

be highly conducting. The most highly conducting material investigated so far has the composition 60% AgI + 20% Ag₂O + 20% MO₃. A room temperature resistivity of only approximately 50 Ω.cm. is reported by Kuwano and Kato (158), while Minami et al (79, 159) find a corresponding value of 70 Ω.cm. for the same material.

Overall it can be seen that incorporating halides into a relatively non-conducting base glass can lead to materials that are very highly conducting indeed. The various authors mentioned above occasionally put forward theories to explain this behaviour, and these theories will be discussed in later chapters.

2.7.5 Fluoride Ion Conducting Glasses.

Some glasses exist in which the mobile ion is the fluoride ion. Early work concentrated on glasses based on BeF₂, AlF₃ or fluorophosphates. These glasses were very resistive, having a resistivity of 10¹⁰ Ω.cm. even at 200°C. (70, 160).

More recently some ZrF₄ based glasses have been investigated (82, 160). These show an improved ionic conductivity, however they still have a room temperature resistivity of the order of 10¹⁰ - 10¹¹ Ω.cm., the activation energy being approximately 75 kJ/mol.

2.7.6 Alkali-Free Glasses.

In general the resistivity of alkali-free glasses is exceedingly high. For example the resistivity of 32% SrO + 68% B₂O₃ at 450°C is reported to be 1.5 x 10¹¹ Ω.cm., with an activation energy of 147 kJ/mol. (161). A similar glass

with Na_2O replacing the SrO has a resistivity of only $3 \times 10^3 \Omega \cdot \text{cm}$. and an activation energy of approximately 70 kJ/mol. (see previous section on alkali borate glasses).

Despite the high resistivities involved, considerable interest has been shown in alkaline-earth silicates (162), alumino-silicates (163), borates (161, 164) and alumino-borates (163, 165, 166). Most of the investigations centre around trying to identify the conducting species and a certain degree of controversy still remains. For barium silicate glasses Evstrop'ev and Khar'yuzov (167) are firmly of the opinion that the mobile species is the Ba^{++} ion. Similarly for calcium silicate glasses Schwartz and Mackenzie (162) believe that it is the Ca^{++} ion that is responsible for conduction. However, for calcium alumino-borate glasses, Owen (165, 166) suggests that the mobile ions are the oxygen ions. This suggestion was further investigated by Hagel and Mackenzie, but they believe their oxygen diffusion results indicate that some other conduction mechanism is more probable, though they hesitate to state which. Hirayama (161) also does not define a specific mechanism, but he does tend to favour the idea of the cation being the mobile species in most cases. He does acknowledge the unusually high resistivity of the calcium alumino-borates and is willing to consider other mechanisms for this glass.

For the purposes of this project, only the alkaline earth borates need to be discussed further. These glasses will be mentioned again in later chapters. Because the compositions used by the various authors differ considerably

it becomes difficult to make a direct comparison in order to note the dependence of the conductivity on the type of alkaline-earth ion that is present. The best that can be done is to compare roughly similar compositions and to look for overall trends. For 38.8% BaO + 61.2% B₂O₃ Hirayama (161) reports a resistivity of $3.2 \times 10^{10} \Omega \cdot \text{cm.}$ at 450 °C, with an activation energy of 166 kJ/mol. His corresponding values for 31.8% SrO + 68.3% B₂O₃ are $1.5 \times 10^{11} \Omega \cdot \text{cm.}$ and 147 kJ/mol. Similarly, for 25.9% CaO + 61.4% B₂O₃ + 12.7% Al₂O₃ Hagel and Mackenzie find values of $4.1 \times 10^{11} \Omega \cdot \text{cm.}$ and 171 kJ/mol. while for 28.5% CaO + 57.1% B₂O₃ + 14.3% Al₂O₃ Owen (165) reports approximately $1.5 \times 10^9 \Omega \cdot \text{cm.}$ and 147 kJ/mol. for the corresponding results. By comparing these and other reported measurements it appears that the dependence of conductivity on the 'type' of alkaline-earth ion is such that conductivity increases in the series Ca < Sr < Ba. This is in spite of the fact that the barium ion is considerably the largest and that the barium glasses are the densest and most viscous (164). The same trend in conductivity is shown in the molten systems (164).

2.8 Ionically Conducting Glass-Ceramics.

The conductivity of a glass-ceramic is of course dependent on the chemical composition of the parent glass. It is also dependent on the volume fraction of crystalline material and on the nature of the crystals that have formed in the heat treatment process.

The usual case is that on conversion from a glass to a glass-ceramic the resistivity of the material increases considerably (45 p.200, 70, 83 p.707).

The degree of increase in resistivity can be quite large. For example the resistivity of a $\text{ZnO} + \text{Al}_2\text{O}_3 + \text{SiO}_2$ glass is increased by at least four orders of magnitude on crystallising (45 p.204).

Similarly, but to a lesser extent, the resistivities of the glasses $\text{AgI} + \text{Ag}_2\text{O} + \text{MO}_3$ are increased by a factor of between 10 and 20 when the crystallised material is investigated (79).

An exception to this general rule can occur however. This happens when the mobile species (usually alkali metal ions) are preferentially ejected from the crystalline phase being formed. This leads to them being in increasing concentrations in the residual glassy phase. This situation can then lead to increased conductivity. However, it must be stressed that this behaviour is comparatively rare and the more usual case is that the conductivity decreases on crystallising. (See 45 p.200 for a thorough discussion).

2.9 Ionically Conducting Ceramics.

Most conventional ceramics are good insulators. However, it can occur in some cases that the combination of the crystal structure and the nature of the atoms or ions involved gives rise to high ionic mobility. Some simple general rules can be applied in order to help predict when good conduction will take place. Firstly there must be a high concentration of the mobile species, secondly a low potential barrier to motion is required, thirdly there must be a large number of available sites of similar energy for the mobile species to move into, and fourthly the structure should be continuous.

The highly conducting materials can be classified into three main groups; firstly alkali metal ion conductors, secondly conductors for which the mobile ion is from the copper/silver group, and thirdly mobile anion conductors.

2.9.1 Alkali-Metal Ion Conducting Ceramics.

One of the most commonly investigated conductors, and one against which other conductors are frequently compared, is sodium β -alumina. Its general formula is $\text{Na}_2\text{O}:11\text{Al}_2\text{O}_3$ but it is commonly written as $\text{NaAl}_{11}\text{O}_{17}$. Its highly conducting properties were first discovered by Yao and Kummer (168) but have since been investigated by many other workers (e.g. 169, 170). The resistivity rather depends on the method of preparation but is typically of the order of $72 \Omega\text{cm}$. at 25°C with an activation energy of 15.8 kJ/mol . (taken from 169). The key to its high conductivity lies in its layer-like structure. This structure is of blocks which contain aluminium and oxygen ions only, which are separated and mirrored in layers containing sodium and oxygen ions only (171 p.496, 172 p.11). Within this layer the sodium ions are very loosely bound and are highly mobile. Hence, conduction is 2-dimensional in single crystals and consequently poly-crystalline materials are used in most applications.

Frequently a different form of β -alumina is used; this is known as β'' -alumina and has the general form $\text{Na}_2\text{O}:X\text{Al}_2\text{O}_3$ where $5 < X < 7$. This phase has a slightly different structure to the β -alumina and a further improved conductivity. The lowest reported room temperature resistivity is approximately $30 \Omega\text{cm}$. (168). The β'' -alumina has

inferior mechanical strength in comparison to β -alumina, so usually a material consisting of a mixture of the two phases is used as a compromise.

Lithium β -alumina is also an interesting ionic conductor, with it having a similar structure to its sodium counterpart. However, its resistivity is rather higher, with a figure of 200 Ω .cm. being reported for room temperature (173). At 300°C it is said to be 30 times less conducting than sodium β -alumina (174).

Few materials can surpass the conductivity of β -alumina. For sodium conduction a recent competitor is the chemical system $\text{Na}_{(1+X)}\text{Zr}_2\text{P}_{(3-X)}\text{Si}_X\text{O}_{12}$. It has been found (175) that within this family the most conducting member is $\text{Na}_3\text{Zr}_2\text{PSi}_2\text{O}_{12}$. At 300°C it has a resistivity of only 5 Ω .cm., which is competitive with β -alumina, however the reported activation energy, 28 kJ/mol., is rather larger than that for β -alumina. The structure of this material is of ZrO_6 octahedra sharing corners with SiO_4 and PO_4 tetrahedra. The skeleton structure so formed has intersecting tunnels in which the sodium ions are free to move.

The corresponding lithium material $\text{Li}_3\text{Zr}_2\text{PSi}_2\text{O}_{12}$ is again found to have a much higher resistivity than the sodium based compound. The conductivity is reported to be lower by a factor of 10^3 (176).

For lithium ion conduction the most conductive material so far reported is $\text{Li}_{14}\text{Zn}(\text{GeO}_4)_4$ which has a resistivity of only 8 Ω .cm. at 300°C (177). At this temperature the resistivity of lithium β -alumina is approximately 110 Ω .cm. (174). The structure of this material is based

on a lattice of $\text{Li}_{11}\text{Zn}(\text{GeO}_4)_4$; the three remaining lithium ions occupy one of two types of interstitial site. These sites have an occupancy of only 16% in one case and 55% in the other case. Furthermore they are interconnected by regions through which the lithium ions can move very easily. Thus, the ideal conditions for fast ionic motion are present.

Another reasonably conducting material, which will be of interest again in later chapters, is the boracite $\text{Li}_4\text{B}_7\text{O}_{12}\text{Cl}$ (also the bromine analogue). At 300°C it has a resistivity of only $100\ \Omega\cdot\text{cm}$. (178). Again, the reason for its high conductivity lies in its structure. According to Levasseur et al (179) the material is built up from a framework of BO_3 and BO_4 units with a sublattice of Li-Cl atoms. The sublattice is formed using only three lithium ions. The fourth ion then occupies a tetrahedral site with an occupation probability of .25. It is this defect structure that gives rise to the high mobility of the lithium ions.

Many other alkali-metal ion conductors exist, e.g. NaInZrS_4 (180), NaSbO_3 (175), Li_3N (181) and $\text{Li}_{1-x}(\text{Zr,Hf})_{2-x}\text{Ta}_x(\text{PO}_4)_3$ (182). Conductivity data for these and numerous other materials, including some potassium ion conductors, can be found in the review article by McGeehin and Hooper (172).

2.9.2 Silver/Copper Ion Conducting Ceramics.

Most highly conducting materials where the mobile ion is the silver ion are based on silver iodide. Silver iodide itself undergoes a phase transition at 149°C from the relatively poorly conducting, low temperature β form to

the highly conducting, high temperature α form. In this α form the iodide ions form a body-centred cubic lattice. For each iodide ion there is a total of 21 interstitial sites that the silver ion could occupy (183 p.286), it is therefore very easy for the silver ion to diffuse and a high 3-dimensional conductivity results. At 150°C the resistivity is only 1 Ω .cm. and the activation energy 4.8 kJ/mol. (184 p.268).

Much of the work on silver ion conducting materials has concentrated on stabilising the high conductivity phase of silver iodide down to room temperature. Three types of approach have been made. Firstly by partial replacement of the iodide ion by another anion, typically S^{2-} , PO_4^{3-} or WO_4^{2-} . For example, $Ag_6I_4WO_4$ has a resistivity of 21 Ω .cm. at room temperature (185 p.19). Secondly, by partial replacement of the silver ion by another cation, typically Rb^+ , NH_4^+ or K^+ . For example $RbAg_4I_5$ has a resistivity of only 8 Ω .cm. at 20°C (184 p.269). Thirdly, by partial replacement of both ion types, with most investigations centring around the system $AgI + HgI_2 + Ag_2S$, e.g. $Ag_8HgS_2I_6$ has a resistivity of 14 Ω .cm. at 25°C (186 p.593).

Apart from silver iodide the other important silver ion conductor is silver β -alumina. This has a similar structure to its sodium counterpart but the reported resistivity is higher, (156 Ω .cm. at room temperature with an activation energy of 16.4 kJ/mol. (168)).

Copper ion conducting materials are in general analagous to the corresponding silver based materials. However, the transition to a highly conducting phase, should

one occur, usually takes place at a higher temperature in the copper based material than in the silver based material. Also, the ultimate conductivity is usually lower. A wide range of conductivity data for copper ion conducting compounds (and for silver ion conducting materials not mentioned above) can be found in the review by McGeehin and Hooper (172).

2.9.3 Anion Conducting Ceramics.

The mobility of anions does not in general approach the mobility of cations. It is only oxygen and fluoride ions that in some cases become reasonably mobile.

The most common fluoride ion conductor is CaF_2 doped with either NaF or YF_3 . In the first case the singly valent alkali metal ion induces fluoride ion vacancies. In the second case the tri-valent yttrium ion induces fluoride ion interstitials. Both situations increase the mobility of the fluoride ion. Nevertheless, the resistivity is still rather high, only decreasing to $100 \Omega\text{.cm.}$ at 700°C (172).

In recent years, interest in the materials MBiF_4 ($M = \text{K, Rb, Tl}$) has arisen (187). These show considerably improved conductivity over the above materials, with the room temperature resistivity being of the order of only $2 \times 10^3 \Omega\text{.cm.}$

For oxygen ion conduction, two classes of material deserve mention. Firstly, there are the oxides ZrO_2 , HfO_2 , GeO_2 or ThO_2 doped with alkaline-earth oxides, Sc_2O_3 , Y_2O_3 or rare earth oxides (172, 188). The reason for the high mobility is that the dopants cause oxygen vacancies in the host materials. However, the resistivities remain rather

high with $4 \Omega \cdot \text{cm.}$ at 1000°C. , plus an activation energy of 63 kJ/mol. , being the best that has been achieved (188).

Improved oxygen ion conductivities have been achieved by Takahashi and co-workers (189) who have used similar dopants as above in a Bi_2O_3 base material. For example $6 \Omega \cdot \text{cm.}$ is reported for $75\% \text{ Bi}_2\text{O}_3 + 25\% \text{ Y}_2\text{O}_3$ at 700°C.

The field of anion conductivity is slowly widening, with anion electrolytes being required for monitoring elements in industrial processes. However such applications are rather specific and general data are not widely available.

CHAPTER 3Materials Preparation and Allied Topics.3.1 Choice of Compositions.

As was mentioned in Chapter 1 (section 1.3), initial information regarding this project came from Borax Research Ltd., (B.R.L), who had found that a highly conducting material could be formed by doping the glass $\text{Na}_2\text{O}:2\text{B}_2\text{O}_3$ (or other sodium borate compounds) with certain halides. The first steps in this project were to confirm the existence of this effect and to ascertain the range of materials in which it occurs.

Results from B.R.L (53) indicated that $\text{Na}_2\text{O}:2\text{B}_2\text{O}_3$ was the best base material to use in order to observe the maximum effect. If any other ratio was used then the degree of enhancement in the conductivity was not as high. Consequently, this base glass was used in the initial experiments and indeed predominated throughout the whole of the project. The use of $\text{Na}_2\text{O}:2\text{B}_2\text{O}_3$ as a base material is also beneficial from another point of view, it is available commercially as the compound $\text{Na}_2\text{B}_4\text{O}_7$, i.e. anhydrous borax. This precludes at least some of the possible weighing errors in making the mixtures to be melted.

B.R.L. had used a number of transition metal halides as dopants. This was because maximum conductivity could be achieved with this type of halide. However, it was decided that work in this project would proceed along different lines. The transition metal ions are, of course, generally multivalent. This adds a further complication to the chemical system so that it becomes more difficult

to know exactly which ions are to be considered as possible current carriers. Perhaps more importantly, it also introduces a possible mechanism for electronic conductivity (see the end of section 2.3). For this reason alternative dopants were considered.

The obvious choice would be to use an alkali-halide dopant, indeed the use of a sodium halide would greatly simplify matters from a compositional point of view. However, here too there are problems. It is well known that alkali halides are only sparingly soluble in anhydrous borax (190, 191), with the iodides being less soluble than the bromides, which are in turn less soluble than the chlorides (190). Consequently, if the enhanced conductivity effect is present in the alkali-halide doped borax materials, it might not be observable simply because there is insufficient halide incorporated into the product.

With these factors in mind it was decided to proceed using dopants consisting of alkaline-earth halides. These halides have cations with only one valency level, and, according to B.R.L., should give a reasonable conductivity enhancement effect.

$\text{Na}_2\text{B}_4\text{O}_7$ is involved in most of the materials to be discussed. For the sake of brevity, it will be understood that where the stated glass composition does not total 100% then the discrepancy will be the total of $\text{Na}_2\text{B}_4\text{O}_7$ included in its makeup, e.g. the glass 20% CaCl_2 + 80% $\text{Na}_2\text{B}_4\text{O}_7$ will simply be referred to as 'the 20% CaCl_2 glass'.

After initial investigations had been completed work progressed to also consider alkali metal halides as dopants,

despite their low solubility, and to investigate other halides such as those of zinc.

Towards the end of the project, work was also carried out on materials in which the base glass was not $\text{Na}_2\text{O}:2\text{B}_2\text{O}_3$ but instead was one of the alkaline-earth borates, $\text{BaO}:2\text{B}_2\text{O}_3$, $\text{SrO}:2\text{B}_2\text{O}_3$ or $\text{CaO}:2\text{B}_2\text{O}_3$, i.e. the form XB_4O_7 in each case. The dopants in these alkali-free materials were the halides of the particular alkaline-earth ion contained in the base material. This particular alkaline-earth oxide / B_2O_3 ratio was chosen in order to provide a direct comparison to those experiments carried out with $\text{Na}_2\text{B}_4\text{O}_7$ as the base glass. The glass with $\text{MgO} + 2\text{B}_2\text{O}_3$ as its base material could not be included in this series because $\text{MgO} + 2\text{B}_2\text{O}_3$ does not form a glass. Indeed, not only would the $\text{MgO}/\text{B}_2\text{O}_3$ ratio have to be altered, but alumina would also have to be included in order to form a glassy product (192, 193). The composition could then become rather complex and useful comparisons would be impossible.

3.2 Preparation of the Glasses.

The glasses used in this project were made using the standard glass forming procedure.

The first stage was the mixing of the chemical constituents. The compounds were obtained from the usual commercial chemical suppliers and were usually of analytical grade. The anhydrous borax was provided by B.R.L. When the base glass was not simply $\text{Na}_2\text{B}_4\text{O}_7$, the extra B_2O_3 was included via the use of boric acid. Occasionally, the metal oxide constituent was not available in the simple oxide form and was introduced into the glass by decomposition of the

carbonate compound. Whenever possible anhydrous halides were used, but from time to time the use of hydrated compounds was unavoidable. After mixing, the powders were put into a dry vessel which in turn was put onto a mechanical roller for a period of not less than twelve hours, i.e. the powders were roll-mixed.

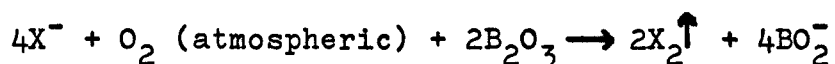
The powders were then melted using platinum crucibles, in air, in an electric furnace. For the glasses based on $\text{Na}_2\text{B}_4\text{O}_7$ the melting temperature was 900°C , and the melting time was 3 hours. However, for the alkaline-earth borate glasses the melting temperature had to be increased to 1200°C . Typically 200 gm. batches were melted.

After the stated melting time the molten glasses were poured into graphite coated steel moulds of the required shape. For the conductivity experiments the mould was a 2.5cm. diameter cylindrical block, shapes for other apparatus will be mentioned in the relevant experimental sections. The resulting solid glasses were then annealed. For most cases when the base glass was $\text{Na}_2\text{B}_4\text{O}_7$ the annealing temperature used was 450°C , and the annealing time was 3 hours. A few variations on this annealing temperature were necessary and will be mentioned individually later. The alkaline-earth borates needed higher annealing temperatures, with barium borate requiring 530°C , strontium borate requiring 580°C and calcium borate requiring 600°C . The method of arriving at the annealing temperature will be described in section 3.4.

If it was necessary to further shape the specimens they were cut using a diamond abrasive saw after the

annealing stage. For example, the 25mm. cylindrical blocks for the conductivity measuring apparatus were cut into discs of 1-2 mm. thickness.

The only serious problem encountered in the glass forming procedure was the partial loss of halogen during the melting time. It is probable that both evaporation of the halide and evolution of the halogen itself take place. According to Dunicz and Scheidt (190) the latter process is a result of the following reaction: (X = a halogen).



Without using sealed melting ampoules, the only method of reducing halogen loss is to melt for a shorter time or at a lower temperature. However, this leads to a reduction in the homogeneity of the product and should be avoided. This project is essentially of a comparative nature and it was therefore considered sufficiently correct to compare final products of known starting composition. After all, it is the initial compositions that would be important in achieving the final physical behaviour. It would also be very difficult to compare a series of similar final products as it would be impossible to know from which starting compositions to make the similar final product series. Consequently, for most purposes, the loss of halogen in melting was ignored, and particular attention was paid in ensuring that all glasses received almost identical melting conditions.

Nevertheless, the loss of halogen on melting was monitored. Most glasses were chemically analysed for their final composition. The analysis was carried out by

staff at B.R.L.'s analytical section. Some sample analytical results are shown in Table 3.1. The following conclusions can be drawn. Firstly that the larger the halide ion the more volatile it is. In melting the 90% $\text{Na}_2\text{B}_4\text{O}_7$ + 10% CaX (X = a halogen) series of glasses, the fluorine content remains unchanged, while approximately 15% of the chlorine and bromine is lost, and virtually all of the iodine. As the amount of halide increases (the series 10% $\text{CaCl}_2 \longrightarrow$ 15% $\text{CaCl}_2 \longrightarrow$ 20% CaCl_2 and also 10% $\text{NaCl} \longrightarrow$ 20% NaCl) the percentage of halogen lost also increases. Furthermore, the degree of loss seems approximately independent of the type of added cation (compare the 10% CaCl_2 and the 10% MgCl_2 glasses). Finally, the increased melting temperature of the glasses based on alkaline-earth borates leads to a large increase in the fraction of halogen that escapes. Great care will have to be taken in discussing and comparing physical properties because of this fact.

Table 3.1

Results of Chemical Analysis

Glass (mol.%)	Halogen wt.% at Weighing	Halogen wt.% in Glass	Approximate Fraction of Halogen remaining
90% $\text{Na}_2\text{B}_4\text{O}_7$ + 10% CaF_2	2.0	2.0	1
90% $\text{Na}_2\text{B}_4\text{O}_7$ + 10% CaCl_2	3.7	3.2	0.86
90% $\text{Na}_2\text{B}_4\text{O}_7$ + 10% CaBr_2	7.9	6.7	0.84
90% $\text{Na}_2\text{B}_4\text{O}_7$ + 10% CaI_2	12.1	0.6	0.05
85% $\text{Na}_2\text{B}_4\text{O}_7$ + 15% CaCl_2	5.6	4.7	0.84
80% $\text{Na}_2\text{B}_4\text{O}_7$ + 20% CaCl_2	7.7	6.0	0.78
90% $\text{Na}_2\text{B}_4\text{O}_7$ + 10% MgCl_2	3.7	3.3	0.89
90% $\text{Na}_2\text{B}_4\text{O}_7$ + 10% NaCl	1.9	1.45	0.76
80% $\text{Na}_2\text{B}_4\text{O}_7$ + 20% NaCl	4.1	2.9	0.70
90% CaB_4O_7 + 10% CaCl_2	3.8	1.0	0.26
90% SrB_4O_7 + 10% SrCl_2	3.0	1.3	0.43
90% BaB_4O_7 + 10% BaCl_2	2.5	1.55	0.62

3.3 Thermal Analysis Techniques.

Knowledge of both the annealing temperatures for the glasses, and of the crystallisation temperature for the process of conversion to glass-ceramics was gained from differential scanning calorimetry (D.S.C.) or differential thermal analysis (D.T.A.).

As a material transforms from one phase to another there is an associated change in free energy. Consequently, heat is either taken in or given out. The glass to crystal transformation lowers the free energy of the material, so consequently the change is exothermic. Both D.S.C. and D.T.A. techniques involve monitoring this free energy change.

3.3.1 Differential Scanning Calorimetry.

In this technique the measured quantity is the rate of heat evolved, or taken in, as the specimen transforms. In practice it is a comparative technique, with the heat input to the specimen being compared with the heat input to an inert reference of similar mass and heat capacity. The difference in heat inputs is then a direct result of the transformation.

The measurement of heat content can allow quantitative studies of the specific heat of the specimen or of the kinetics of crystallisation, however for the purposes of this project only the crystallisation temperature was required. In this mode of operation, the sample and reference are simply heated so that their temperatures increase at a constant rate. When the specimen transforms, and gives out heat, it requires less power from the

apparatus to maintain the constant temperature rise than does the reference material. This difference is then observed on the outputs from the calorimeter.

It is possible to use either monolithic or powdered specimens. As this project deals with properties of bulk materials the corresponding form of the specimens was usually chosen. Typically, 100 mg. specimens were used. In the case of a powder specimen, the surface free energy per unit volume is vastly increased and this tends to promote crystallisation, i.e. the crystallisation peak occurs at a lower temperature. The difference in crystallisation temperature for the bulk material and for the powdered material is dependent on particle size and on the surface free energy. If a material has a high surface energy it tends to surface crystallise, and this phenomenon was observed in some of the samples investigated in this project. This will be mentioned again later.

D.S.C. measurements were made on most samples as a matter of course. The form of the observed trace is rather similar in all cases and there seems little point in displaying all the curves that were obtained. Consequently, only specimen curves are shown, and these comprise Figs. 3.1 - 3.4.

In general, D.S.C. is a more sensitive and quantitative technique than D.T.A., and was used preferentially throughout the project. The only limitation with D.S.C. is that it becomes unreliable at very high temperatures. The equipment used was a Seteram model III calorimeter and was limited to use below 827°C. This caused no

D.S.C.

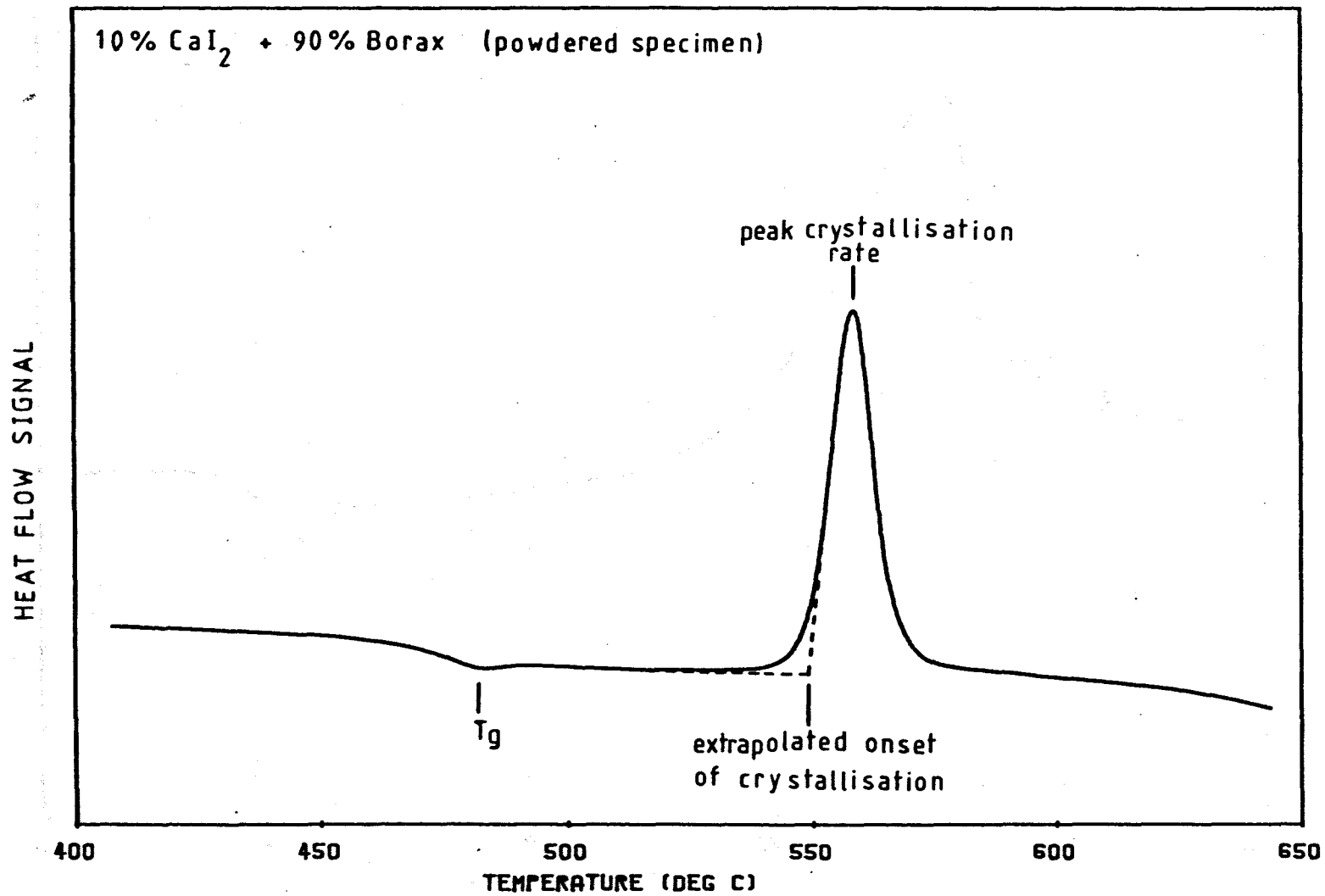


FIGURE 3.1

FIGURE 3·2

D.S.C.

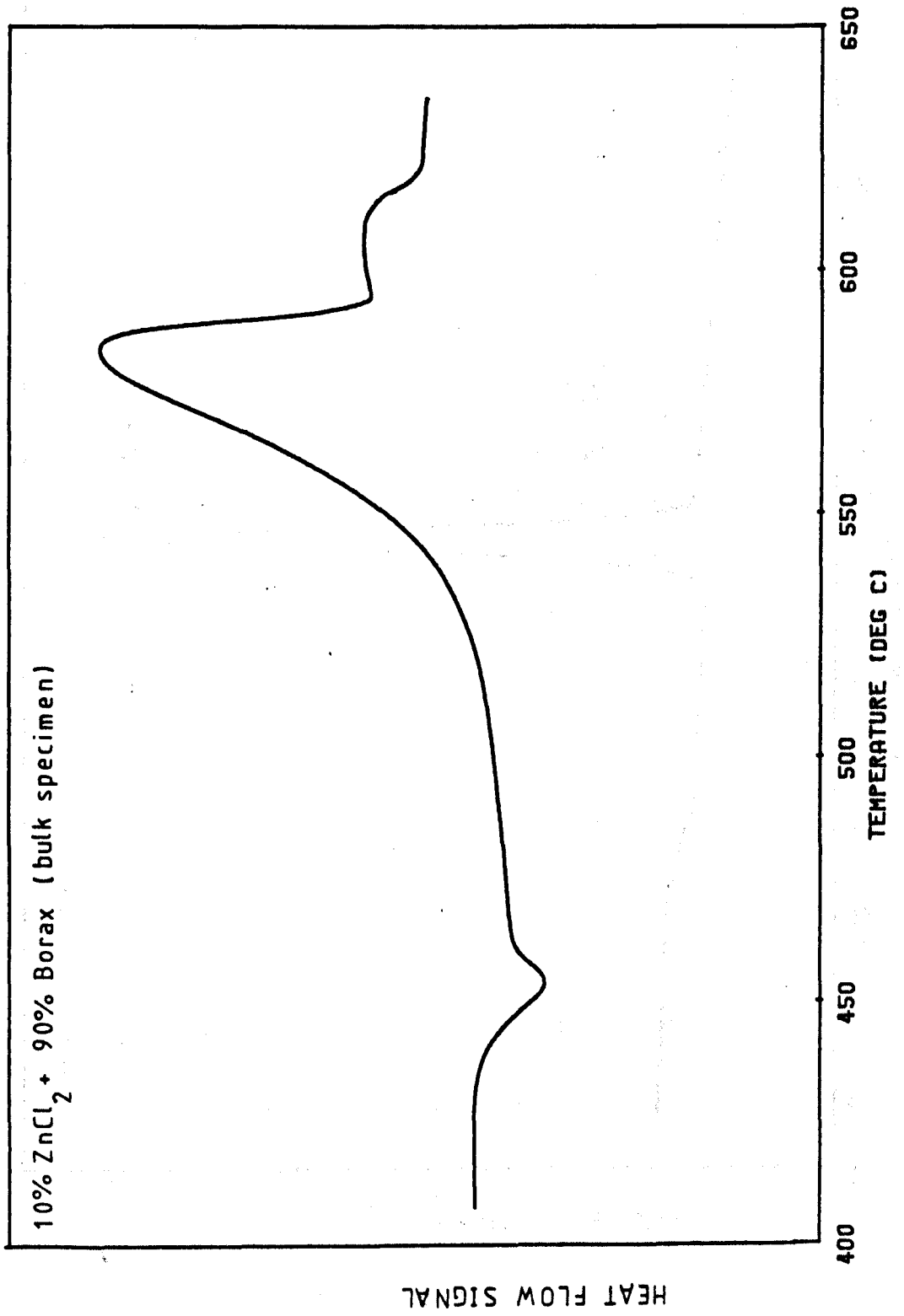


FIGURE 3-3

D.S.C.

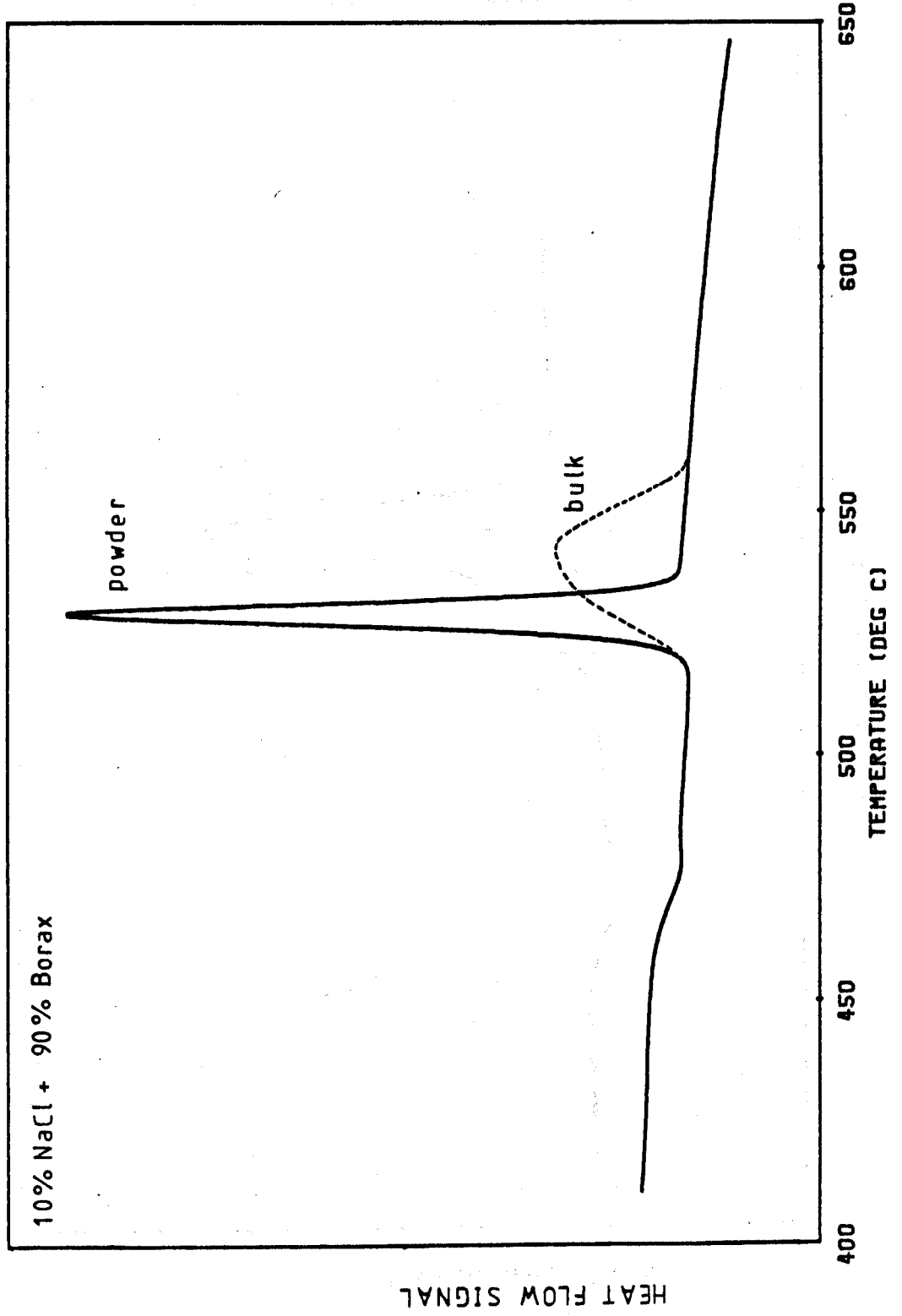
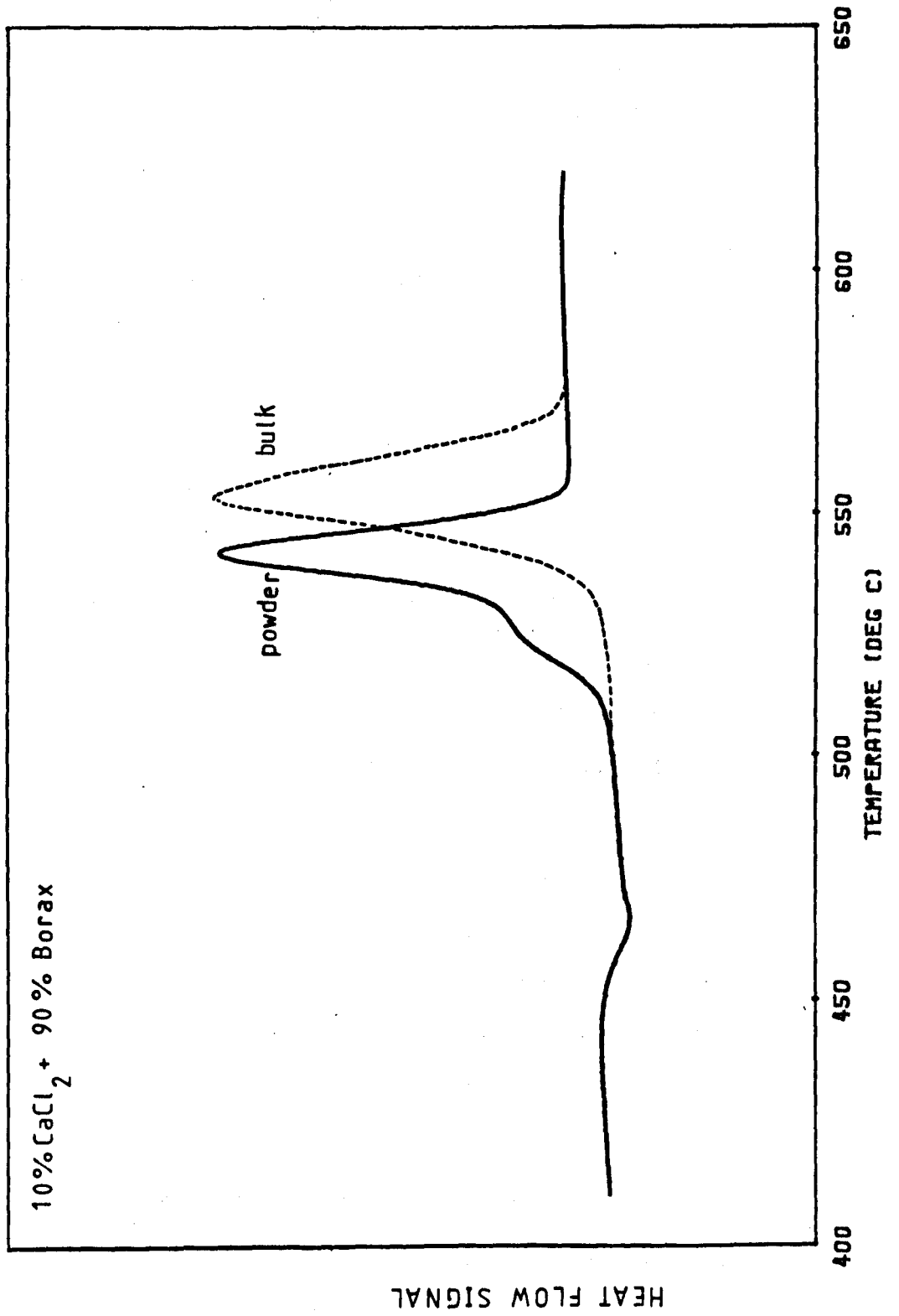


FIGURE 3.4

D.S.C.



problem with the glasses based on $\text{Na}_2\text{B}_4\text{O}_7$ but for certain of the alkaline-earth borate based glasses it was necessary to use a D.T.A. method.

3.3.2 Differential Thermal Analysis.

This is a very similar technique to D.S.C., again it is a comparative technique requiring the presence of an inert reference. The main difference lies in the method of detecting the heat changes. In D.T.A. the two samples are simply heated at a constant rate and the difference in temperature between them monitored. Under ideal conditions, over most of the temperature range this difference would be zero. However, when the specimen transforms it is slightly heated or cooled and a temperature difference is registered. The particular apparatus used was constructed at Warwick and is capable of performing measurements up to 1400°C . However, because of the availability of the D.S.C. equipment it was used only very occasionally. A sample observation is shown in Fig. 3.5.

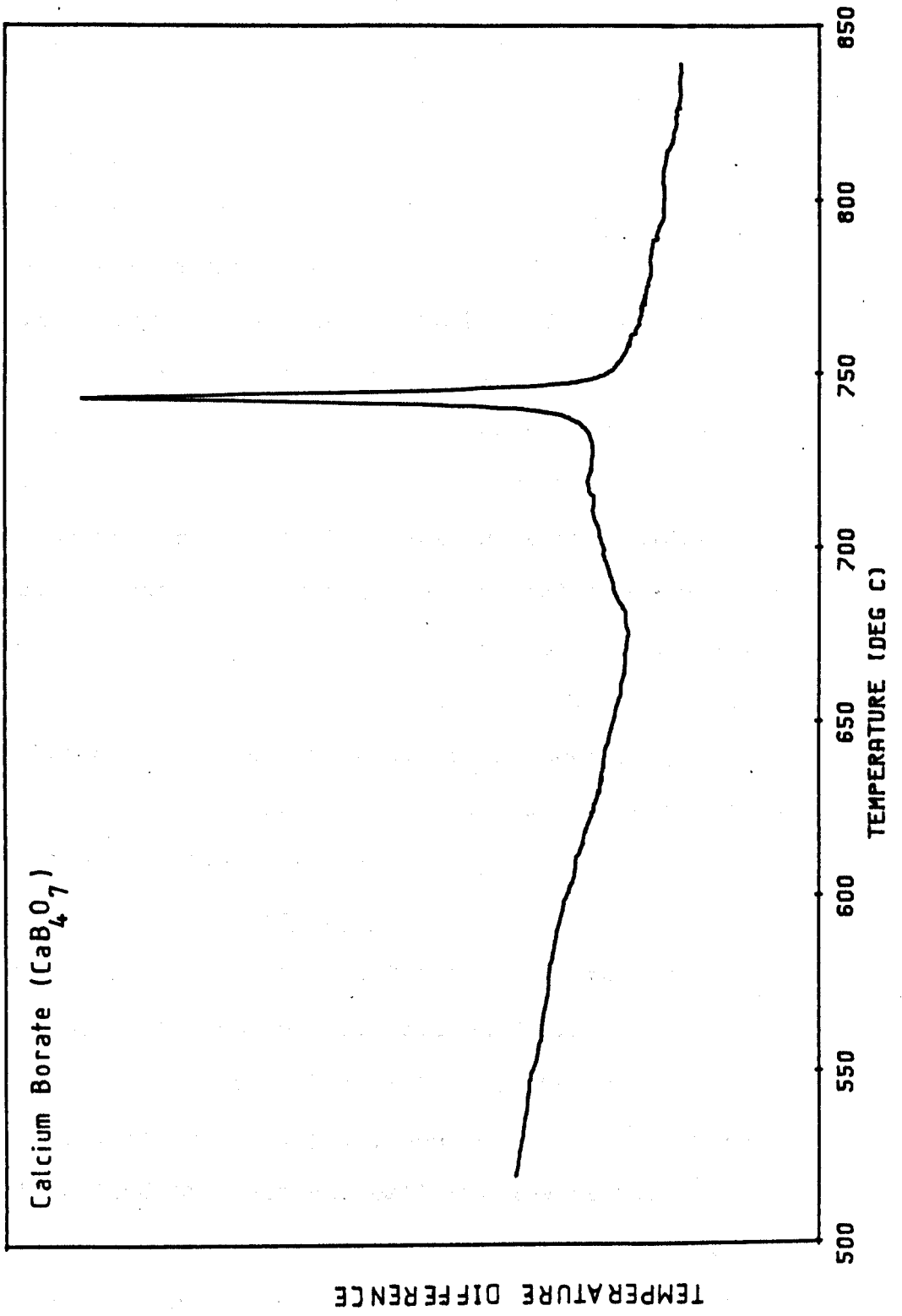
3.4 Heat Treatments.

3.4.1 Estimation of the Annealing Temperature.

Section 3.2 gave information regarding the annealing stage in the glass forming process. In order to understand how the annealing temperatures were found from the D.S.C. investigations a short discussion on the glass transition temperature, T_g (see Fig. 3.1), is necessary. For a glassy material the curve of volume versus temperature shows a distinct change in slope at a particular temperature. Above this temperature the material has the same expansivity as the liquid even though it is quite highly viscous. In

FIGURE 3·5

D.T.A.



this state it is correctly described as a 'super-cooled liquid'. Below this temperature the material has a much lower thermal expansion coefficient, in some cases approaching that of the corresponding crystalline solid, and it is in this temperature range that the material should be correctly known as a glass. The temperature at which this change of slope occurs defines T_g . Actually, T_g can take a range of values as it is slightly dependent on the cooling rate involved.

Effectively, as the material is heated through T_g the number of degrees of freedom associated with its structure increases, i.e. there is an endothermic transformation which can be observed by thermal analysis. Just below T_g the properties of the glass can change slowly with time, so that it is in this region that the annealing temperature must lie. It will be noticed that this fact correlates the values of T_g observed in Figs. 3.1 - 3.5 with the annealing temperatures quoted in section 3.2. (For a detailed discussion of T_g and annealing temperatures see 5 p.2-5 and p.61-64, and 194 p.4-6).

3.4.2 The Re-crystallisation Process.

As was stated in section 1.2 the usual conversion process involves two stages; nucleation followed by crystal growth. The crystal growth temperature is easy to assess from thermal analysis, however it is much more difficult to find the best nucleation temperature. Indeed, it becomes rather a matter of trial and error. Furthermore it soon became apparent, see below, that the addition of halides to anhydrous borax greatly affected

the nucleation properties. It would have been an impossible task to investigate the nucleation temperature for each composition. Consequently, it was decided to use a simplified heat treatment procedure consisting of a single dwell temperature in the vicinity of the crystallisation temperature. It would then be a much easier task to compare directly the properties of various compositions.

Generally the dwell temperature chosen was between the onset of crystallisation and the peak rate of crystallisation (see Fig. 3.1) though occasionally temperatures just outside this range were used. Electron microscopical studies (see later) demonstrated that the dwell temperature was very critical in relation to the size of the crystallites found in the final product. In the lower reaches of the crystallisation temperature range the crystallites were small, and a considerable time was needed to crystallise the sample fully, i.e. a low crystal growth rate was observed which allows many crystals to nucleate. At the upper reaches of the temperature range the crystallites were large and the material crystallised quickly, i.e. a high crystal growth rate with few nuclei. In this latter situation there was a tendency for the sample to deform.

Overall the most commonly used heat treatment was a rise from room temperature at 5°C per minute to a certain 'middle of the range' temperature, followed by a dwell of 2 hours to crystallise the sample.

The effect on the crystallisation of varying the heat treatment dwell temperature is shown by Fig. 3.6.

FIGURE 3.6

THE EFFECT OF HEAT TREATMENT DWELL
TEMPERATURE ON CRYSTALLISATION

10% NaCl + 90% Borax

Heat Treatment : 2 Hours at Stated Temperature



No h.t.



500°C



512°C



525°C



538°C



550°C

This depicts samples of a typical composition (90% $\text{Na}_2\text{B}_4\text{O}_7$ + 10% NaCl) after heat treatment at the stated temperature for a dwell time of 2 hours.

(h.t. = heat treatment).

The nucleation brought about by the addition of a halide is illustrated by Figs. 3.7 - 3.10. These show a series of glasses with the composition of borax plus varying amounts of NaCl. In the pure borax sample, large crystals can be seen which tend to crack the specimen. In the doped samples the grain size is much reduced, leading to less deformed samples. This difference is emphasised in Fig. 3.11 which shows a close-up comparison of a typical re-crystallised sample of firstly pure borax, and secondly borax with the addition of 10% NaCl.

Note also, from Figs. 3.7 - 3.10, that as the halide is added crystallisation tends to occur more readily at a lower temperature.

FIGURE 3.7

100% Borax

Heat Treatment: 500°C for Stated Time



No h.t.



rise time only



½ hr



1 hr



2 hrs



4 hrs



8 hrs



16 hrs

FIGURE 3.8

10% NaCl + 90% Borax

Heat Treatment : 500 °C for Stated Time



No h.t.



rise time only



½ hr



1 hr



2 hrs



4 hrs



8 hrs



16 hrs

FIGURE 3.9

20% NaCl + 80% Borax

Heat Treatment : 500 °C for Stated Time



No h.t.



rise time only



1/2 hr



1 hr



2 hrs



4 hrs



8 hrs



16 hrs

FIGURE 3.10

30% NaCl + 70% Borax

Heat Treatment : 500 °C for Stated Time



No h.t.



rise time only



1/2 hr



1 hr



2 hrs



4 hrs



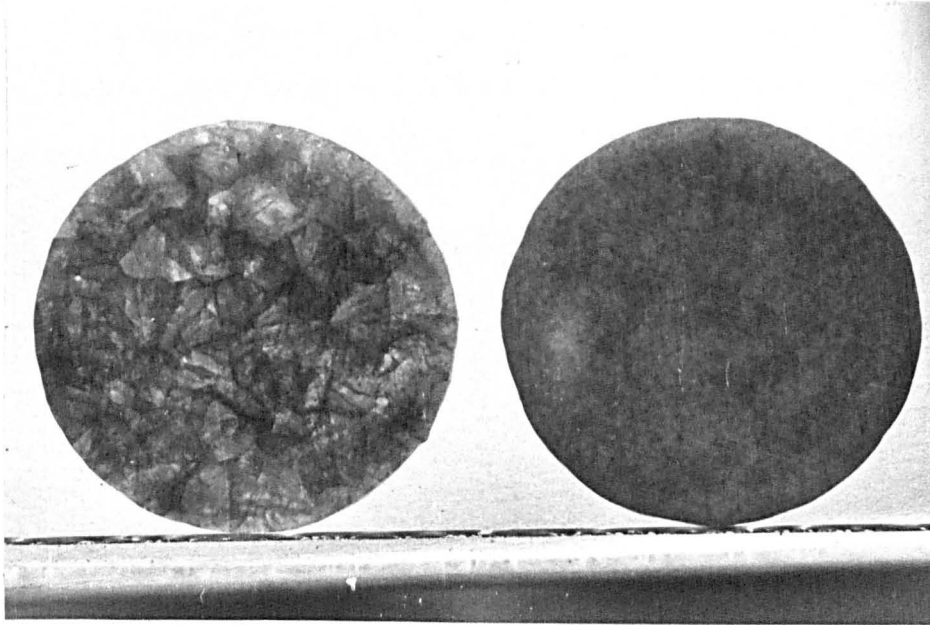
8 hrs



16 hrs

FIGURE 3·11

ILLUSTRATING THE DEPENDENCE OF
GRAIN SIZE ON COMPOSITION



A

B

A. 100 % Borax

B. 10% NaCl + 90% Borax

Heat Treatment : 2 Hours at 550 °C

CHAPTER 4

Experimental Techniques.

4.1 Electrical Conductivity.

4.1.1 Connections to the specimen and the arrangement within the furnace.

The specimens for the electrical conductivity apparatus were discs of 25mm. diameter with a typical thickness of 2mm. Three electrode contacts were made to the sample. These electrode contacts were formed by sputtering gold layers onto the surface of the specimen. Appropriate masks were used to obtain the design shown in Fig. 4.1.

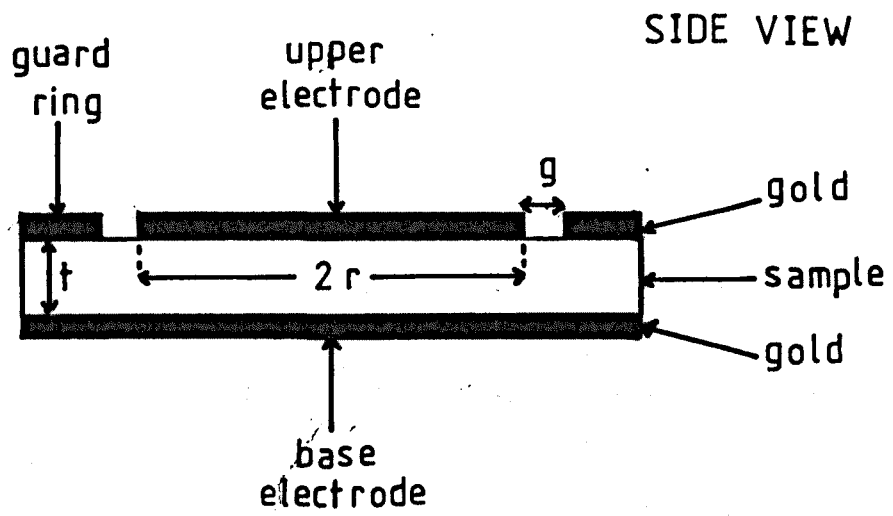
Within the furnace, contacts to the gold electrodes were made via screw arrangements. Good contact was ensured by painting around the gold/screw interface with a colloidal silver suspension which dries to a highly conducting layer. The overall apparatus is shown in Fig. 4.2.

The furnace took a considerable time to stabilise at a particular temperature and it was found, through measurements on standard glasses, that sufficient accuracy could be achieved if measurements were made during heating at a slow, constant rate. Consequently, this second method of performing the experiment was adopted, with a heating rate of 3°C per minute being used on every occasion. The thermocouple was positioned very close to the specimen.

Once the resistance, R_s , of the specimen had been found, the resistivity, ρ , could be calculated by using the following expansion (195 p.105):

FIGURE 4.1

ELECTRODE ARRANGEMENT



$r = 0.64 \text{ cm.}$

$g = 0.11 \text{ cm.}$

TOP VIEW

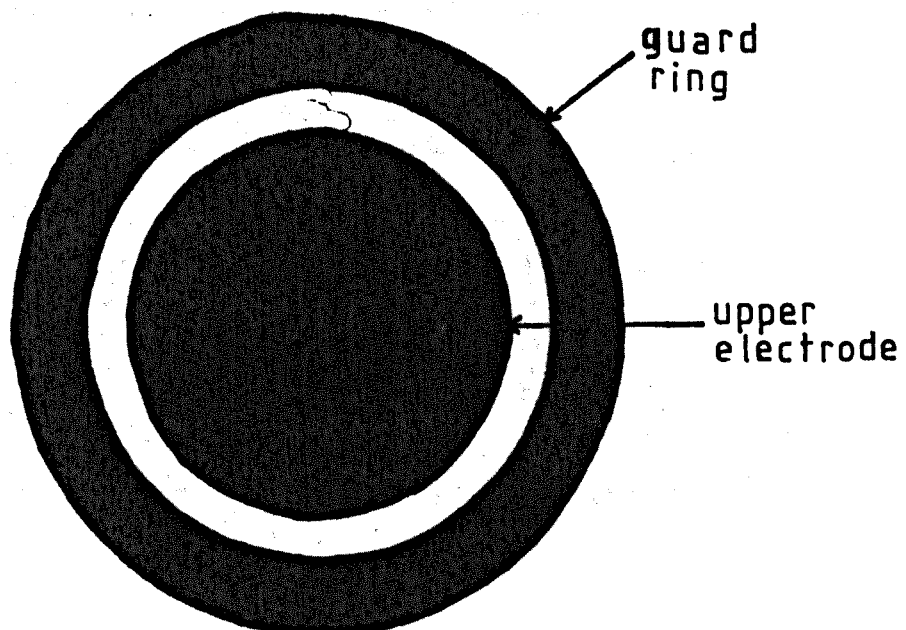
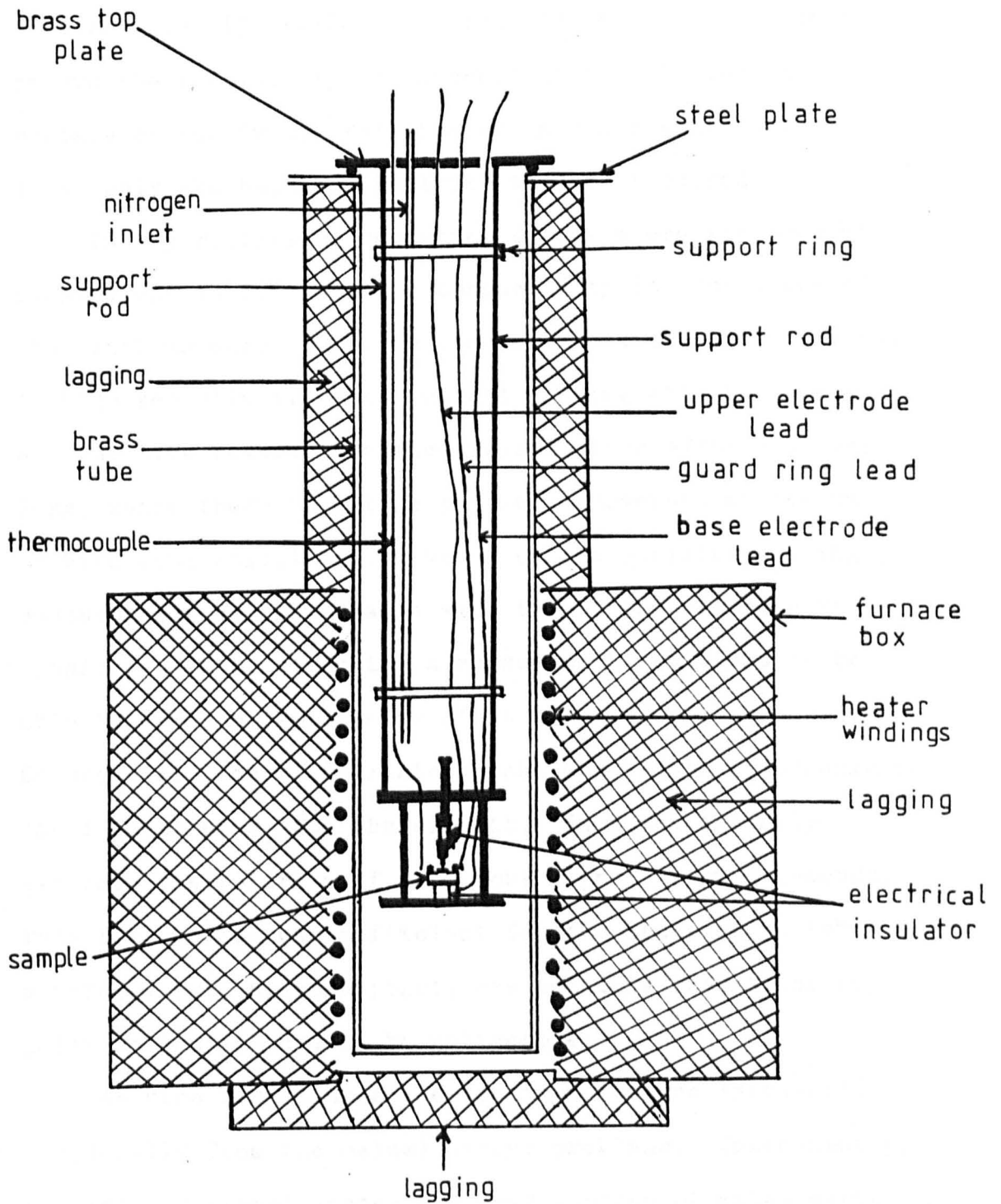


FIGURE 4·2

FURNACE ARRANGEMENT



$$\rho = R_s \cdot \frac{\pi (2r + g)^2}{4t}$$

$$\rho = R_s \cdot \frac{1.528}{t \text{ (cm.)}} \Omega \cdot \text{cm.}$$

4.1.2 D.C. Circuitry.

The three electrode arrangement has been used by many workers (e.g. 195 p.104). It can, in certain configurations, remove the possibility of inadvertently including any surface conductivity contribution in the measurements. It is only the bulk conductivity that is required.

In any resistance measuring system where the mode of measurement is D.C. and the conductivity is ionic, one of the problems encountered is the polarisation of the specimen. At high resistivities the current flowing will be very small and the time needed to notice polarisation effects is very long, hence there is little problem. However, at medium or high conductivities the value of the resistance being measured can quickly change with time. One of the aims considered in constructing a measuring circuit was to be able to measure resistances of as wide a range as possible. Consequently, an 'electronic clock' and switching arrangement was incorporated into the circuit. This mechanically switched the polarity of the input signal every 5 seconds. This time period was sufficient for the observer to take a reading but, up to a point, was not long enough for any polarisation effects to be noticeable.

At high resistances electronic noise and 'pick-up' (especially from the mains) become problems. Consequently, a 'floating earth' system was used instead of mains earth, and careful attention was paid to shielding various wires

and connections.

The overall electronic circuit used is shown in Fig. 4.3. The circuit utilises an ANCOM 15A-7D amplifier which is a hybrid low noise device especially suited to uses involving small currents. In this mode its input impedance is of the order of $10^{14}\Omega$. With the amplifier wired as shown, the resistivity of the sample could be found from the simple equation:

$$R_s = R_f \cdot \frac{V_{in}}{V_{out}}$$

R_f was always kept very much smaller than R_s , and was changed periodically during the experiment. It follows that there is very little voltage drop between the central electrode and the output. Consequently, the output can be fed to the guard ring which results in the guard and central electrodes being at approximately the same potential. Thus, no surface current can flow to the central electrode and interfere with the measurement of the bulk conductivity.

4.1.3 A.C. Circuitry.

The D.C. circuit described above performed perfectly well over a large resistance range. However, it soon became apparent that, at elevated temperatures, highly conducting materials begin to polarise, not only within the 5 seconds allowed by the switching electronic clock, but at too fast a rate to make D.C. measurements a sensible technique. A standard A.C. type system would have to be used. Nevertheless, it was still the D.C. conductivity that was of primary interest, so to avoid any frequency dependent effects it was decided to use a low frequency.

D.C. MEASURING SYSTEM

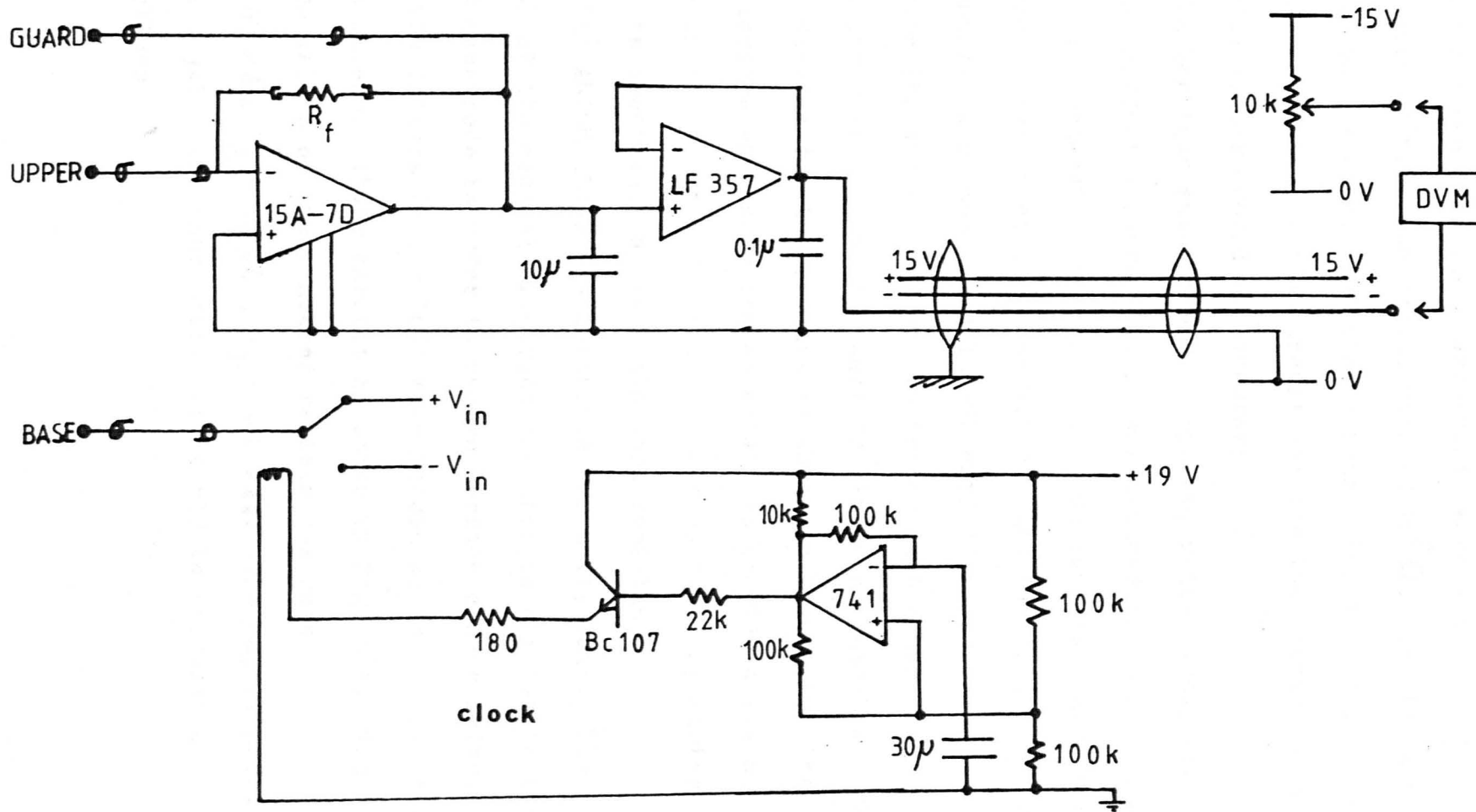


FIGURE 4.3

Ultimately, 27Hz was found to be appropriate.

Originally it was thought that the best procedure would be simply to use the existing D.C. circuitry in an A.C. mode and perform the whole experiment in this way. However, in this revised form the measurements were swamped with noise even at moderate resistances of $10^8 \Omega$, i.e. the A.C. mode is much more susceptible to noise than is the D.C. mode. Further shielding of the circuit and the incorporation of suitable filters would be necessary.

Rather than amend the D.C. system, which itself was working perfectly correctly, it was decided to construct a completely separate A.C. circuit. Measurements could then be carried out in either mode without any adaptation being necessary. A second ANCOM 15A-7D amplifier was used in this new circuit, which, in order to try and avoid any intra-circuitry noise, was kept as simple as possible. The block diagram for the circuit is shown in Fig. 4.4. The oscilloscope was incorporated solely to provide a visual check on the input and output signals so that any distortions could be observed. R_0 is a standard resistance.

The ANCOM 15A-7D is connected for unity gain. The signal at the central electrode can then be applied to the guard electrode in order to remove surface conductivity.

The filters (196 p.169) were needed as an aid in reducing noise levels. Their circuit is shown in Fig. 4.5. The chosen values of the numbered resistances were $R_1 = 47 \text{ k}\Omega$, $R_2 = 68 \Omega$, $R_3 = 100 \text{ k}\Omega$. The capacitance, C, was $2.2 \mu\text{F}$. The characteristics could be calculated as follows:

A.C. MEASURING SYSTEM

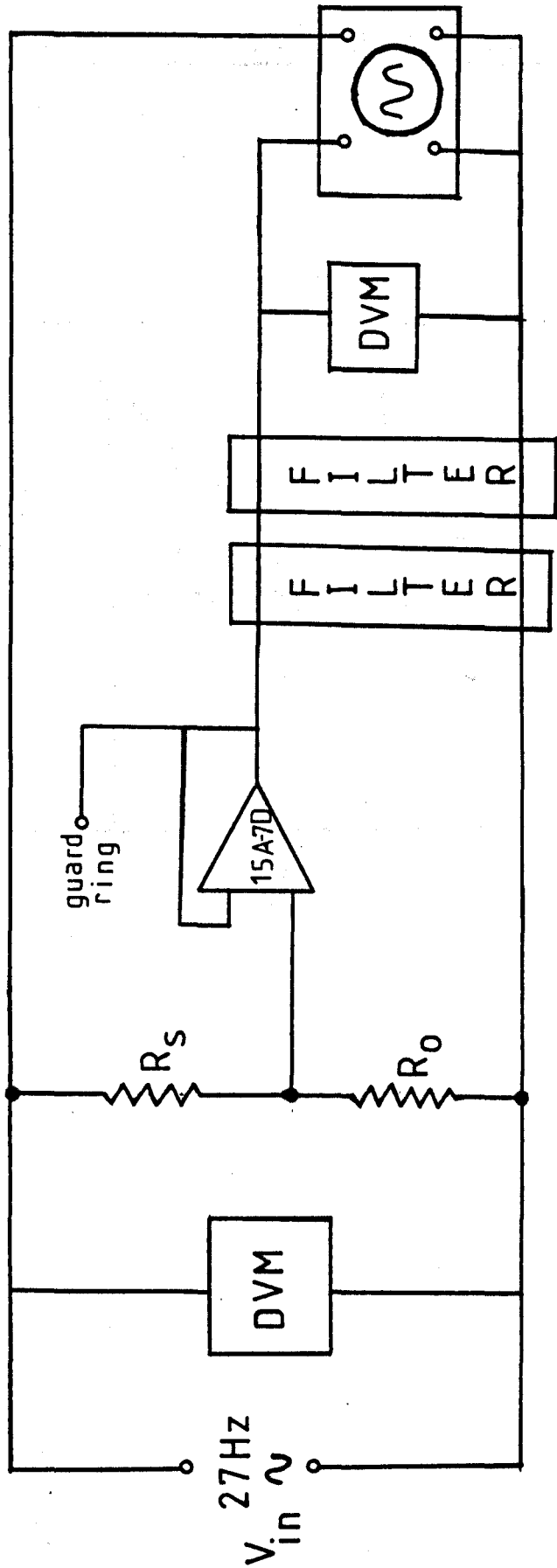
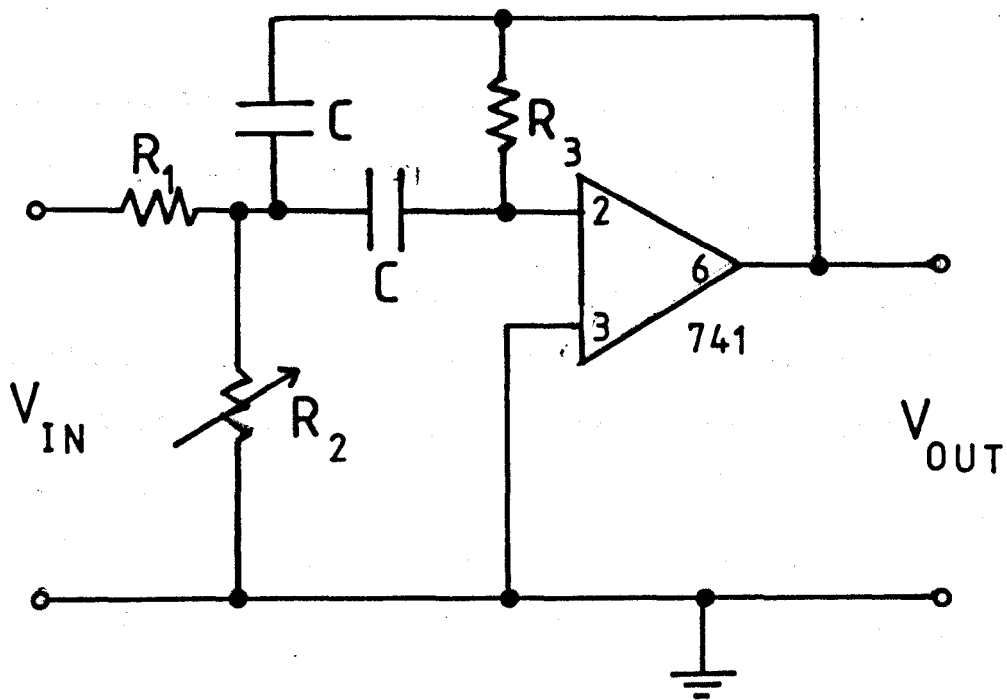


FIGURE 4.5

MULTIPLE FEEDBACK ACTIVE BAND PASS
FILTER



The resonant frequency, f_o , is given by:

$$f_o = \frac{1}{2\pi C} \left(\frac{R_1 + R_2}{R_1 \cdot R_2 \cdot R_3} \right)^{\frac{1}{2}} = 27\text{Hz}$$

The bandwidth, Δf , is found from:

$$\Delta f = \frac{1}{\pi C R_3} = 1.4\text{Hz}$$

The amplification at resonance, A , can also be calculated:

$$A = \frac{R_3}{2 \cdot R_1} = 1.06$$

It is worth noting that R_2 alters f_o but not Δf or A ; it can therefore be used as a tuning control.

As can be seen, the measuring frequency of 27Hz corresponds to the resonance frequency of the filter. The amplification factor at resonance is virtually unity, hence the signal passes through unaffected and no further adjustment of the output voltage is necessary. With the amplifier connected as shown, the following formula applied:

$$\frac{V_{in}}{V_{out}} = \frac{R_s + R_o}{R_o}$$

$$R_s = R_o \left(\frac{V_{in}}{V_{out}} - 1 \right)$$

Resistances of up to 10^{10} ohms could be measured accurately with this system. Just as importantly, given the application, measurements could be made down to only a few ohms.

The combination of the D.C. and A.C. systems allowed measurements to be made from 10^{13} ohms to 10 ohms. Occasionally the electrical properties of the specimen

resulted in its resistivity lying totally within the range of one of the types of measuring systems throughout the whole of the temperature scan. More usually the measuring system was switched during the course of the experiment. This only entailed changing the three inputs to the specimen electrodes and was easily accomplished. Invariably, the two systems gave consistent results at the changeover.

4.1.4 Results for Standard Glasses.

As a check on the accuracy of the conductivity measuring apparatus, some standard glasses of known conductivity were measured.

Firstly a sample of Float Glass was obtained from Pilkington Bros. who also supplied conductivity data. The results obtained are plotted in Fig. 4.6, together with the data supplied by Pilkington Bros. It can be seen that there is excellent agreement.

Secondly, anhydrous borax glass was made and its conductivity measured. The results obtained are plotted in Fig. 4.7. The reproducibility of the graph was investigated by making a second sample and measuring its conductivity as a comparison. This second set of data is also shown in Fig. 4.7. There is very good agreement between the results for the two specimens. The graph yields an activation energy of 73 ± 4 KJ/mol. and the room temperature resistivity is approximately 10^{11} ohms. This is in excellent agreement with other reported results (see Table 2.2) and is indeed identical with data referred to by Namikawa (137).

These trial experiments clearly demonstrate the reliability and accuracy of the conductivity measuring equipment.

FLOAT GLASS

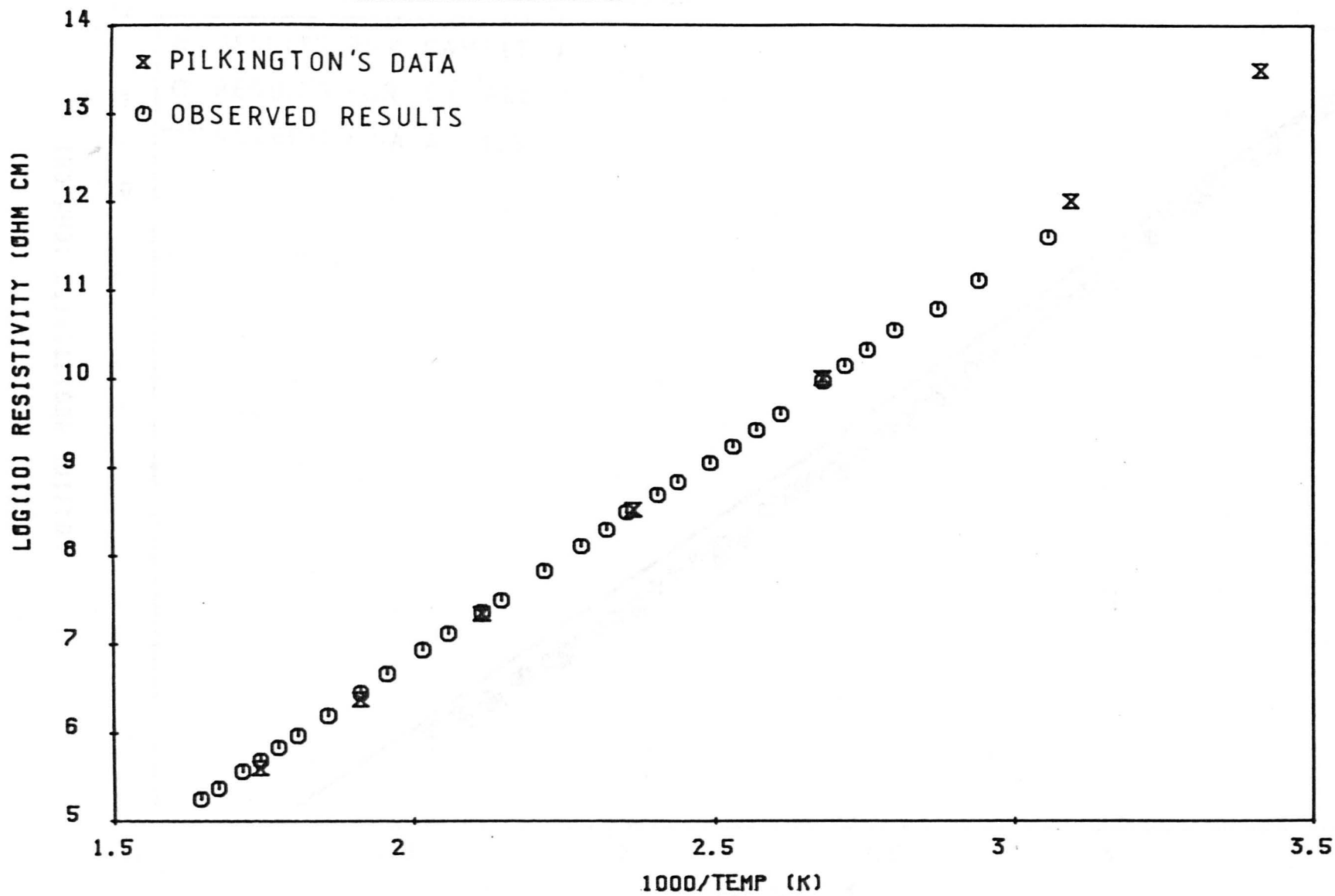


FIGURE 4.6

PURE BORAX GLASS

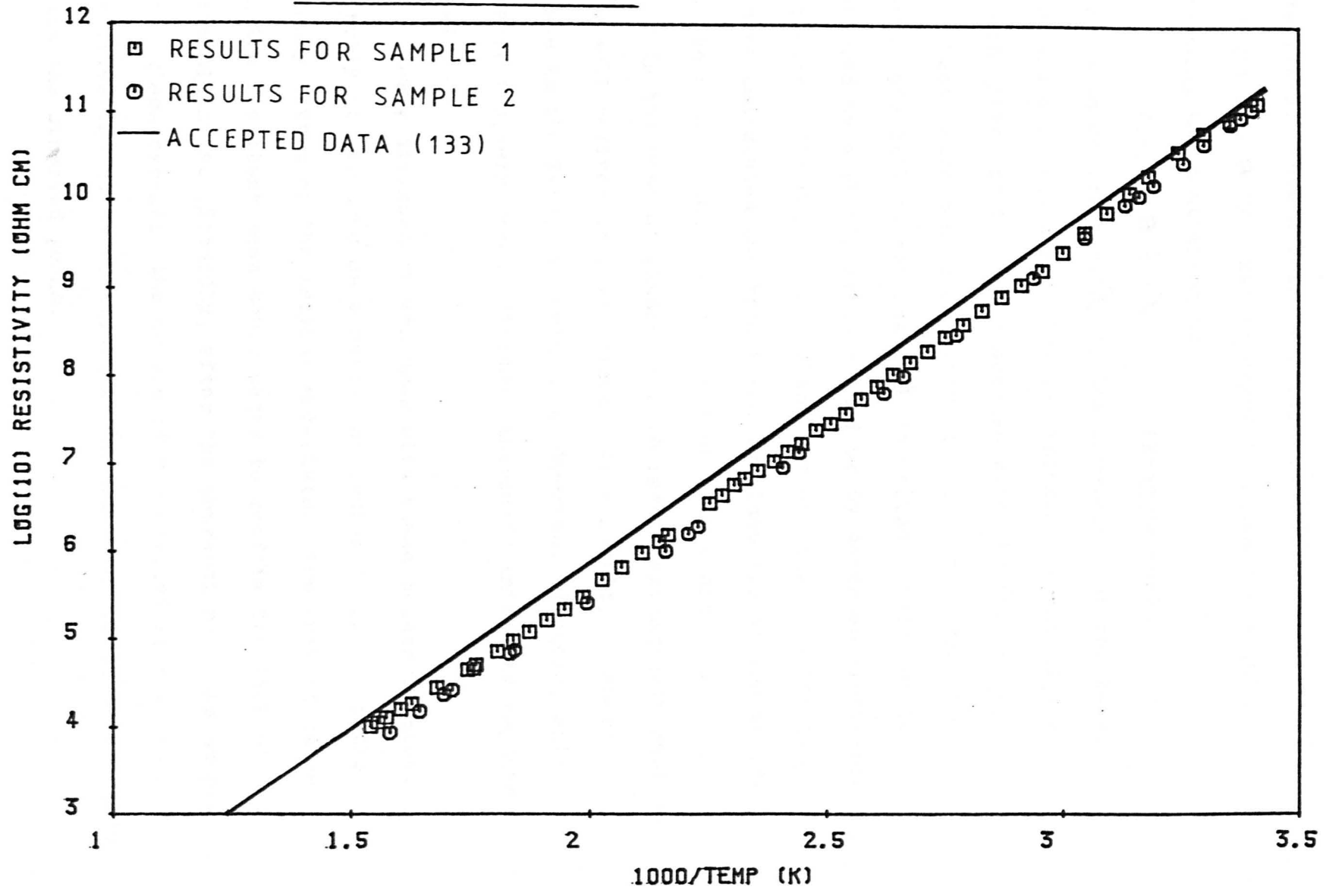


FIGURE 4.7

4.2 X-ray Diffraction.

X-ray diffraction analysis is a technique used by a very wide range of solid state physicists and materials scientists. When a beam of X-rays is diffracted through an angle of 2θ by a set of crystal planes the equation governing the scattering is:

$$2.d.\sin \theta = n\lambda \quad (\text{Bragg's Law})$$

where n is an integer, λ is the wavelength of the X-ray beam and d is the perpendicular distance between adjacent atomic planes of the set concerned with the scattering.

Most experimental apparatus involve monitoring the X-ray intensity as the angle θ is varied. This can be achieved by a photographic method or by using an electronic detector. The set of 'd' values corresponding to the peaks can be calculated and from these the identity of the sample can be established via a comparison with standard results.

In the case of glasses a more random arrangement replaces the well defined crystal planes. As a result, no sharp peaks in the X-ray intensity are observed. Instead, only one or two very broad, diffuse, increased intensity regions occur.

X-ray diffraction was used with these points in mind. Firstly it was used as a matter of course to check on the glassy nature of the initial materials. The lack of peaks in the resultant scan would serve to confirm the lack of crystallinity. Secondly, after the conversion of the sample to a glass-ceramic, the nature of the crystal species could be investigated by calculating the set of d-spacings associated with the observed peaks.

Initial work was carried out using a standard Debye-Scherrer powder camera technique. This method is well known and is described in detail by many authors (e.g. 86 p.44, 88 p. 27, 197 p.130, 198 p.10). The sample is used in fine powder form and covers a cylindrical fibre within the camera. X-ray sensitive photographic film is mounted around the specimen. Due to the vast number of crystallites that are present there will always be some at a convenient angle to diffract the incoming X-ray beam. Hence, cones of rays diverge from the specimen and strike the photographic paper in arcs. These arcs can then be related back to the d-spacings. The X-ray generator was constructed by Philips Electronic Instruments and the radiation used was copper $K\alpha$ i.e. a wavelength of 1.542 Å.

Midway through the project an X-ray diffractometer became available. This apparatus provides an improved technique and was subsequently used in preference to the powder camera. Again, the construction of the apparatus and the method used is well known and discussed in detail elsewhere (e.g. 197 p.161, 198 p.29). As in the above case the generator was made by Philips Electronic Instruments and copper $K\alpha$ radiation was used. The goniometer arrangement was of the horizontal type. Either a powdered or a bulk sample could be used, however the 25mm. disc samples that were used in the conductivity apparatus (see previous section) proved to be an ideal size for the sample-holder. Consequently this type of sample was used on most occasions.

The basic principle of operation is that, with the X-ray beam being horizontal, the sample is rotated about a

vertical axis through the point where the X-rays hit the sample. Coupled with this rotation is the rotation of a detector about the same axis. The coupling is such that if the specimen turns through an angle θ , then the detector arm rotates through 2θ . The output from the detector then transfers to a pen recorder.

4.3 Electron Microscopy.

4.3.1 General Observations.

Scanning electron microscopy was carried out on several samples using a Cambridge 250 Stereoscan microscope. The specimen preparation was as follows. Firstly, the samples were set in plastic resin in order to facilitate polishing and general handling. Polishing was accomplished via the combined use of silicon carbide abrasive paper and, for a fine finish, diamond paste. Finally, to avoid charging up of the sample in the microscope, the specimen was coated in a thin layer of carbon by an evaporation technique.

The initial use of the microscope was to investigate the dependency of the crystallite size on the heat treatment temperature during the glass to glass-ceramic conversion. It was envisaged that the crystallite size could change drastically with the heat treatment temperature, and that this could affect the resultant conductivity.

Generally an electron accelerating voltage of 20KV was used throughout these observations. Any voltage higher than this tended to damage the samples.

4.3.2 The Use of E.D.A.X.

The scanning electron microscope that was used also incorporated an 'energy dispersive analysis by X-ray'

(E.D.A.X.) system. Such an apparatus analyses the characteristic X-rays given off by the sample and relates the observed spectrum to the elemental composition. Unfortunately, the apparatus is insensitive to elements below sodium in the periodic table. Hence, it can not investigate the presence of boron or oxygen in the samples. This makes true quantitative work rather difficult but nevertheless the technique provides an excellent comparison for the other elements that are present.

Usually it is the K type X-ray lines that are used. However, for elements such as barium, where the energy of the K X-ray lines is above 20KV, observations can be carried out on the L X-ray lines without any difficulty.

E.D.A.X. could be carried out on the specimen as a whole or on regions within the sample. This second facility proved especially useful as it allowed compositional comparisons to be made between the crystallites and the residual glassy phase. Consequently, any preferential influx or expulsion of certain elements to or from the crystalline phase could be investigated.

4.3.3 Determination of the Conducting Phase.

A rather novel technique was used to qualitatively compare the relative conductivities of the crystalline and residual glassy phases in the glass-ceramics. As was stated above, the usual procedure was to coat the specimen in a layer of carbon in order to prevent charging. However, in this technique only half of the specimen was covered. The aim was that, in the uncoated section, the more resistive region would indeed charge up and be conspicuous due to the characteristic charge-glow that occurs in this situation.

Whereas, in the more conductive phase region the charge would be conducted away, and the area would not glow.

The graphite coated section was used as a control for this experiment and could also be used for 'normal' observations.

In the event, it was found that if the usual electron accelerating voltage of 20KV was used on the uncoated area, then both phases charged up quickly. In order to achieve satisfactory results the accelerating voltage had to be reduced to 5KV.

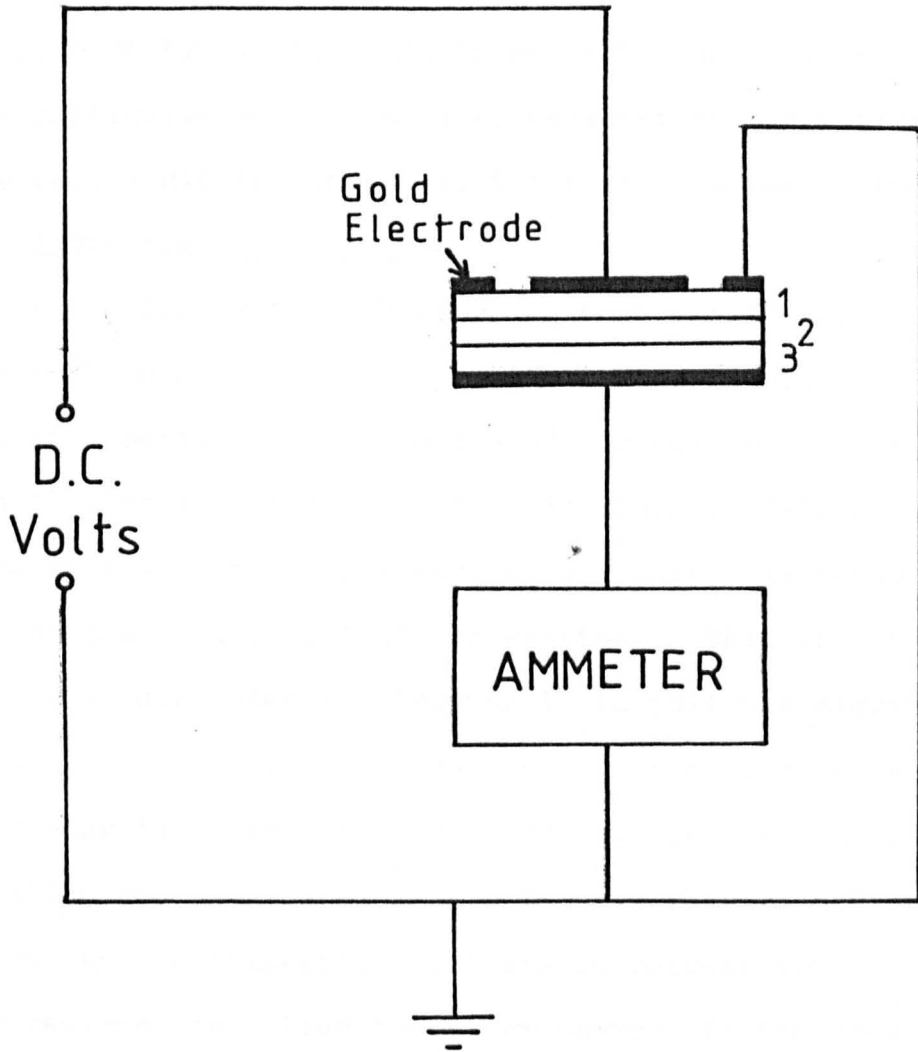
4.4 Triple Disc Experiments.

In pure $\text{Na}_2\text{B}_4\text{O}_7$ the mobile ion responsible for conduction is the sodium ion (see Chapter 2, section 2.7.2). However, in a sample such as 90% $\text{Na}_2\text{B}_4\text{O}_7$ + 10% CaCl_2 the situation is far less clear cut. The possibility that the most mobile ion is the chloride ion, or even the calcium ion, and not the sodium ion can not simply be discounted. The situation has to be checked and the nature of the conducting species verified. The 'triple disc experiment' is one method of achieving this.

In these experiments three of the 25mm. disc specimens (as used in the conductivity apparatus - see sections 3.2 and 4.1) of the same composition were arranged on top of each other. A large D.C. potential was then put across them for several hours, and the current through the bulk of the specimen was monitored by an electrometer. The general arrangement is shown in Fig. 4.8. The gold electrodes and contacts to them were made as for the conductivity measuring apparatus (see section 4.1.1).

FIGURE 4·8

'TRIPLE DISC' ARRANGEMENT



The surfaces providing contact between the discs were highly polished with great care. The aim of the experiment was that, as the specimens polarised, it would prove possible for the mobile species to transfer from disc to disc, thus these ions would increase in concentration near the appropriate electrode. While maintaining the applied potential the discs could be separated and then analysed either by chemical analysis or by E.D.A.X. An increase in the relative concentration of a particular ion in the disc adjacent to the appropriate electrode would indicate that ion to be the mobile species.

4.5 Thermopower Experiments.

Historically most thermopower experiments have been performed on electronically conducting materials. If one part of a semi-conductor is heated the number of conduction band electrons in that region is increased. This creates a concentration imbalance and, as a result, electrons diffuse towards the cooler part of the specimen. This in turn creates a back potential tending to inhibit the migration. Eventually equilibrium is reached with the back potential cancelling the concentration gradient. In the equilibrium situation the electrical back potential that is set up, divided by the temperature difference between the hot and cold regions, is called the thermopower. If the conduction had been via holes the thermopower would have had an opposite sign. Consequently, simple measurement of the thermopower can give the sign of the charge carrier.

A somewhat analagous situation arises in the case of crystalline ionic conductors. In these materials the conductivity mechanism is usually either interstitial ion

motion or vacancy motion. In either case the number of such defects is temperature dependent, thus the necessary situation for a thermopower effect to be observed is achieved. Similar arguments can usually be made for other ionic conductivity mechanisms.

Ionic thermopower effects have been investigated by a few authors (199-202) with considerable interest centering on the silver halides.

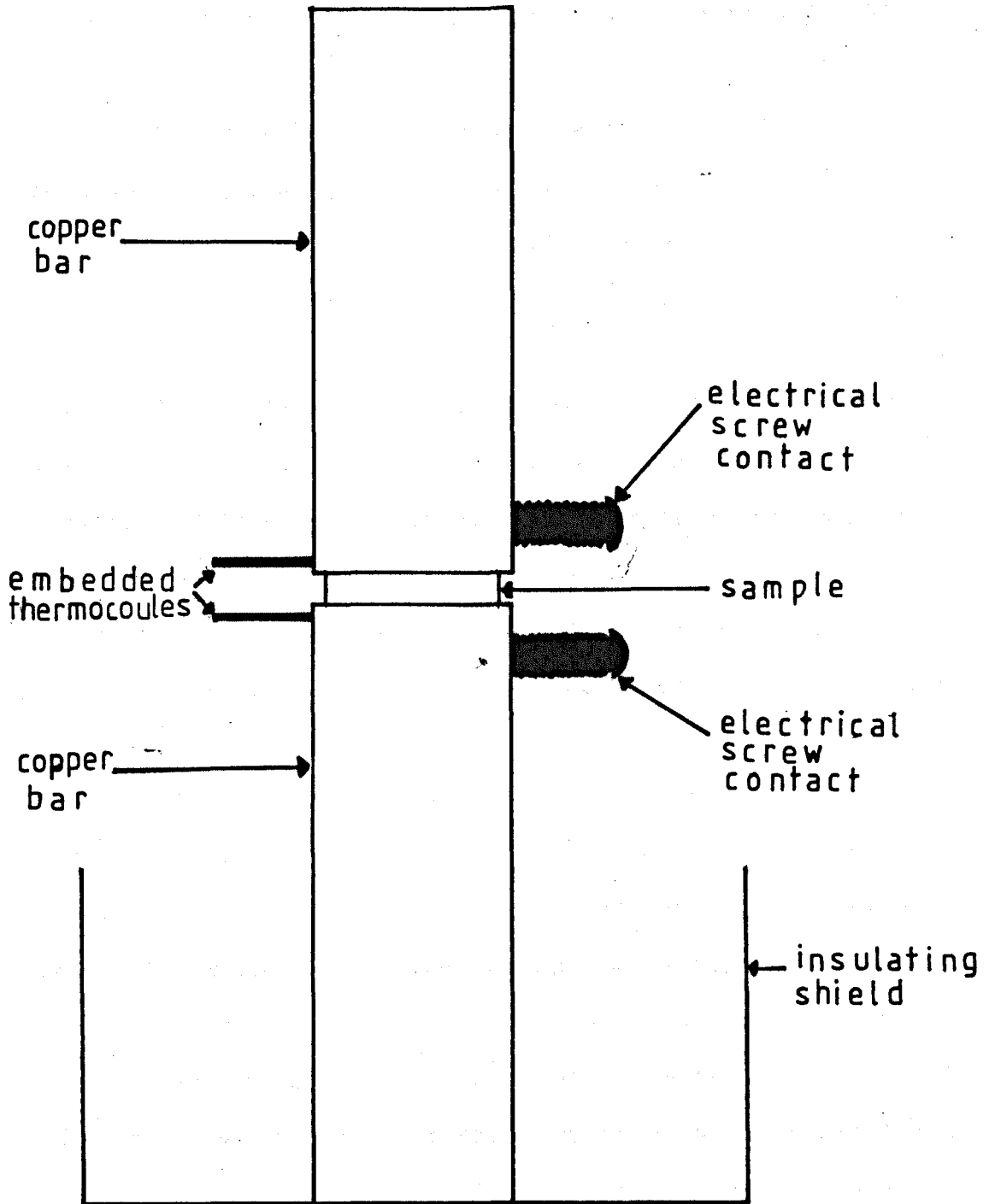
For the purposes of this project it was never the intention to perform detailed quantitative experiments to ascertain, for example, thermopower versus temperature curves. All that was required was evidence concerning the sign of the charge carrier that would back up, or otherwise, the results from the triple disc experiments mentioned in the previous section. With this single notion in mind the basic apparatus shown in Fig. 4.9 was set up. Again a 25mm. disc sample was found to be convenient. The temperature difference across the sample was measured via the two thermocouples which were embedded as close as possible to the specimen. The thermo-voltage developed was measured on an electrometer, with contact to the copper bars being made via brass screws sunk into the material.

The upper copper bar could be warmed by using either electrical heating tapes or a bunsen flame. Alternatively, the lower bar could be cooled by surrounding it with ice.

Good electrical contact to the specimen was achieved by one of two methods. Firstly, the established gold sputtering technique was used. The gold was sputtered over the upper and lower surfaces of the disc and then colloidal silver

FIGURE 4.9

THERMOPOWER APPARATUS



painted over this to provide a complete interface between the gold and the copper bar. The second method simply entailed using a layer of colloidal graphite. Both methods seemed equally successful.

It may be envisaged that contact potentials between the various metals could effect the results obtained. This was checked by removing the sample but using the same 'sandwich' of metals in the sample gap. No results of a comparable magnitude were obtained. Similarly if an inert sample was used no thermopower voltage arose.

4.6 Infra-red Absorption.

The atomic units within a glass or a glass-ceramic have characteristic vibrational modes, with the frequency of these vibrations often falling in the infra-red region of the spectrum. Consequently, infra-red absorption spectroscopy is a powerful tool for the investigation of structural units on a local scale. Vibrations of individual bonds and of atomic groups can both be observed provided they fall within the relevant frequency range.

For all investigations a double beam spectrometer was used. In such apparatus two identical beams emanate from the infra-red source. The specimen is positioned in the path of one of the beams, whilst the second beam enters the spectrometer directly. A comparison of the infra-red intensity in the two resultant beams yields the degree of absorption by the specimen. The double beam technique avoids errors such as absorption by the atmosphere, which might otherwise be thought to be due to the specimen.

The main problem in the preparation of specimens for use

in infra-red absorption measurements was due to the fact that borate materials tend to absorb rather strongly over a wide range of frequencies. This means that very thin specimens had to be used in order to observe structure within the absorbing regions. This was beyond the scope of normal grinding and polishing techniques, hence special procedures had to be employed.

One method that was used was the KBr disc technique. This is a standard technique used by many workers. In this procedure the powdered sample was mixed with powdered anhydrous KBr, generally in an approximate ratio of 1:8. The mixture was then put into an hydraulic press and a disc formed. The pressure used was approximately 10 tons on a $\frac{1}{2}$ inch die, and the thickness of the resulting disc was typically 0.1mm. The KBr shows very little absorption over most of the infra-red range and therefore acted as an inert matrix through which the specimen was thinly dispersed. This method has been criticised on several counts. Firstly, it subjects the specimen to high pressures which may distort or change the normal structure. Secondly, it has proved impossible to remove water contamination completely. Thirdly, the strength and shape of the absorption peaks have been found to be dependent on particle size. Fourthly, the possibility of chemical reactions altering the compounds that are present can not be ruled out (for further discussion on the validity of the KBr disc technique see, for example, 203 p.122, 204, 205, 206).

Despite these drawbacks this procedure, or similar procedures, has been used by a host of authors. It is a

simple technique to use and has been effective in a wide range of cases. For binary sodium borate glasses, serious water contamination and peak distortion were found only to be present at low sodium content (206). However, at concentrations above approximately 10% Na₂O, the KBr disc method was found to give similar spectra to those obtained by other techniques. The predominant base glass used in this project was 33.3% Na₂O + 66.7% B₂O₃, consequently the KBr disc technique has been used with a reasonable degree of confidence. It was used for both glasses and re-crystallised glass-ceramics.

The second method used to produce thin samples was to blow bubbles from the molten glass. A steel tube of 7mm. internal diameter was dipped into the melt and withdrawn with a globule of glass attached to the end. When the glass had cooled to a reasonable viscosity (a visual estimate made easier with experience) a bubble was blown. The wall thickness was generally of the order of a micron. The specimen was then immediately mounted in the sample holder and the infra-red absorption measurements taken. Delays of hours or, in some cases, even minutes resulted in 'fogging' of the specimen. The resulting spectra were usually of superior quality in comparison to those taken with the KBr disc method, provided a sufficiently thin specimen could be obtained.

While the above 'blown bubble' technique could be attempted quite readily for glassy samples, problems arose when the infra-red absorption spectrum of a re-crystallised sample was required. Not surprisingly, the heat treatment of such thin samples met with rather less than complete success. The films tended to crinkle and deform in the heat treatment

furnace, with the resulting crystalline products being many times thicker than the initial glassy sheets. Nevertheless, it was usually found that the edge of one such product could be used to obtain a reasonable spectrum.

Both the KBr disc technique and the blown bubble method were used repeatedly during the course of the project.

Measurements were made on three spectrometers. Initially a Grubb-Parsons 'Spectromaster' spectrometer was used. This instrument was rather old and it was quite difficult to obtain reasonable results. However, some spectra were obtained using the blown film method and will be presented later. During a period of time spent working at Borax Research Ltd. a Pye-Unicam SP 1100 spectrometer was available. This model covers the range 4000cm^{-1} to 400cm^{-1} which includes most of the region of interest for borate based materials. Numerous spectra were taken on this apparatus, the vast majority of which involved the KBr disc technique. Finally, a Perkin Elmer model 983 spectro-photometer was used. This instrument also incorporated a Perkin Elmer model 3600 data station which provided facilities for data storage and handling. The range associated with this spectrometer is 5000cm^{-1} to 180cm^{-1} . The extension of the range to lower wavenumbers than had previously been available proved particularly useful. Both KBr disc and blown film measurements were made on this instrument.

4.7 Nuclear Magnetic Resonance (N.M.R.)

4.7.1 Aims.

The work on N.M.R. has progressed along two fronts. Firstly, to investigate the boron nucleus and to ascertain

whether the addition of a halide dopant in any way alters its co-ordination state in the resultant glass. Secondly, to observe the resonance due to the sodium nuclei and to note if it is changed substantially when the doped material is heat treated. The apparatus used was a Varian VF16B wide line N.M.R. spectrometer.

4.7.2 Theory.

Detailed theory on N.M.R. will not be entered into here, but a thorough treatment can be found in many texts (for example 207-219). Only a few brief results need to be mentioned. The boron and sodium nuclei have spin $3/2$, hence, due to the quadrupolar interaction, in single crystals their N.M.R. spectra would consist of three equally spaced lines, see Fig. 4.10. However, in polycrystalline and glassy materials, the relative position of the outer satellite lines is not fixed, hence they become very broad and are often un-observable, see Fig. 4.11. Thus, only the central line is usually observed.

In some cases this central line is itself broadened by second order quadrupolar effects. If this is so, then the frequency width, $\delta \nu$ is given by (217, 220, 221):

$$\delta \nu = \frac{25 C^2}{192 \nu_0}$$

where ν_0 is the central frequency and C is called the coupling constant.

If C is very small then second order quadrupolar effects are not important and the width of the line is due to simple dipolar effects.

In most N.M.R. experiments it is the derivative of the absorption peaks that is observed. This has to be integrated

FIGURE 4.10

TYPICAL N.M.R. SPECTRUM FOR A NUCLEUS
WITH SPIN $3/2$ IN A CRYSTALLINE MATERIAL

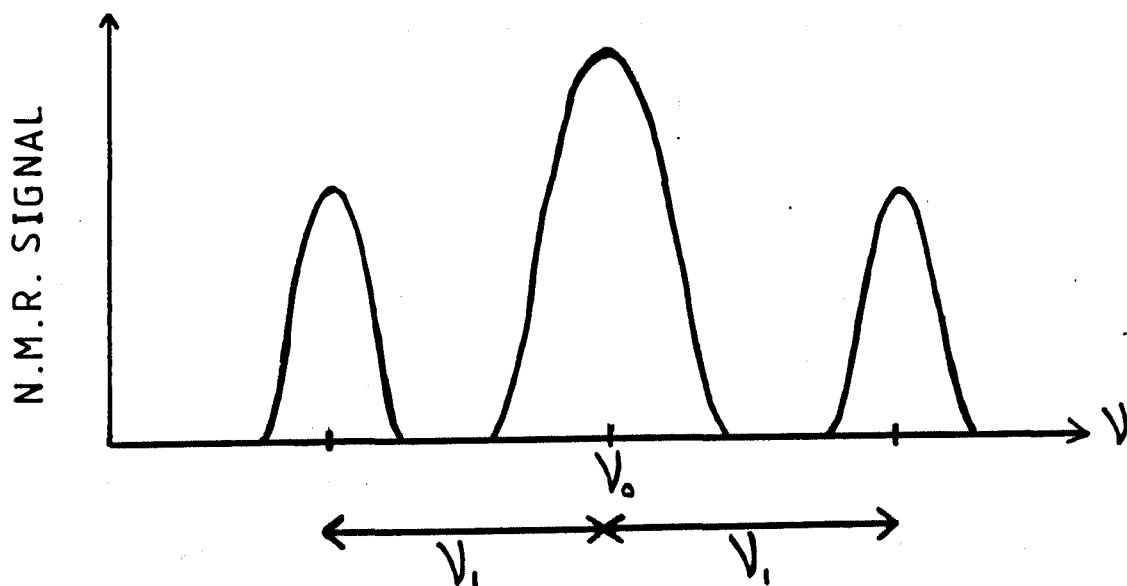
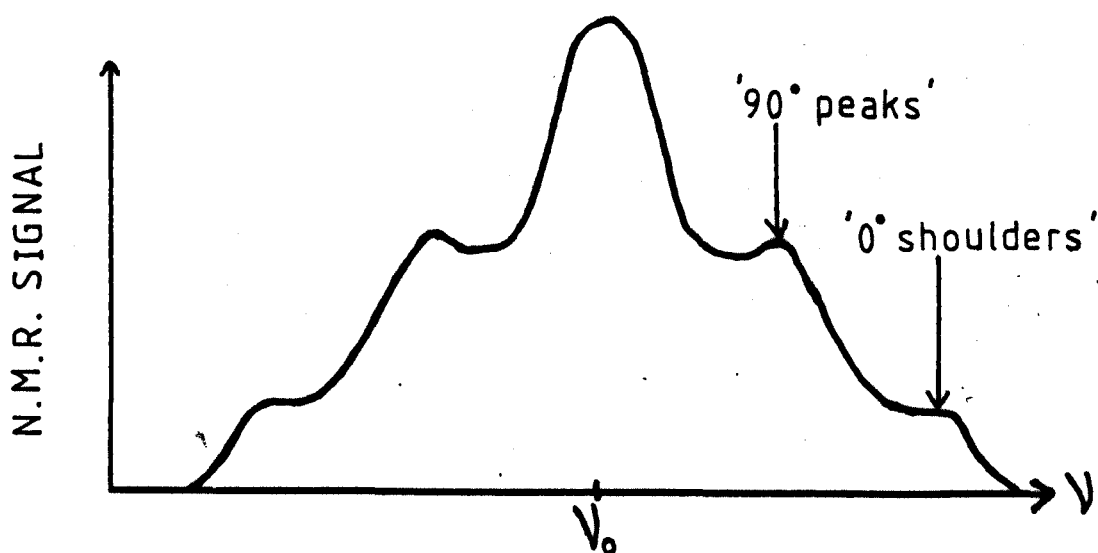


FIGURE 4.11

AS ABOVE BUT FOR A POLYCRYSTALLINE
OR GLASSY MATERIAL



if it is necessary to utilise the true absorption curve.

4.7.3 Boron Studies.

The boron nucleus, ^{11}B , has been investigated in a wide range of materials by a host of workers. Such materials include boric oxide and binary glasses (217, 221-238), ternary glasses (239-249), boro-silicates (217, 250-257), boron containing single crystals (258, 259), poly-crystalline minerals (260-265) and other compounds (266-271). In more recent years advances have been made in two areas. Firstly, with the use of the ^{10}B isotope. This is proving a more sensitive tool than ^{11}B (272-277). Secondly, in the theoretical interpretation of lineshapes with the use of computer simulation predictions (278-293).

In borate glasses boron can exist in 3 co-ordination or 4 co-ordination with oxygen. In the case of 3 co-ordination the coupling constant is quite large at 2.76 MHz (217, 221, 227, 230, 263, 267, 283). This gives broadening due to second order quadrupolar effects and the resulting line is also rather assymmetric. The highly symmetric arrangement for the 4 co-ordinated state gives a vanishingly small coupling constant, hence the line is not broadened by second order quadrupolar effects and is very narrow. Hence, it is possible to observe both types of resonances simultaneously, and the relative fraction of each type of state can be calculated.

Boric oxide itself is considered, usually from X-ray results, to be made up of wholly 3 co-ordinated boron in both the glassy (294-302) and crystalline form (303, 304), though the presence of groups made up from the triangular units remains open to debate. The N.M.R. results of various

workers agree with this idea of 3 co-ordination for boron in the simple oxide (217, 221, 227, 230, 263, 267, 283). If Na_2O is added to B_2O_3 one possibility is that on adding one unit of Na_2O the added oxygen becomes bonded to two of the previously 3 co-ordinated boron atoms, making then 4 co-ordinated. The two Na^+ ions then enter interstices. Hence, considering the formula $X\text{Na}_2\text{O}:(1-X)\text{B}_2\text{O}_3$, there must be a total of $2X$ boron atoms in 4 co-ordination. The total number of boron atoms is $2(1-X)$, consequently if N_4 is the fraction of borons that are 4 co-ordinated then:

$$N_4 = \frac{2X}{2(1-X)} = \frac{X}{1-X}$$

The absorption peak from 3 co-ordinated boron is very broad. Hence, as X increases, the strength of this signal becomes very weak, and it tends to disappear into noise. Thus, at high X , the result for N_4 from a simple measurement of peak heights becomes artificially high and large discrepancies from true results occur. (226, 227). Ways of correcting this effect have been developed (226, 227), however, this calibration procedure will not be entered into in the work performed in this project and comparisons will only be made to the early raw data of Silver and Bray (221). The relative N_4 results to be given can be directly compared to the ' c/a ' values quoted in that work.

Correctly calibrated results for various borate glasses are given by Bray and O'Keefe (227), this work illustrates that N_4 follows the predicted formula until $X > 30\%$. For sodium borate with $X > 30\%$ N_4 falls rather below the predicted value, though the limit of glass formation is reached before there is much discrepancy. In the case of

lithium borate the glass formation region is extended, and it is found that N_4 falls back to zero at $X = 70\%$. It must be mentioned that some of these high lithium content results should be questioned; the glass forming region for lithium borate does extend further than for sodium borate, but 70% Li_2O is considerably beyond the region generally accepted in which a clear homogenous glass can be formed (193, 305).

The glasses investigated at Warwick were melted in platinum at 1000°C . for 3 hours, cast into cylinders at 1.5cm. diameter and annealed at 455°C . The samples in this form could be mounted directly into the spectrometer without any modification. The re-crystallised materials were obtained by heat treating the cylinders at 520°C .

4.7.4 Sodium Studies.

The N.M.R. spectrum of sodium in sodium borate glasses is much less well documented than that of boron. Indeed, considering the alkali borate glasses, the most frequently investigated alkali metal nucleus is lithium (217, 223, 306, 307), with caesium also coming under considerable scrutiny (232, 308, 309). The sodium resonance is more usually investigated in materials such as β -alumina (310-318), crystalline minerals (319, 320), NaTiS_2 (321) and other compounds (322-326).

The reason that the Na resonance in sodium borate glasses is so infrequently investigated is that it is very difficult to observe. Indeed, in his early work, Bray states that the resonance cannot be observed (221). Furthermore, even in crystalline borates, the Na resonance cannot be seen unless the material is hydrated (320). Bray has since revised his

opinion and has displayed an observed Na resonance in glassy $\text{Na}_2\text{O}:2\text{B}_2\text{O}_3$ (217, p.116). The difficulty in observing the resonance is put down to the fact that the coupling constant would vary greatly with each sodium ion, due to its random placement in the network.

Observations were made at 12.0 MHz in a steady field of 10.7 KG. It was found that in order to avoid saturating the N.M.R. signal a rather low input R-F field had to be used. If this input was reduced still further then the signal to noise ratio decreased.

4.8 Density Measurements.

The extent by which additions change the network of a base glass can be seen from density measurements. It is a simple, but nevertheless very useful, investigatory technique.

A standard Archimedian type method was used, with chloroform being the immersion fluid. The sample was weighed first in air, M_a , and then in chloroform, M_c . The upthrust, $M_a - M_c$, is then given by:

$$M_a - M_c = dc.V$$

where V is the volume of the sample, and dc is the density of chloroform.

Hence,
$$M_a - M_c = dc \cdot \frac{M_a}{d}$$

where d is the density of the sample,

$$d = \frac{dc \cdot M_a}{M_a - M_c}$$

The sample was attached to the weighing balance by very thin wires in order to reduce any effects due to surface tension at the liquid interface. The mass of the wires was subtracted from any weighing result. Samples of considerable

mass (~ 25 gms.) were used so that accurate results were easily obtained. Such measurements were repeated on several occasions in order to estimate the possible experimental error.

As well as standard density results, also of interest is the average linear separation of the boron atoms, S . This gives an indication of how open the boron network is. S^3 is the volume of glass per boron atom, so that the reciprocal of S^3 is the number of boron atoms per unit volume.

$$S = \left(\frac{1}{\text{No. of B atoms per unit vol.}} \right)^{1/3}$$

$$S = \left(\frac{1}{d \times \text{no. of B atoms per unit mass}} \right)^{1/3}$$

The number of boron atoms per unit mass can be calculated from the composition.

CHAPTER 5

Results for Electrical Conductivity and Related Topics.

5.1 Electrical Conductivity.

When considering the results obtained for the various doped materials it is usually interesting to draw a direct comparison with the results obtained for anhydrous borax glass. Consequently, in most figures the results for the anhydrous borax glass are reproduced alongside the results for the doped material. For the sake of consistency the pure borax results are always plotted with the \square symbol, and for ease of comparison the graphs are plotted on the same scale wherever possible.

5.1.1 Glassy Materials based on Anhydrous Borax.

Early work in the project concentrated on glassy materials. In all the glassy systems investigated a very high degree of reproducibility of conductivity results was achieved. Fig. 4.7 showed the similarity of the results obtained when repeating conductivity measurements on borax glass. This close matching of curves is typical for all the glasses investigated. It is estimated that each conductivity value is correct to within approximately 8%, and that the activation energy calculated from the gradient of the curves is correct to within approximately 5%. This is based on analysis of repeated runs on several glasses, and on the direct comparison with standard glasses discussed in section 4.1.4.

Table 5.1 gives atomic percentage compositions of some of the glasses to be mentioned later in this chapter.

For reasons stated in section 3.1 the first addition to anhydrous borax glass that was investigated was CaCl_2 . Three

Table 5.1
Glass Compositions

Overall Composition	Atomic Percentages				
	Na	O	B	Added Cation	Added Halide Ion
100% borax	15.4	53.8	30.8	-	-
10% (Mg,Zn)CaCl ₂ (F,Br,I) + 90% borax	15.0	52.5	30.0	0.8	1.7
15% (Ba)CaCl ₂ + 85% borax	14.8	51.7	29.6	1.3	2.6
20% CaCl ₂ + 80% borax	14.5	50.9	29.1	1.8	3.6
10% NaCl(F,Br) + 90% borax	16.0	52.9	30.3	-	0.8
20% NaCl + 80% borax	16.7	51.9	29.6	-	1.9
30% NaCl + 70% borax	17.5	50.5	28.9	-	3.1
8.77% NaCl + 7.89% B ₂ O ₃ + 83.34% borax	15.4	53.2	30.6	-	0.8

glasses of different composition were made: 90% borax + 10% CaCl₂, 85% borax + 15% CaCl₂ and 80% borax + 20% CaCl₂. The conductivity results for the 10% CaCl₂ glass and the 20% CaCl₂ glass are shown in Fig. 5.1, together with the results for pure borax as a comparison. For the sake of clarity the measurements for the 15% CaCl₂ glass are not shown here, but they lie intermediate to the other two combination glasses and are displayed in a later figure (Fig. 5.3).

It can be seen that there is a considerable decrease in

RESISTIVITY PLOT

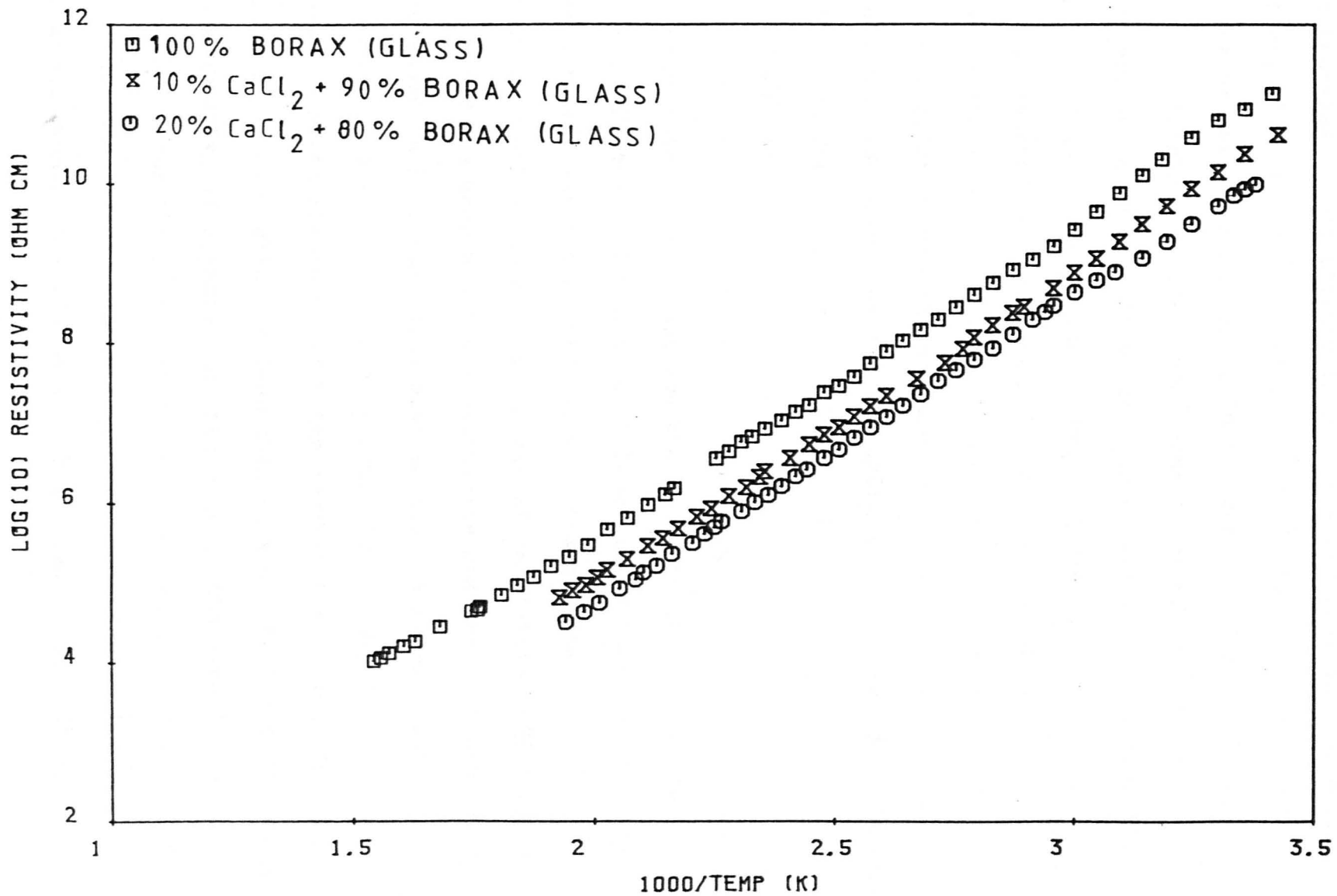


FIGURE 5.1

resistivity on adding the halide. A decrease of over an order of magnitude is observed at room temperature for the 20% CaCl_2 glass. At this stage it is difficult to comment as to whether the decrease in resistivity is due to a decrease in activation energy, (i.e. a change in slope) or if it is due to a change in the pre-exponential factor in the conductivity equation, (i.e. an increase in the number density of effective charge carriers which results in a lower intercept). See section 2.4 for a discussion on the conductivity equation. The activation energy measured for the doped glasses does not differ from that of the pure borax glass by more than the possible error range associated with the measurement. The calculation for the activation energy of the 20% CaCl_2 glass yields $73 \pm 4 \text{kJ/mole}$, while that for borax (see section 4.1.4) was similarly $73 \pm 4 \text{kJ/mole}$.

No presumptions were made as to which ion had to necessarily be present in order to achieve the conductivity enhancement effect. However, it was thought less likely that the improved conductivity was due specifically to the calcium ion. In order to check on this idea a glass of composition 10% MgCl_2 + 90% borax was made and its conductivity measured. The results are shown in Fig. 5.2; also plotted are the results for the 10% CaCl_2 glass. A decrease in resistivity compared to pure borax is again observed, with the resistivity of the 10% MgCl_2 glass being also slightly less than that of the 10% CaCl_2 glass. Consequently, it appears that the size of the alkaline-earth ion influences the degree of decrease of resistivity at least to a certain extent. These ideas are supported by the results of measurements on a 15% BaCl_2 + 85% borax glass. These

RESISTIVITY PLOT

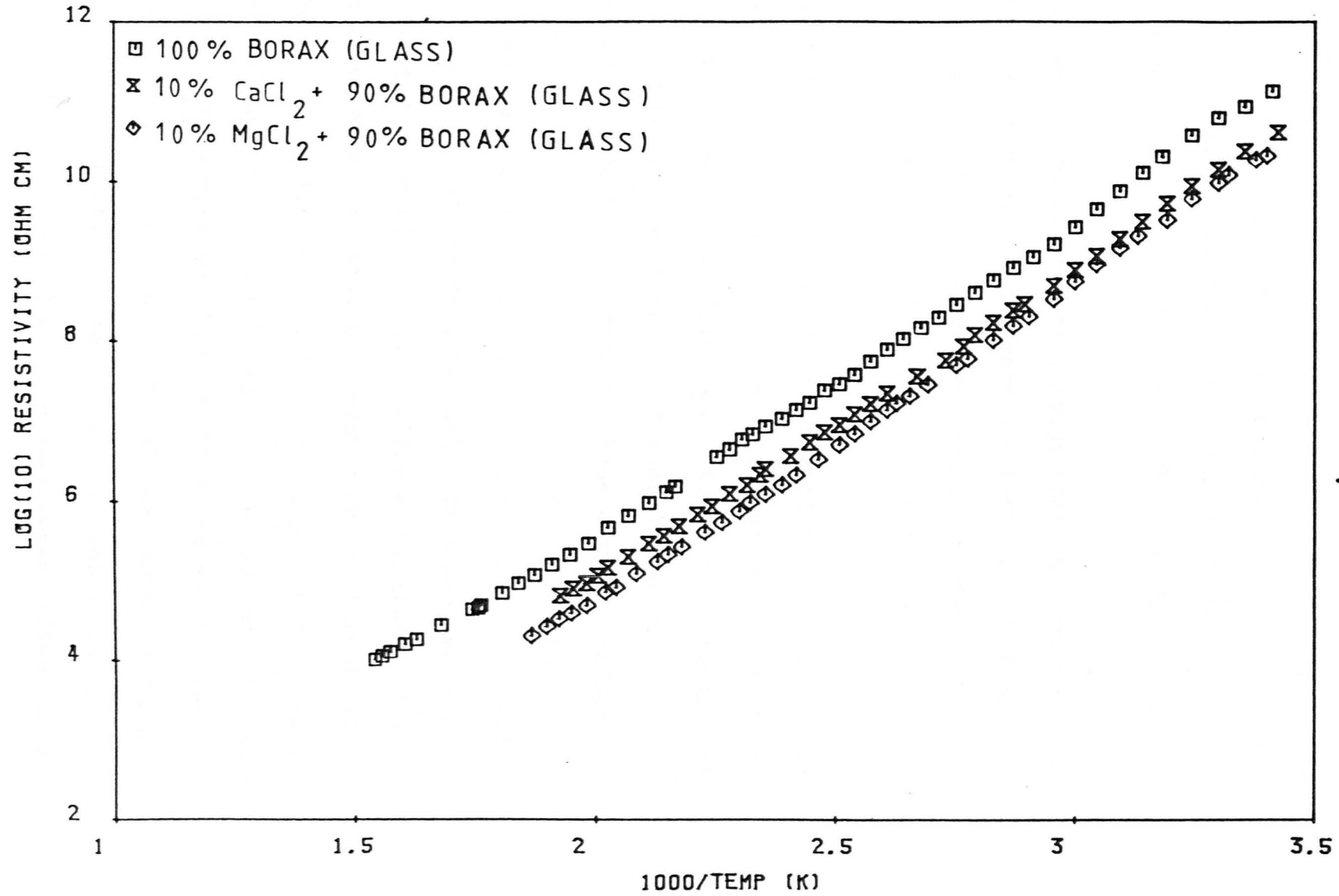


FIGURE 5.2

measurements are shown in Fig. 5.3, which also displays the results for the equivalent calcium chloride glass. It is observed that BaCl_2 enhances conductivity to only a small degree and certainly not as much as CaCl_2 . Thus, it appears that for the addition of alkaline-earth chlorides to borax the degree of resistivity decrease follows the pattern $\text{Ba} < \text{Ca} < \text{Mg}$, which, of course, is the order of decreasing ion size.

It may be thought rather strange that the addition of a chloride to borax should decrease the resistivity at all. It should be remembered that the addition of an alkaline-earth oxide to a sodium borate glass results in a conductivity reduction (151).

In order to remove any doubts regarding the validity of the above results, glasses of the following two compositions were made: 10% MgO + 90% borax and 10% CaO + 90% borax. As expected these samples showed an increased resistivity in comparison to pure borax. Because these samples conform to the expected behaviour there is no reason to distrust the results for the halide doped samples, i.e. it is confidently believed that the decreased resistivity is a real effect.

Having considered various alkaline-earth ions in the dopant material the natural progression was to investigate the dependency of the decreased resistivity effect on the type of halide ion. With this aim in mind two further glasses were made. These were 10% CaBr_2 + 90% borax and 10% CaF_2 + 90% borax. The former of these two glasses showed similar conductivity properties to that of the 10% CaCl_2 glass; the results are shown in Fig. 5.4. The enhancement effect seems

RESISTIVITY PLOT

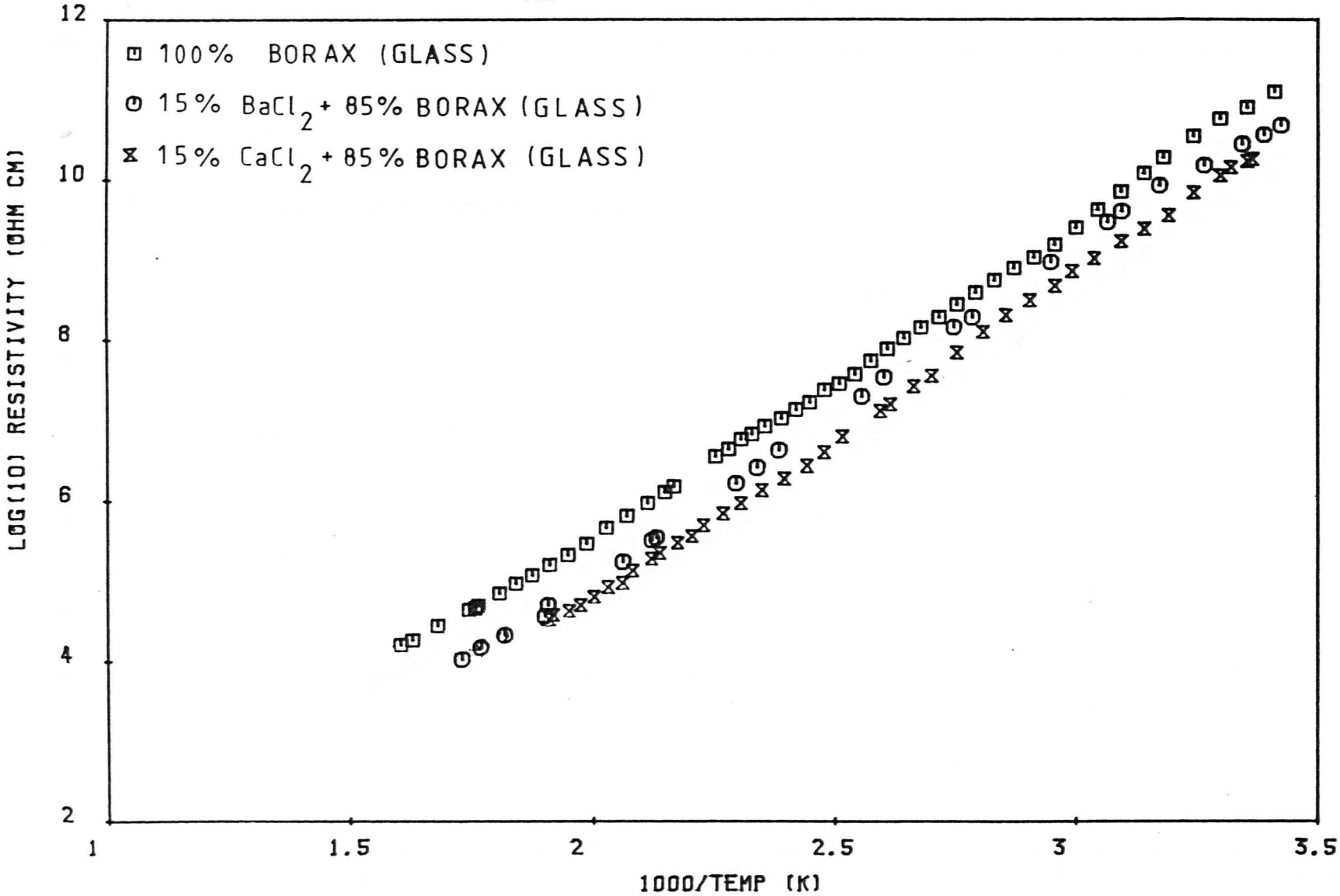


FIGURE 5.3

RESISTIVITY PLOT

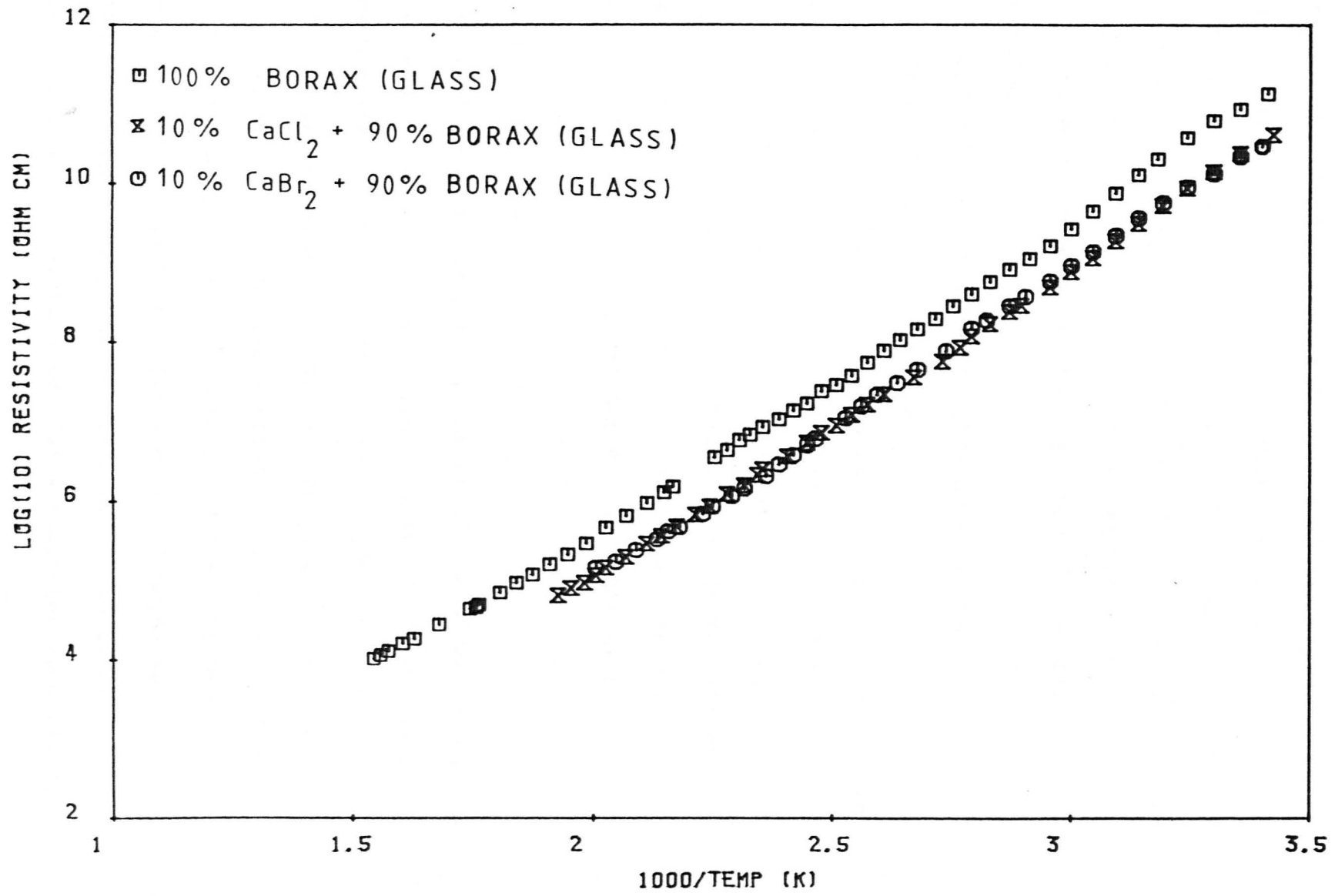


FIGURE 5.4

virtually independent of whether the anion is bromine or chlorine. However, the situation is very different for the 10% CaF_2 glass, the results for which are shown in Fig. 5.5. Far from there being a decreased resistivity in comparison to pure borax, over most of the temperature range the resistivity is considerably increased. There is also quite a noticeable increase in activation energy, the measured value is 78 ± 6 kJ/mole. The results were confirmed when the experiments were repeated on other glasses of the same composition.

In order to complete investigations on using calcium halides as dopants, a glass of composition 10% CaI_2 + 90% borax was made and its conductivity measured. The results are shown in Fig. 5.6, apparently the material had a resistivity virtually identical to that of pure borax. The reason for this soon became obvious when chemical analysis results on the glass were obtained. Almost all of the iodine had volatilised during melting, see table 3.1. This high volatility precludes iodides from being used as dopants unless the melting procedure is amended greatly.

As mentioned earlier, the presence of the alkaline-earth ions should, if anything, be detrimental to the conductivity of the material. Consequently, it was decided to attempt to improve conductivity by using NaCl despite the reported lower solubility in borax (see section 3.1). It was found that up to 30% NaCl could be incorporated into the borax base while still being able to achieve a clear, homogenous glass. At this upper limit a high quench rate had to be employed, and the annealing temperature carefully monitored in order to

RESISTIVITY PLOT

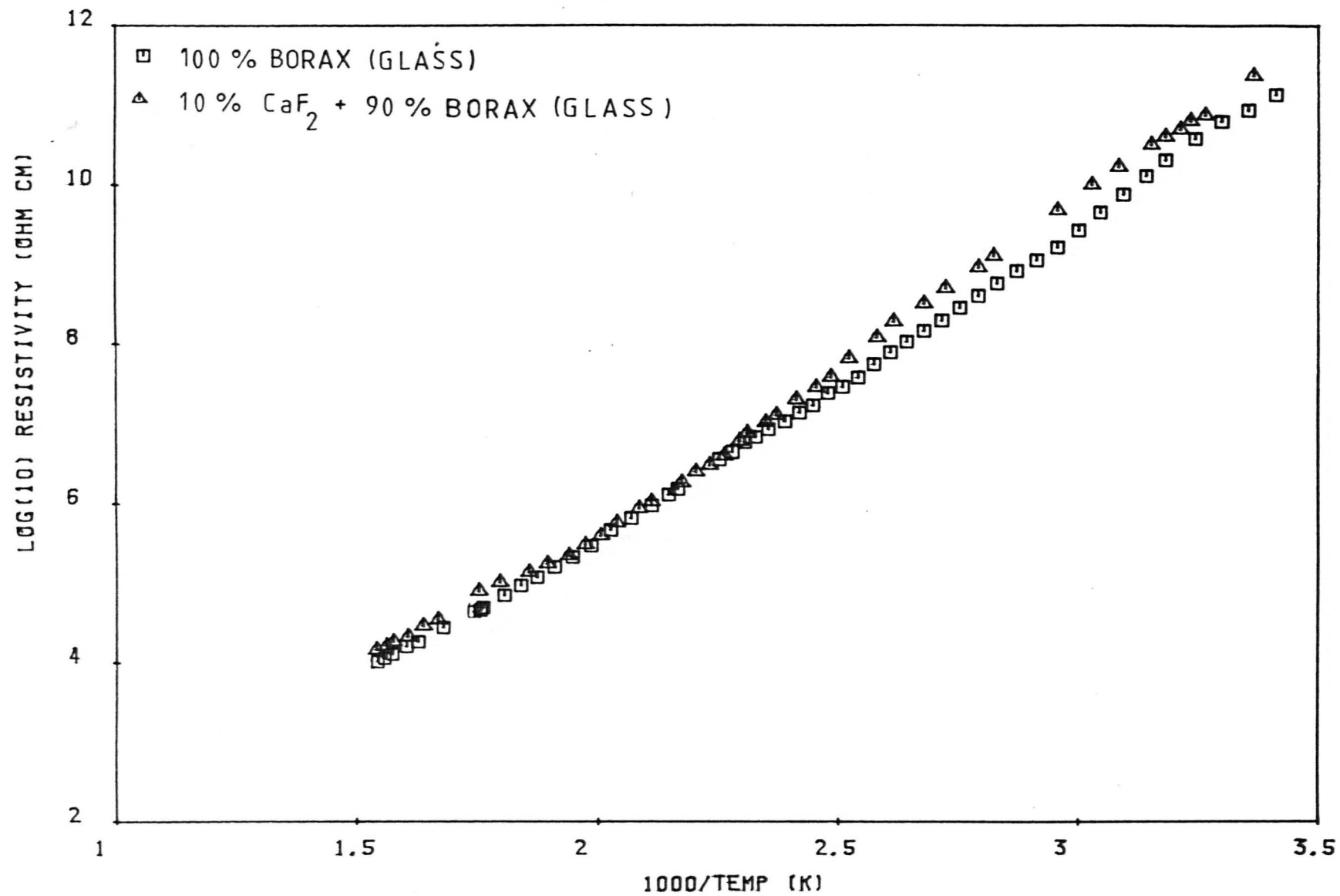
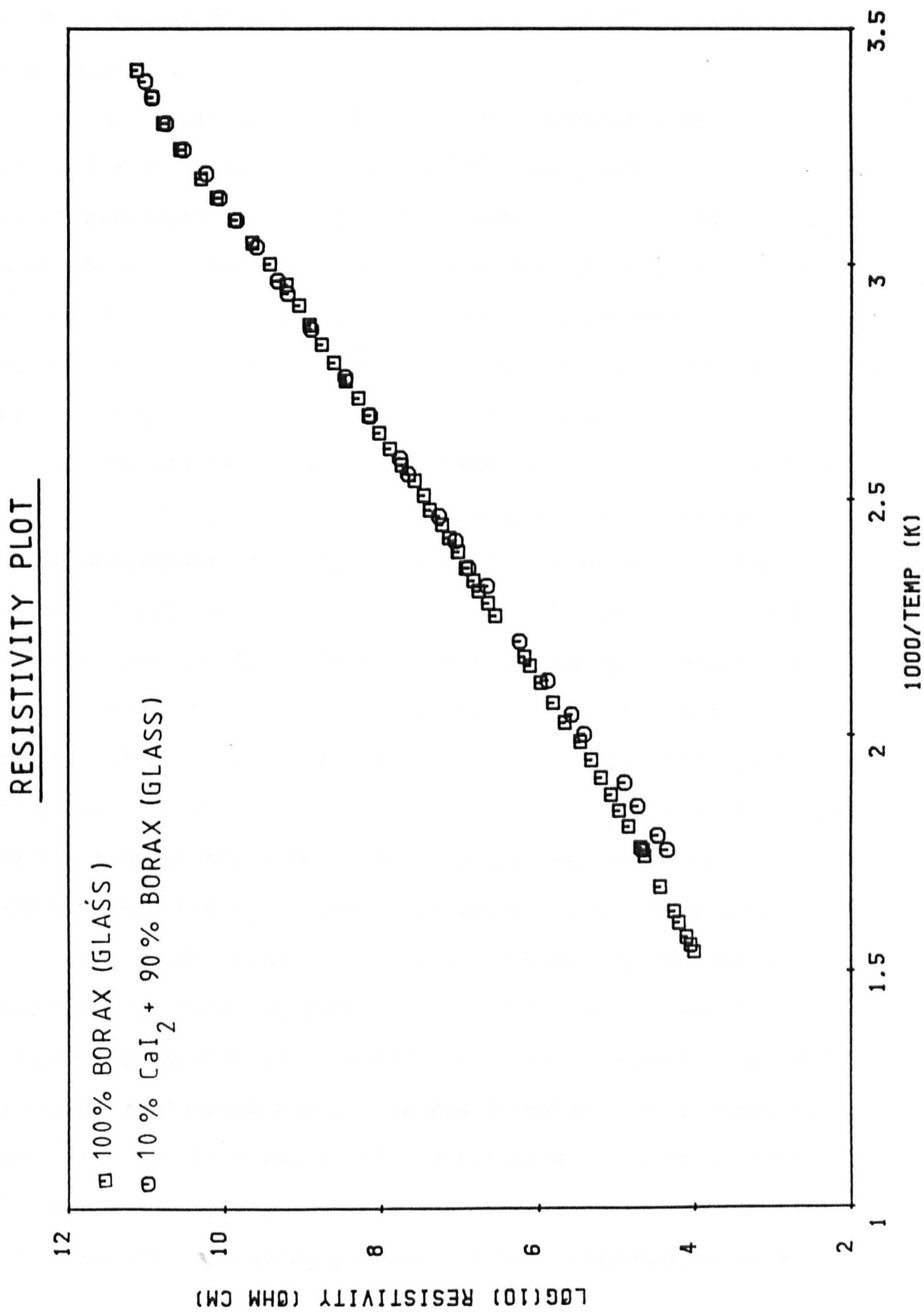


FIGURE 5.5

FIGURE 5.6



prevent the material from crystallising. It should be noted that the addition of 30% NaCl puts considerably fewer chloride ions into the glass than does 20% CaCl_2 , see Table 5.1. It is for this reason that it is considered that NaCl is 'relatively less soluble'.

Glasses were made of the following compositions:

10% NaCl + 90% borax, 20% NaCl + 80% borax, 30% NaCl + 70% borax. The conductivity results for these materials are shown in Fig. 5.7. It can be seen that there is a steady reduction in resistivity as the percentage of halide in the glass is increased. There also appears to be a steady reduction in activation energy, it is down to 63 ± 3 kJ/mole for the 30% NaCl glass.

It was realised that these three compositions, as well as introducing chloride ions into the glass, also increase the atomic percentage of sodium ions in the material. Without further investigations it could not be definitely concluded that the decrease in resistivity was due to the presence of the chloride ions. Instead it could be said that the improvement resulted from the increase in sodium ion concentration. The glass of composition 8.77% NaCl + 7.89% B_2O_3 + 83.34% borax has the same atomic percentage of sodium as borax, and approximately the same atomic percentage of chloride ions as a 10% NaCl + 90% borax glass. The conductivity results for this ternary glass are shown in Fig. 5.8. A considerably reduced resistivity is observed, compared to pure borax. This decreased resistance can not be due to extra sodium ions, it must therefore be a result of the presence of chloride ions.

Conductivity measurements were also made on two further sodium halide containing glasses. These compositions were

RESISTIVITY PLOT

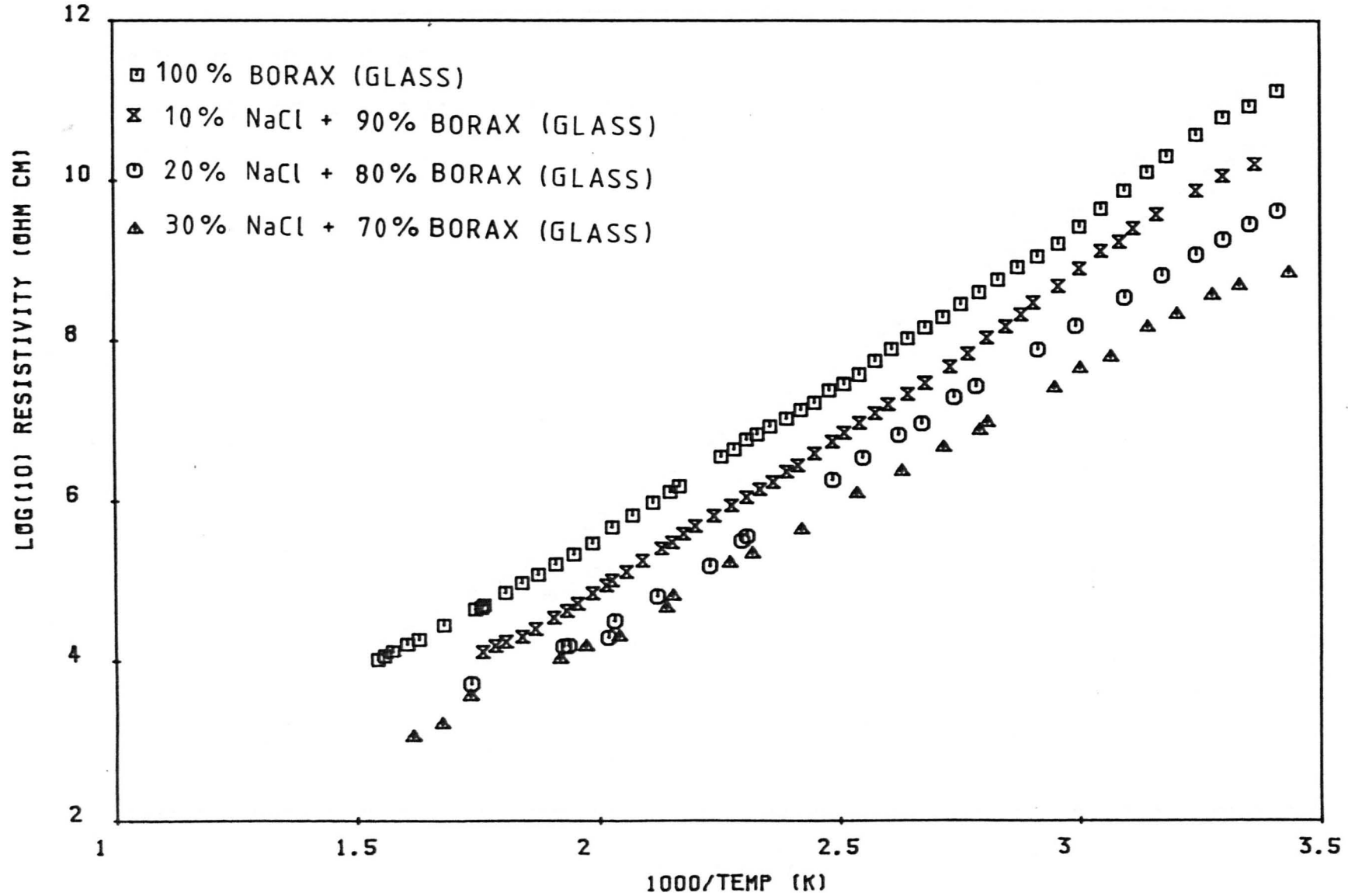


FIGURE 5.7

RESISTIVITY PLOT

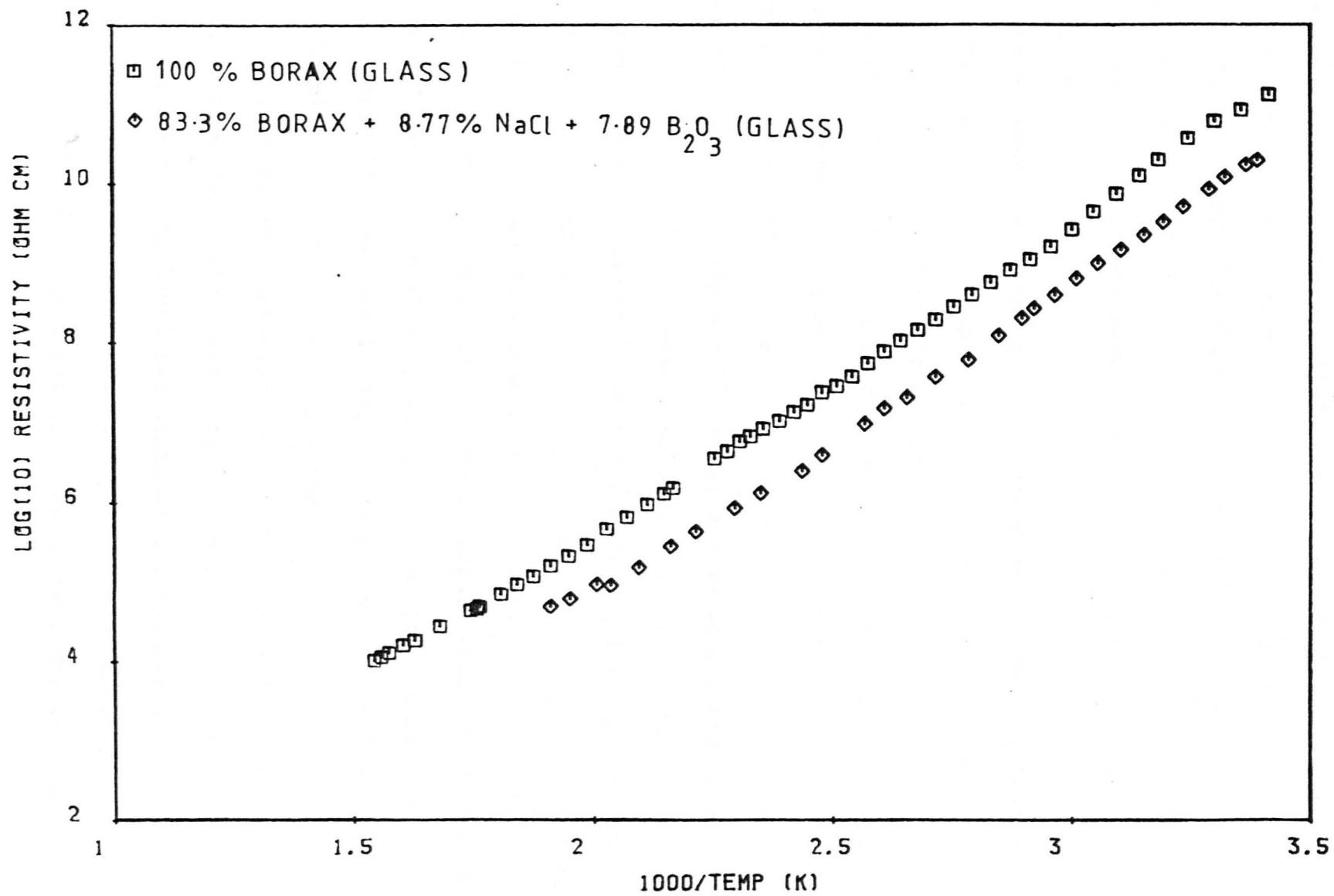


FIGURE 5.8

10% NaBr + 90% borax and 10% NaF + 90% borax. The results are plotted in Fig. 5.9. Over most of the temperature range there seems to be a general decrease in resistivity as the size of the added halide ion increases. It is also observed that a reduction in activation energy accompanies the decrease in resistivity. The activation energy for the glass doped with fluoride is 80 ± 2 kJ/mol., while that for the glass doped with bromide is 68 ± 5 kJ/mol. All these results will be discussed further in Chapter 7.

These measurements are all of considerable interest, however the reduction in resistivity is not sufficient that the doped glasses could be considered 'good ionic conductors'. The original liaison with B.R.L. had led to the belief that far greater effects would be observed. Although B.R.L. had found that the greatest reductions in resistivity were obtained with transition metal halide dopants (see section 3.1), considerable enhancement had been obtained with alkaline-earth halides. A large effect had also been observed using ZnCl_2 as the additive. For this reason the next glass melted was of the composition 10% ZnCl_2 + 90% borax. The results of conductivity measurements on this glass are shown in Fig. 5.10. As with most of the doped glasses measured previously, a small decrease in resistivity of up to an order of magnitude is found in comparison to pure borax. However, this reduction was certainly not of the extent expected.

Further detailed discussions with B.R.L. regarding melting procedure, chemicals used, measuring apparatus, etc., resulted in the discovery of at least two distinct differences in experimental technique between work reported here and work carried out at B.R.L. The first of these differences was that

RESISTIVITY PLOT

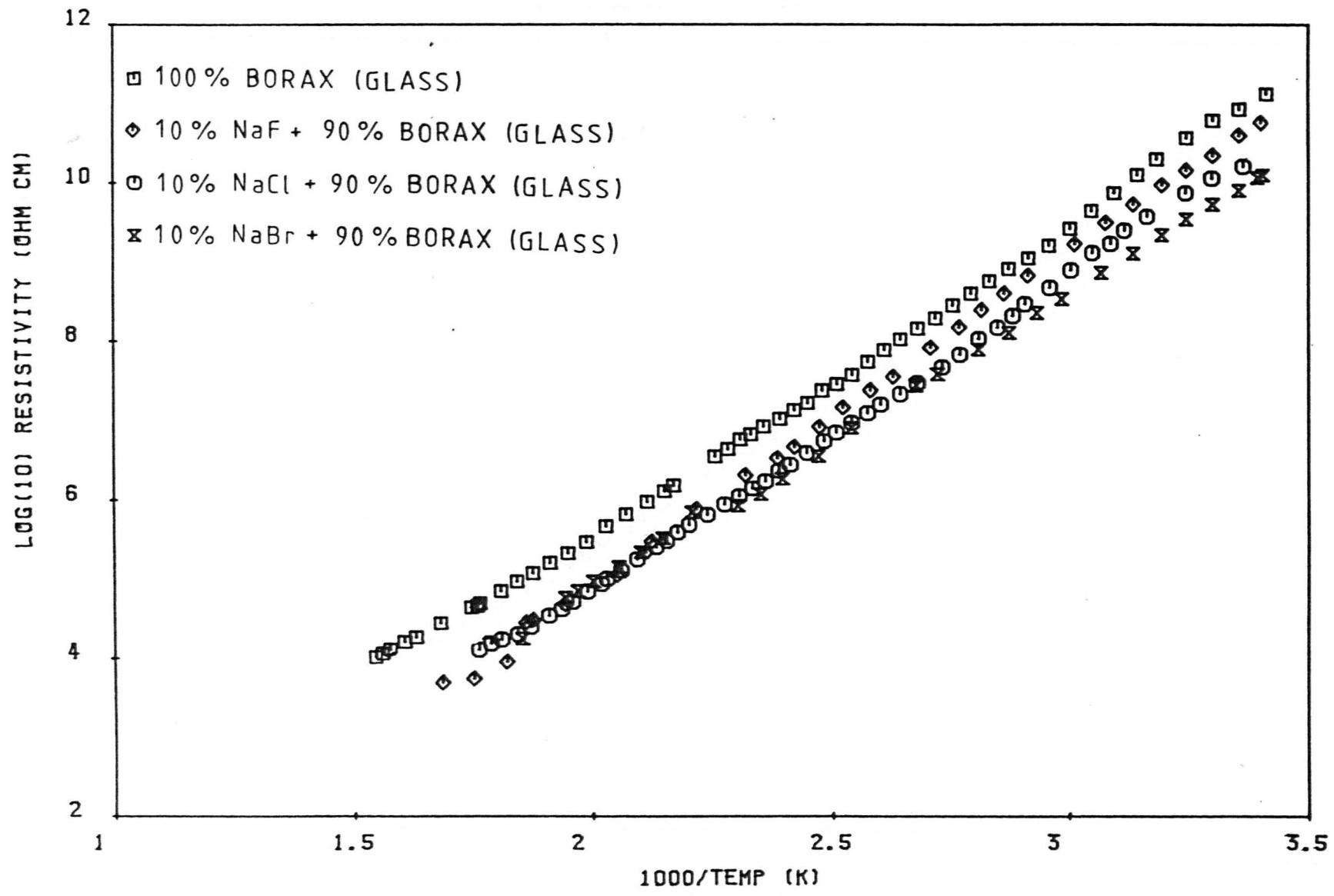


FIGURE 5.9

RESISTIVITY PLOT

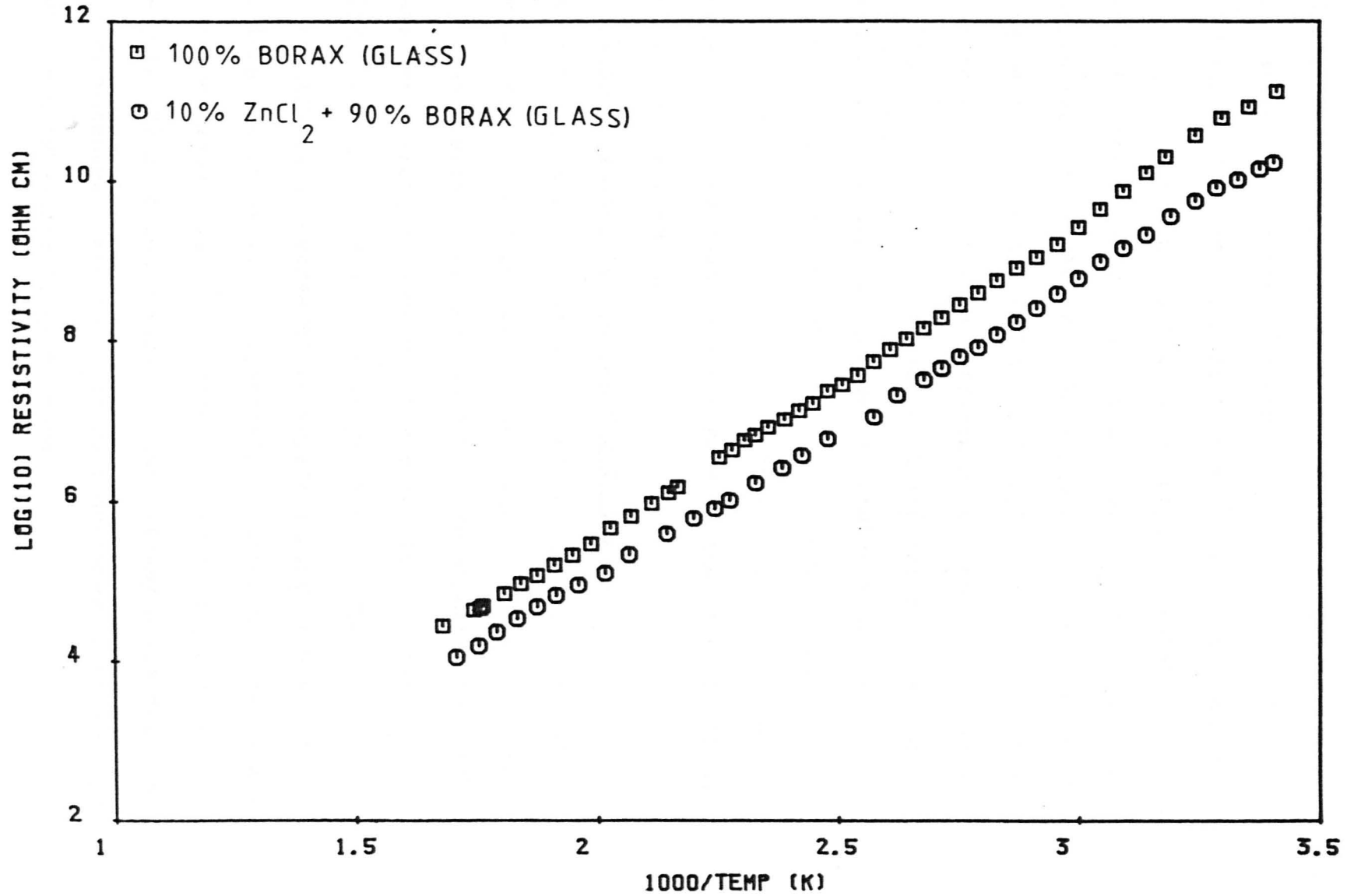


FIGURE 5.10

B.R.L. had used a nitrogen atmosphere in the melting furnace, in contrast to a normal air environment. Secondly, no fast quench step was involved in the B.R.L. glass formation procedure; consequently it was possible that their glasses had crystallised to a certain extent.

The first of these possibilities was checked by making a 10% MgCl_2 + 90% borax glass in a nitrogen atmosphere and measuring its resistivity. The results are shown in Fig. 5.11; also shown are the results for the glass of the same composition that was melted in an air atmosphere. Allowing for experimental error there is apparently no difference between the two sets of results. This similarity was confirmed for other glass compositions. It could be confidently stated that the discrepancy in results reported here and those observed by B.R.L. was not due to the atmosphere in the melting furnace.

Consequently, attention was turned to the possibility of crystallising the glasses.

5.1.2 Glass-Ceramics based on Anhydrous Borax.

At this point it is worth re-stating the fact that the vast majority of glass-ceramics have a higher resistivity than their parent glasses (see section 2.8). In glasses the mobile ions are less strongly bound and the potential barriers impeding their motion are, on average, lower. The only case where resistivity is decreased on crystallising is when the mobile ions are strongly preferentially ejected into the glassy phase at the glass/crystal interface. This concentration build-up in the more conducting residual glassy phase can, in a few circumstances, lead to an overall decrease in resistivity. However, this behaviour is quite rare.

RESISTIVITY PLOT

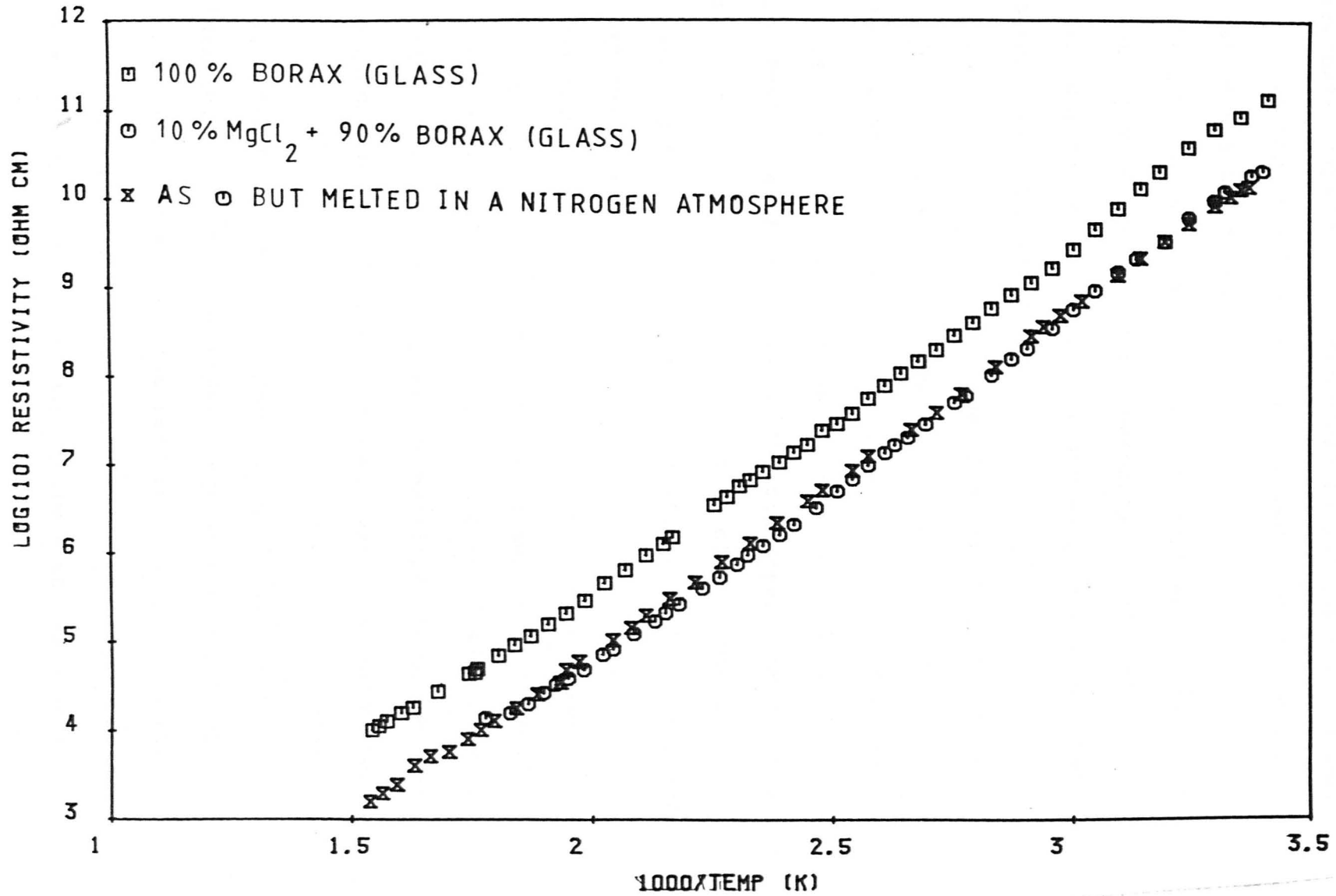


FIGURE 5-11

For reasons stated in section 3.4 the recrystallisation process was a single stage heat treatment. The crystallisation dwell temperature was chosen as a result of D.S.C. or D.T.A. measurements, this was also discussed in section 3.4. Unless otherwise stated, the time the samples remained at the dwell temperature was two hours.

The samples subjected to heat treatment were first cut into the 2.5cm. discs that were necessary for the conductivity measuring apparatus. Thus, no further shaping was required after the conversion process.

Because of the large decrease in resistivity predicted by B.R.L., the first glass to be re-crystallised was the 10% ZnCl_2 + 90% borax sample. Specimens were heat treated at one of three temperatures: 700°C, 600°C or 550°C. The samples heat treated at either of the two upper temperatures appeared crystalline throughout the bulk of the material. A certain degree of deformation had occurred with the specimen heat treated at 700°C.

Resistivity measurements on the samples proved very interesting. It was found that the specimens heat treated at either 600°C or 700°C exhibited a resistivity which, at room temperature, was over four orders of magnitude lower than the parent glass, and up to five orders of magnitude lower than that of pure borax glass. There was only a slight difference, if any, between the samples crystallised at 600°C and those crystallised at 700°C. The experiments were repeated on several occasions and the above results verified. Admittedly, there was considerable scatter associated with the measurements, rather more than with the glasses, however the decreased

resistivity effect was undeniable and quite startling.

This increased experimental scatter was found on all subsequent measurements on re-crystallised materials. Consequently, at least five sets of data were taken for each heat treatment temperature on each composition. To plot all the collected data points graphically would lead to considerable congestion on the figure, especially where comparisons are being made between different heat treatments. Consequently, in most cases for the re-crystallised specimens, only the best fitted line will be drawn on the resistivity plot. At the very worst the discrepancy between the drawn line and any individual result may be up to a factor of four. Although this is considerable for a single result, the logarithmic scale of the resistivity plot makes the situation tolerable. The question of this scatter will be returned to later.

The best fitted results for the zinc chloride doped materials heat treated at 700°C and 600°C are shown in Fig. 5.12.

The specimens of the above composition re-crystallised at 550°C were observed to behave rather differently. The guard ring arrangement, for the connections to the specimen in the resistivity apparatus, allows the removal of surface conductivity contributions from the required bulk resistivity value (see section 4.1). However, whether or not the guard ring is connected usually alters the result by only up to a few percent, i.e. the surface conductivity is much smaller than the bulk value. In the case in question the complete opposite was true. The surface conductivity was much larger than that through the bulk. With knowledge of the results obtained for the specimens re-crystallised at higher temperatures, the obvious conclusion

RESISTIVITY PLOT

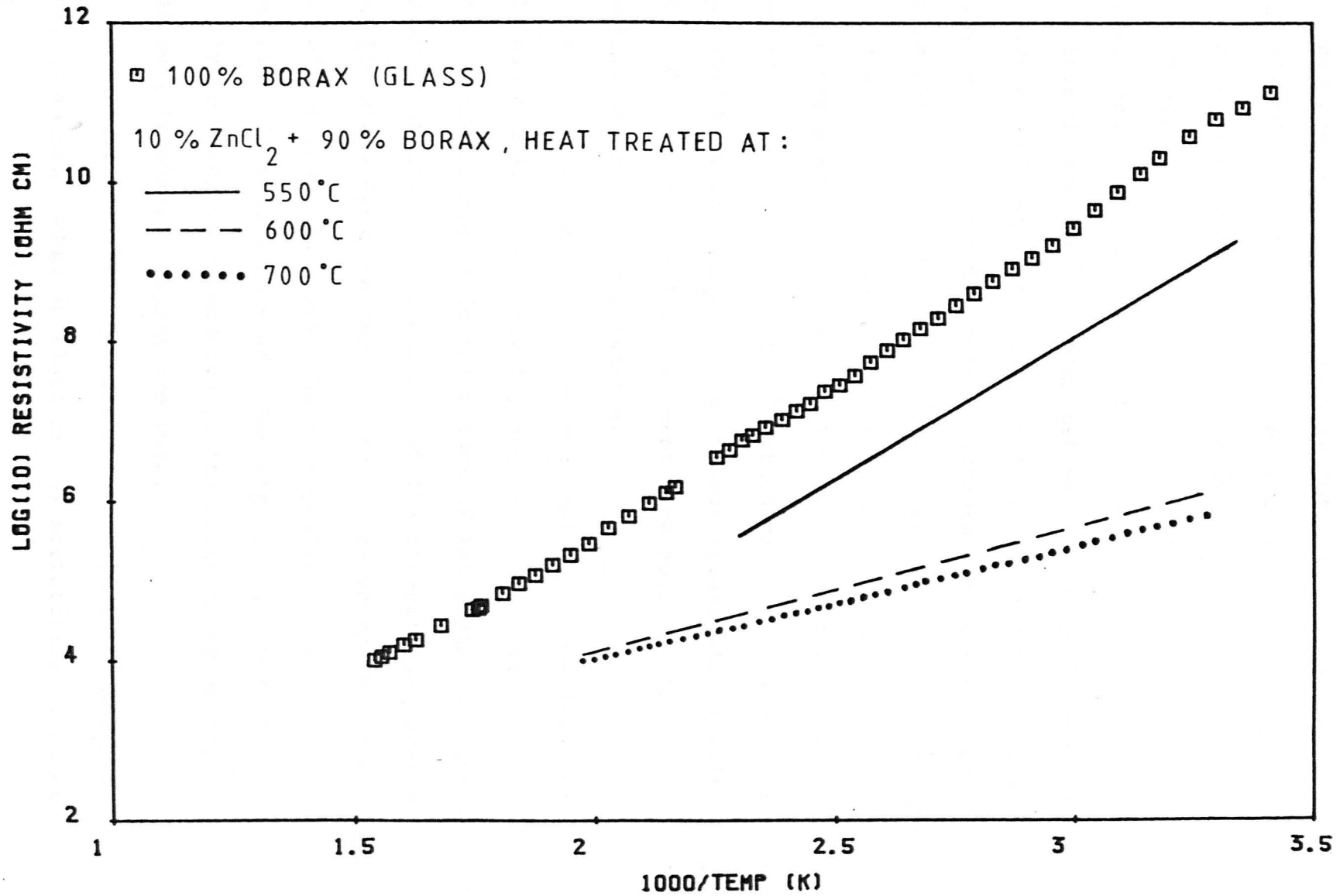


FIGURE 5-12

to draw was that this specimen had surface crystallised. Indeed, this was quite obvious from the appearance of the disc. The layer-like structure is shown clearly on an electron micrograph (see Fig. 6.14). Bulk resistivity measurements are difficult to perform on such samples because any slight error in removing the surface conductivity contribution will distort measured results considerably. Nevertheless, the observed results are also shown in Fig. 5.12. No other composition showed such a strong tendency to surface crystallise.

Having verified that a large resistivity reduction could be achieved via a heat treatment procedure, the emphasis of the work shifted back to the original lines of the investigation, i.e. the use of alkaline-earth halides as dopants. Glassy disc specimens of the composition 10% CaCl_2 + 90% borax were subjected to the same re-crystallisation process as the above ZnCl_2 doped materials; i.e. two hour heat treatments at either 700°C, 600°C or 550°C. All specimens were well crystalline throughout the bulk of the material.

Conductivity measurements showed that all three types of sample had a similar resistivity, and that its value was several orders of magnitude below that of the glassy specimen. In order to indicate the magnitude of the experimental scatter, dotted lines are drawn on the results figure which show the extent of the individual measured data points. The 'best fitted line' is also displayed. See Fig. 5.13. There is virtually no apparent dependence of the resistivity on the actual heat treatment temperature used.

One further interesting observation is that the results indicate a marked change in slope in the resistivity curve at

RESISTIVITY PLOT

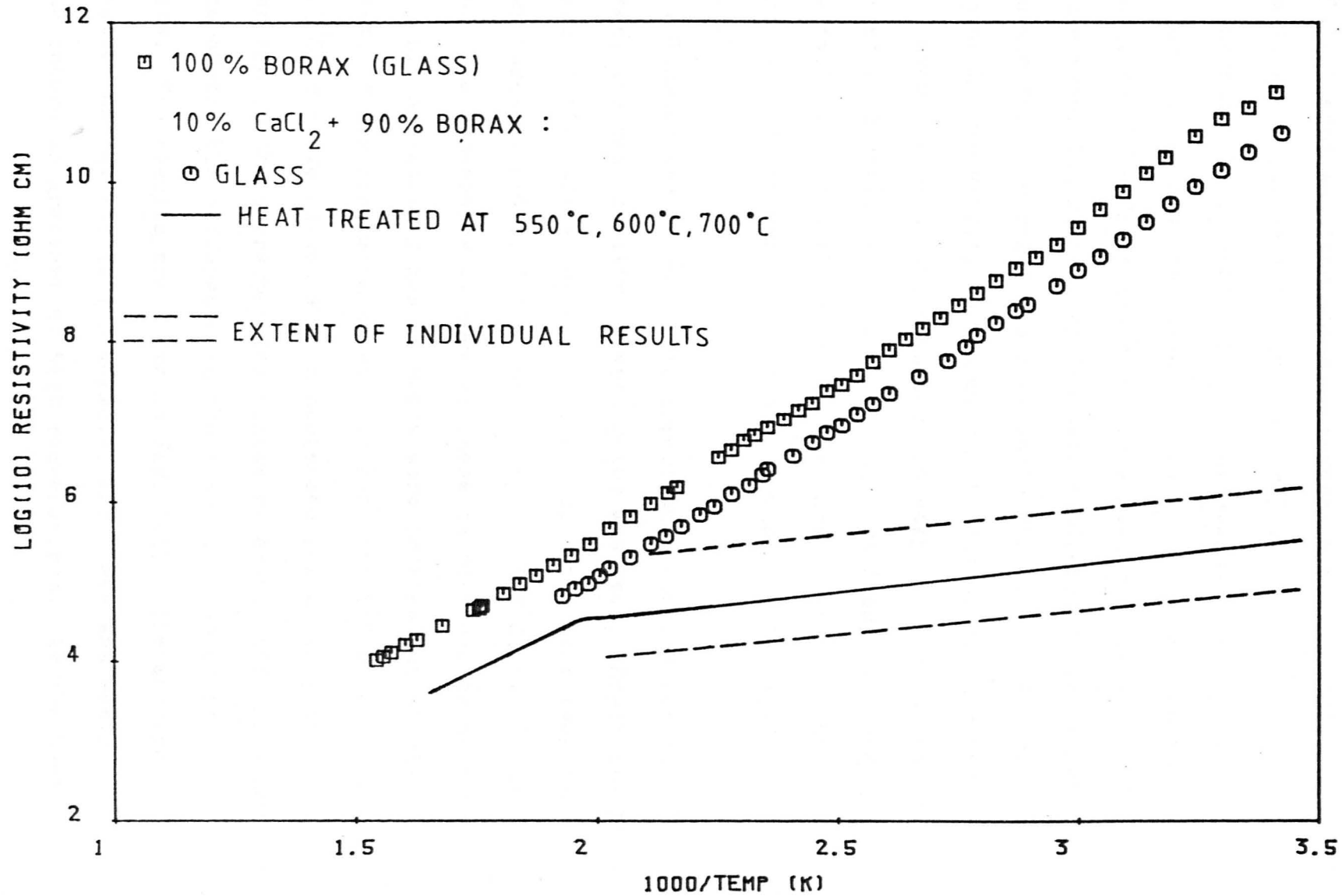


FIGURE 5-13

high temperatures. Indeed, in the high temperature region the trend in resistivity seems to follow that of the parent glass very closely, both in activation energy and absolute value. This phenomenon was observed with several other compositions and will be discussed fully in Chapter 7.

Another alkaline-earth halide investigated for its use as a resistivity reducing agent was BaCl_2 . Glassy samples of composition 15% BaCl_2 + 85% borax were re-crystallised at 550°C , and the resulting glass-ceramics were subjected to resistivity measurements. The results are shown in Fig. 5.14. A large decrease in resistivity in comparison to the original glass is achieved. Indeed, the behaviour is very similar to that observed when doping with CaCl_2 , though the final observed resistivity is not quite as low. The sharp change in the slope of the resistivity curve at elevated temperature is again present.

Following the lines of the experiments carried out on glasses, the next additive investigated was NaCl . Re-crystallised samples of 10% NaCl + 90% borax were made using heat treatment temperatures of 650°C , 600°C , 550°C , 538°C , 525°C , 512°C and 500°C . The appearance of some of these samples can be seen in Fig. 3.6. Resistivity measurements were carried out on all samples. Those specimens which were heat treated at a temperature of 525°C or above showed a much decreased resistivity in comparison to the corresponding glassy material, and there was little observable difference in the resistivities of these samples. The results are shown in Fig. 5.15. The measured activation energy was 26 ± 5 kJ/mole, and there was again a marked change in gradient at high temperatures. As the heat

RESISTIVITY PLOT

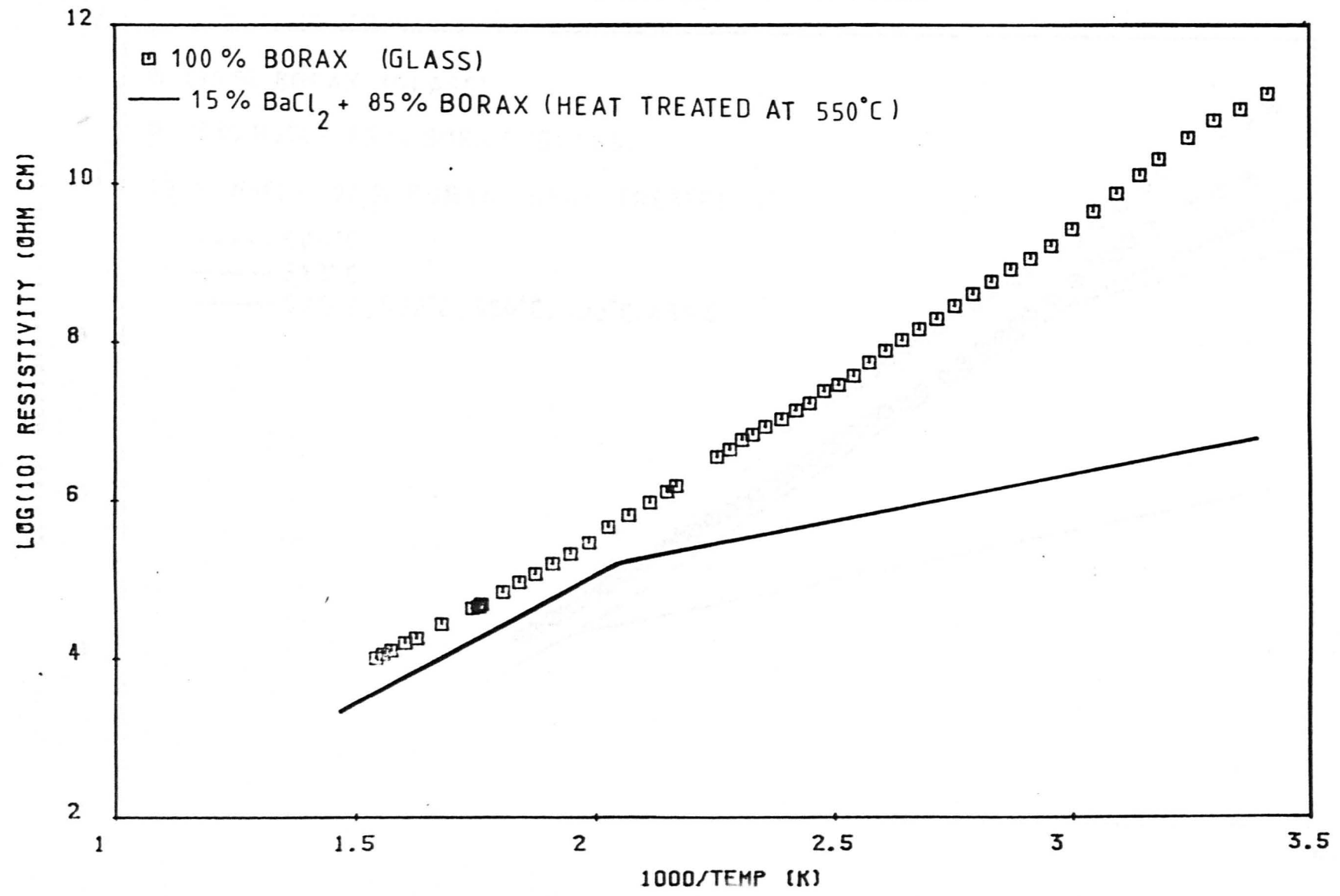


FIGURE 5.14

RESISTIVITY PLOT

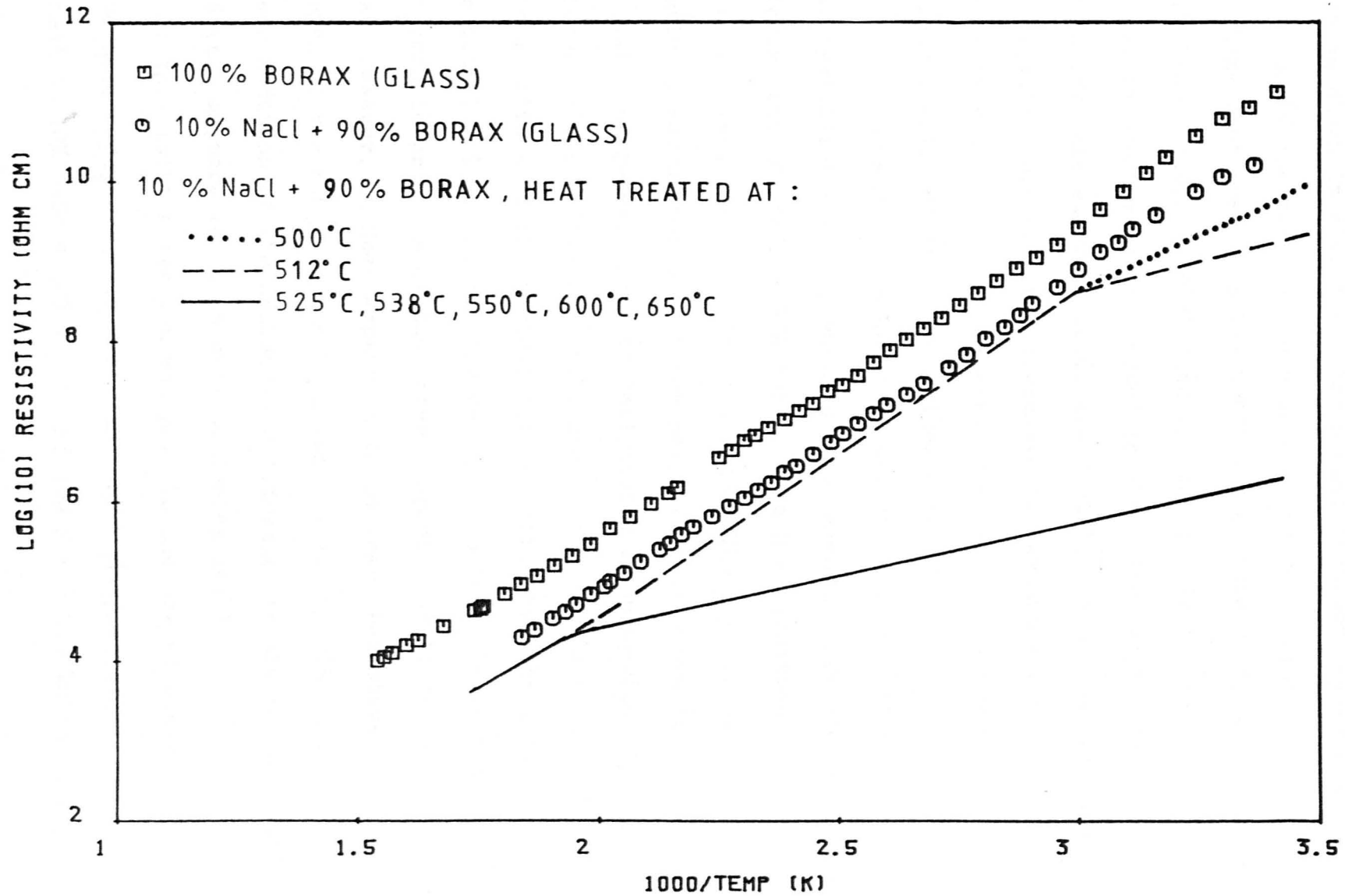


FIGURE 5.15

treatment temperature was reduced below 525°C the measured resistivities quickly rose back towards that of the parent glass. This overall effect is mirrored by the form of the samples as shown in Fig. 3.6. For a heat treatment temperature of above 525°C the specimens are opaque and well crystalline, while those heat treated below 525°C are decidedly glassy.

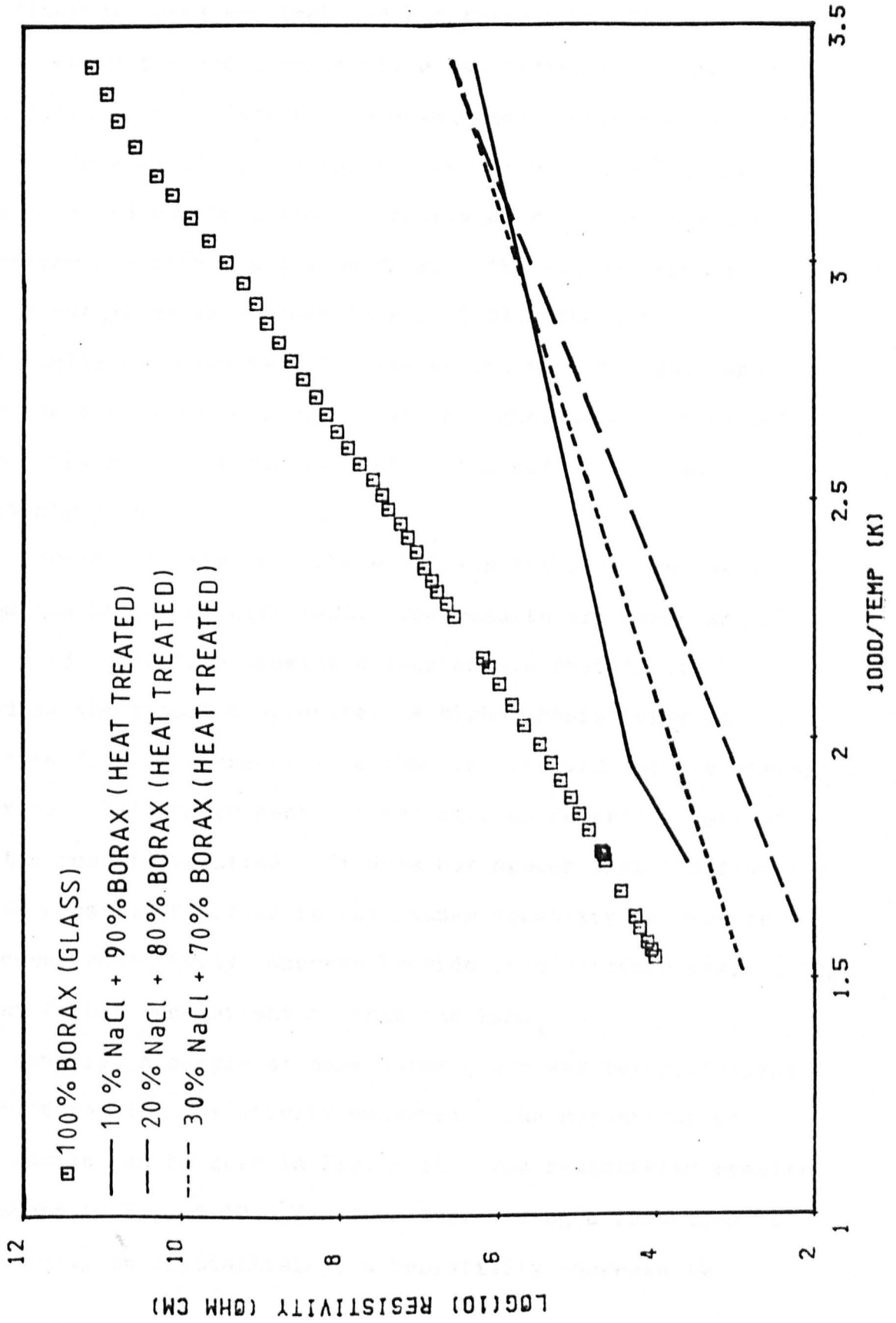
A clear pattern is beginning to emerge. As the heat treatment temperature is increased to above the temperature at which crystals start to form, the resistivity of the material drops rapidly. However, a temperature is reached where the resistivity reduction is a maximum. Heat treatment above this temperature will result in no further decrease.

The use of NaCl as an additive was further investigated by re-crystallising glassy samples of composition 20% NaCl + 80% borax, and 30% NaCl + 70% borax. The heat treatment temperature used was 525°C in each case. The results of resistivity measurements on these materials are shown in Fig. 5.16. Large decreases in resistivity in comparison to the parent glasses (see Fig. 5.7) are obtained. In relation to the magnitude of the resistivity reduction brought about by crystallisation, the difference in resistivity between the glass-ceramic products of the three compositions is quite small. However, it does appear that the least resistive material in the range is the specimen containing 20% NaCl. Further addition of the halide is detrimental to the conductivity. There thus appears to be an optimum doping level.

At this point attention was paid to the use of other sodium halide dopants, i.e. NaBr and NaF. Samples of composition 10% NaBr + 90% borax and 10% NaF + 90% borax were

FIGURE 5-16

RESISTIVITY PLOT



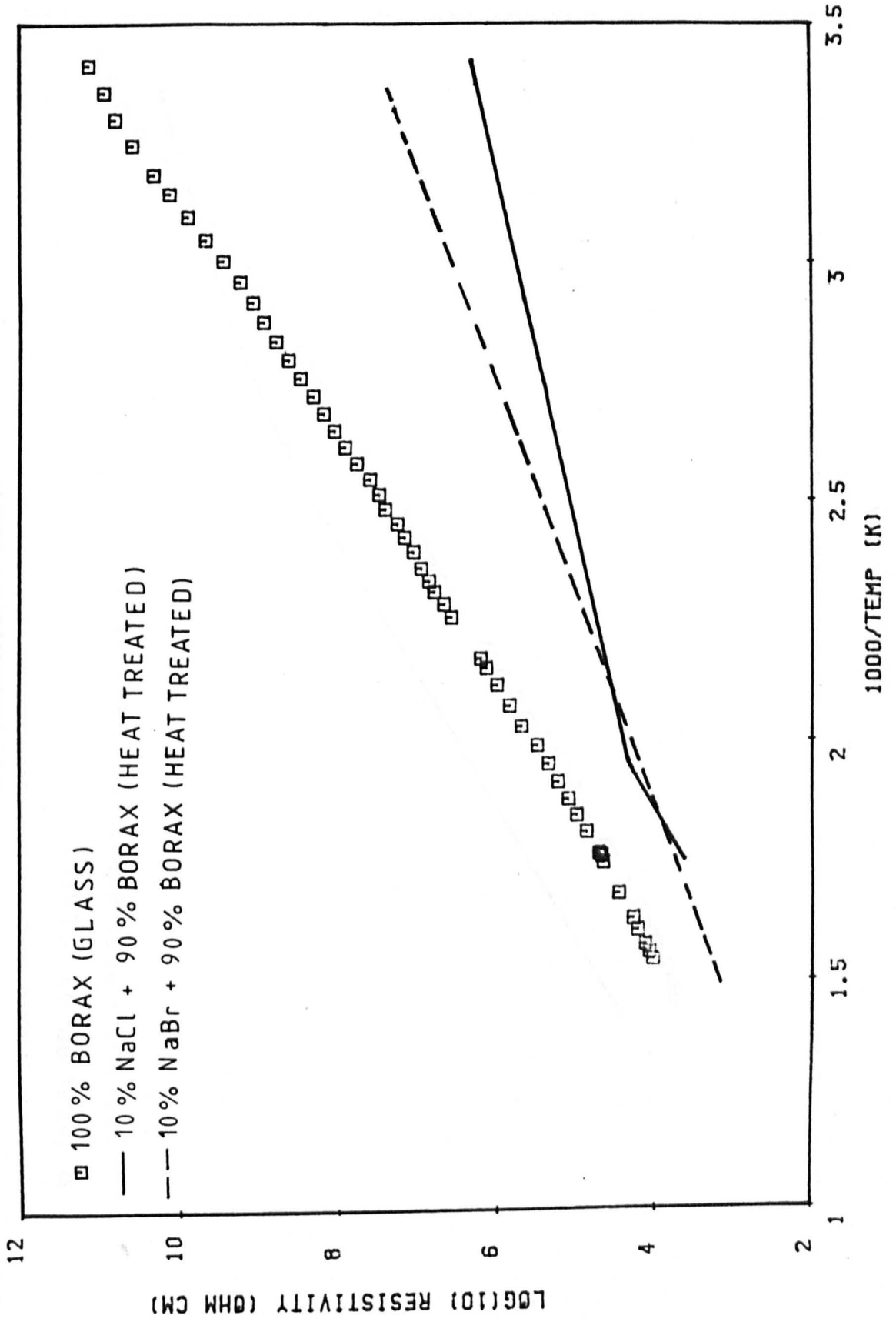
re-crystallised from the parent glasses. A heat treatment temperature of 525°C was used in the case of the bromide doped glass, however it was found that at this temperature the fluoride doped specimen did not fully crystallise, consequently the dwell temperature was increased to 550°C for this latter case. Resistivity measurements were then carried out on these samples. As can be seen from Fig. 5.17, the bromide doped sample showed a greatly decreased resistivity in comparison with its glassy form. (The measurements for the parent glass were shown in Fig. 5.9). The ultimate resistivity achieved is not quite as low as with NaCl, and also the activation energy is rather higher at 42 ± 6 kJ/mole. Nevertheless, the decreased resistivity effect is most certainly present.

However, in the case where NaF was the added halide the situation is rather different. The results are shown in Fig. 5.18. Far from showing a decrease in resistivity the trend is the complete opposite. A higher resistivity is observed for the glass-ceramic than is observed for the glassy material. This experiment was repeated on several occasions and the results verified. It does not appear that the fluoride ion is capable of acting in the manner necessary to promote decreased resistivity, whereas bromide ions decrease resistivity almost to the same extent as chloride ions.

Finally, a sample of pure borax glass was re-crystallised at 550°C and its resistivity measured. The appearance of this sample can be seen in Fig. 3.11. The resistivity results are shown in Fig. 5.19. Far from there being a reduction in resistivity on crystallising, a resistivity increase is

FIGURE 5-17

RESISTIVITY PLOT



RESISTIVITY PLOT

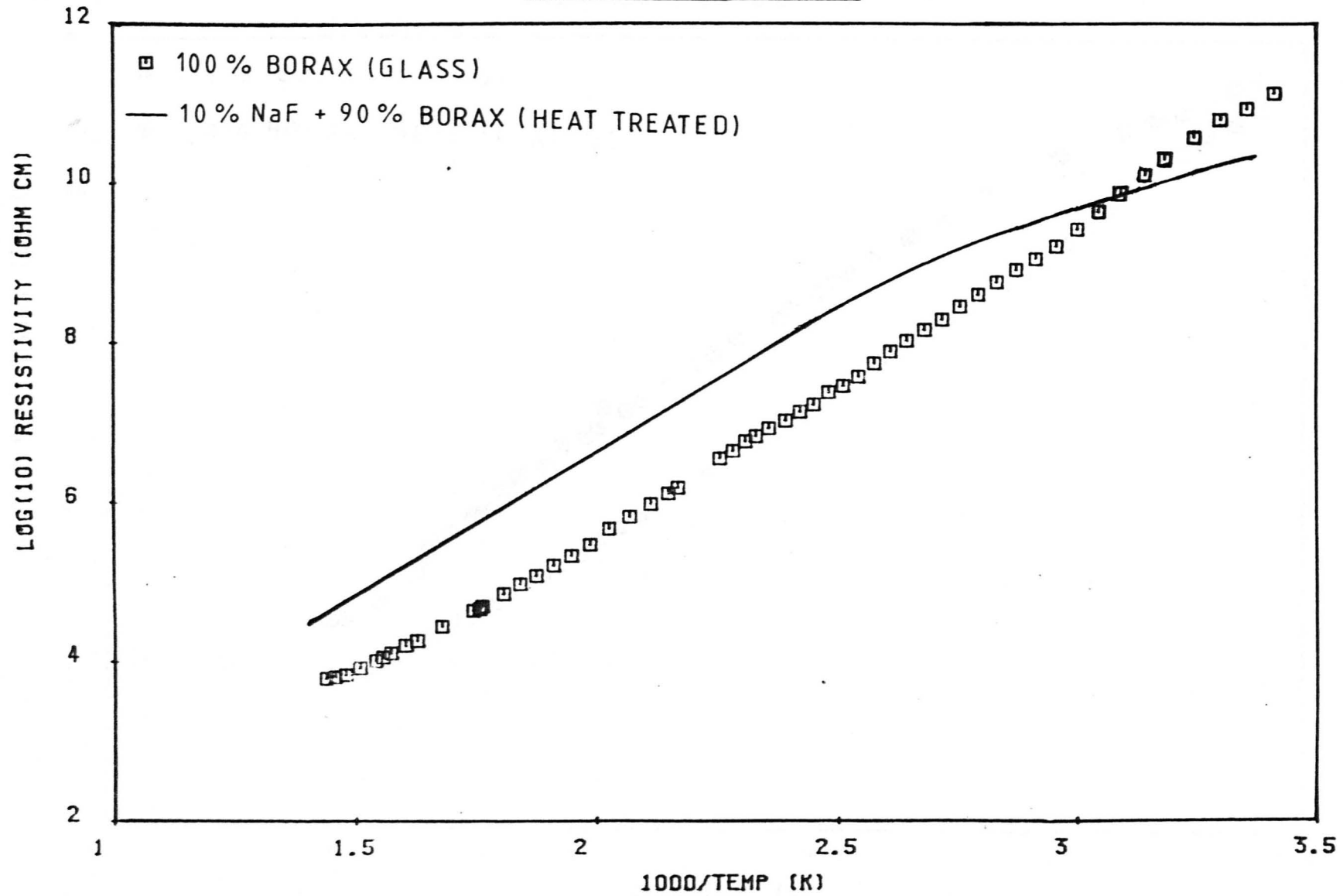


FIGURE 5.18

RESISTIVITY PLOT

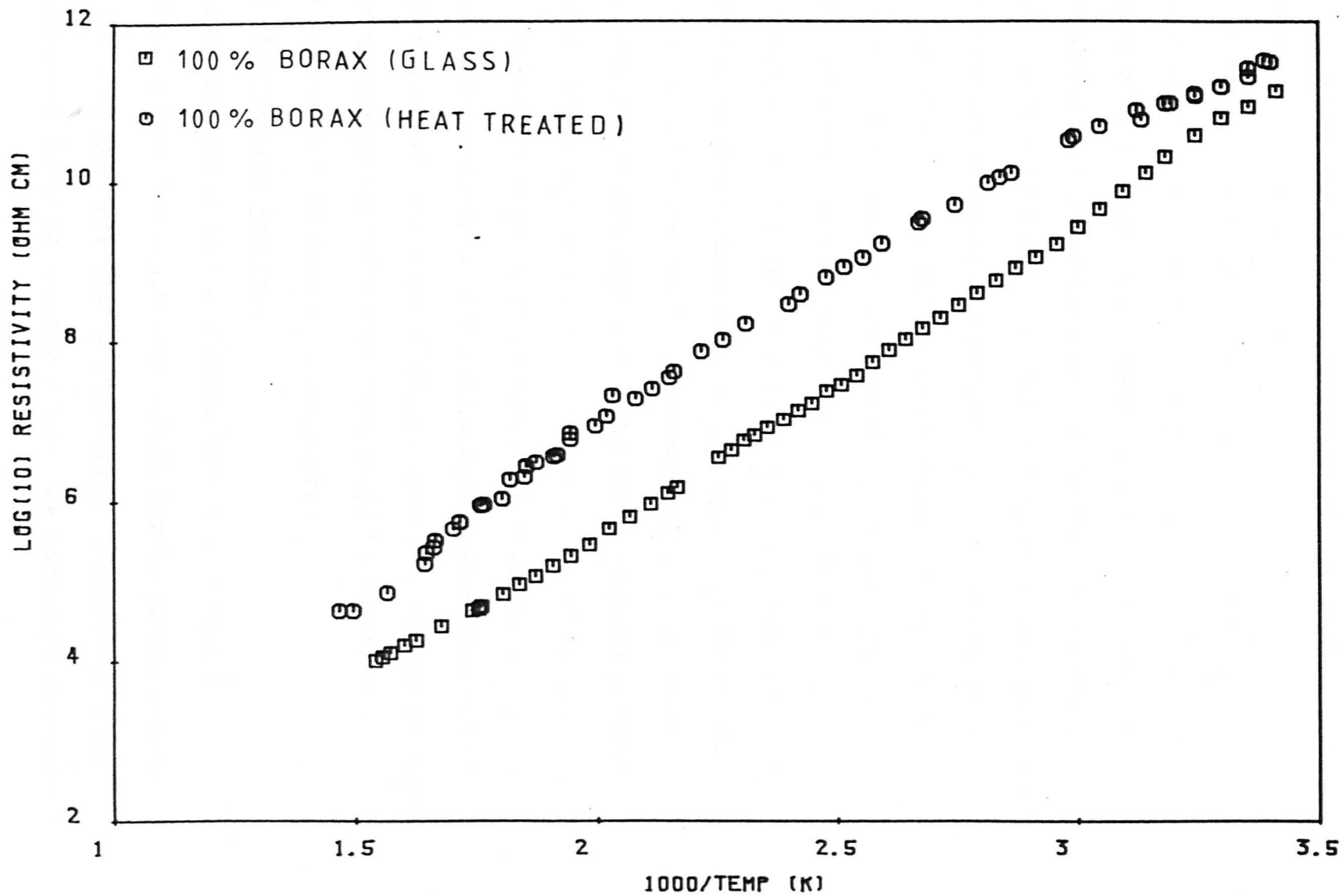


FIGURE 5.19

observed. This is the more usual trend on transforming a glass to a glass-ceramic. Furthermore this result shows that the decrease in resistivity observed on re-crystallising a doped specimen is a direct consequence of the doping, and is not some artificial effect.

In summary, when borax is doped with certain halides the resistivity of the product can be reduced by over five orders of magnitude, in some cases, when the initial glassy material is converted to a glass-ceramic. It is most certainly the presence of the halide ion itself that is necessary in order to promote this resistivity reduction. The type of metal cation involved in the halide is of secondary importance. Chloride ions and bromide ions seem to act quite similarly but fluoride ions do not produce the large decrease in resistivity. The low resistivity that is achievable is not critically dependent on a precise doping level, though the resistivity reduction can be increased slightly by choosing an optimum percentage addition. The lower percentage limit of dopant necessary in order to achieve a marked resistivity decrease has not been fully investigated here and is an obvious area of interest for future work. Room temperature resistivities of less than $10^6 \Omega \cdot \text{cm}$. have been easily obtained and it is highly possible that this could be further reduced using different heat treatment procedures.

5.1.3 Alkali-free Borates.

Alkaline-earth borate glasses have a much higher resistivity than the equivalent alkali borate glass, indeed they are very good electrical insulators. Furthermore, as was discussed fully in section 2.7.6, the mechanism responsible

for the electrical conductivity in these glasses is still under considerable discussion.

Towards the end of this project it was decided to investigate the effect of the addition of halides on the electrical properties of some alkaline-earth borate glasses, and also to explore the effects of heat treating the samples. The halide additions used were chlorides, XCl_2 , such that there was only one type of alkaline-earth ion present. Thus, glasses of the form 100% XB_4O_7 and 90% XB_4O_7 + 10% XCl_2 were formed, where X = Ca, Sr, Ba. Glasses based on magnesium borate could not be investigated due to the fact that the product does not form a glass at this composition.

A melting temperature of $1200^\circ C$ was used in all cases. Annealing temperatures and crystallisation temperatures were found by D.S.C. and D.T.A. techniques (see section 3.4). It was found that both these temperatures varied with the type of cation involved. The barium borate based glasses were annealed at $530^\circ C$, the strontium borate based glasses at $580^\circ C$ and the calcium borate based glasses at $600^\circ C$. A similar trend was discovered for the crystallisation temperatures. It was possible to crystallise the barium borates at $700^\circ C$, while the strontium borates required $720^\circ C$, and the calcium borates required $750^\circ C$.

The resistivities of the undoped materials are so high that they cannot be measured at room temperature with existing apparatus. The samples have to be taken to approximately $350^\circ C$ before the resistivity can be measured. In general Arrhenius type behaviour is exhibited as the temperature is varied, though it must be appreciated that the difficulty in measuring

such high resistivities gives rise to considerable scatter about the fitted straight lines. The experiments have been repeated and the results confirmed. The observed resistivity curves for the three sets of materials are shown in Figs. 5.20 - 5.22. Again, to avoid confusion from the plethora of data points, only the fitted straight lines are shown.

As might be expected, the undoped materials all show very high resistivities with the re-crystallised materials showing a rather higher activation energy and, over most of the temperature range utilised, a higher resistivity than the parent glass. Alkaline-earth borate glasses have been investigated by other authors, but it is not a simple matter to compare the results obtained by them to the results given here, as the XO/B_2O_3 ratio used does not coincide. However, a comparison table is given in Table 5.2, where the quoted results are taken from work on compositions nearest to those used here. It can be seen that at least order of magnitude correlation is shown, which is all that can be expected given the difference in compositions and the extreme temperatures and resistivities involved.

The results for the doped glasses are not very different from the undoped glasses, the activation energy is very similar indeed. The doped glasses are slightly more resistive, which is the opposite trend to that shown with the glasses based on sodium borate, but overall the effect is not very startling.

It is with the re-crystallised doped specimens that the results become most interesting. Once again a reduced

RESISTIVITY PLOT

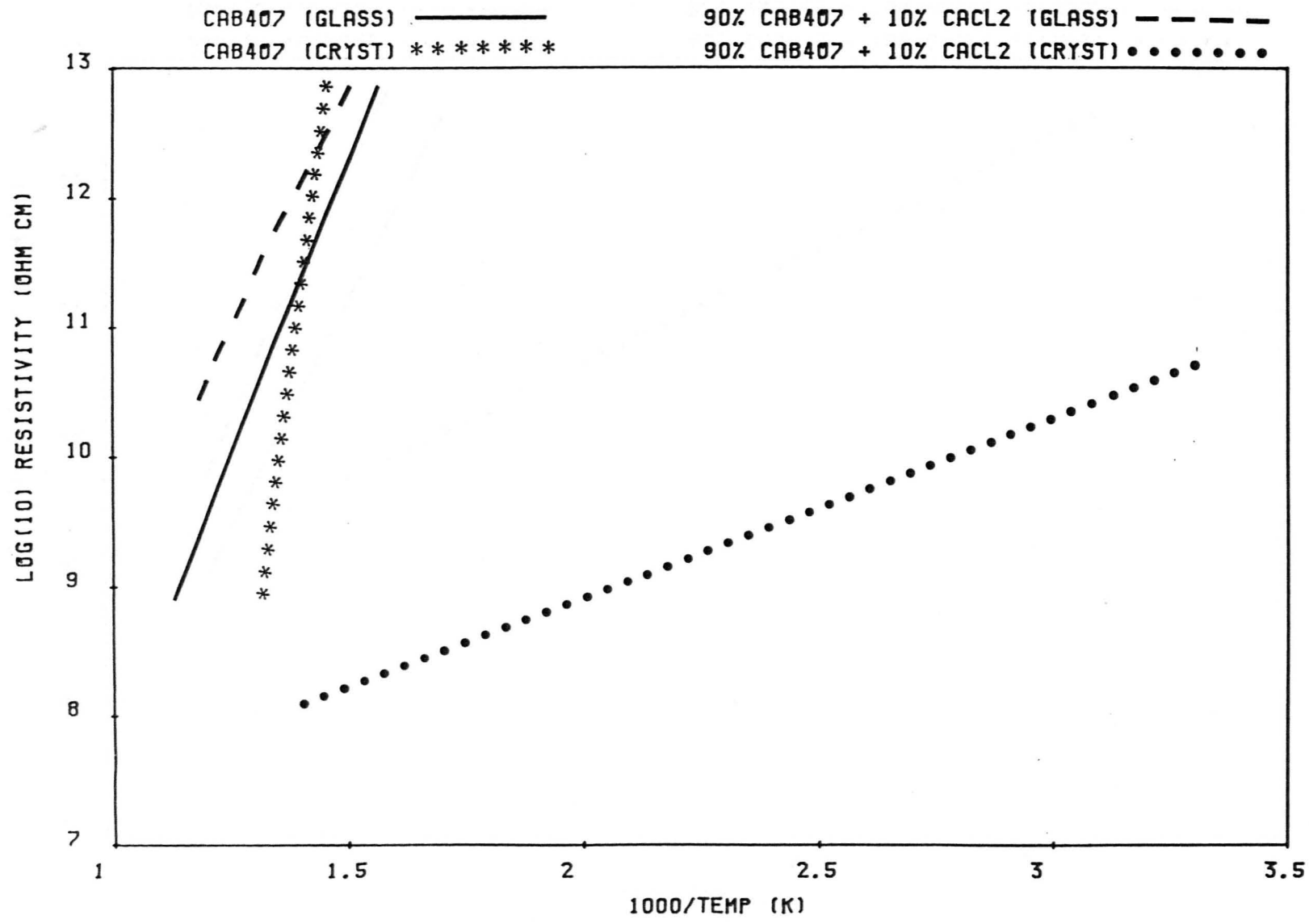


FIGURE 5.20

RESISTIVITY PLOT

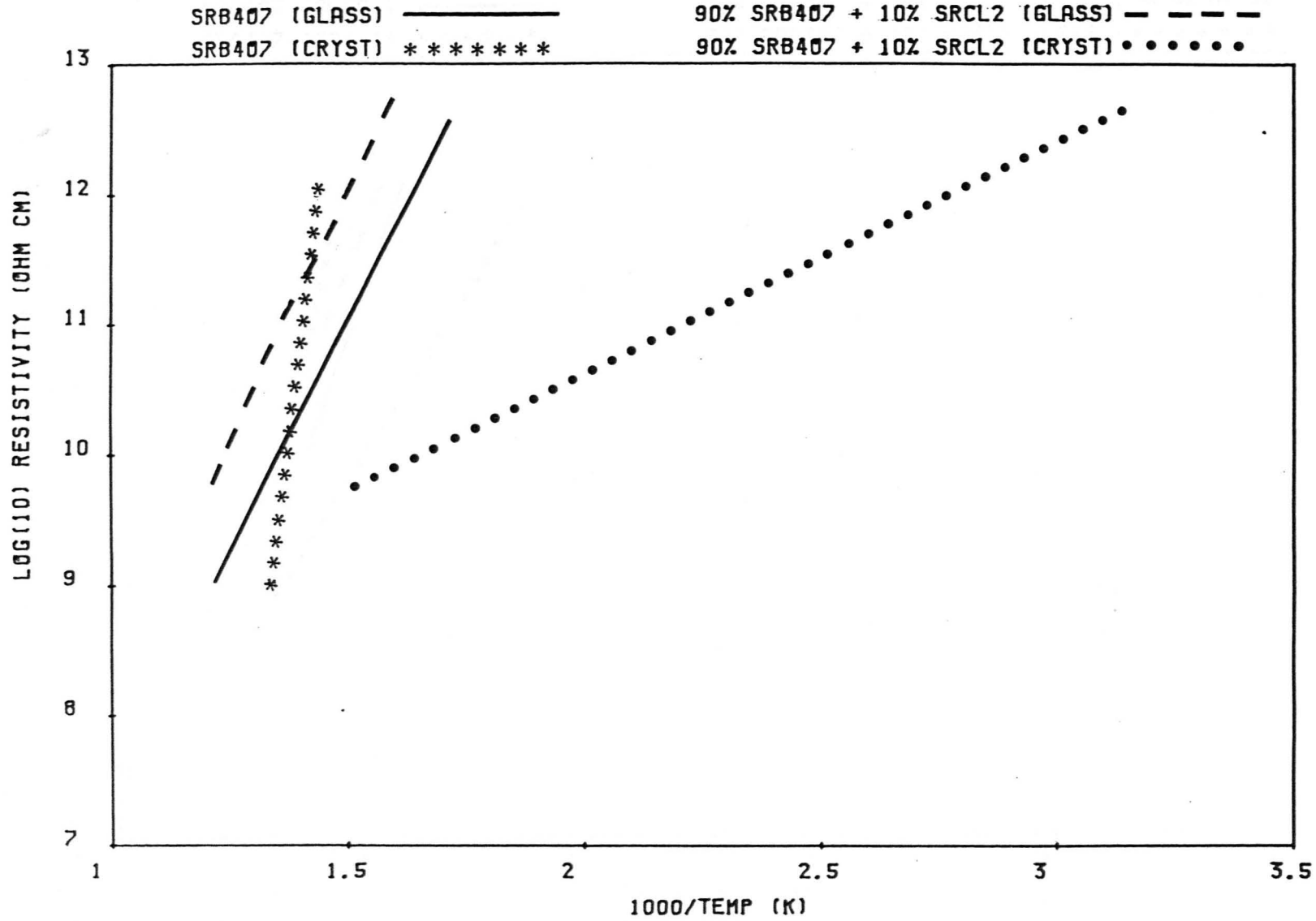


FIGURE 5.21

RESISTIVITY PLOT

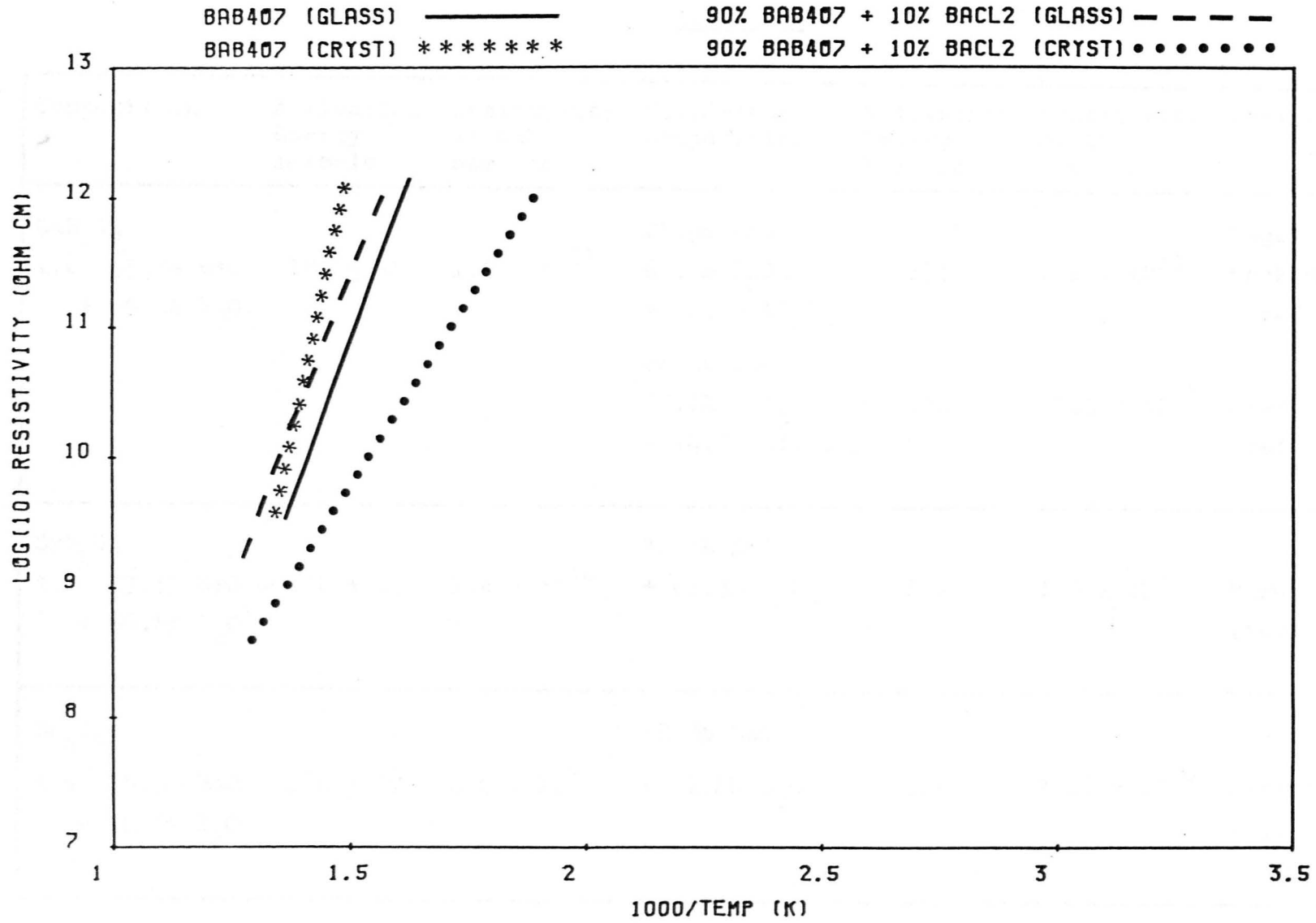


FIGURE 5.22

Table 5.2

Composition	Activation Energy kJ/mole	Resistivity at 450°C ohm. cm.	Comparison Composition	Activation Energy kJ/mole	Resistivity at 450°C ohm. cm.	Worker
CaB_4O_7 i.e. 33.3% CaO + 66.6% B_2O_3	181 ± 15	1.6×10^{11}	25.9% CaO 61.4% B_2O_3 + 12.7% Al_2O_3	171	4.1×10^{11}	Hagel and Mackenzie (ref. 5)
			28.5% CaO 57.1% B_2O_3 + 14.3% Al_2O_3	170	1.5×10^{11}	Owen (ref. 1)
SrB_4O_7 i.e. 33.3% SrO + 66.6% B_2O_3	136 ± 18	1.4×10^{10}	31.8% SrO + 68.3% B_2O_3	147	1.5×10^{11}	Hirayama (ref. 6)
Ba_4O_7 i.e. 33.3% BaO + 66.6% B_2O_3	184 ± 17	4.9×10^9	38.8% BaO + 61.2% B_2O_3	166	3.16×10^{10}	Hirayama (ref. 6)

resistivity effect is observed. It is most noticeable with the calcium borate based material. Here the resistivity is so decreased that measurements can be made even at room temperature. The room temperature resistivity is of the order of $10^{11} \Omega \cdot \text{cm}$. and the activation energy is reduced to $26 \pm 4 \text{ kJ/mole}$. The effect is also very prominent in the strontium borate based material, with the activation energy being $34 \pm 5 \text{ kJ/mole}$. In the barium borate based specimens the resistivity reduction is rather less, but the effect is certainly still present.

Overall there seems to be a general consistency throughout the results and an apparent dependence of the resistivity reducing effect on ionic size. It is quite remarkable that not only can the addition of a halide bring about such a marked resistivity reduction, but also that the effect can be observed in such a wide range of borate materials.

5.1.4 Electronic Conductivity.

It was found that if any specimen was allowed to polarise in a D.C. voltage, the final current flowing was below the limit detectable in an electrometer. Thus the electronic component of conduction can be assumed negligible in respect to the ionic component.

5.1.5 Further Comments.

The resistivity measurements create many points of interest and also provoke a number of questions, some of which will be mentioned below. However, before diverging from the measurements themselves, a further point must be made regarding the scatter of results for the re-crystallised samples. Almost overshadowed by the large 'random' scatter of results, there appears to be

an underlying trend that the resistivity of the sample increases with the number of measuring cycles. Because of the relative size of the effect compared to the 'random' scatter it is difficult to produce a meaningful graph illustrating the change. However, a set of repetition curves for a sample in which this effect was particularly large is shown in Fig. 5.23. It is emphasised that the observed increase is usually considerably less than this. A large number of 'same sample' repetitions is not possible due to deterioration of the gold electrodes and of associated contacts.

The overall impression is of some sort of relaxation effect, though this interpretation is open to question because the highest temperature attained in the conductivity measurements, approximately 400°C , is still considerably lower than the heat treatment re-crystallisation temperature. Thus there are no kinetic reasons why further relaxation should take place. The area obviously provides interesting features for future work, though the task of separating this effect from random scatter could prove difficult.

Returning to the resistivity results in general, several questions need to be answered. Firstly, it must not simply be assumed that the decrease in resistivity is brought about by increased sodium ion mobility, or even an increase in the effective number of ions available for conduction. The possibility that, in these doped re-crystallised materials, the halide ion itself is directly responsible for charge conduction cannot be ruled out without recourse to further evidence.

The re-crystallised specimens consist of at least one

RESISTIVITY PLOT

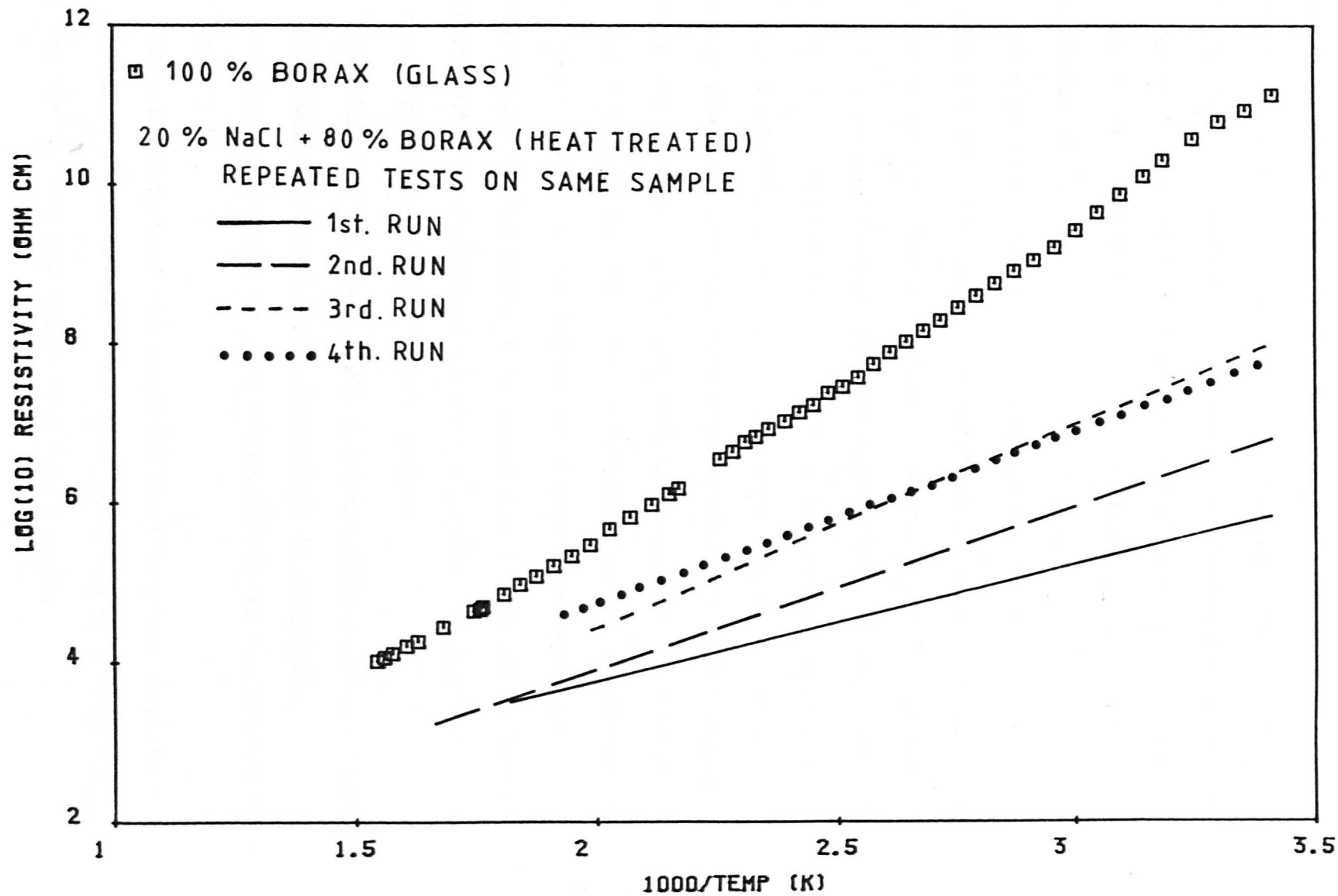


FIGURE 5.23

crystalline phase plus a residual glassy phase. It was mentioned earlier (section 5.1.2) that in the few cases reported previously where crystallisation brings about decreased resistivity it was the glassy phase, not the crystalline phase, that was more conducting. It must be asked whether the resistivity reduction brought about in the present case is a manifestation of the same effect. Thus it must be established whether it is the glassy phase or the crystalline phase that is highly conducting.

Even if experiments prove that it is the glassy phase that is highly conducting, the crystalline phase should be identified as a matter of course. Naturally, if it happened that the conducting phase was the crystalline phase, then this identification procedure would become of greater importance.

The environment of the various ions should be probed to look for changes that occur on crystallisation. This would include any changes in bonding and/or co-ordination number.

The experimental work to be reported in the remainder of this chapter, and in the following chapter, attempts to discover some of the answers to these questions, or at least to carry out investigations so that a greater insight into the conductivity mechanism can be gained.

5.2 Determination of the Relative Resistivity of the Crystalline and Glassy Phases in the Glass-Ceramic Materials.

The technique used in these investigations was discussed in section 4.3.3.

The composition of the material used in these experiments was 10% CaCl_2 + 90% borax. The re-crystallisation temperature used was 700°C , and the dwell time was 2 hours.

FIGURE 5·24

Micrograph: Overview of sample used in 'charging-up' experiment.

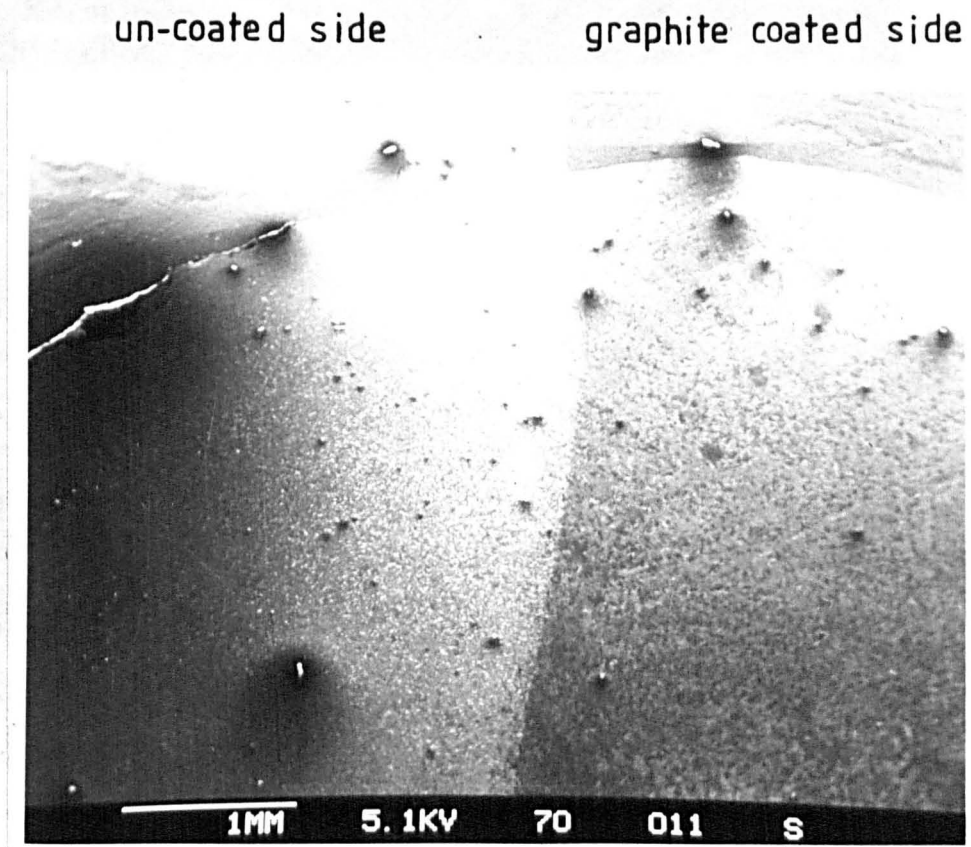


FIGURE 5·25

Micrograph: Close-up of boundary region

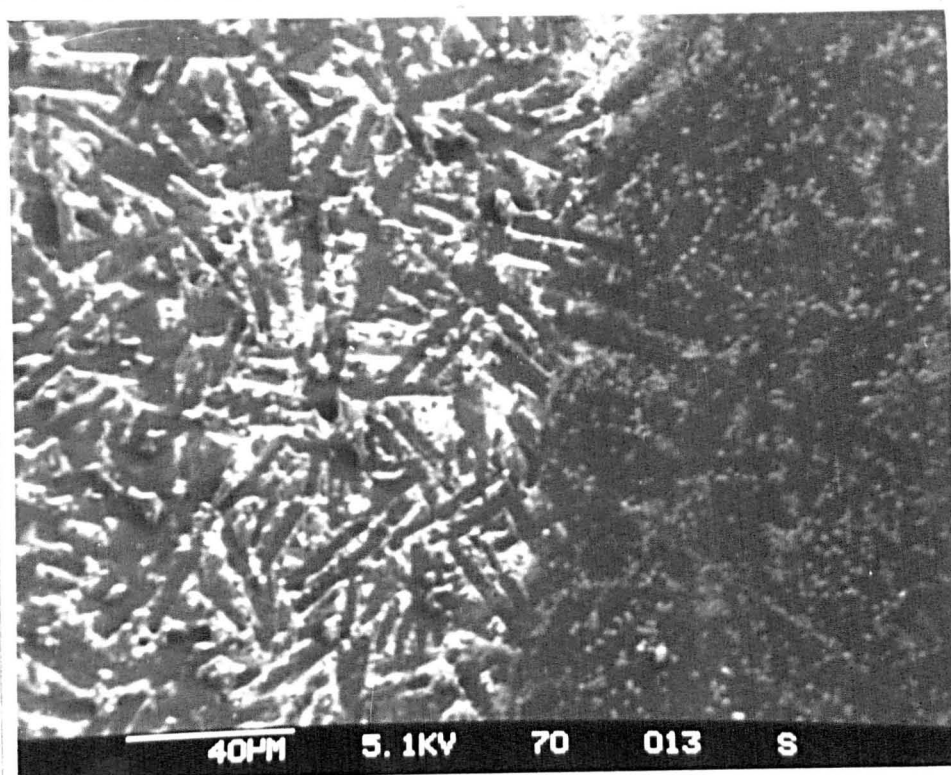


FIGURE 5-26

Micrograph: Close-up of un-coated region

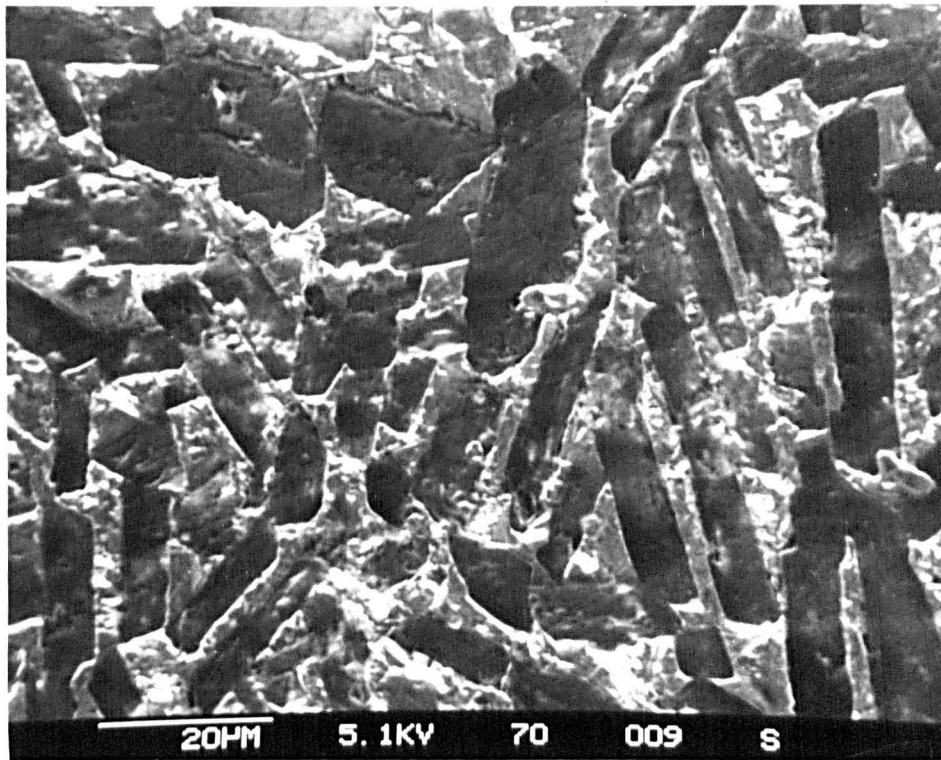
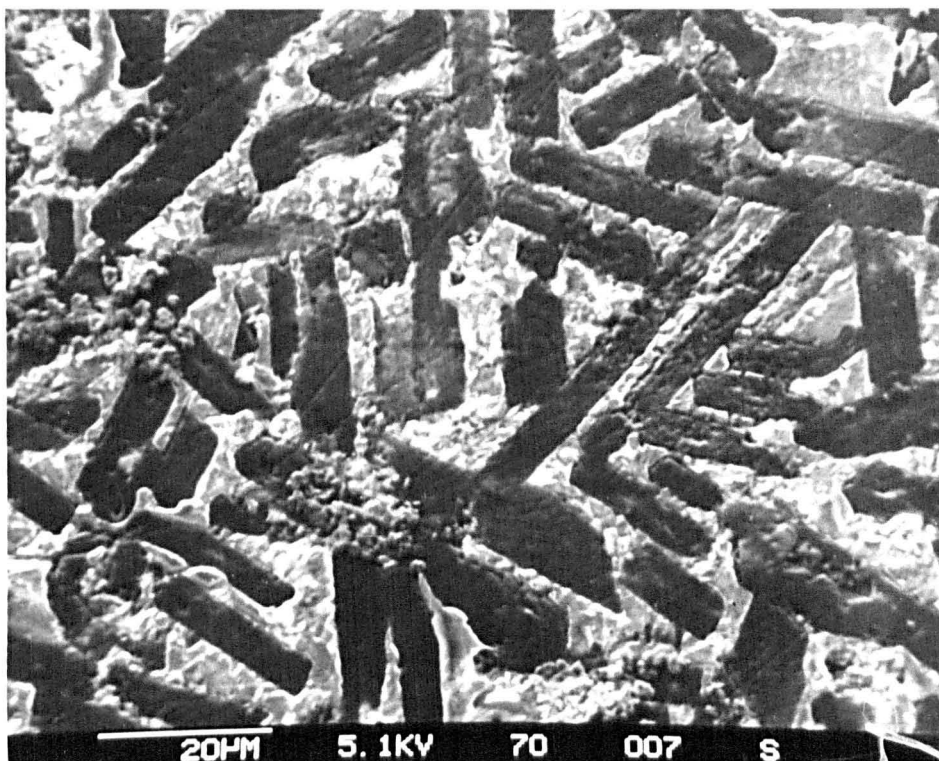


FIGURE 5-27

Micrograph: Close-up of un-coated region



An overall view of the sample is shown in Fig. 5.24. The border between the region coated in graphite and the uncoated region is easily observable. Fig. 5.25 shows this dividing line in rather more detail. Even at this stage the charge glow within the uncoated region can be seen to be clinging to only certain areas. Figs. 5.26 and 5.27 show the uncoated region at high magnification. It is very easy to see that the crystallites remain charge free, while the residual glassy phase is subject to considerable charging. The difference is very marked indeed.

This set of photographs clearly demonstrates that the crystalline phase is capable of conducting charge away, while the residual glassy phase is not. Thus, it can be concluded that the low resistivity of these doped, re-crystallised materials is due to the crystalline phase that is formed being a good conductor. The effect is not due to an increased concentration of sodium ions in the glassy phase.

This result has put increased importance on establishing definitely which ion is the mobile species in these low resistivity materials, on determining the crystal phase that is present and on looking for changes in the environment of the various ions on crystallisation.

5.3 Thermopower Experiments.

The background to this technique and the equipment used was discussed fully in section 4.5. The results will be used to confirm, or otherwise, the findings of the 'triple disc' experiments to be reported in the next section.

Several of the low resistivity, re-crystallised, borax based samples were utilised in the experiments. A consistent

result was always achieved. It was found that independent of the dopant used, be it CaCl_2 , NaCl , ZnCl_2 , NaBr , etc., when a temperature gradient was applied to the specimen the colder surface became positive with respect to the hotter surface. This indicates that the charge on the mobile ion is positive. This fact was not affected by the overall temperature of the sample.

This result was evidence that the mobile ion was the sodium ion. Of course, it was not possible to rule out that the mobile ion, dependent on the particular dopant, was that of calcium or zinc etc., but it was felt that this was less likely. Perhaps it is best to say that this result indicates that the conduction is not due to highly mobile halide or oxygen ions.

5.4 Triple-Disc Experiments.

The apparatus used and the experimental procedure are described fully in section 4.4.

The viability of the procedure was first explored using a re-crystallised sample of composition 20% NaCl + 80% borax. The triple-disc arrangement was polarised at 90V, at room temperature, for a period of approximately 24 hours. The initial current flowing was of the order of 100 μA , and this fell during the course of the experiment to be below the noise level of the electrometer (10^{-10}A).

E.D.A.X. analysis of the three discs after polarisation are shown in Figs. 5.28 - 5.30. Fig. 5.28 shows the analysis of the disc that was nearest the positive electrode, Fig. 5.29 shows the analysis of the central disc, and Fig. 5.30 shows the analysis of the disc that was nearest the negative

FIGURE 5.28

E.D.A.X. Analysis : Disc nearest positive electrode
Relative peak heights shown

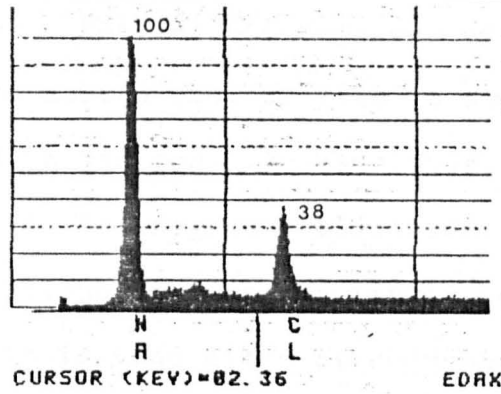


FIGURE 5.29

E.D.A.X. Analysis : Centre disc

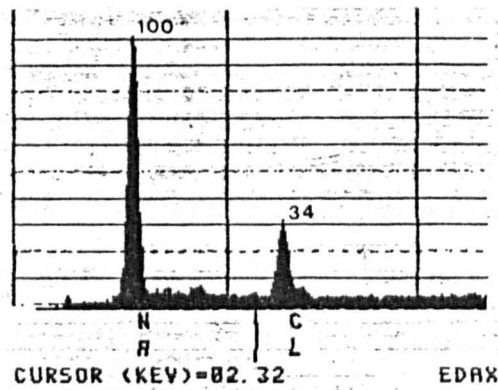
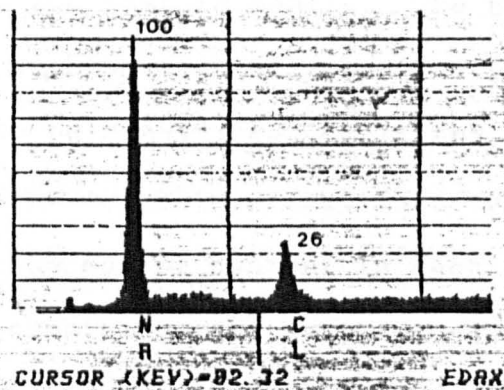


FIGURE 5.30

E.D.A.X. Analysis : Disc nearest negative electrode



electrode. It can be seen that there is a small but observable decrease in the chlorine/sodium ratio as the negative electrode is approached. However, it must be realised that at this stage it can not be stated whether this is due to the chlorine ions having moved to the positive electrode, or the sodium ions having moved to the negative electrode. Before this can be decided a stationary reference ion is needed.

With this in mind discs of composition 15% BaCl_2 + 85% borax were utilised. It could not be envisaged that the large barium ion would be mobile to any relevant extent, it would consequently act as a reference in all three discs, against which the presence of other ions could be gauged. In order to try to increase the resulting degree of polarisation of the triple-disc arrangement, three improvements were made compared to the first experiment described above. Firstly, the polarising voltage was increased from 90V to 150V. Secondly, the experiment was carried out at an elevated temperature; 180°C . Thirdly, the time allowed for polarisation was increased to one week.

Figs. 5.31 - 5.33 show the E.D.A.X. analysis of the three discs. It can be seen that the sodium/barium ratio increases quite drastically as the negative electrode is approached. As this cannot be attributed to a change in the percentage of barium that is present, the conclusion to be drawn is that it is the sodium ion that is mobile. The chlorine/barium ratio is much more constant. Strangely, the percentage of chlorine does appear to be rather reduced in the disc near the positive electrode. However, this effect is overshadowed by the variation of the sodium content in each disc. Consequently, this result, combined with the thermopower measurements of

FIGURE 5.31

E.D.A.X. Analysis : Disc nearest positive electrode
Relative peak heights shown

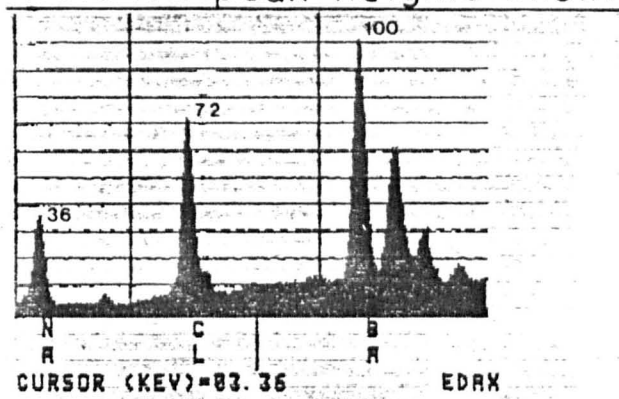


FIGURE 5.32

E.D.A.X. Analysis : Centre disc

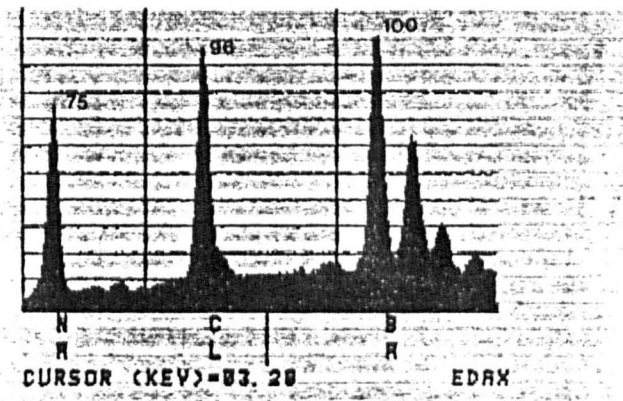
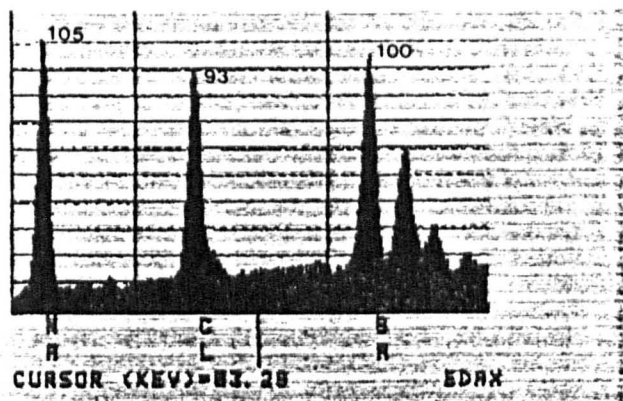


FIGURE 5.33

E.D.A.X. Analysis : Disc nearest negative electrode



the previous section, provides conclusive evidence that, in these low resistivity materials, the ion responsible for conduction is that of sodium.

CHAPTER 6

Results for Structural Investigational Techniques.

6.1 X-Ray Diffraction.

As discussed in section 4.2 X-ray diffractational studies were used for two broad reasons. Firstly, to monitor the initial glassy materials, in order to demonstrate that they were indeed glassy products and that no trace crystallinity was present. Secondly, to identify the nature of the crystalline phase that evolved on heat treating the samples.

Early work utilised the well-known Debye-Scherrer powder technique but later a diffractometer became available for use. The experimental apparatus, general theory, and the technique used were also discussed in section 4.2.

6.1.1 Studies on Glassy Materials.

The X-ray diffraction pattern of most of the glassy products was taken as a matter of course after cooling from the annealing furnace, or after having been cut into discs. The nature of the work was purely qualitative, so there is little point in re-producing all the curves that were observed. Instead, only sample curves illustrating the appearance of the diffraction pattern for a glassy material, and for the same material after a re-crystallisation heat treatment, will be given.

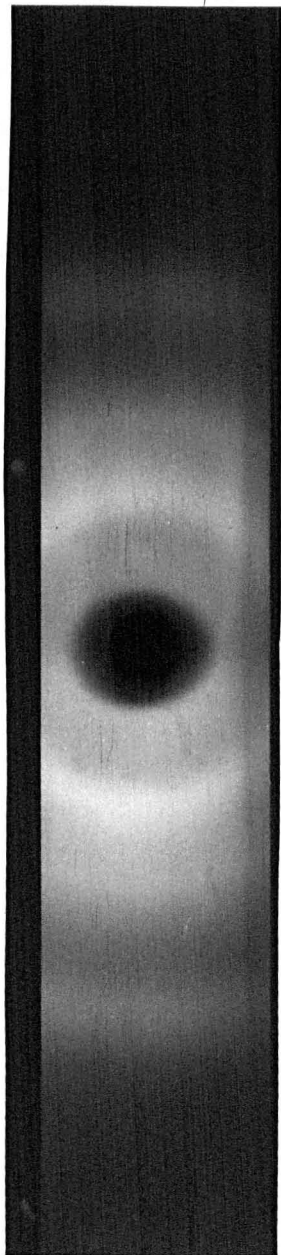
The Debye-Scherrer powder diffraction pattern of the material of composition 10% NaCl + 90% borax is shown in Figs. 6.1 and 6.2. Fig. 6.1 shows the pattern for the glassy product, while Fig. 6.2 is the pattern taken after a heat treatment at 700°C. There is a clear difference. The diffraction lines on Fig. 6.2 demonstrate the crystalline nature of the product, while the diffuse haloes of Fig. 6.1 are indicative

FIGURE 6.1

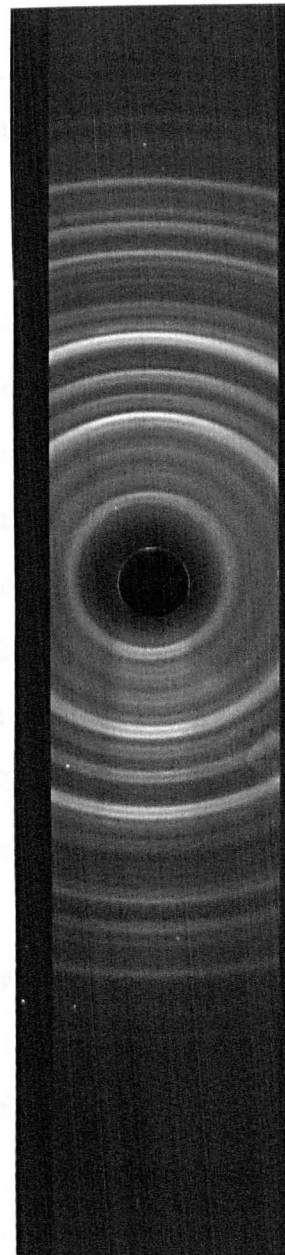
FIGURE 6.2

X-Ray Diffraction Patterns of
10% NaCl + 90% Borax

Glassy
Material



Heat Treated
Material



of a glass.

This difference is also well illustrated when a diffractometer is used to record the X-ray pattern. Fig. 6.3 shows the result for the glass of composition 20% NaCl + 80% borax. The broad haloes are clearly seen. Figs. 6.4 and 6.5 are curves for the same material which has been subjected to further heat treatment. The specimen used for Fig. 6.4 is only partially crystalline, while that used for Fig. 6.5 is more fully crystalline. The heat treatment used was a dwell of 500°C for 4 hours and 16 hours respectively. The samples were shown in Fig. 3.9.

6.1.2 Studies on the Re-crystallised Materials.

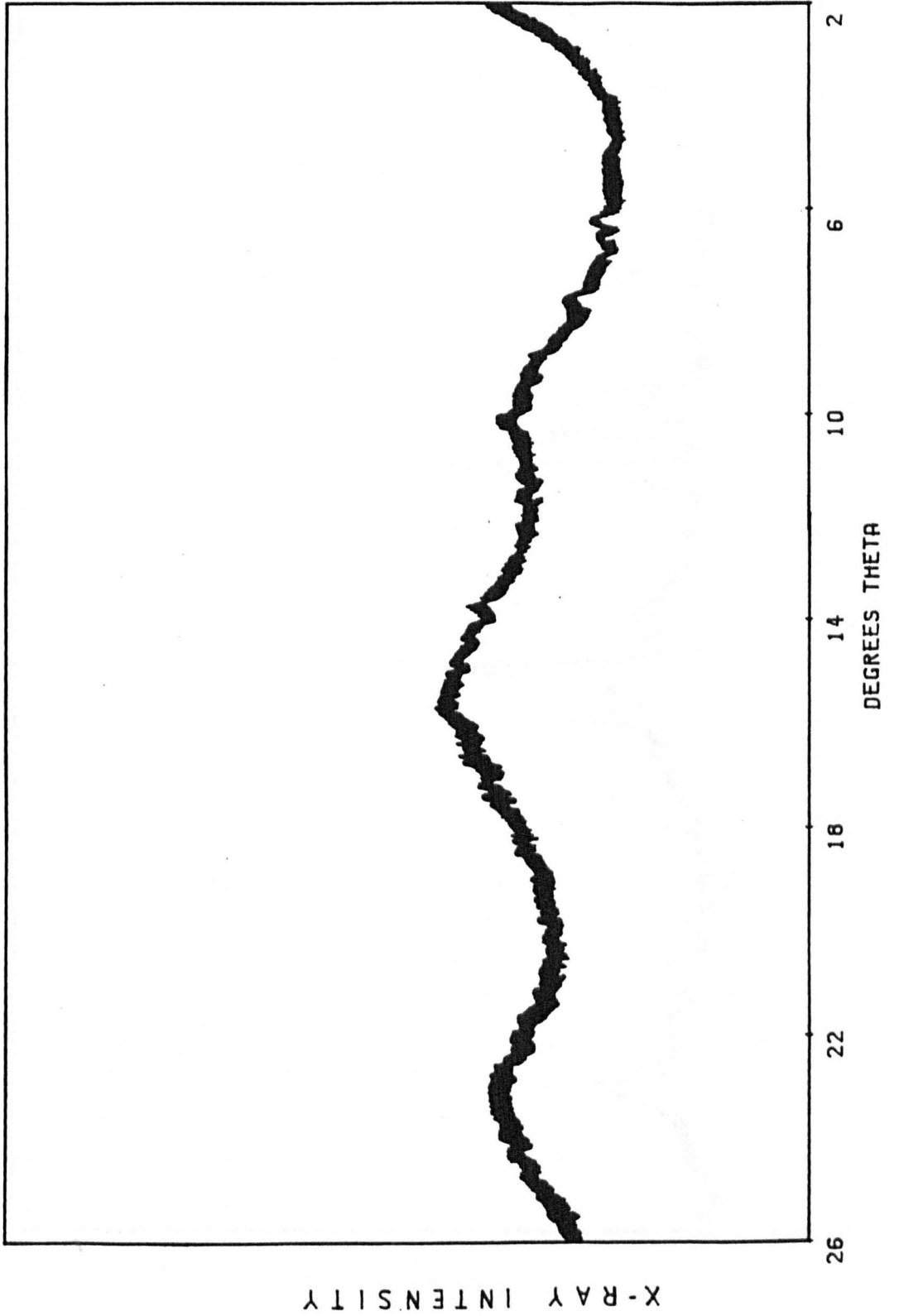
The compositions investigated, and the order in which they were examined follows the pattern set by the conductivity measurements. Consequently the first re-crystallised material subjected to this mode of study was 10% ZnCl₂ + 90% borax. The specimen utilised had been heat treated at 700°C for 2 hours. At this stage the Debye-Scherrer technique was still being used, the observed X-ray diffraction pattern is shown in Fig. 6.6. The d-spacings resulting from analysis of the pattern are given in Table 6.1. Also shown in this table are the compounds that are thought responsible for each given line. Most of the lines can be allocated in this way. The A.S.T.M.S. powder diffraction reference lists were used as the source of information.

Several points of interest arise from the analysis. Firstly that there is no trace of any halide compound. The ZnCl₂ appears to have dissociated at some stage in the melting or re-crystallisation process. As the constituent ions are most certainly still present in the sample the question is provoked regarding their roles and positions within the material.

FIGURE 6-3

DIFFRACTOMETER TRACE

20 % NaCl + 80 % BORAX (GLASS)



DIFFRACTOMETER TRACE

20% NaCl + 80% BORAX (SEMI-CRYSTALLINE)

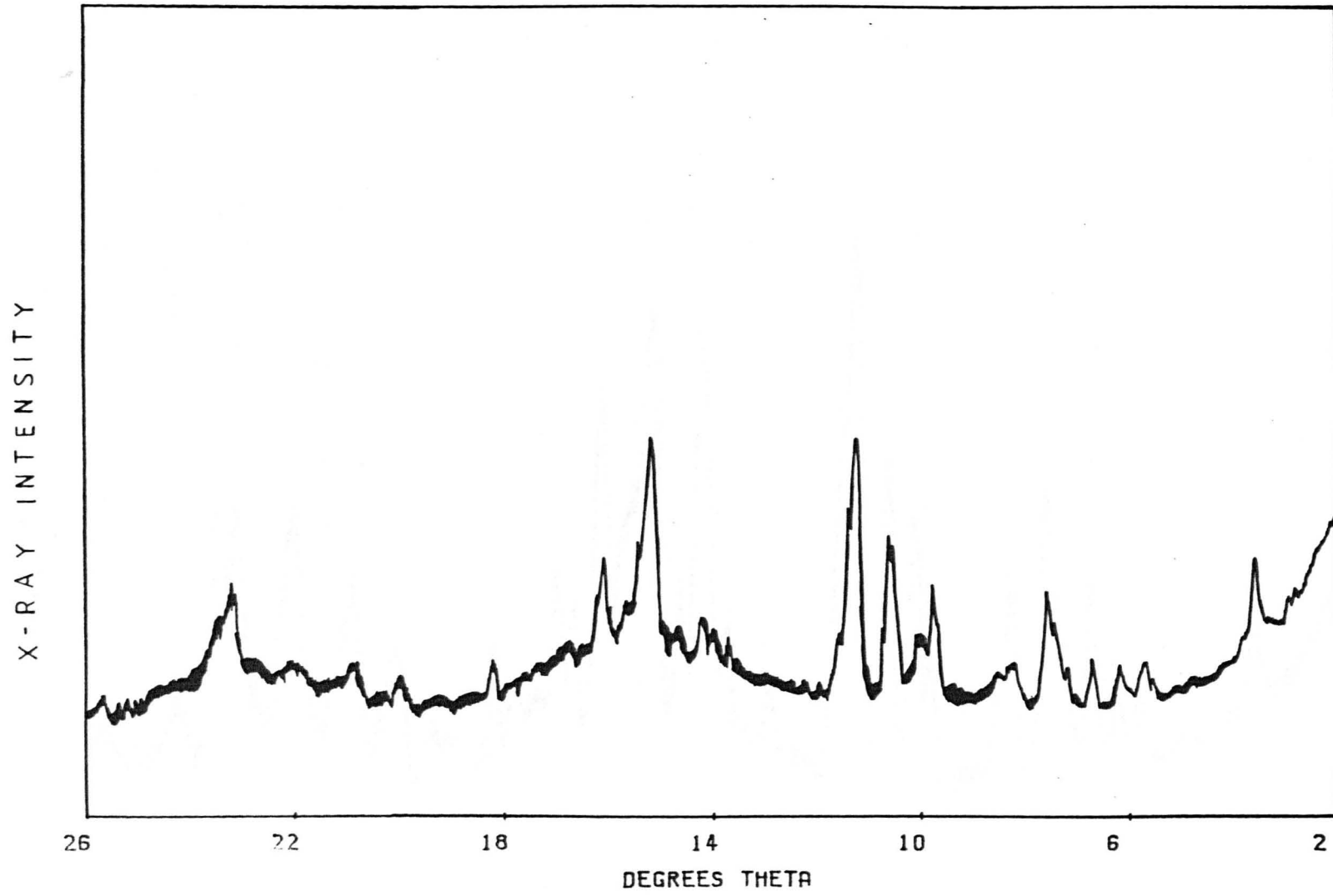


FIGURE 6.4

FIGURE 6·5

DIFFRACTOMETER TRACE

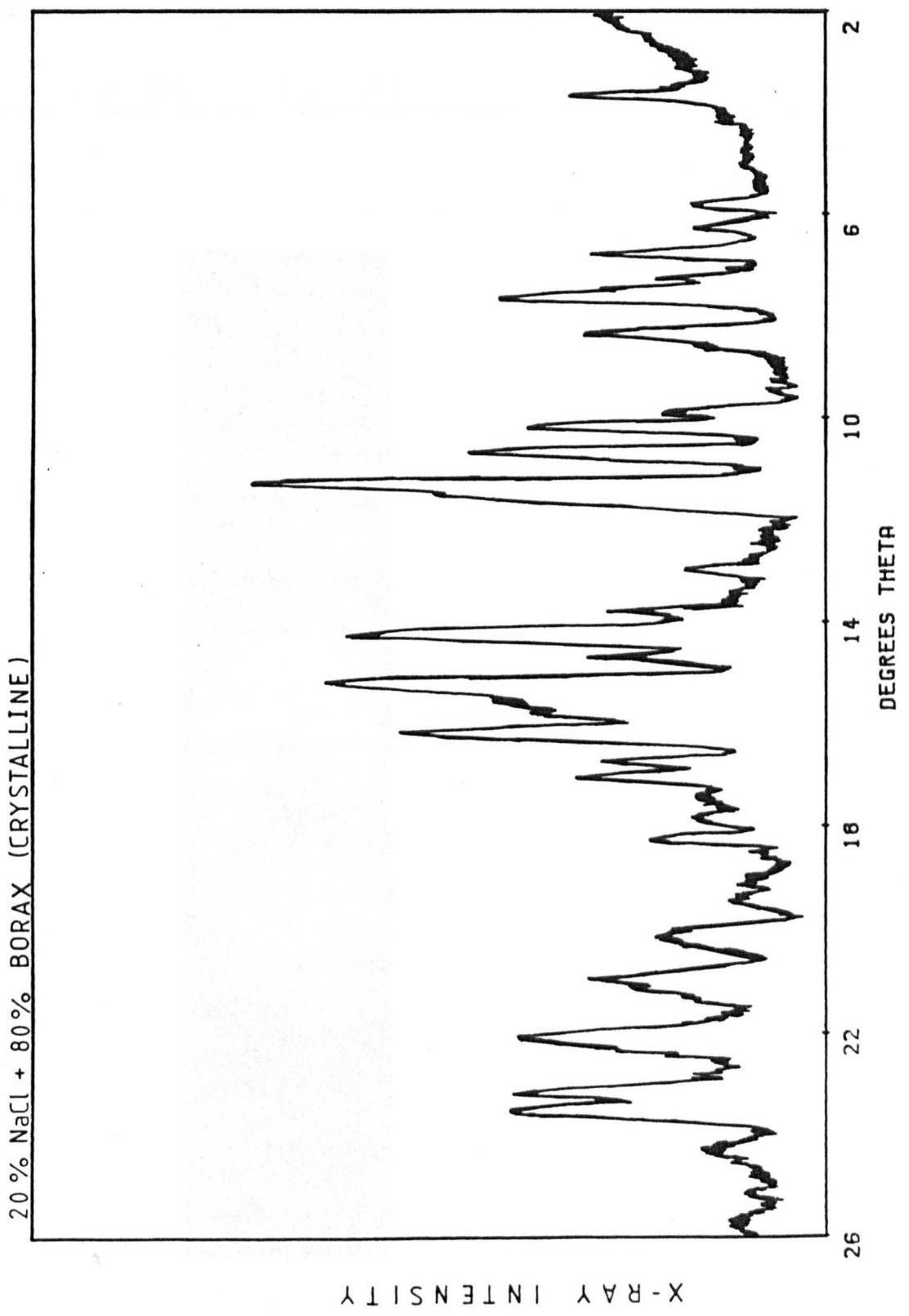


FIGURE 6·6

X-Ray Diffraction Pattern Of

10 % $ZnCl_2$ + 90 % Borax

Heat Treated Specimen

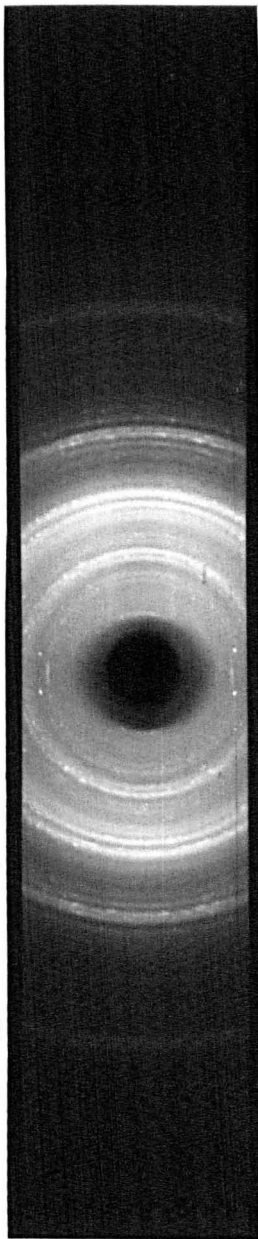
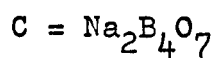
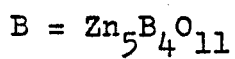


Table 6.1

Analysis of the Debye-Scherrer X-ray Diffraction Pattern
 for 10% ZnCl_2 + 90% Borax.

d-spacing \AA	Strength of Diffraction Line	Correlation
6.17	medium	-
5.73	medium	-
5.29	weak	A at 5.29 \AA
5.05	weak	-
4.12	medium	A at 4.11 \AA
3.92	medium	C at 3.92 \AA
2.94	medium	B at 2.94 \AA
2.88	medium	A at 2.89 \AA or B at 2.86 \AA
2.76	weak	-
2.63	weak	B at 2.66 \AA
2.53	weak	A at 2.55 \AA
2.13	weak	C at 2.12 \AA
1.96	medium	B at 1.96 \AA
1.92	medium	A at 1.95 \AA
1.77	weak	-
1.68	weak	B at 1.68 \AA



The zinc ions have been assimilated to form one of two types of zinc borate phase. It is these phases that dominate the diffraction pattern. Given the original composition it is presumed that there must also be large amounts of one or more phases of sodium borate present. Indeed, two diffraction lines are allocated to such species. It is believed that only relatively few lines are observed for these sodium borate phases because of the great scattering power of the zinc ion in comparison to that of a sodium ion.

The next material investigated was of composition 10% CaCl_2 + 90% borax. The specimen had been re-crystallised by heating at 700°C for 2 hours. A Debye-Scherrer technique was again used on this occasion. The analysis of the resulting diffraction pattern is shown in Table 6.2. Rather similar observations can be made to those noted in the previous case. Firstly, no halide phase is indicated despite the presence of chloride ions in the material. Secondly, most of the diffraction lines can be accounted for by relatively well-known borate phases. The calcium ion, being much smaller than the zinc ion, does not mask the contribution from the sodium borate phase, the presence of which is clearly indicated.

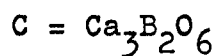
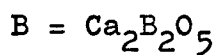
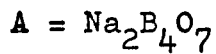
Following this it was decided to scrutinise the products formed when NaCl is added to borax. The same compositions were used as were utilised in the conductivity measurements, i.e. 100% borax, 10% NaCl + 90% borax, 20% NaCl + 80% borax and 30% NaCl + 70% borax. Six different heat treatments were used for each of the compositions. These consisted of a dwell at a temperature of 500°C for either $\frac{1}{2}$ hour, 1 hour, 2 hours, 4 hours, 8 hours or 16 hours. The resulting specimens were

Table 6.2

Analysis of the Debye-Scherrer X-ray Diffraction Pattern

for 10% CaCl_2 + 90% Borax.

d-spacing \AA	Strength of Diffraction Line	Correlation
6.51	weak	A at 6.49 \AA
5.79	weak	B at 5.71 \AA
5.23	medium	A at 5.23 \AA
4.32	medium	B at 4.32 \AA
4.14	medium	-
3.91	medium	A at 3.91 \AA
3.08	v. weak	B at 3.09 \AA
2.94	medium	B at 2.95 \AA
2.89	medium	B at 2.87 \AA
2.76	weak	C at 2.76 \AA
2.66	weak	A at 2.67 \AA or B at 2.67 \AA
2.45	v. weak	A at 2.45 \AA
2.15	v. weak	C at 2.16 \AA
2.04	v. weak	C at 2.04 \AA
1.92	medium	C at 1.90 \AA
1.89	v. weak	B at 1.87 \AA



displayed in Figs. 3.7 - 3.10. A diffractometer was used in these and subsequent investigations in preference to the Debye-Scherrer technique. Analysis of the various diffraction patterns showed that the nature of the phases present for each particular composition was virtually independent of the length of the heat treatment (though of course the degree of crystallinity varied). Consequently there is little point in displaying all 24 curves concerned in this section of work. Instead, only typical curves for well crystalline specimens of each composition will be shown. These form Figs. 6.7, 6.8, 6.5 and 6.9.

At first glance the diffraction patterns look quite different, however careful analysis has shown that similar phases are present on each occasion; it is the relative proportion of each phase that is changing. Consequently the position of major peaks for one composition corresponds only to a minor peak in another composition, and vice versa. The analysis is summarised in Table 6.3.

It was a rather complicated task performing the analysis. The main problem was the very large number of peaks encountered. They frequently overlap, causing irregularities in line shape and doubts over the appearance or non-appearance of shoulders etc. Further difficulties arise in the interpretation because many of the peaks from different sodium borate phases occur at very similar angles. Nevertheless, the analysis has been performed carefully and the observed trends are put forward with reasonable confidence.

Again no trace of a halide phase is observed, not even for the 30% NaCl composition. At this stage it seems probable that the halide ions are either distributed through the residual

DIFFRACTOMETER TRACE

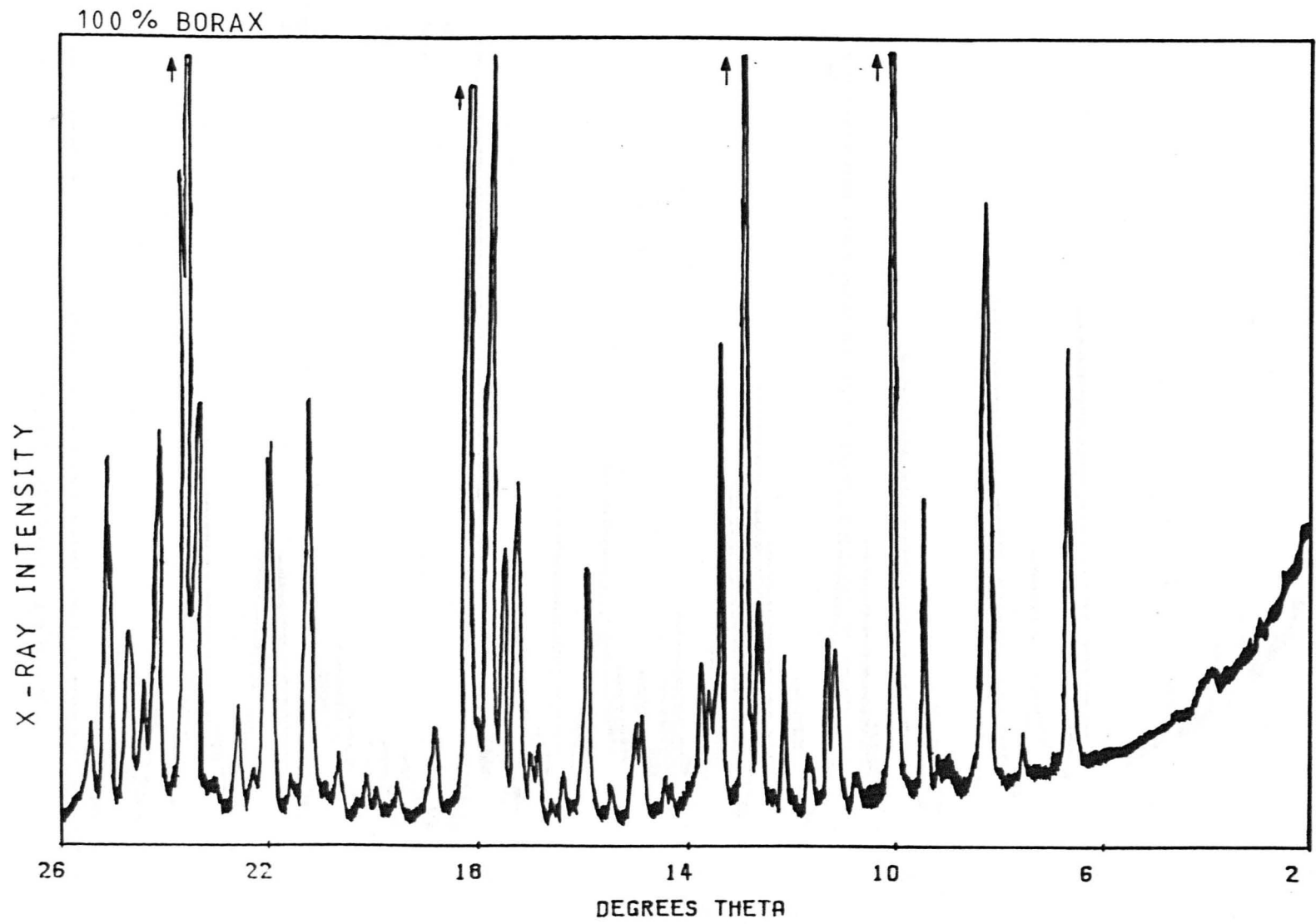


FIGURE 6.7

DIFFRACTOMETER TRACE

10 % NaCl + 90 % BORAX

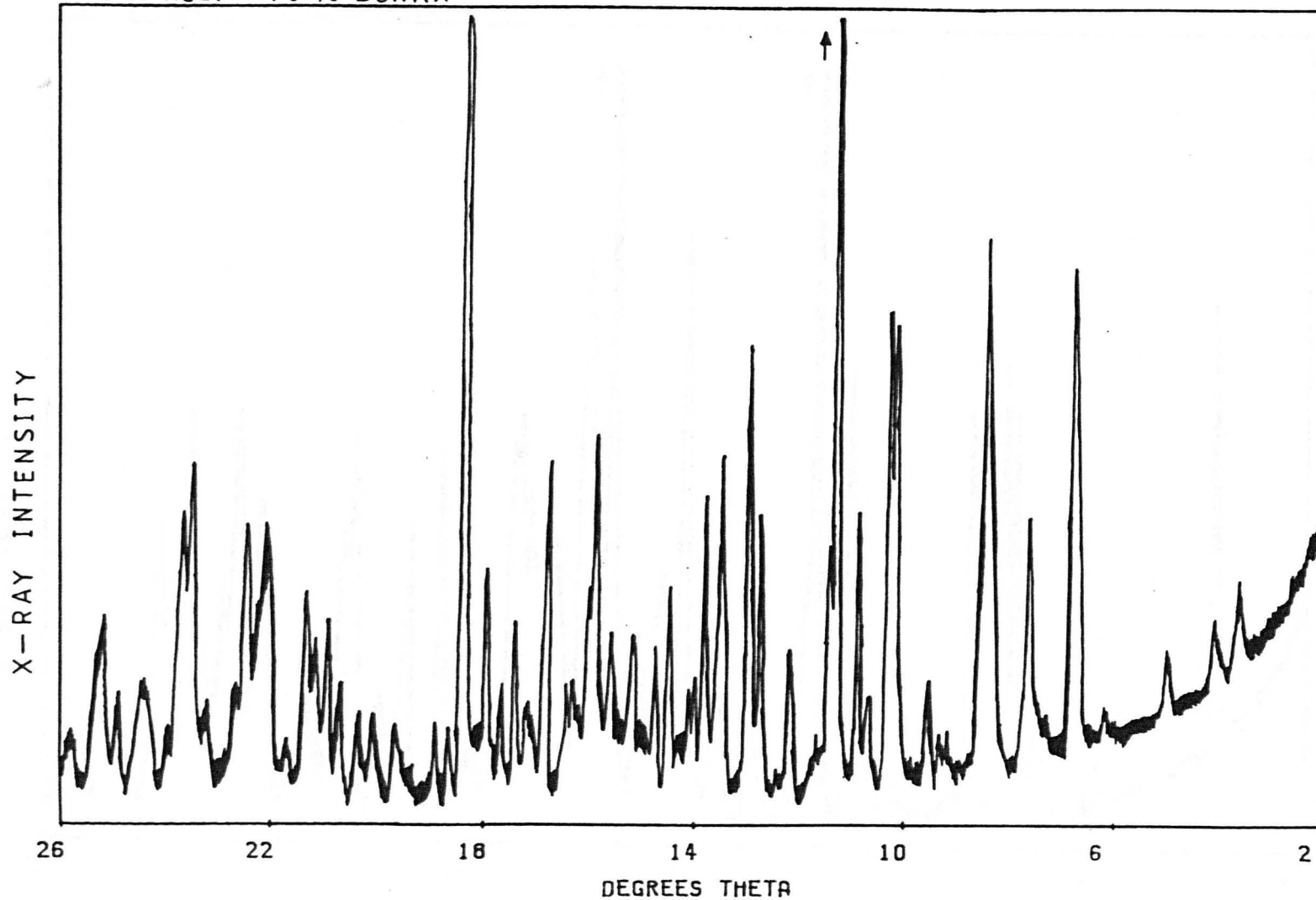


FIGURE 6.8

DIFFRACTOMETER TRACE

30 % NaCl + 70 % BORAX

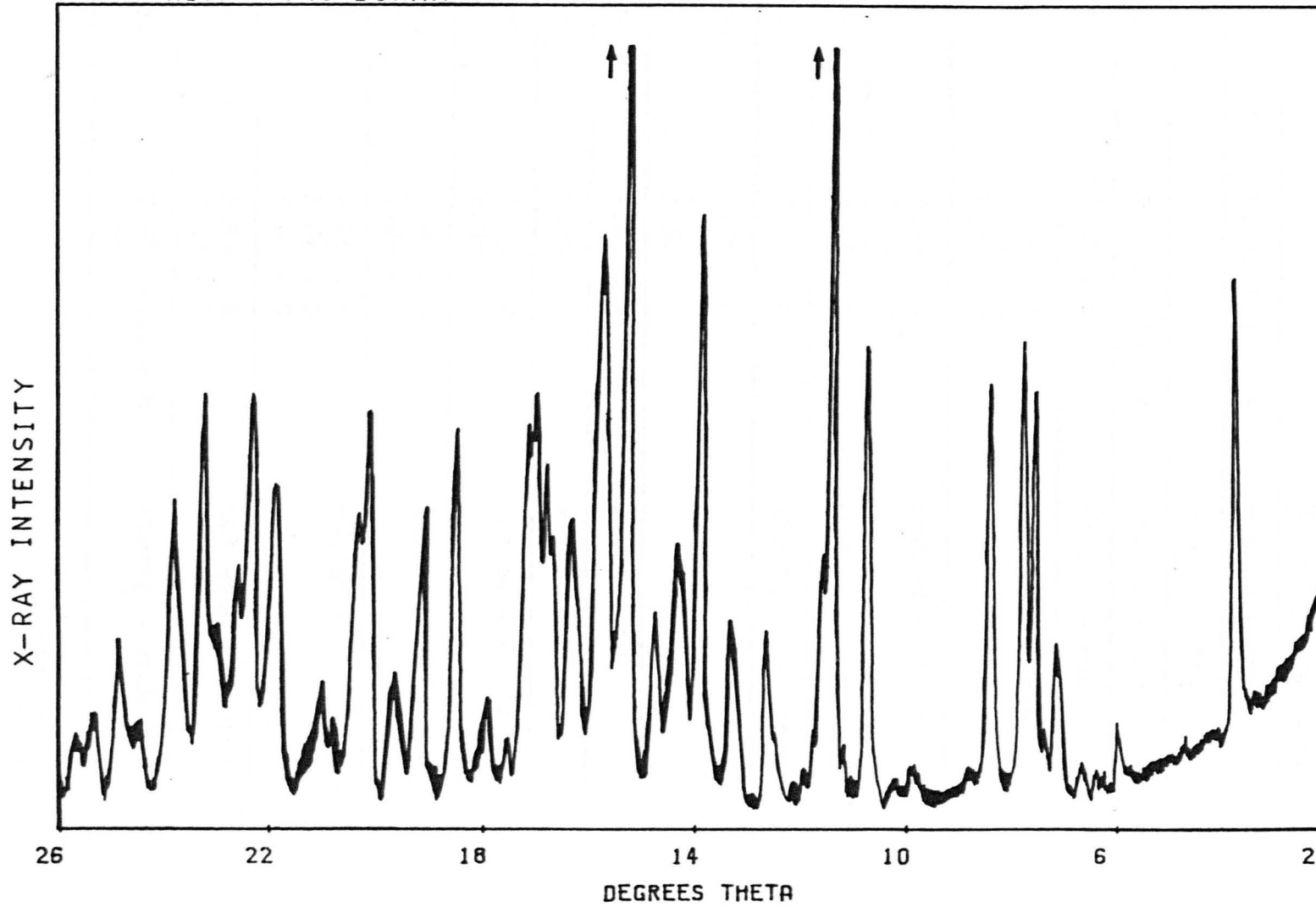


FIGURE 6.9

Table 6.3

Analysis of the Diffraction Patterns for
a Series of Materials.

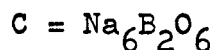
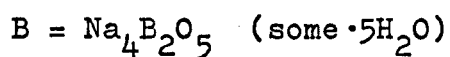
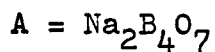
NaCl + Borax.

d-spacing (Å)	Correlation attempt	Strength and trend 0% NaCl → 30% NaCl
6.5	6.55, 6.49 - A	medium - weak
5.8	-	weak - medium
5.3	5.35, 5.23 - A	strong - medium
4.40	4.41 - A	strong - weak
4.33	4.32 - A 4.29 - B 4.33 - C	v. weak - weak
3.93	3.93 - A 3.90 - B	medium - strong
3.52	3.48 - A	medium - not seen
3.45	3.43 - A	strong - not seen
3.33	3.30 - A 3.32 - B 3.32 - C	medium - weak
3.08	3.05 - B	weak - medium
3.01	2.99 - B	weak - medium
2.92	2.93 - B 2.95 - C	not seen - strong
2.83	2.83 - B 2.83 - C	medium - strong
2.76	2.67 - A 2.68 - B 2.67 - C	not seen - medium
2.64	2.65 - B 2.63 - C	not seen - medium
2.52	2.58, 2.51 - B 2.52, 2.51 - C	strong - weak

cont'd...

Table 6.3 (...cont'd)

d-spacing (\AA)	Correlation attempt	Strength and trend 0% NaCl \rightarrow 30% NaCl
2.48	2.45 - A 2.48 - B 2.47 - C	strong - weak
2.24	2.21 - B 2.25, 2.27 - C	v. weak - medium
2.12	2.12 - A 2.14 - B 2.15 - C	medium - weak
2.04	2.02, 2.05 - A 2.02 - B 2.02 - C	medium - medium
1.93	1.93 - A 1.95 - B 1.92 - C	medium - medium
1.91	1.92 - A 1.90 - B 1.91 - C	strong - medium



glassy phase, or they effectively act as an impurity in one or more of the crystal phases, or they play a role in both of these situations. There is also no trace of any sodium halo-borate phase.

Most of the lines can be accounted for by the presence of three sodium borate phases, $\text{Na}_2\text{B}_4\text{O}_7$, $\text{Na}_4\text{B}_2\text{O}_5$ and $\text{Na}_6\text{B}_2\text{O}_6$. The diffraction lines due to $\text{Na}_2\text{B}_4\text{O}_7$ tend to be strongest at low concentrations. This is not very surprising as $\text{Na}_2\text{B}_4\text{O}_7$ is the chemical composition of the undoped parent glass. The strength

of the contribution from $\text{Na}_4\text{B}_2\text{O}_5$ increases with NaCl content. It should be noted that this phase has a higher sodium content than $\text{Na}_2\text{B}_4\text{O}_7$, a fact which is mirrored by the composition of the present glasses in question, i.e. 30% NaCl + 70% borax has a higher atomic percentage of sodium than 100% borax (see Table 5.6). These trends seem quite consistent though an anomaly does appear to exist for the line corresponding to a d-spacing of 2.52 Å.

The presence of $\text{Na}_6\text{B}_2\text{O}_6$ is rather more debatable. On no occasion can its presence alone account for a particular diffraction line. However, it must be included in the list of possible phases because all its strong lines are present on the observed diffraction pattern.

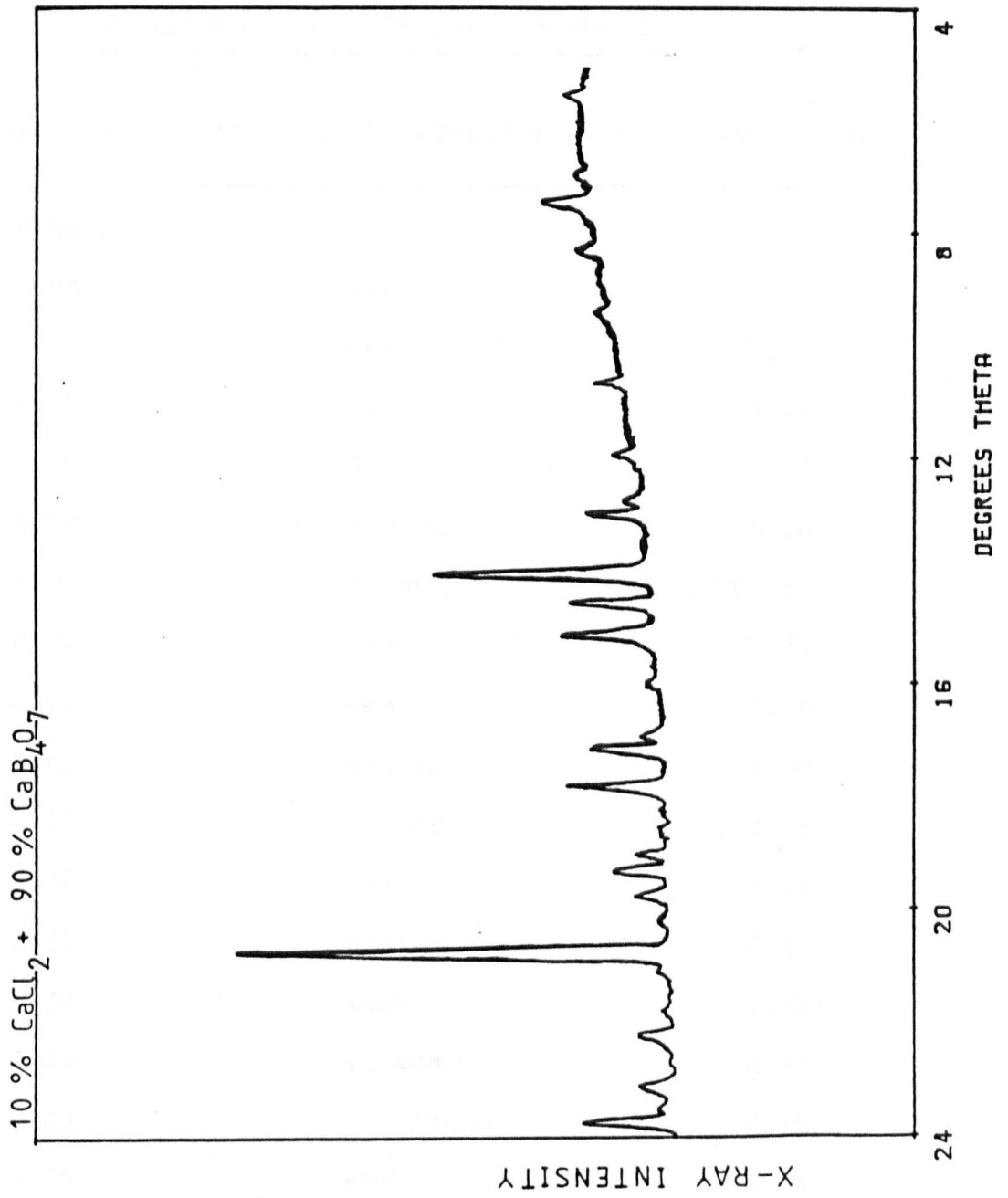
A further point of interest is that all the phases have a sodium content equal to, or greater than, the parent glass. This means that the residual glassy material is comparatively deficient in sodium. This fact supports the evidence produced in the previous Chapter, that it is the crystalline material, not the residual glassy phase, that is highly conducting.

X-ray diffraction analysis was also undertaken for the alkali-free materials. The observed diffraction pattern for a re-crystallised sample of composition 10% CaCl_2 + 90% CaB_4O_7 is shown in Fig. 6.10. Analysis of this trace shows that the crystalline phase is conclusively CaB_2O_4 . The correlations are shown in Table 6.4. It should be noted that this transformation would leave the residual glassy phase severely depleted in calcium in comparison to the original glass.

As has been discovered in all previous cases, no trace of a halide phase, nor of a halo-borate phase, is present in the diffraction pattern. This is perhaps the most startling outcome

FIGURE 6.10

DIFFRACTOMETER TRACE



of the X-ray diffraction investigations.

In general, relatively common crystalline phases have been found to appear on crystallisation of the mixed glasses. These alone cannot account for the large increase in conductivity.

Table 6.4

Analysis of the Diffraction Pattern for a Sample of
Re-crystallised 10% CaCl₂ + 90% CaB₄O₇.

<u>d-spacing</u> <u>Å</u>	<u>Strength of Diffraction Line</u>	<u>Correlation</u>
5.98	weak	-
3.75	weak	-
3.57	weak	3.57
3.45	medium	3.44
3.19	v. strong	3.12
3.09	medium	3.10
2.97	strong	3.00 or 2.95
2.81	weak	2.81
2.67	weak	2.66
2.63	medium	2.60
2.53	strong	2.53
2.38	weak	2.41
2.35	weak	2.35
2.30	weak	2.31
2.25	v. weak	2.23
2.19	v. strong	2.14
2.05	weak	2.04
1.98	weak	2.00

cont'd...

Table 6.4 (...cont'd)

<u>d-spacing</u> <u>Å</u>	<u>Strength of Diffraction Line</u>	<u>Correlation</u>
1.92	strong	1.94 or 1.92
1.88	weak	1.84
1.70	weak	1.68
1.69	weak	
1.53	weak	1.50
1.37	weak	1.37
1.33	weak	1.34

6.2 Electron Microscopy.

In support of the work on crystal phase identification, carried out by X-ray diffraction studies, the physical appearance of the crystals was examined by scanning electron microscopy (S.E.M.), and the chemical composition of the specimens was analysed semi-quantitatively by associated E.D.A.X. measurements. The apparatus and technique used was discussed fully in Section 4.3.

It was decided to concentrate on two compositions that showed typical behaviour as far as electrical conductivity was concerned. The first composition chosen was 10% ZnCl_2 + 90% borax. It was thought that this composition would exhibit interesting features microscopically due to its tendency to surface crystallise (see Section 5.1.2). This indeed proved to be the case. Micrographs of a specimen heat treated at 700°C for 2 hours are shown in Figs. 6.11 and 6.12. The specimen was in the usual disc form. Fig. 6.11 shows the flat surface of the disc, Fig. 6.12 is a

FIGURE 6·11

Micrograph: 10 % $ZnCl_2$ + 90 % BORAX
Surface of a disc specimen

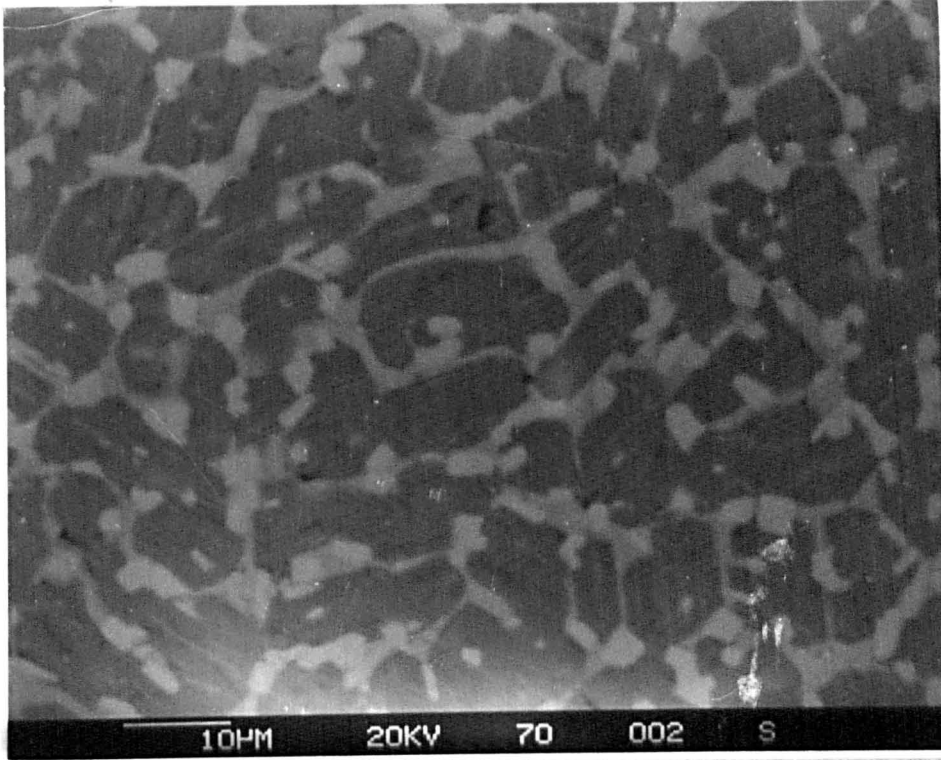
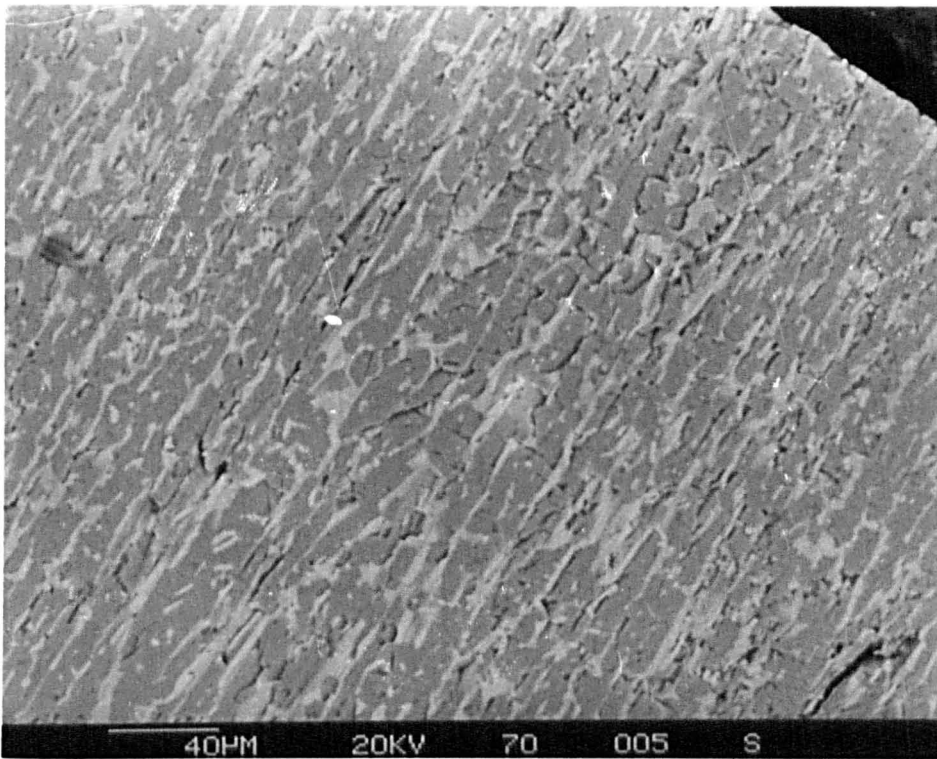


FIGURE 6·12

Micrograph: As above, cross-sectional view



cross-section through the disc. In this latter figure, the flat surface of the disc is shown in the upper right-hand corner of the micrograph in order that the orientation of the specimen may be ascertained.

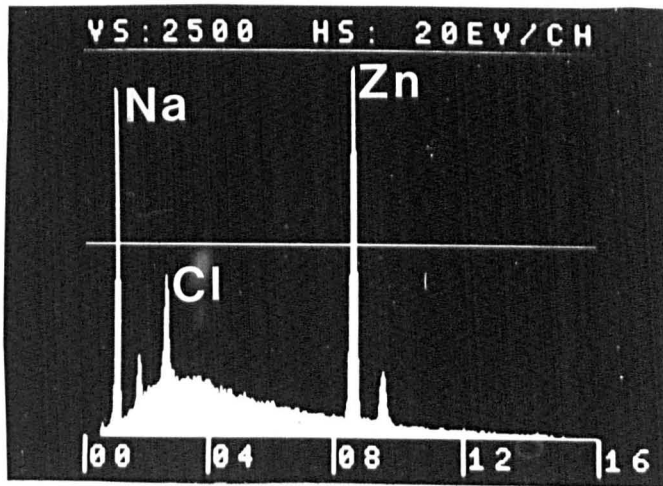
The micrographs were obtained using back-scattered imaging. This process enhances atomic number contrast rather than topographical features. Thus the regions of the material containing heavy elements appear lighter in the electron micrographs than those regions containing only elements of low atomic number.

On both figures two types of 'light' crystals can be seen against a darker background. The E.D.A.X. probing of these light and dark areas, see Figs. 6.13A and 6.13B, reveals that the zinc atoms are almost wholly contained within the 'light' phases and that chlorine atoms are distributed throughout all the material. These findings greatly support the previous X-ray work in which this sample was found to consist of two zinc borate phases, which it is believed correspond to the lighter regions, plus a borax phase, now considered to be the darker background. It is probable that the background is made up of a mixture of crystal and glassy borax phases; it is not possible to differentiate between them because of lack of atomic number contrast.

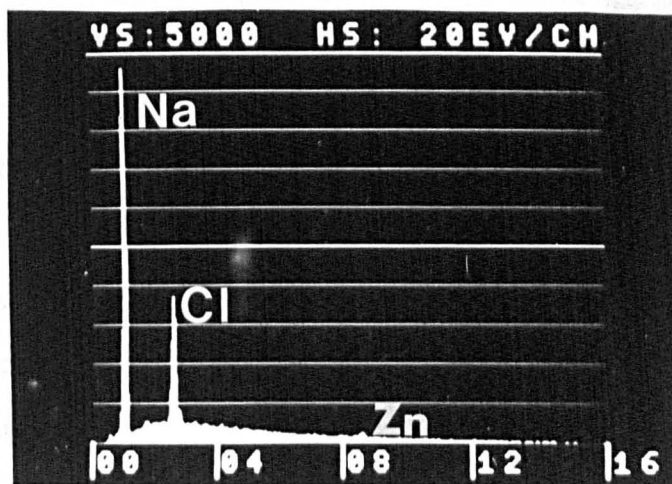
One further interesting effect with this material is the apparent preferred orientation of the crystals. Figs. 6.11 and 6.12 clearly show that the crystals have tended to grow perpendicular to the flat surface of the disc. One manifestation of this effect is the appearance of surface crystallisation. This was mentioned earlier in Section 5.1.2. This surface crystallisation

FIGURE 6.13

A: E.D.A.X. Analysis of 'light' areas of Fig. 6.11



B: E.D.A.X. Analysis of 'dark' areas of Fig. 6.11



is best illustrated by observing a specimen that has been heat treated at a lower temperature, and is only partly crystalline. Such a sample is shown in Fig. 6.14; it had been heat treated at 550°C for 2 hours. Despite the specimen being rather fractured the cross-section shows three distinct regions; two crystalline regions near the surfaces of the disc, plus a glassy interior.

Another point that should be mentioned concerns the size of the crystallites. Figs. 6.11 and 6.12 show a sample heat treated at 700°C, and in this case the crystals are typically of the order of a few microns in width by perhaps ten microns in length. This is quite large and no problems at all are encountered in their observation. However, if the heat treatment temperature is reduced to 600°C or 550°C then the situation changes completely. No individual crystallites could be observed in either of these latter cases. The size of the crystallites had been reduced to below the resolution of the electron microscope and/or the degree of contrast between the two regions had been severely diminished.

The second composition to be investigated by electron microscopy was 10% CaCl_2 + 90% borax, with heat treatments of 2 hours at 700°C, 600°C and 550°C being used. No preferred crystal orientation, or surface crystallisation, was observed. The appearance of the specimen is shown in Fig. 6.15A, and in greater detail in Fig. 6.15B. Again, one or more light crystalline phases can be seen against a dark background. Back scattered electron imaging was used.

E.D.A.X. studies on the two regions are shown in Figs. 6.16 and 6.17. The dopant metal ion, this time the calcium ion, is again more prevalent in the lighter phase. With knowledge of the X-ray results for this sample (see earlier), the obvious

FIGURE 6.14

Micrograph: 10 % $ZnCl_2$ + 90 % BORAX
Heat Treated at $550^{\circ}C$
Cross-Sectional View

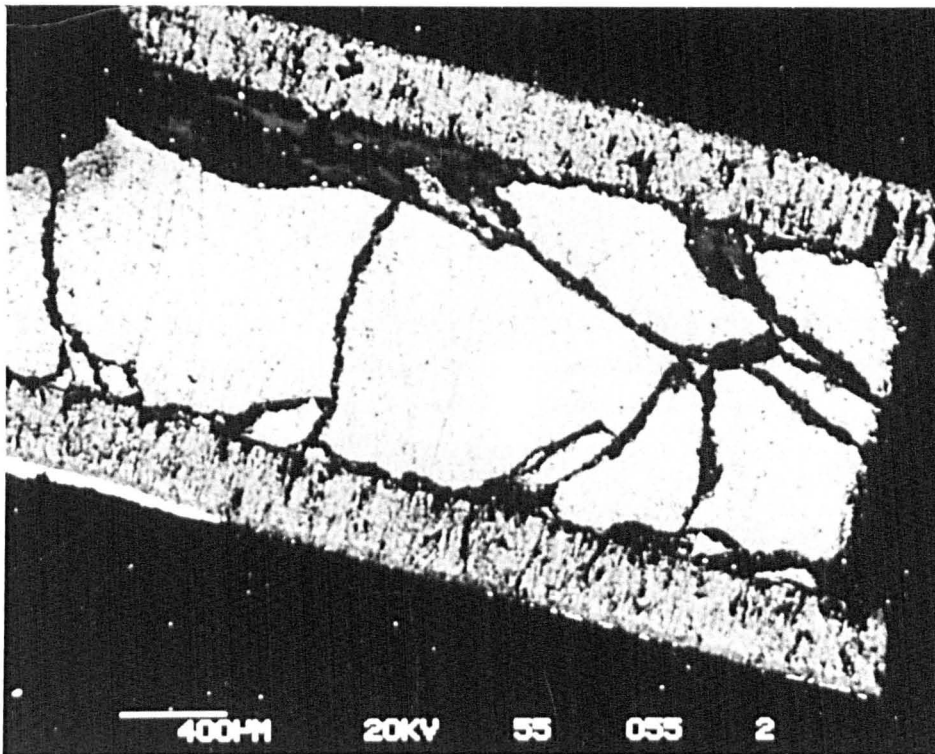
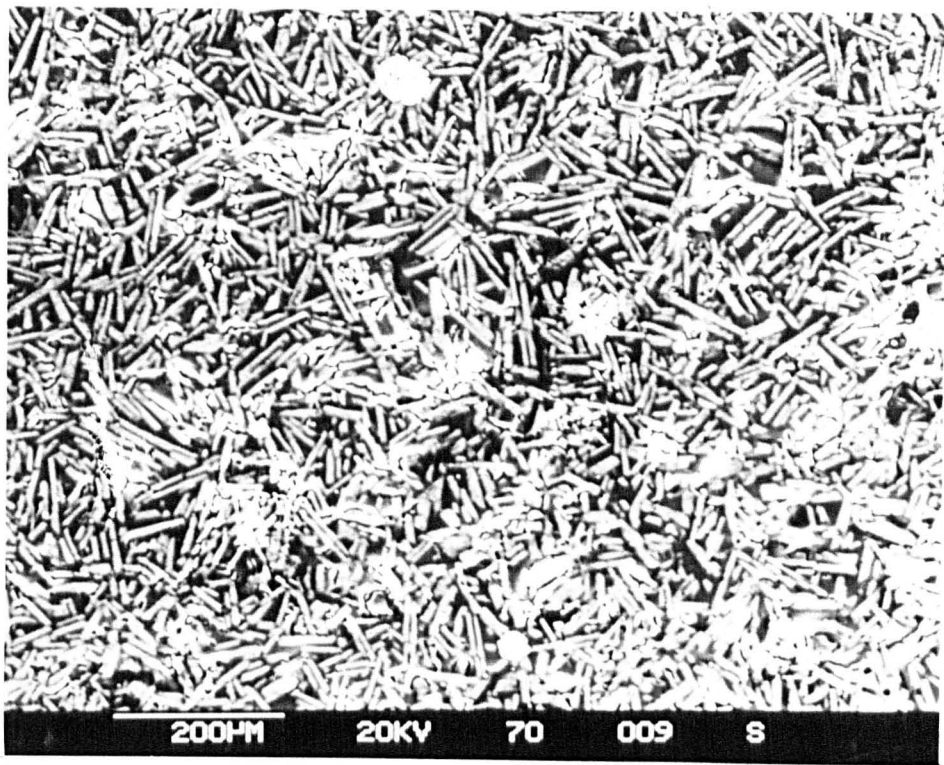


FIGURE 6.15

A Micrograph: 10% CaCl_2 + 90% BORAX
Heat Treated at 700°C



B Micrograph: As above, close-up

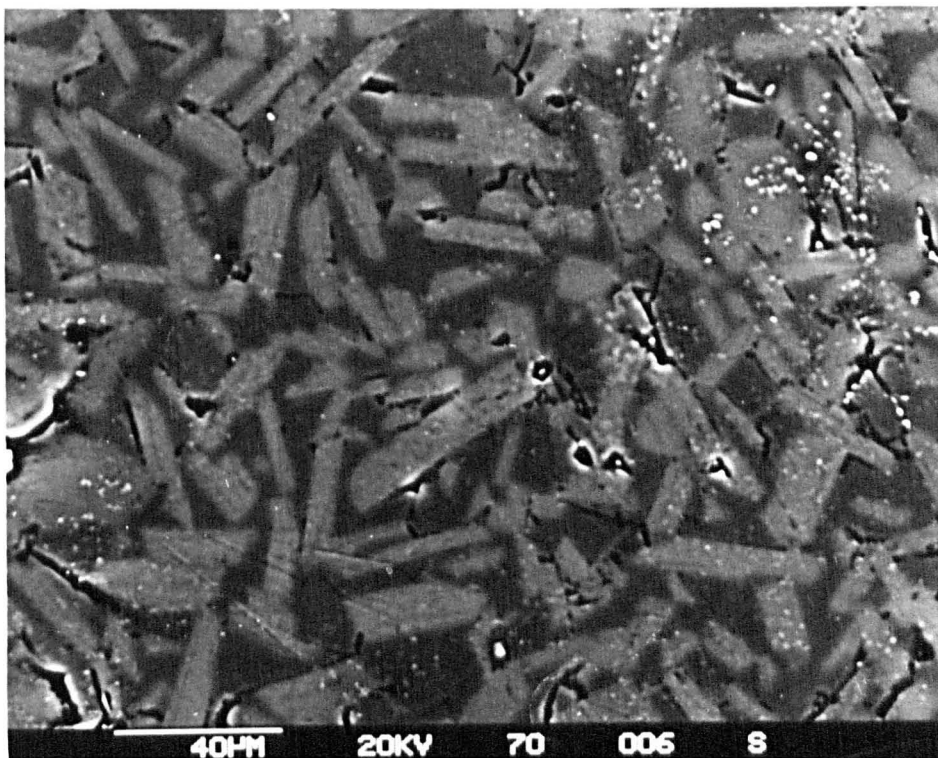


FIGURE 6.16

E.D.A.X. Analysis of 'light' areas of Fig. 6.15

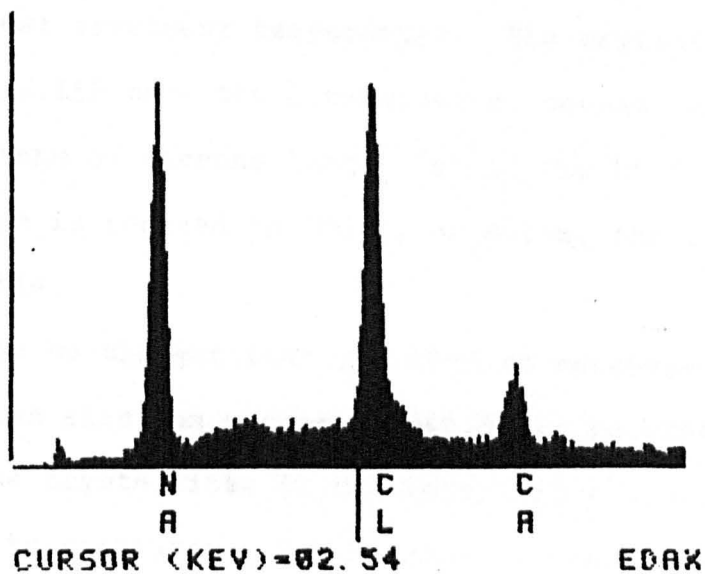
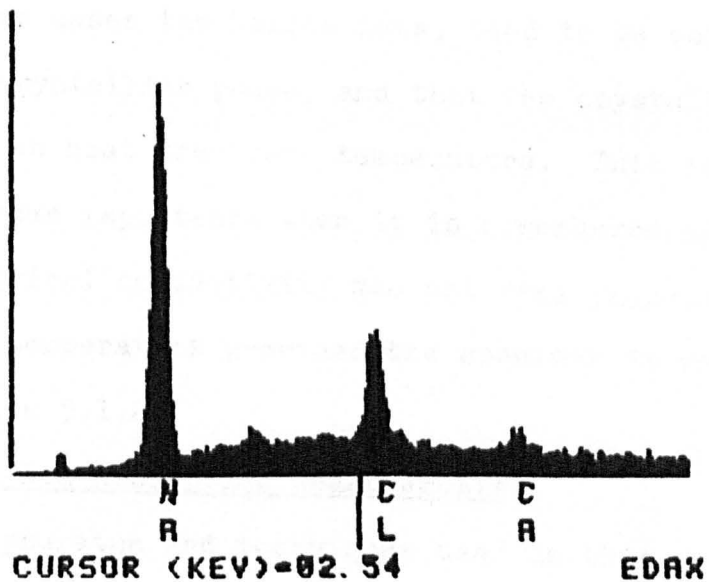


FIGURE 6.17

E.D.A.X. Analysis of 'dark' areas of Fig. 6.15



conclusion is that the specimen contains calcium borate crystals in a borax background.

Another consistency observed is the dependence of crystallite size on heat treatment temperature. The crystallites in Figs. 6.15A and 6.15B have the dimensions of several microns; some are even tens of microns long. Yet if the heat treatment temperature is reduced to 600°C, or below, the crystals become unobservable.

It may be thought that the obvious recourse was to utilise transmission electron microscopy (T.E.M.) in order to try to observe the crystallites in the materials subjected to lower heat treatment temperatures. T.E.M. shows a considerable advantage over S.E.M. in terms of resolution limits. However, advice was received that simple borate materials are far too volatile to stand up to the intense electron beam associated with T.E.M. and hence the exercise would prove fruitless.

In summary, it has been found that the dopant metal ions, and in some cases the halide ions, tend to be concentrated in the emerging crystalline phase, and that the crystallite size is very dependent on heat treatment temperature. This latter statement is of extreme importance when it is remembered that it was found that electrical conductivity was not very dependent on heat treatment temperature provided the specimen is well crystalline (see section 5.1.2).

6.3 Infra-Red Absorption Measurements.

The apparatus and techniques used in this work are discussed fully in section 4.6.

The infra-red absorption properties of boric oxide and simple binary sodium borate glasses have been investigated by many

authors (e.g. 203 - 206, 327 - 332). Naturally, the glass with the borax composition has been included in some of the tests. It is generally reported that the absorption spectrum for this glass consists of at least two broad bands, centred on approximately 1350cm^{-1} and 990cm^{-1} , plus a smaller band at 710cm^{-1} . Various authors report that the central of these bands is subdivided into two bands at 950cm^{-1} and 1050cm^{-1} , though the idea of this further subdivision being caused by the presence of water is mentioned by some (e.g. 329).

A summary of previously reported infra-red absorption curves for sodium borate glasses is given in Table 6.5. The influence of alkali content on the strength of various bands is indicated, as is the allocation of particular molecular vibrations to each absorption peak. It is not surprising that the absorption bands found for the glass of the borax composition, i.e. a relatively high alkali content, are those predominantly associated with tetrahedrally co-ordinated boron.

Unless stated in the text, all the spectra to be discussed here were obtained by using the KBr disc method (see section 4.6).

Borax glass was used as the starting point in this study; the absorption spectrum obtained is shown in Fig. 6.18. It can be seen that there is good agreement between this spectrum and the established reported results. There appears to be little or no splitting of the central band. In order to investigate the effect of water the glass was allowed to become damp prior to measurement. The absorption spectrum for this sample is shown in Fig. 6.19. Indeed, not only does the central band subdivide but several other subdivisions occur also. This shows that considerable care has to be taken in maintaining the dryness of

INFRA-RED ABSORPTION SPECTRUM

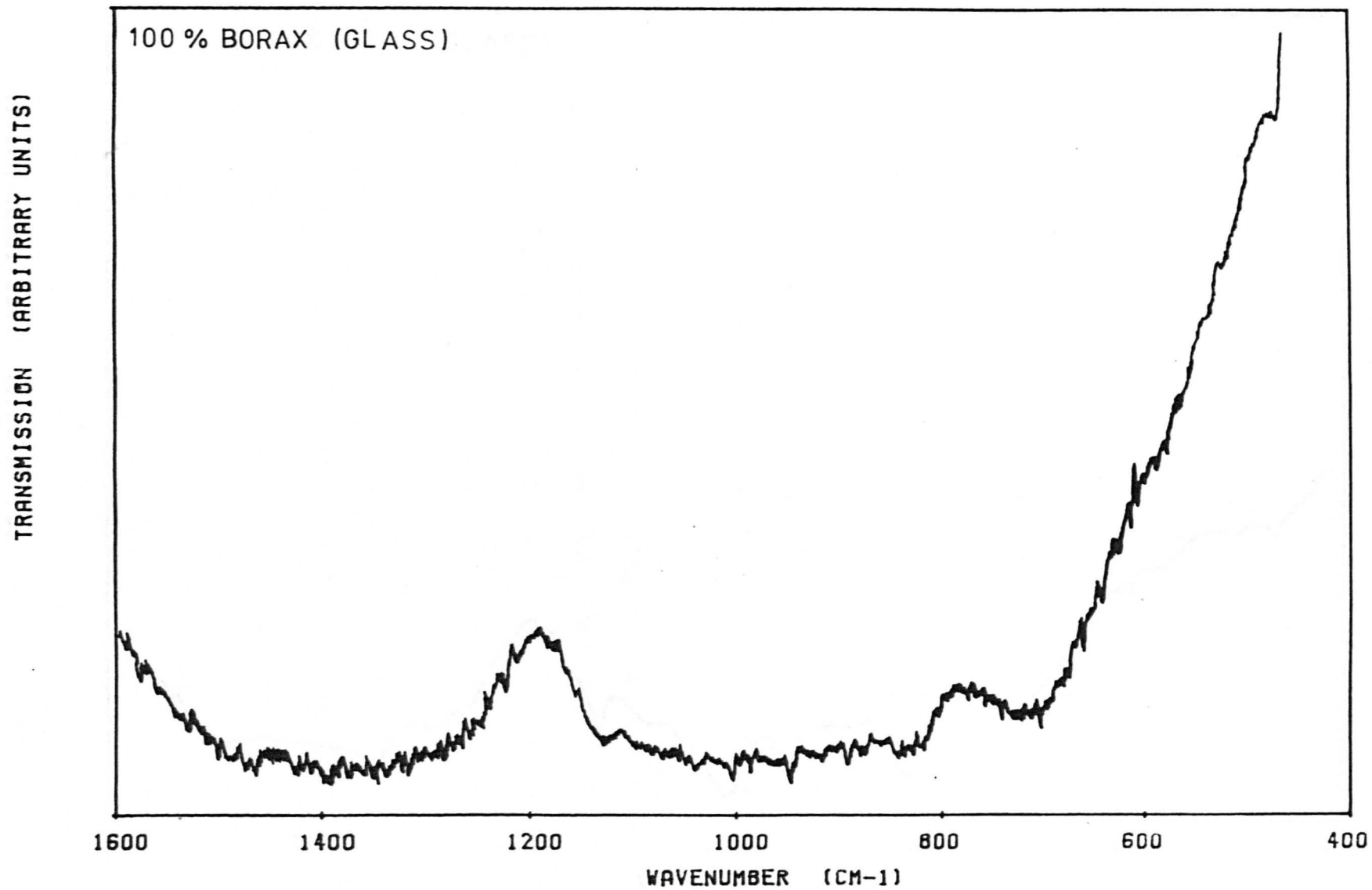


FIGURE 6.18

FIGURE 6.19

INFRA-RED ABSORPTION SPECTRUM

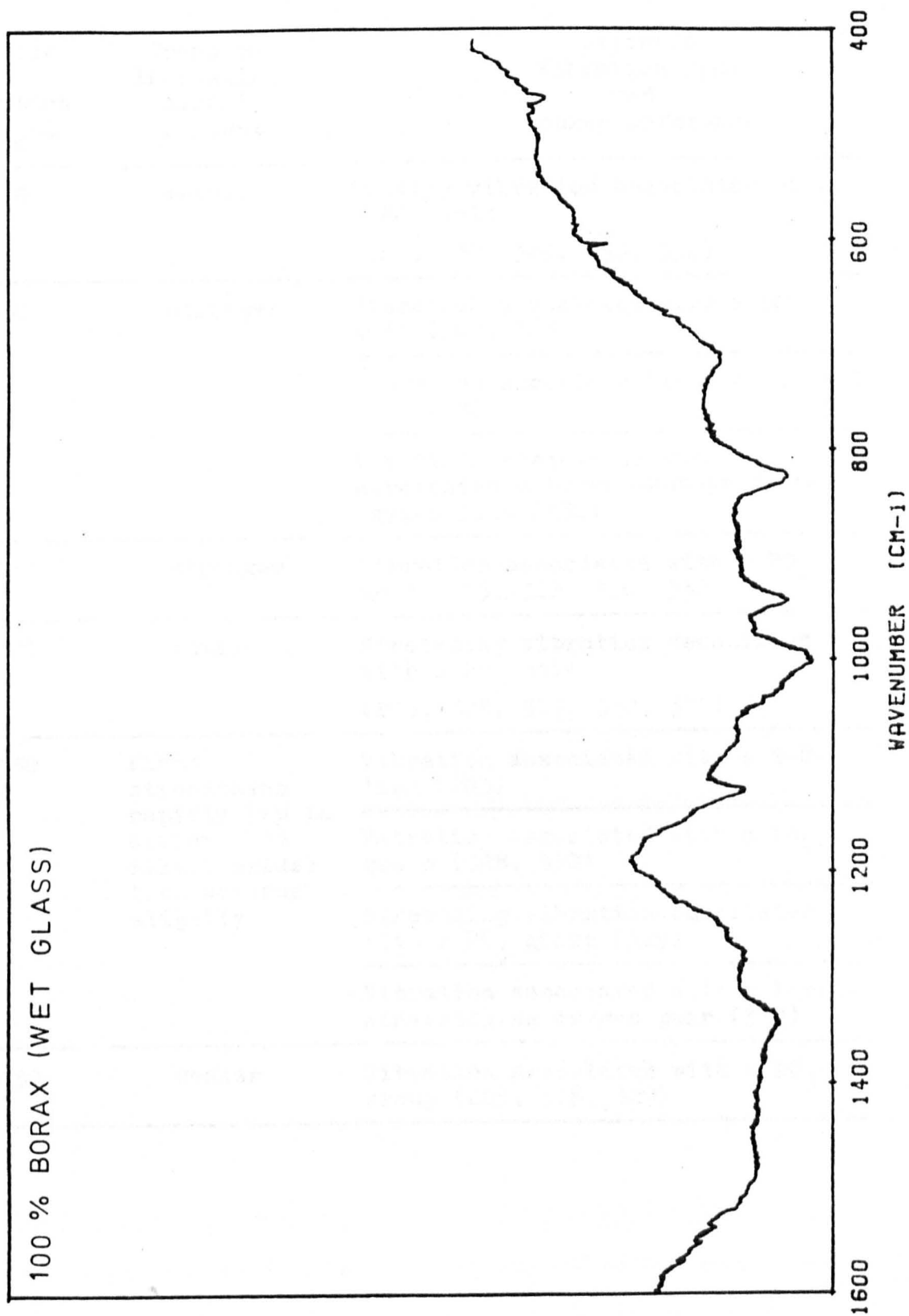


Table 6.5

Published Infra-red Absorption Data
for Alkali-Borate Glasses.

Position of Absorption Peak cm^{-1}	Trend on Increasing Alkali Content	Reported Vibration Type and Source Reference
710	weaker	Bending vibration associated with a BO_3 unit (205, 328, 329, 330, 332)
950	stronger	Vibration associated with a BO_4 unit (205, 328) Vibration associated with a boroxol unit (332) Vibration associated with stretching a boron—non-bridging oxygen link (330)
1050	stronger	Vibration associated with a BO_4 unit (205, 328, 330, 332)
1270	weaker	Stretching vibration associated with a BO_3 unit (205, 328, 329, 330, 332)
1350	First strengthens rapidly (up to approx. 15% alkali oxide) then weakens slightly	Vibration associated with a B-O-B link (205) Vibration associated with a BO_4 group (328, 330) Stretching vibration associated with a BO_3 group (329) Vibration associated with a boron-non-bridging oxygen pair (332)
1450	weaker	Vibration associated with a BO_3 group (205, 328, 329)

specimens if useful comparisons of spectra are to be made. This point was noted and due consideration was given to it.

Virtually all of the glasses studied regarding their electrical conductivity properties were also scrutinised by infra-red absorption measurements. However, to avoid unnecessary repetition, only a few illustrative examples will be given here.

Fig. 6.20 shows the absorption curve for the glass of composition 10% ZnCl_2 + 90% borax. The important point to be noted is the almost exact similarity to that observed with pure borax. The added halide does not appear to have altered the infra-red absorptive properties to any noticeable degree.

The curve obtained from the glass of composition 20% CaCl_2 + 80% borax is shown in Fig. 6.21. Even at this relatively high level of doping there is no definite change in the observed trace compared to pure borax.

Indeed, similar curves were obtained irrespective of the type of dopant used. Glass containing 20 mol.%, and occasionally as much as 30 mol.%, of added halides were regularly scrutinised and on no occasion were any new features on the absorption curve definitely identified.

It becomes necessary to surmise where changes in the absorption curve may have been expected, though even here the situation is far from clear cut. If the added halide ion becomes bonded in some way to the boron atom then bending or stretching modes resulting from this linkage would be one possibility. However, at the present time it is not believed that vibrational frequencies for such pairings in a glassy network have been published. The nearest similar data appears to be that concerned with crystalline boron trihalides, and it is thought that

INFRA-RED ABSORPTION SPECTRUM

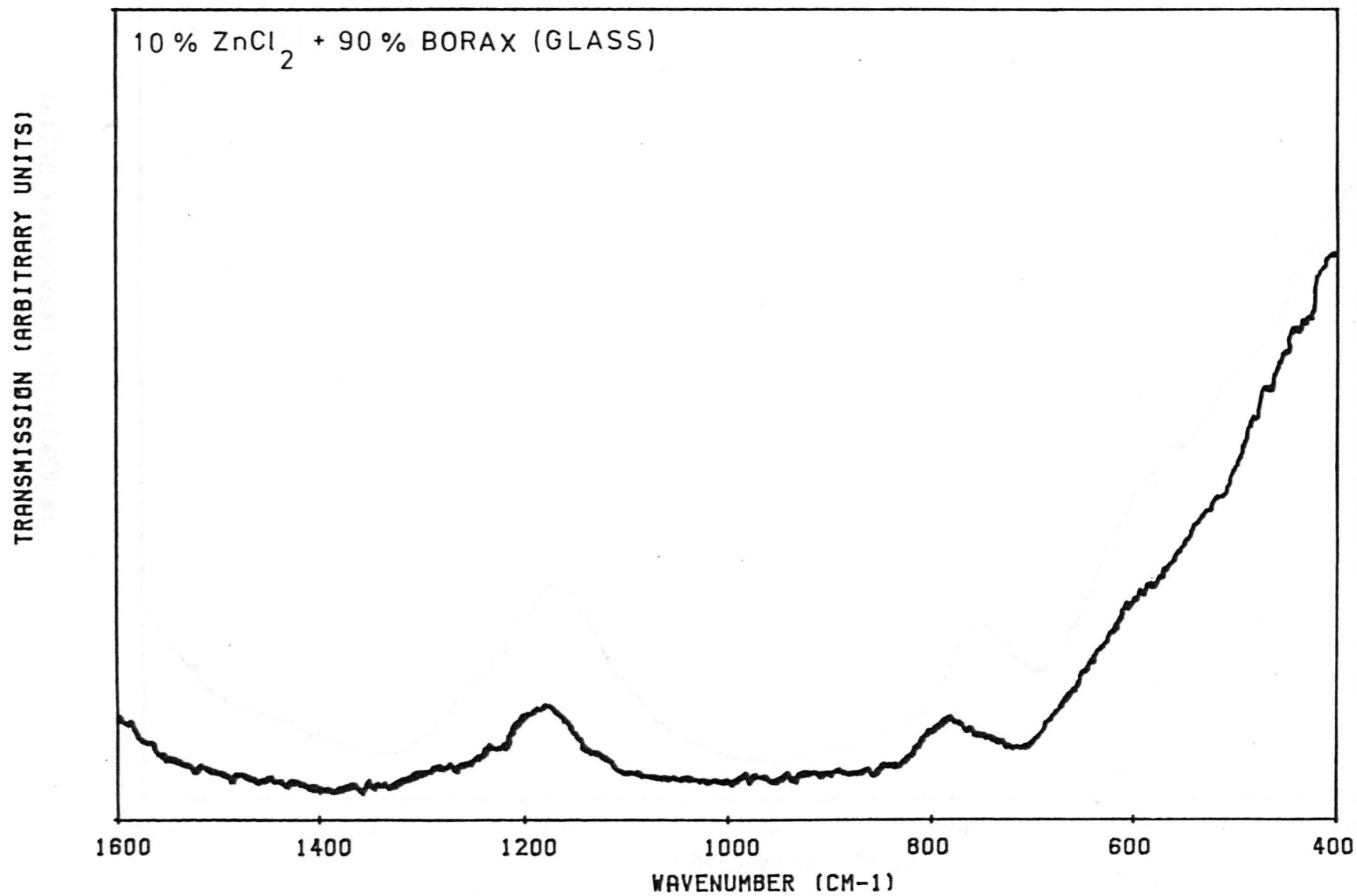


FIGURE 6.20

INFRA-RED ABSORPTION SPECTRUM

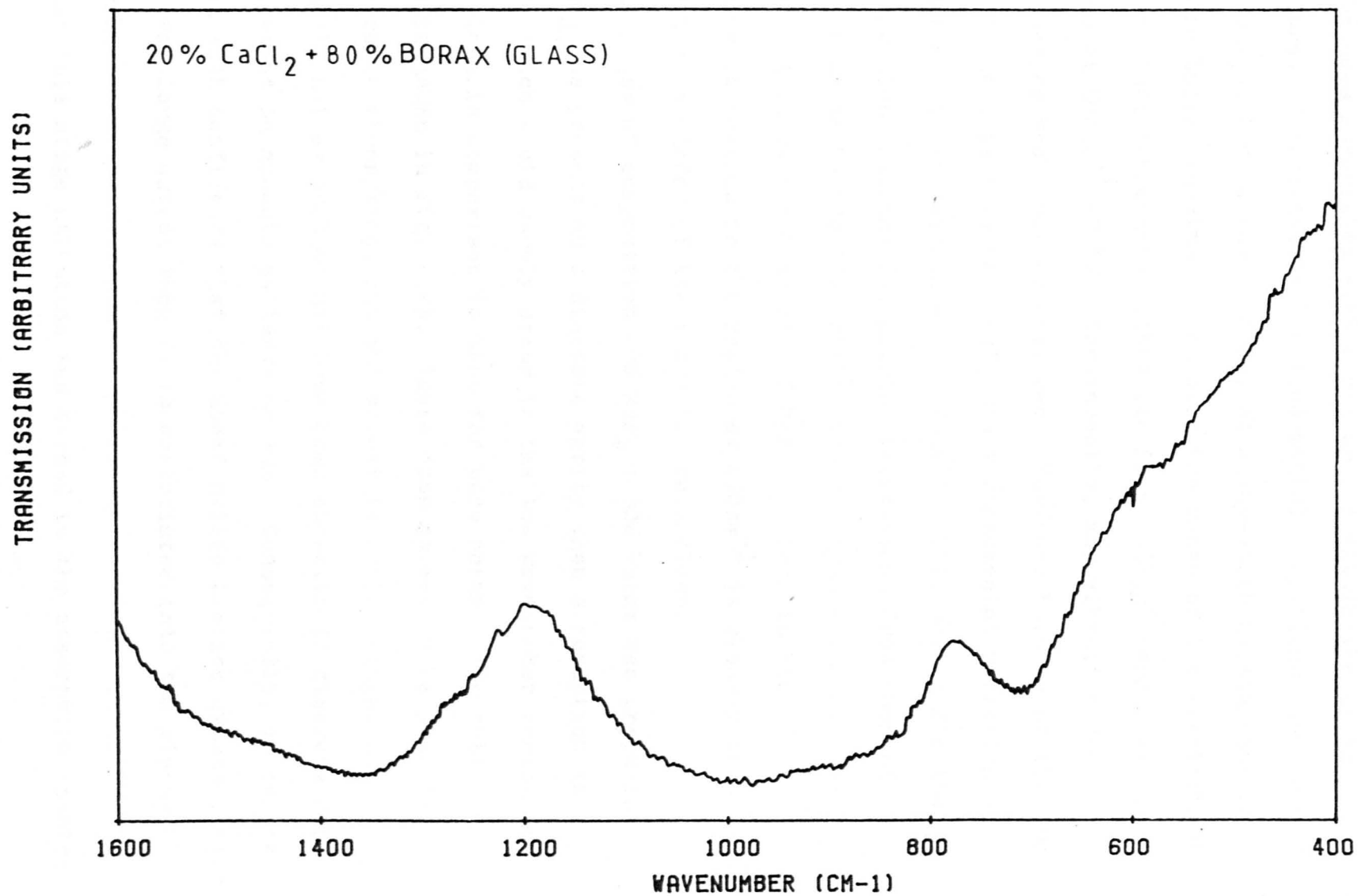


FIGURE 6.21

comparing the two situations would scarcely be valid.

Alternatively the possibility arises as to whether the halide ion remains discretely bonded to the added cations, or even becomes associated with a sodium ion within the glassy structure. Unfortunately the fundamental vibrations associated with most sodium halide bonding, alkaline-earth halide bonding and zinc halide bonding lie outside the range of the spectrometer, e.g. the NaCl fundamental vibration is at 366cm^{-1} and that for NaBr is at 302cm^{-1} (333). Consequently, any vibration due to such species would not be observed. However, because of the low mass of the ions involved, MgF_2 has a fundamental vibration at the rather higher wavenumber of 470cm^{-1} . This represents the only occasion that the fundamental vibrational frequency of an alkaline-earth halide lies within the observable range. The absorption curve for a sample of MgF_2 is shown in Fig. 6.22. A strong absorption in the region of 470cm^{-1} is clearly seen, while the remainder of the trace is featureless.

A glass of composition 20% MgF_2 + 80% borax was prepared. If MgF_2 was present as a discrete entity then a reduction in transmission would surely occur in the low wavenumber region for this glass in comparison to that for pure borax. The obtained curve is shown in Fig. 6.23. There does appear to be a small increase in absorption, but the effect is rather slight and certainly not as much as may have been expected if discrete MgF_2 was present in amounts as large as 20%. Consequently, it can be stated with confidence that the added halide becomes disassociated to a very large extent when it is assimilated into the glassy network.

At this stage attention was turned to the absorption spectra

INFRA-RED ABSORPTION SPECTRUM

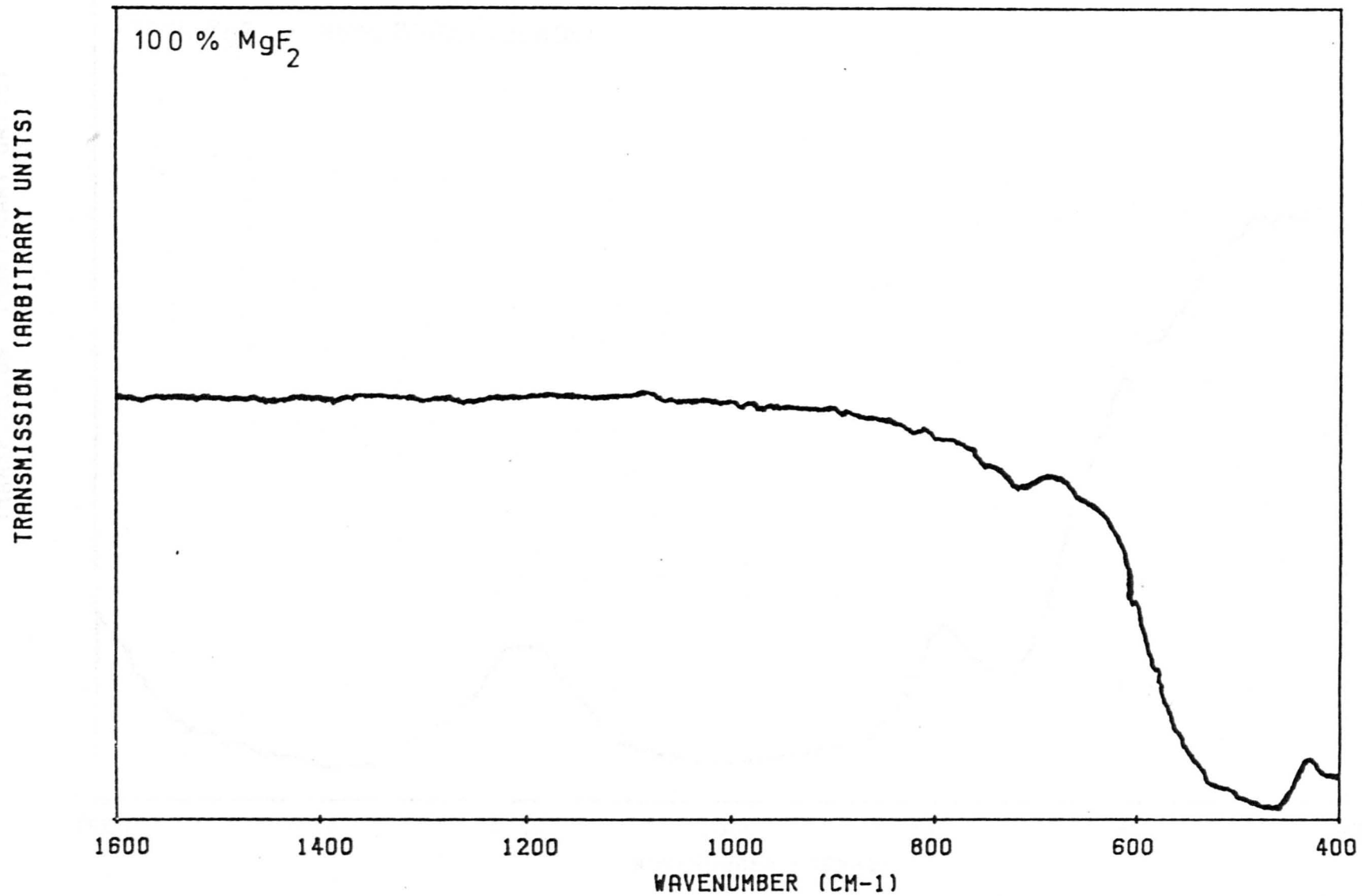


FIGURE 6.22

INFRA-RED ABSORPTION SPECTRUM

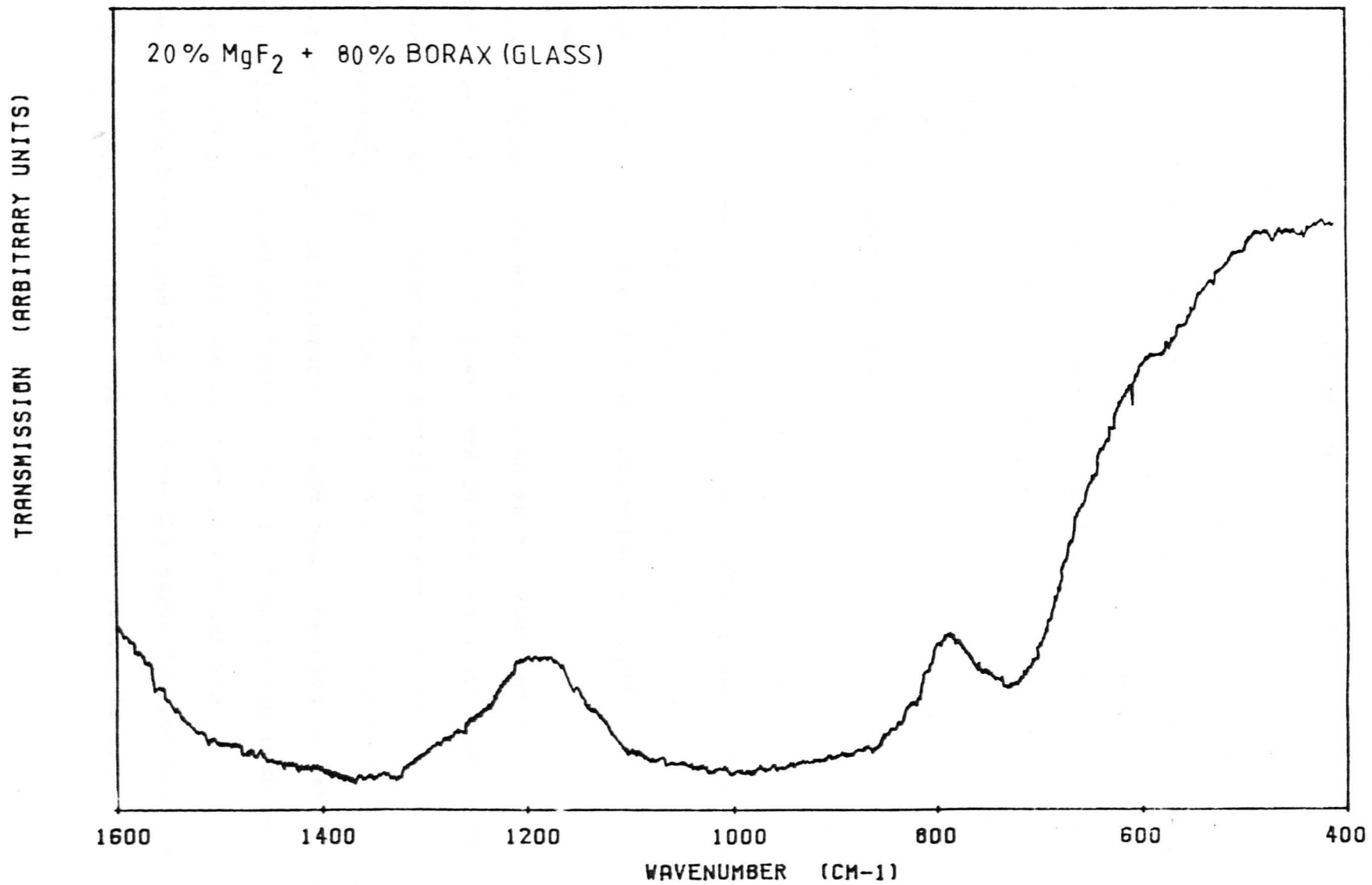


FIGURE 6.23

of re-crystallised materials. Again the main aim of the work was to look for changes in the observed curves brought about by the halide additives.

Firstly a specimen of re-crystallised pure borax was investigated. The resulting trace was then used as a comparative reference. The curve is shown in Fig. 6.24, and it can be seen that a very large number of absorption bands were observed. This study is very much of a comparative nature and so no attempt was made to assign the bands. The re-crystallisation procedure used for this specimen was a heat treatment at 550°C for 2 hours. This was the same heat treatment that was used in the resistivity investigations. Indeed, in order that direct comparisons could be made between resistivity results and infra-red absorption measurements this general rule was applied in all the cases to be discussed here, i.e. the heat treatments used can be ascertained by reference to section 5.1.2. If in this previous section more than one heat treatment was used on a particular composition, then the procedure giving most typical resistivity results was reproduced for the purpose of these infra-red absorption measurements.

A very wide range of compositions were investigated, including virtually all of those used in the resistivity studies. Only some typical specimen curves will be shown, and for comparative purposes the chosen curves will be for the heat treated versions of the illustrative compositions used in the above section on glassy specimens. Fig. 6.25 shows the results obtained for a re-crystallised specimen of composition $10\% \text{ZnCl}_2 + 90\% \text{borax}$, and Fig. 6.26 is the curve for $20\% \text{CaCl}_2 + 80\% \text{borax}$. The quality and resolution of the traces is rather

INFRA-RED ABSORPTION SPECTRUM

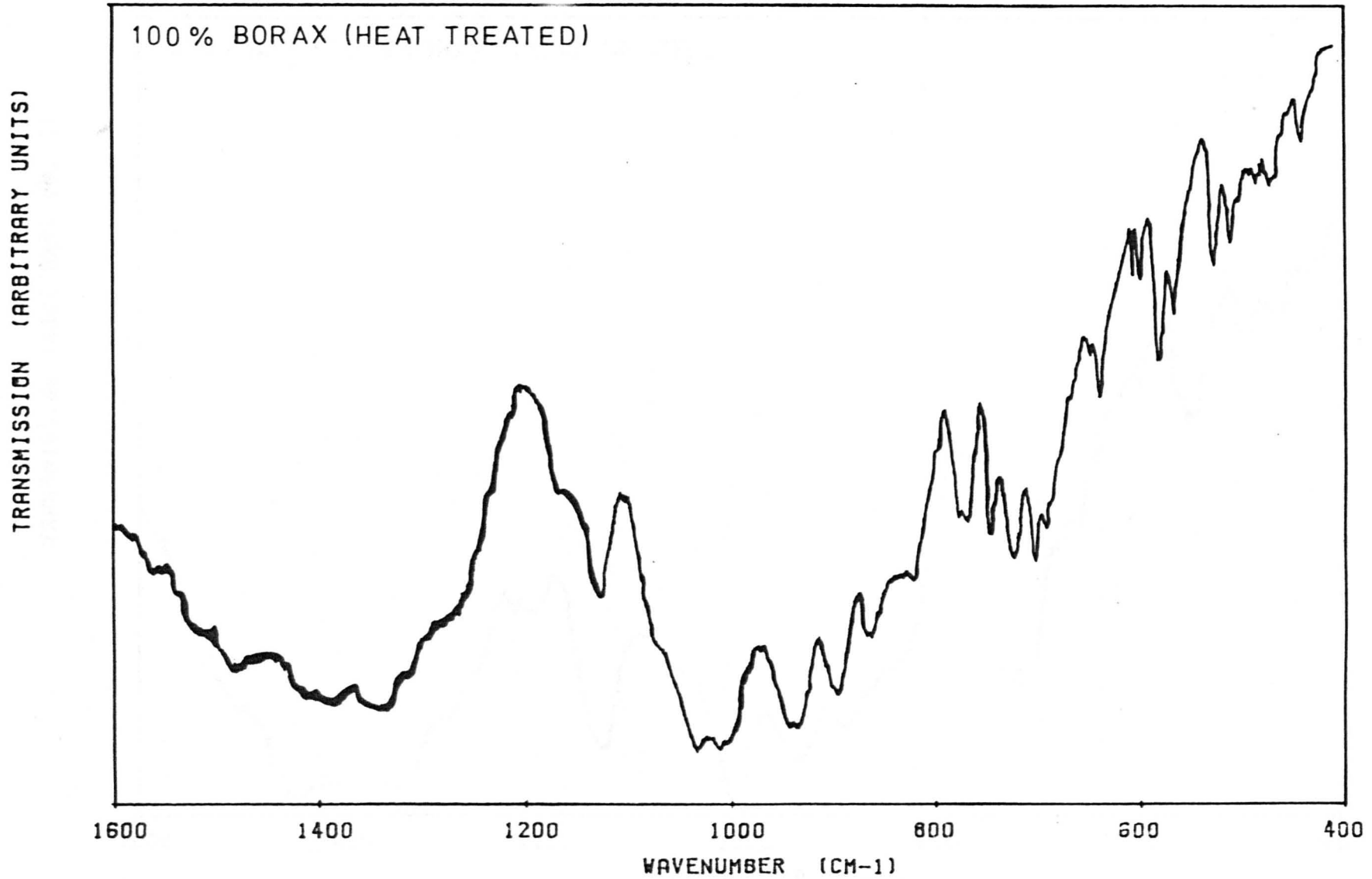


FIGURE 6.24

INFRA-RED ABSORPTION SPECTRUM

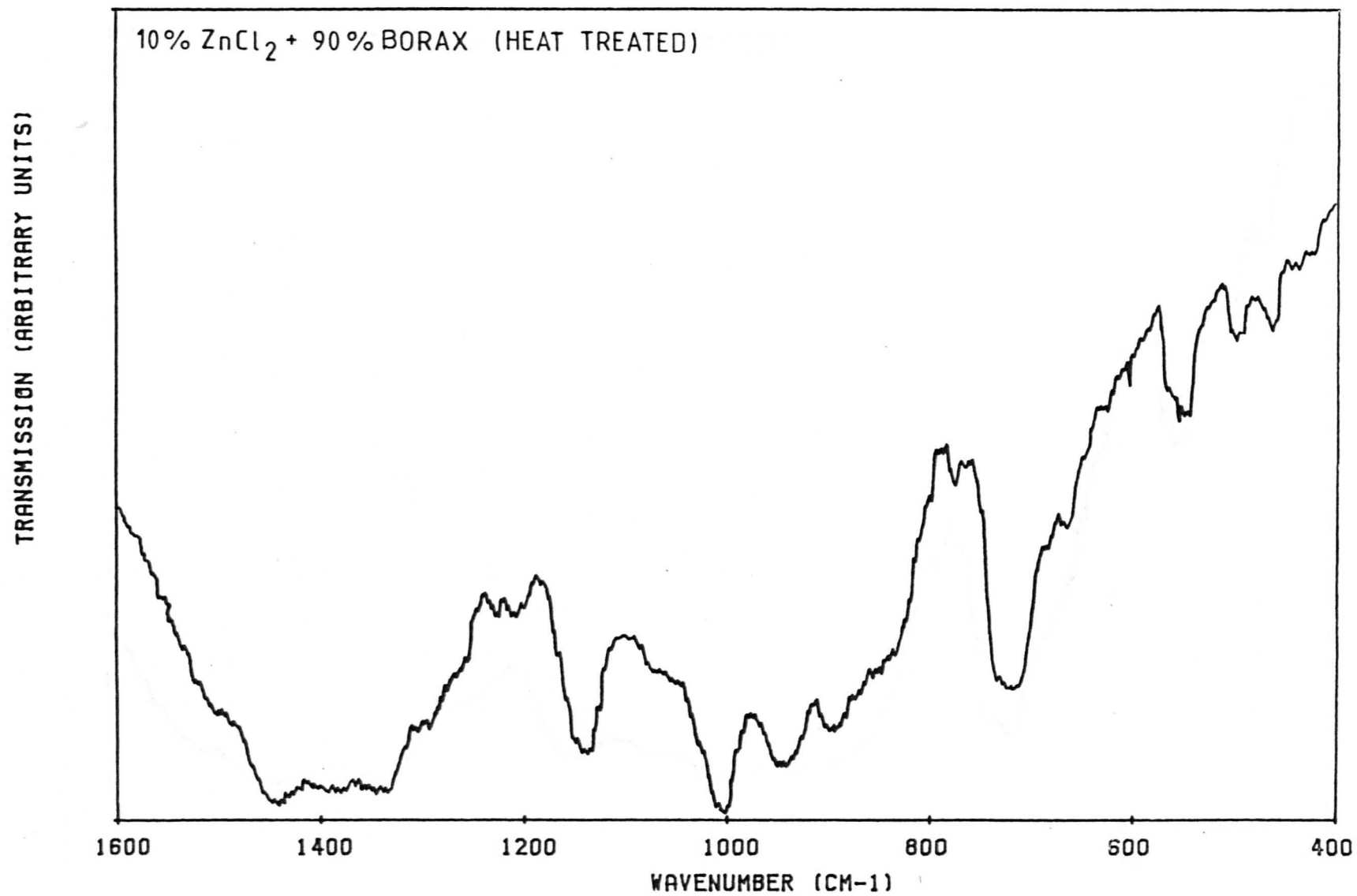


FIGURE 6.25

INFRA-RED ABSORPTION SPECTRUM

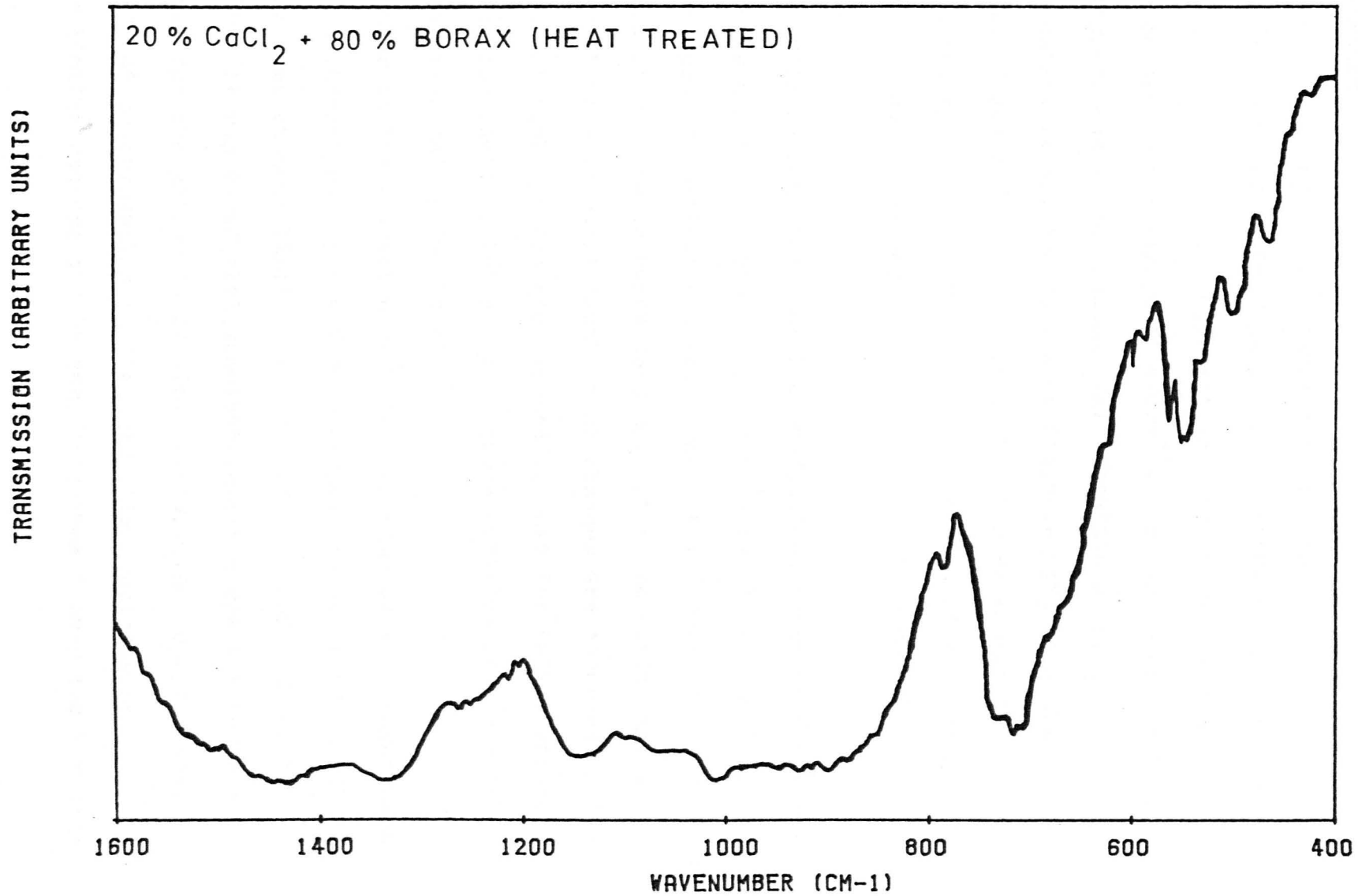


FIGURE 6.26

variable but other than this there is no conclusive difference between these curves and that for re-crystallised pure borax. This similarity is the general result found in all the compositions.

Fig. 6.27 displays the curve obtained for a sample of composition 20% MgF_2 + 80% borax. Overall the trace resembles the results for the other compositions, but a small extra band is noticeable in the region of 470cm^{-1} . As mentioned earlier, this corresponds to the fundamental vibration of MgF_2 . Consequently, it appears that some discrete MgF_2 is still present. However, the vibration is not strong enough to have been caused by all the MgF_2 in the composition of the material, i.e. the added halide remains disassociated to a very large extent.

It will be realised that the conclusions drawn in the work on re-crystallised materials are the same as those resulting from the glassy specimen studies. These are firstly that the addition of halides to borax does not alter the boron-oxygen structural network sufficiently that changes are observed in the main vibrational spectra and, secondly, that the halide becomes greatly disassociated but a few discrete entities may, and in some cases certainly do, remain.

Later in the project some thin film studies were undertaken and a spectrometer with a wider wavenumber range became available. The lower wavenumber limit that could be used was reduced to 180cm^{-1} . It was found that somewhat improved spectra could be obtained for the glassy materials. However, not surprisingly, attempts at re-crystallising the thin film specimens met with rather limited success and no real improvement over the KBr disc

INFRA-RED ABSORPTION SPECTRUM

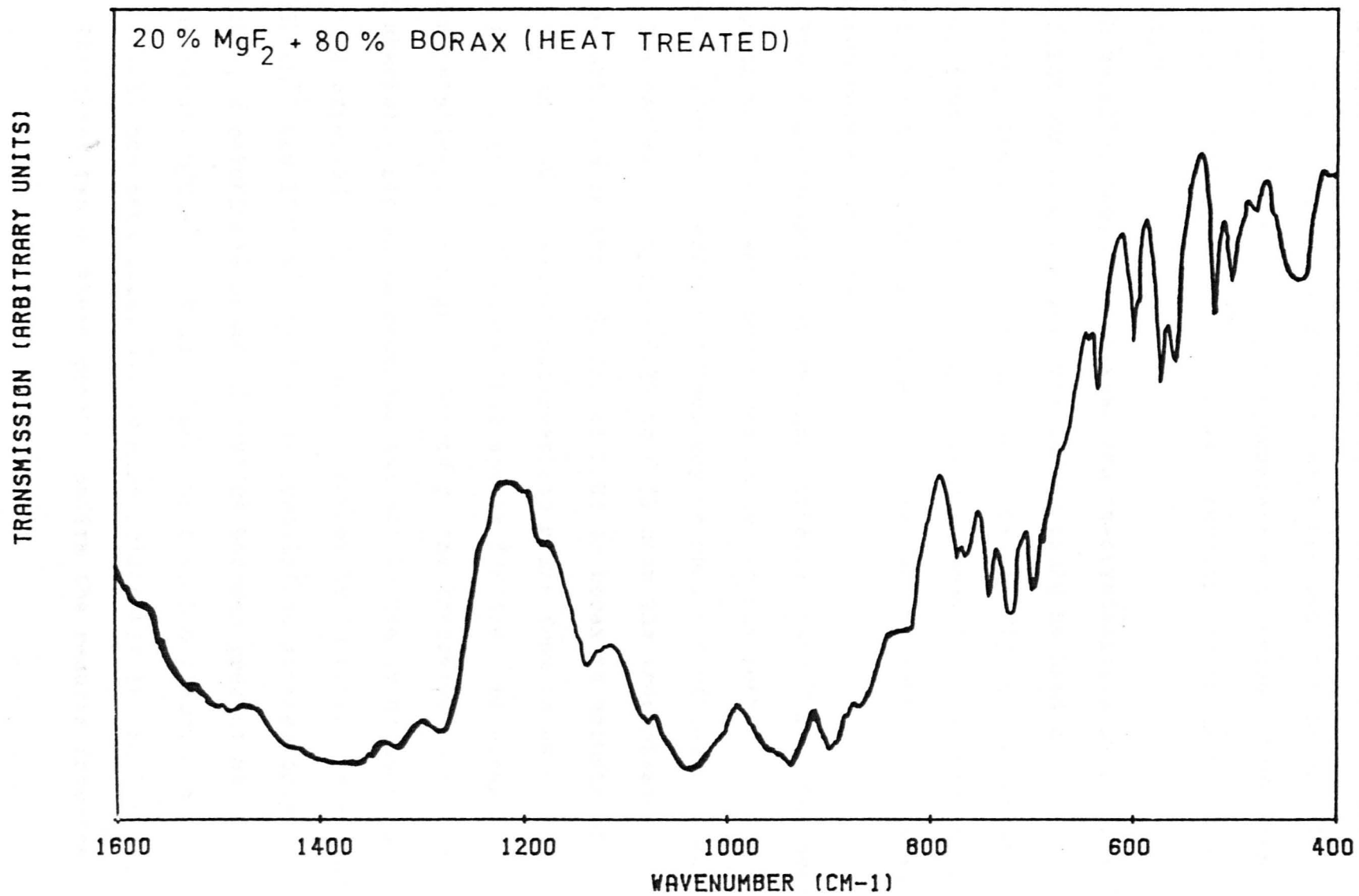


FIGURE 6.27

technique was obtained for this type of material. The heat treatment procedure was again designed to reproduce that used in the resistivity work (section 5.1.2).

An additive studied extensively for its effect on electrical properties was NaCl. The fundamental vibration of this salt is at 366cm^{-1} (333), which is now conveniently in range. Consequently, it was the addition of NaCl that was concentrated on in this new technique.

Naturally, samples of glassy and re-crystallised pure borax were first run in order that the curves could be used as a reference. The spectra obtained are shown in Fig. 6.28. It will be seen that the curve for the glass does show improved resolution over that obtained by the KBr method, though, of course, the main features remain the same.

Fig. 6.29 shows the absorption curve for pure NaCl. The deep trough in the lower wavenumber region is clearly seen, and this gives an idea of where the effect may be on its addition to borax.

The series of Figures 6.30 to 6.32 show the transmission curves obtained on the addition of NaCl to borax in amounts of 10%, 20% and 30%. Several observations arise from these curves. Firstly, the strong features that appear for the pure borax remain relatively unchanged. Secondly, the transmission in the NaCl absorbing region is reduced, but not by nearly as much as might be expected. Thirdly, small, narrow bands gradually appear at 1570cm^{-1} and 1730cm^{-1} in the re-crystallised samples only. Fourthly, a relatively broad absorption becomes present at approximately 530cm^{-1} . This occurs for both the glassy and re-crystallised materials, but is more noticeable in the latter.

The first two of these points confirm the results from the

FIGURE 6.29

INFRA-RED ABSORPTION SPECTRUM

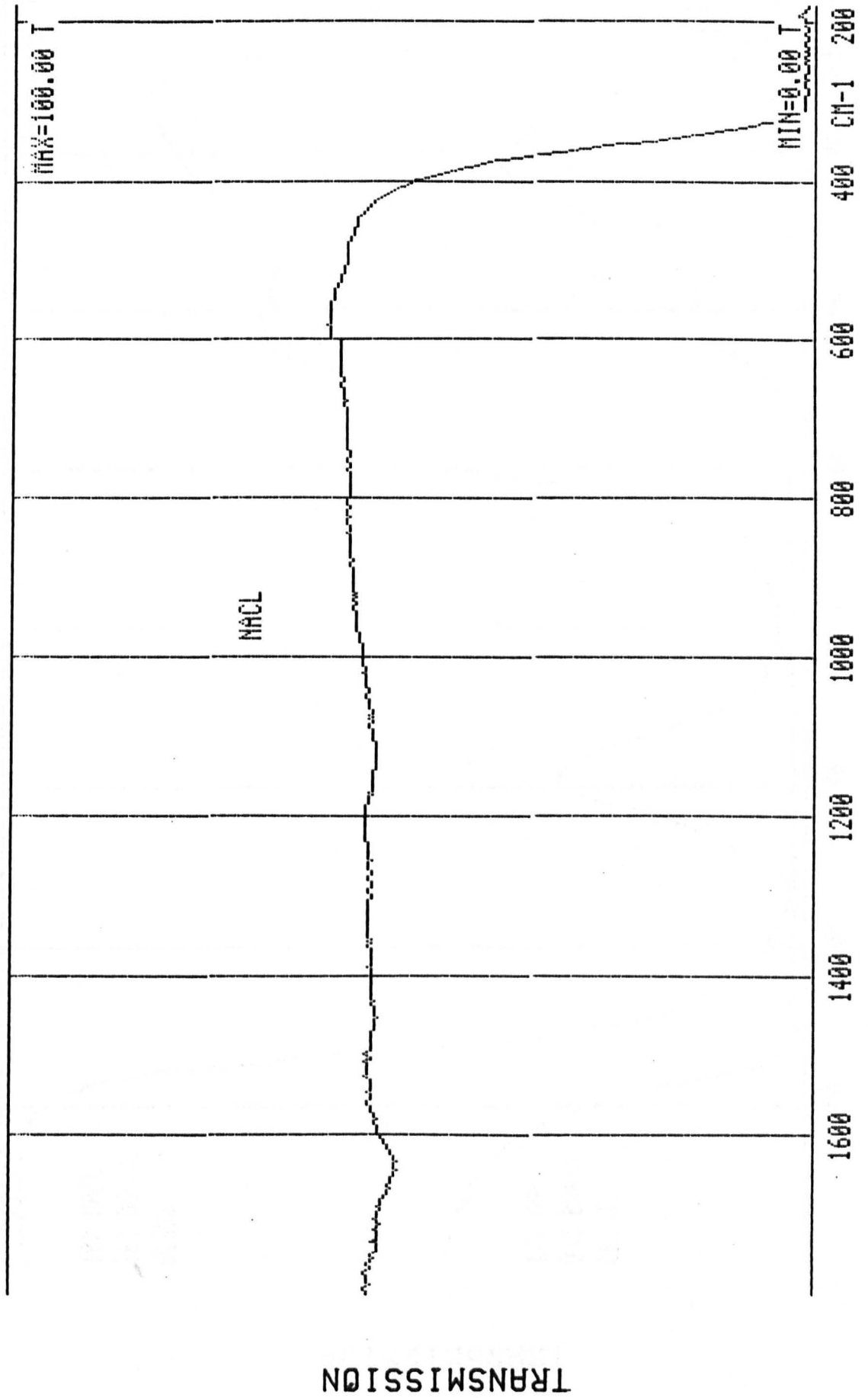
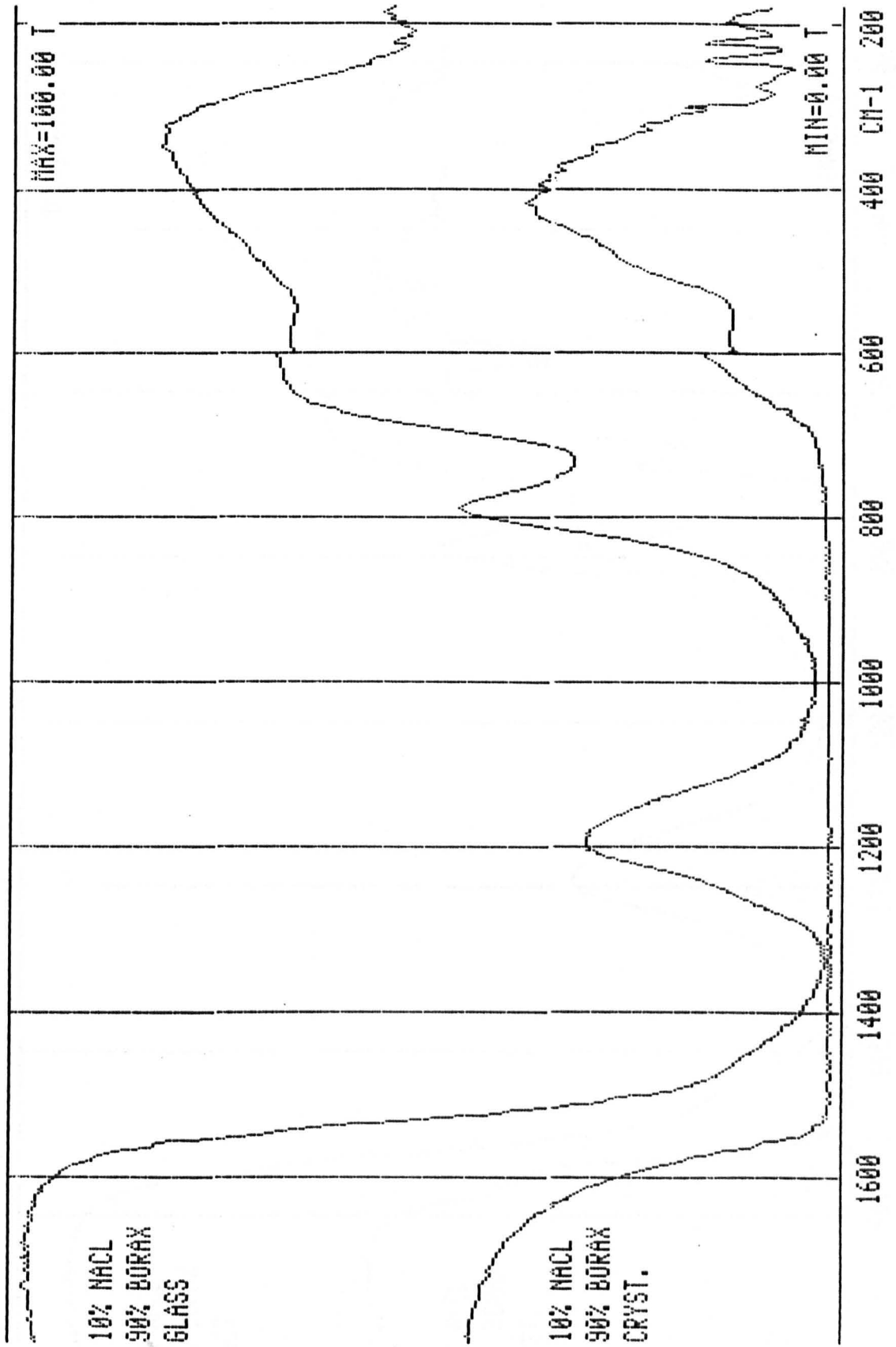


FIGURE 6.30

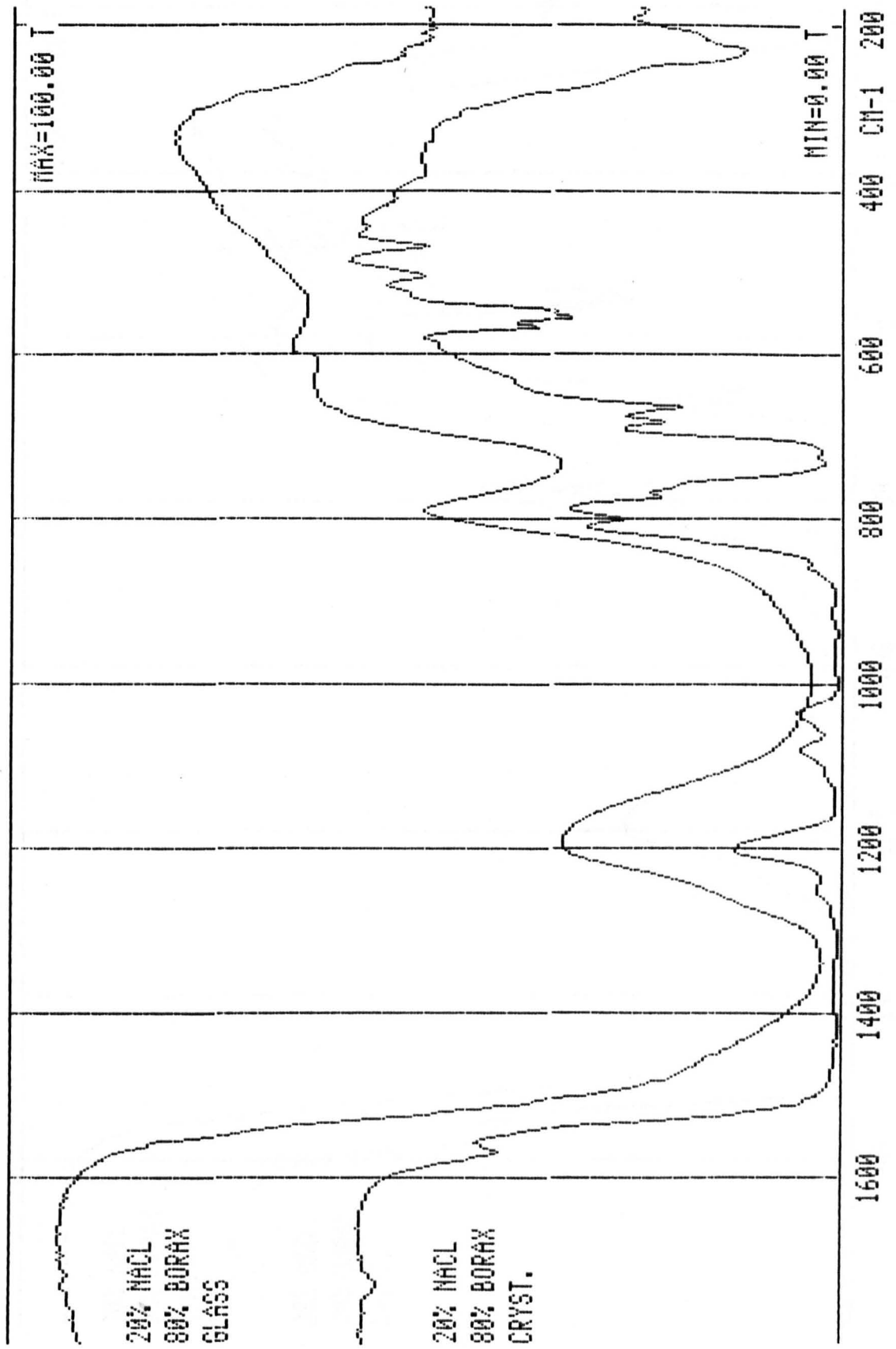
INFRA-RED ABSORPTION SPECTRUM



TRANSMISSION

FIGURE 6.31

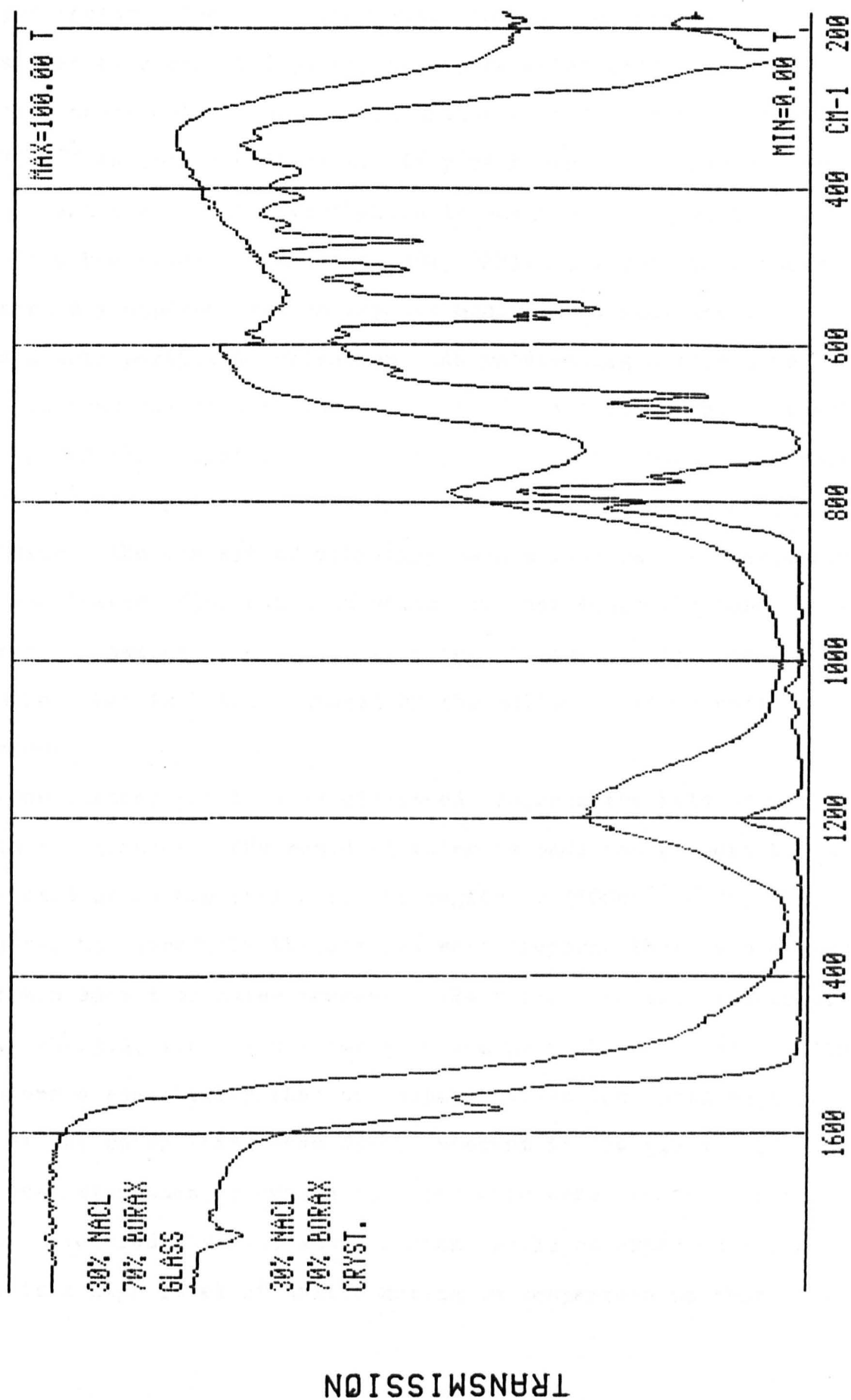
INFRA-RED ABSORPTION SPECTRUM



TRANSMISSION

FIGURE 6.32

INFRA-RED ABSORPTION SPECTRUM



earlier experiments using the KBr disc technique and have already been discussed. The two narrow bands have not been assigned to any particular molecular vibrations. The stated frequencies do not appear to correspond to any of the reported crystalline borate vibrational modes. The situation with the broader vibration at 530cm^{-1} is rather different. In pure borax it is present only as a slight trough but nevertheless it has been assigned to a certain O-B-O bending vibration (204, 327). However, there does not seem any apparent reason why the addition of NaCl should enhance this particular vibration. An interesting alternative idea concerns the role of the sodium ions. A theoretical approach (334) gives the vibrational wavenumber of a Na-O diatomic molecule as 526cm^{-1} , which is certainly in the vicinity of the observed vibration. The concept of vibrating Na-O polyhedra has previously been considered (335) but such units have not generally been observed. However, the possibility that it is this form of vibration that is being enhanced by the halide doping cannot be ruled out.

One further point to be discussed concerns the role of water within the glasses. Any residual water is made conspicuous by an associated broad absorption in the region of 3500cm^{-1} (204, 336). No matter how carefully the glasses were prepared there was always a certain amount of water present. The halide ion is, of course, singly charged, i.e. it has the same charge as the OH^- ion. It is therefore a possibility that the dopant halide ion could replace some of the water that tends to be inherent in the glass. If this were true then, provided the specimens were treated exactly alike, a reduced inherent water content would be expected where there is a high level of halide doping in comparison to that

where there is lighter doping. This could be monitored by observing the strength of the water absorption at 3500cm^{-1} . This study was undertaken for the series of NaCl doped glasses reported above. The resulting absorption curves are shown in Fig. 6.33 where the transmission axis has been considerably expanded in order to make the detail more easily observable. It can be seen that the band does appear to be rather stronger for the lightly doped materials. This is therefore considerable evidence that at least some of the added halide ion directly replaces hydroxyl ions within the glasses.

Finally, some work on alkali-free borates remains to be reported. Binary alkaline-earth borates have been studied to a much smaller extent than have binary alkali borates, though some published results exist (e.g. 330). It is not believed that halide doped tertiary materials have been studied. As usual, materials of the same compositions as those used in the corresponding resistivity work were investigated. The KBr disc technique was the method utilised, and again only specimen results will be given.

The observed infra-red absorption curve for binary glassy CaB_4O_7 is shown in Fig. 6.34, and the corresponding curve for a re-crystallised sample is shown in Fig. 6.35. It will be seen that Fig. 6.34 is very similar to the equivalent curve for glassy borax. Indeed this same result is found for the other corresponding binary alkaline-earth borates that were investigated and it is also the findings of other workers (e.g. 330). It is generally concluded that equivalent glassy alkali and alkaline-earth binary borates have a very similar boron oxygen network.

The curve for re-crystallised CaB_4O_7 does show several

INFRA-RED ABSORPTION SPECTRUM

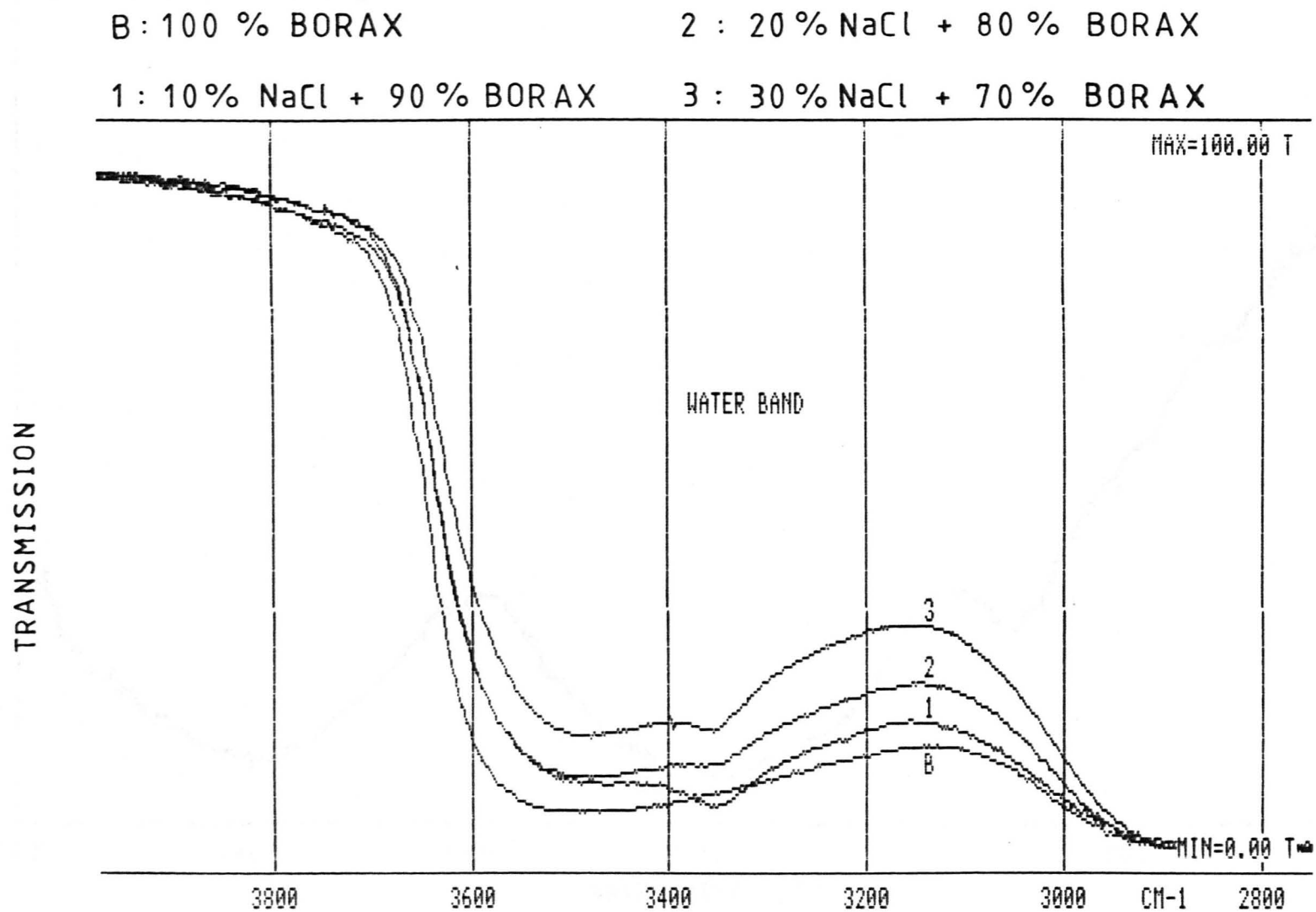


FIGURE 6.33

FIGURE 6.34

INFRA-RED ABSORPTION SPECTRUM

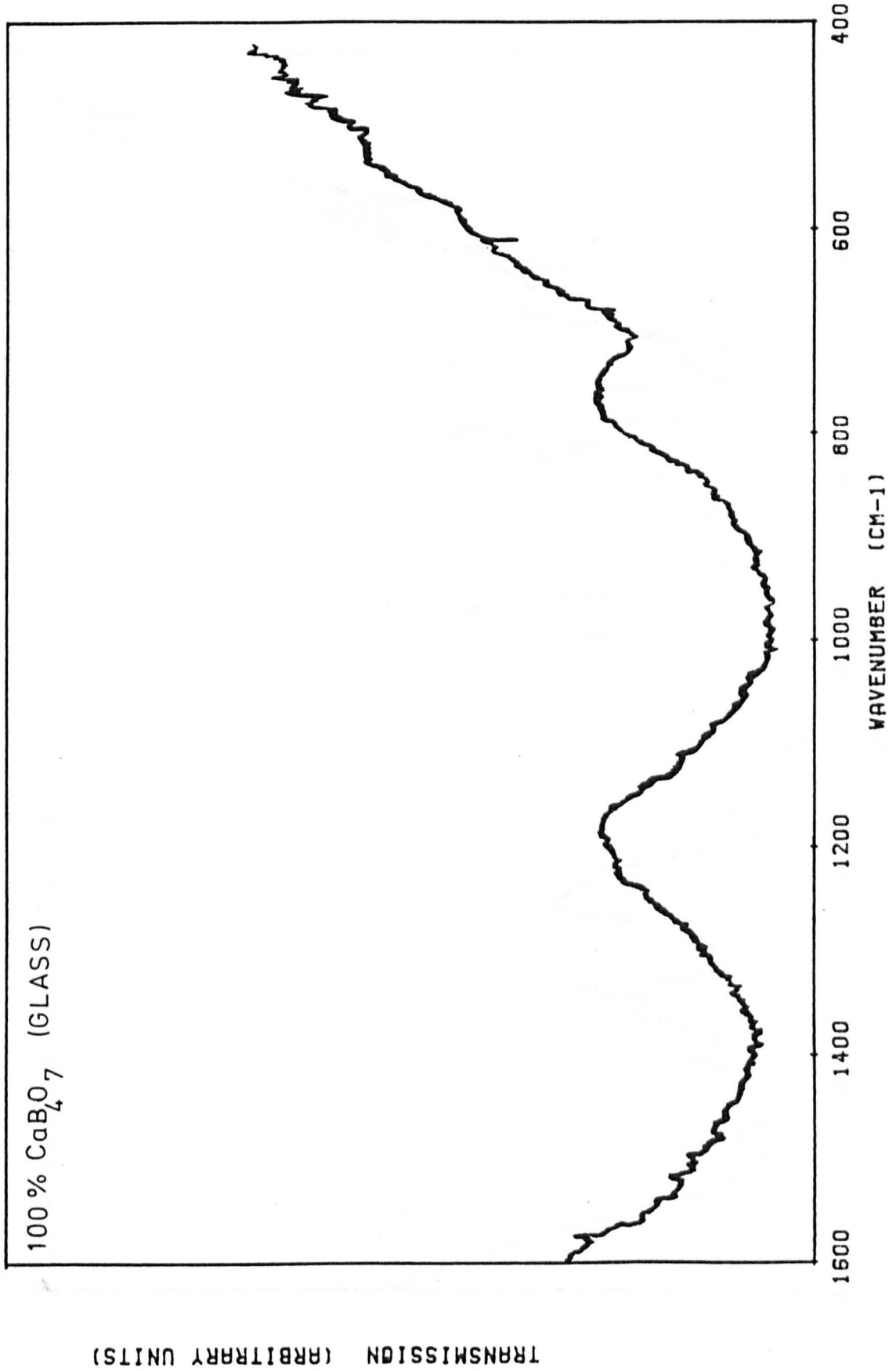
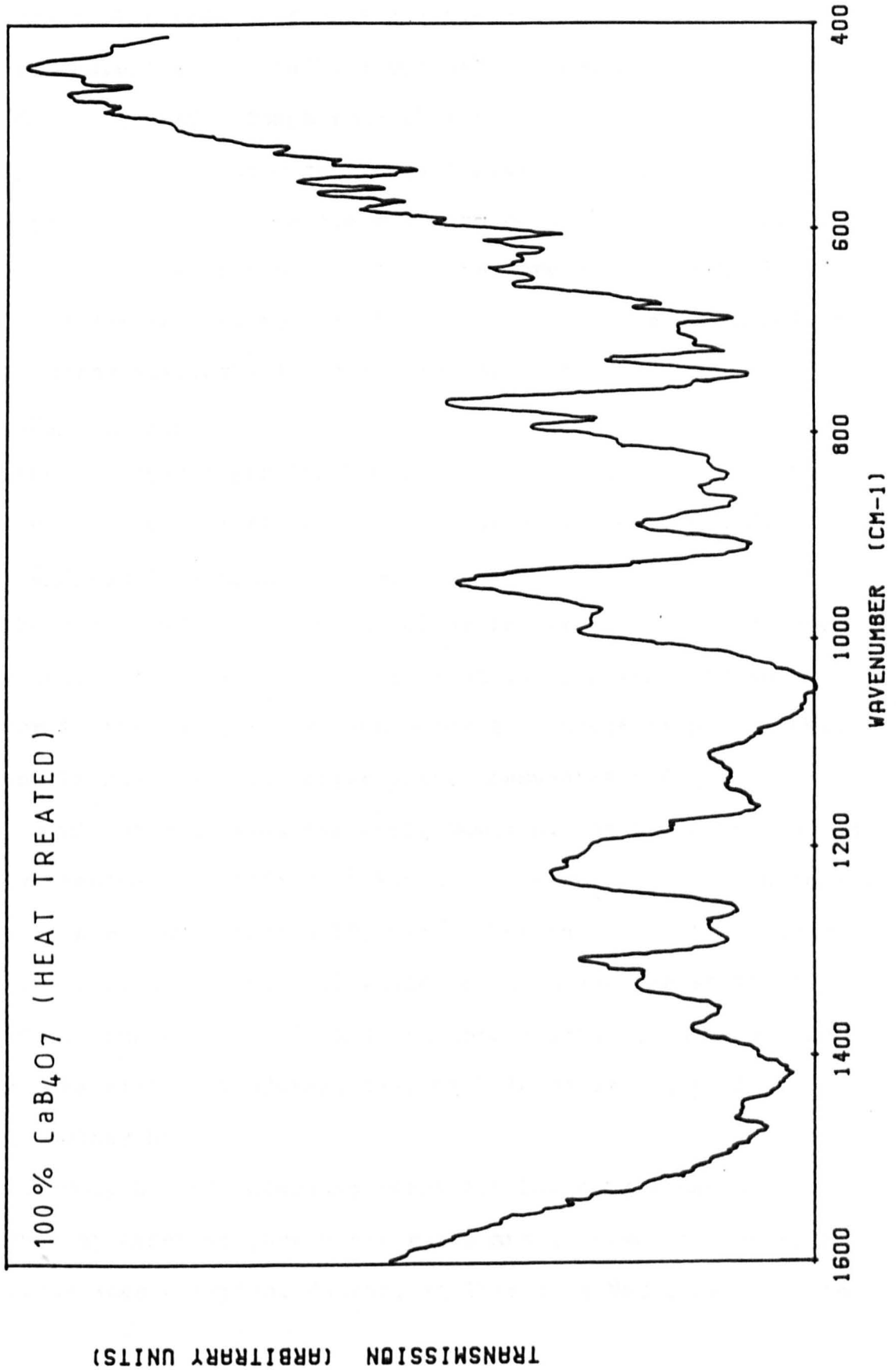


FIGURE 6.35

INFRA-RED ABSORPTION SPECTRUM



differences in comparison to that of re-crystallised borax, but this is hardly surprising as different crystal species are under investigation.

Curves obtained for glassy and re-crystallised specimens of the doped material (10% CaCl_2 + 90% CaB_4O_7) are shown in Figs. 6.36 and 6.37. Apart from slight differences in spectral quality, both curves show great similarity to their binary counterparts. Other doped compositions behaved correspondingly.

These are the same observations as were made in the case of the alkali borate samples, which indicates that the added halide ion is acting similarly in both types of material.

6.4 N.M.R. Studies.

General ideas regarding N.M.R., the apparatus used and the method of sample preparation were discussed in section 4.7.

6.4.1 Studies on the Boron Nucleus.

The nature of this work is rather in the same vein as some of the infra-red investigations in that it is attempting to discover if the added halide ion bonds to a boron atom. If this so then the resulting molecular unit, presumably a BO_3Cl group, would be such that the environment of the boron nucleus is greatly changed. In effect it would have more of the characteristics of a BO_4 unit than a BO_3 unit. Consequently, the observed value of N_4 (see section 4.7) would be increased, or at least changed to some extent. To a first approximation, in this bonding scheme, the effect of adding, say, NaCl to borax, is similar to adding further Na_2O .

The most natural starting point for investigations is to utilise a specimen of pure borax glass and to observe whether N_4 is altered when a typical dopant, in this case NaCl , is added to

INFRA-RED ABSORPTION SPECTRUM

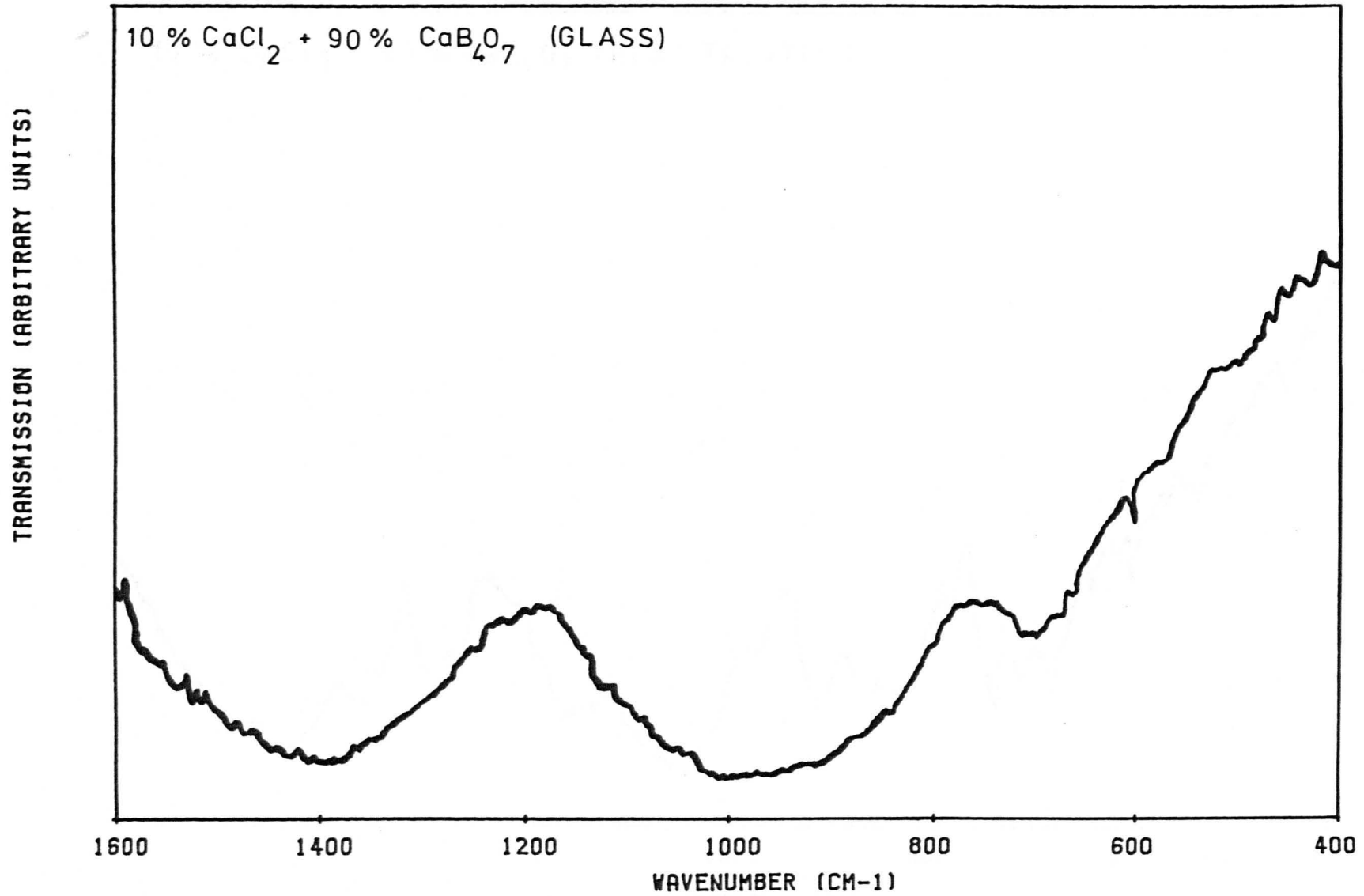


FIGURE 6.36

INFRA-RED ABSORPTION SPECTRUM

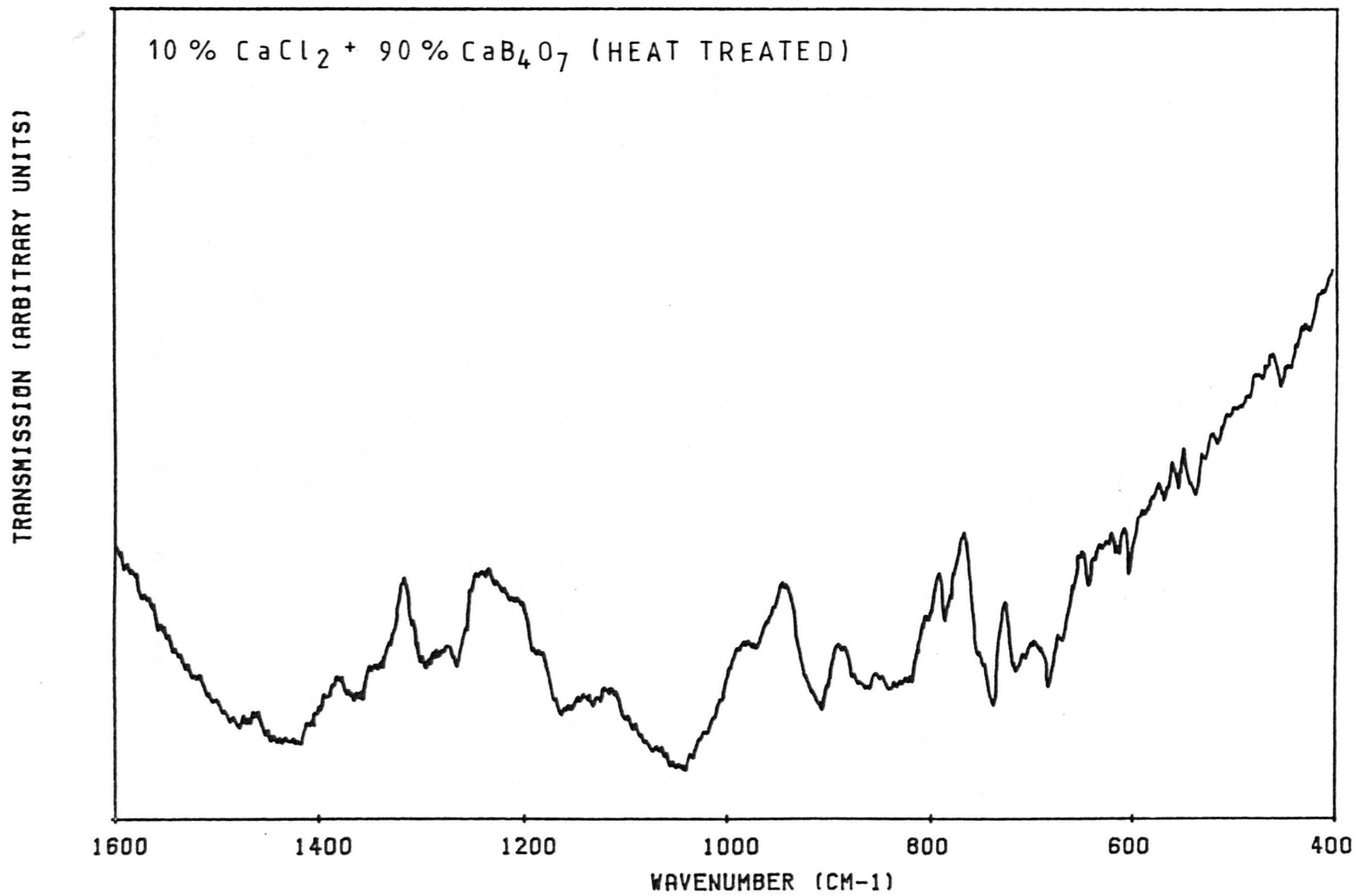


FIGURE 6.37

it. Certainly this was undertaken, however it should be recognised from the start that there is a problem associated with this composition. Consider the following argument. Borax glass contains 33.3% modifying oxide + 67.7% B_2O_3 . If the structural effect of adding a halide is as discussed above then a glass of composition 30% NaCl + 70% borax can be described to a first order approximation as equivalent to containing 41.7% total modifier + 58.3% B_2O_3 . However, according to the raw data of Bray (227) N_4 rises to a shallow peak at approximately 38% modifier, and so there is little difference between N_4 values for 33.3% and 41.7% modifier. This means that for these compositions the observed boron N.M.R. spectra would be expected to be similar irrespective of whether the halide ion bonded to the boron atom, or whether its addition did not affect boron co-ordination at all. Nevertheless, for the sake of completeness and uniformity, pure and doped borax based glasses were the first materials investigated. Tests on theoretically more illuminating compositions follow from this.

The observed resonance for pure borax glass is shown in Fig. 6.38. The frequency used was 10.72 MHz with a steady field of 7.85 KG and a sweep-field of 250 G. These values were kept constant for all further observations. As expected, a large, narrow resonance, together with a smaller, broader, asymmetric resonance can be clearly seen. For the broad line the peak to peak separation of the derivative signal is 89 ± 6 KHz, which gives a coupling constant (see section 4.7) of 2.7 ± 0.1 MHz. This is in good agreement with the published values mentioned earlier (section 4.7).

BORON NUCLEAR RESONANCE

100 % BORAX (GLASS)

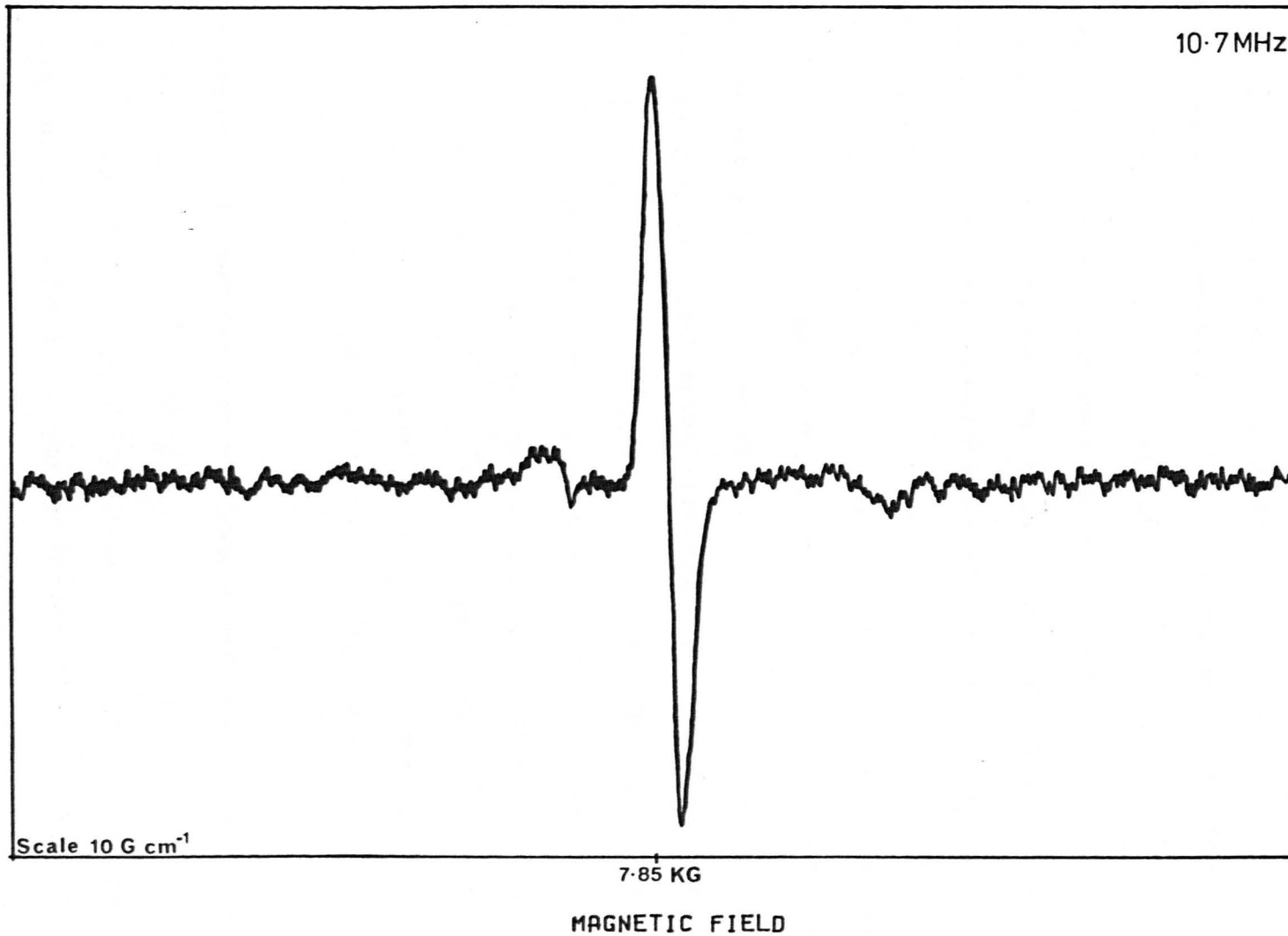


FIGURE 6.38

The resonance obtained for the doped glass (30% NaCl + 70% borax) is shown in Fig. 6.39 and the resonances observed using the corresponding pure and doped re-crystallised products are shown in Figs. 6.40 and 6.41. The resonances of the pure and doped pairings show a very great similarity, a result that was forecast in the above discussion. Numerical values of N_4 for each specimen, averaged over several runs, are given in Table 6.6. It appears that N_4 is slightly reduced in the case of the re-crystallised materials, but the difference is not very significant. As mentioned previously, these values can be directly compared to the raw ' c/a ' values in the work of Silver and Bray (221) on binary borate glasses. There is good agreement.

Considerable thought was given to deciding which compositions would next be investigated. The rate of change of N_4 with composition is greatest just above approximately 10% modifying oxide (221, 227). However, at this oxide content NaCl is only very sparingly soluble in the parent glass (190). Consequently, it was decided to compromise and base experiments on an intermediate composition, 20% Na_2O + 80% B_2O_3 . This allows both a reasonable rate of change of N_4 with composition and a fair degree of chloride solubility, approximately 12% (190), though the actual doping level used was 10%.

The observed resonances for the pure binary material and for the doped specimens, in both the glassy and re-crystallised form, are shown in Figs. 6.42 - 6.45. Numerical values for N_4 averaged over several observations are given in Table 6.7. It will be noticed that there is a small but perceptible increase in N_4 for the doped sample in both the glassy and re-crystallised types of specimen. Consequently, it can be stated that, to a certain

BORON NUCLEAR RESONANCE

30 % NaCl + 70% BORAX (GLASS)

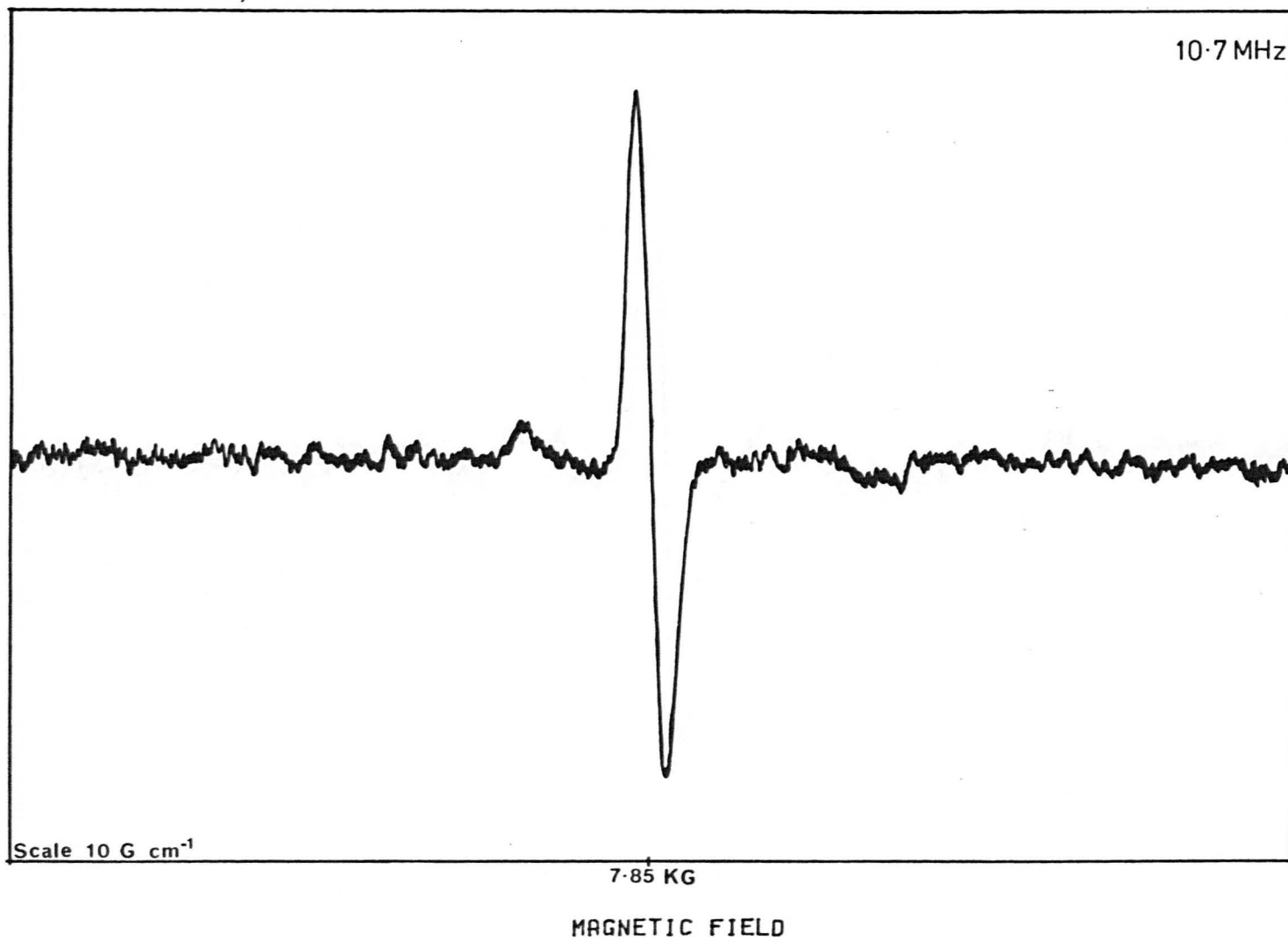


FIGURE 6.39

BORON NUCLEAR RESONANCE

100% BORAX (HEAT TREATED)

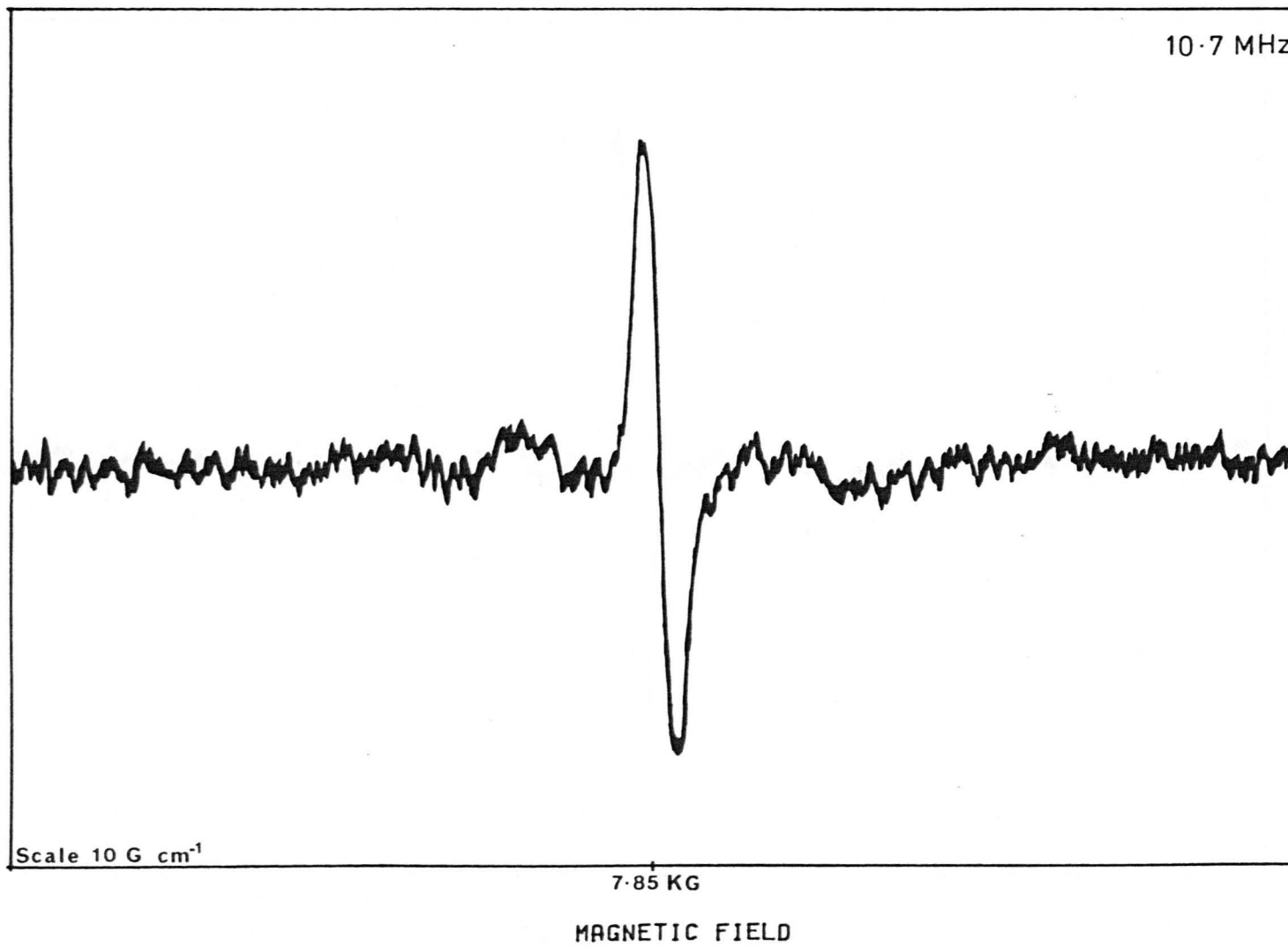


FIGURE 6.40

BORON NUCLEAR RESONANCE

30% NaCl + 70% BORAX (HEAT TREATED)

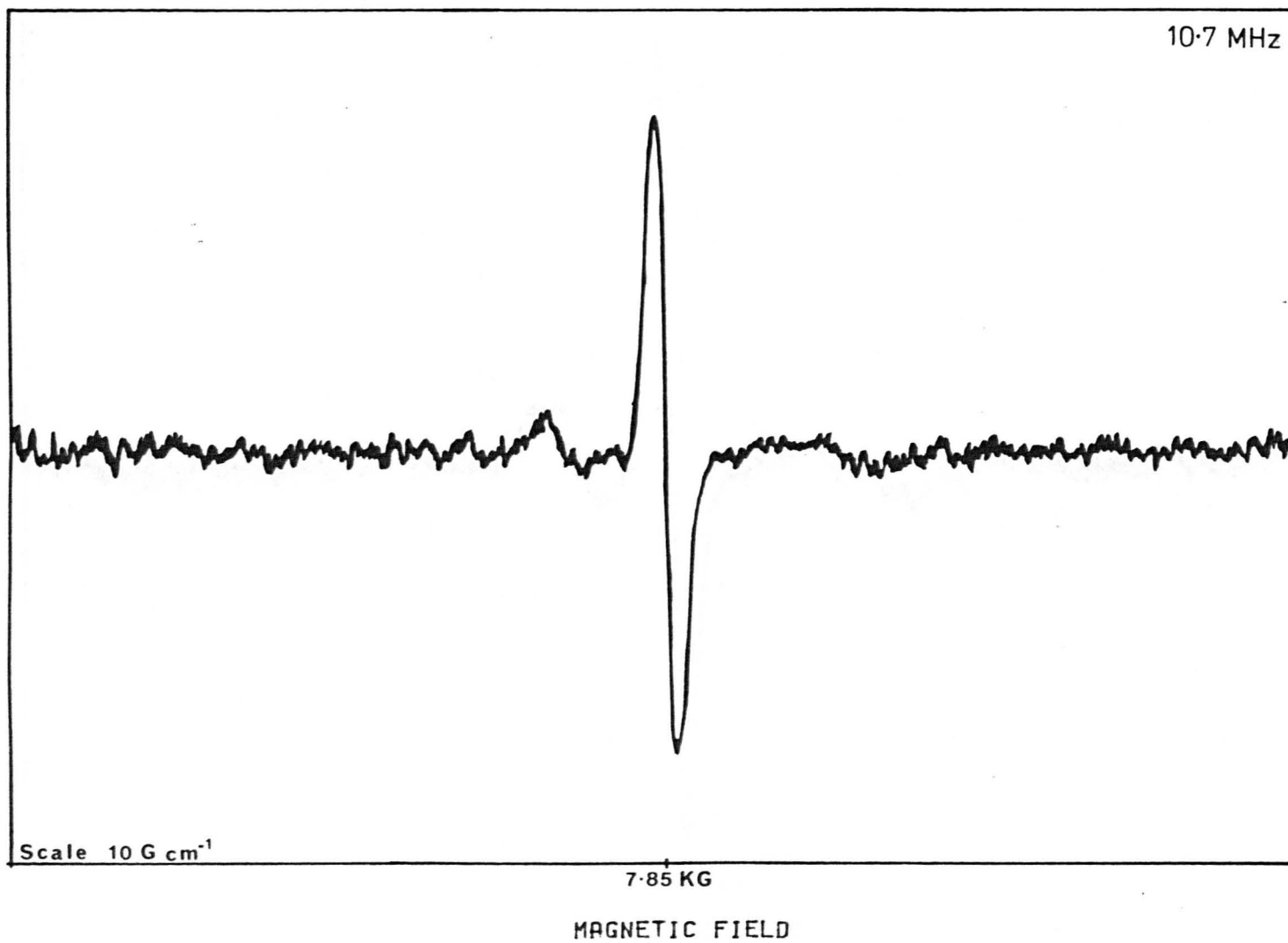


FIGURE 6.41

BORON NUCLEAR RESONANCE

20% Na₂O + 80% B₂O₃ (GLASS)

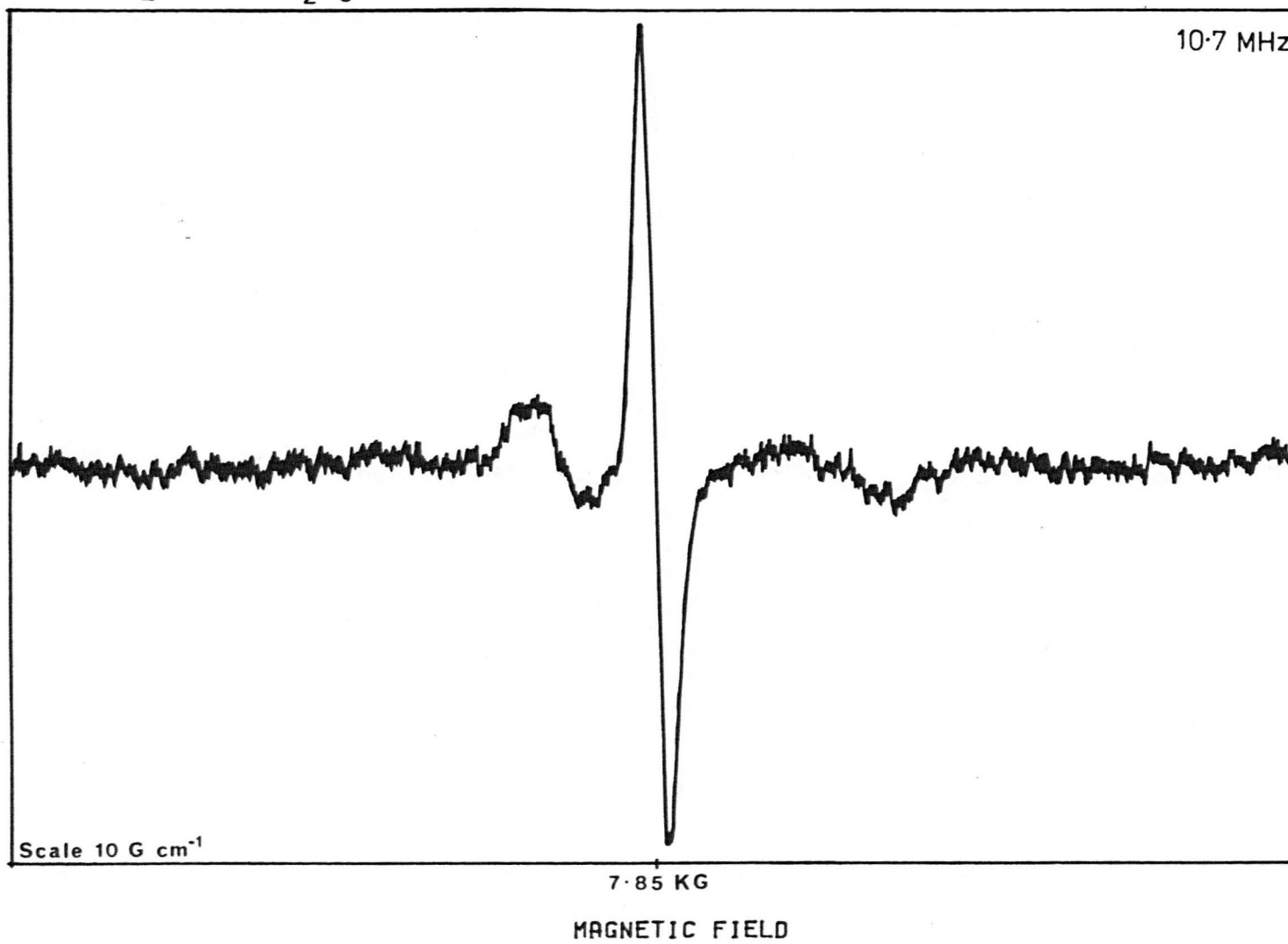


FIGURE 6.42

BORON NUCLEAR RESONANCE

10% NaCl + 18% Na₂O + 72% B₂O₃ (GLASS)

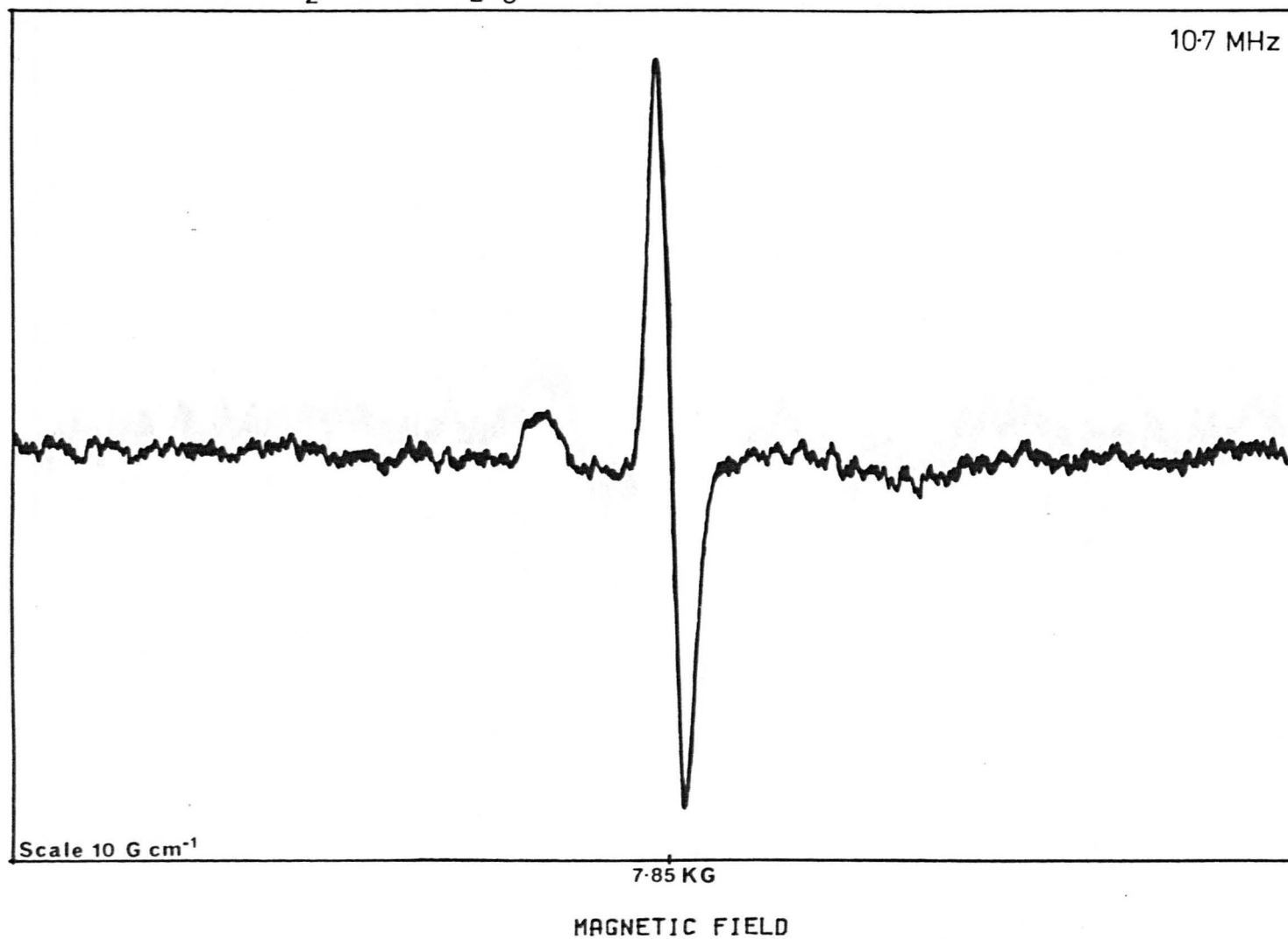


FIGURE 6·43

BORON NUCLEAR RESONANCE

20% Na₂O + 80% B₂O₃ (HEAT TREATED)

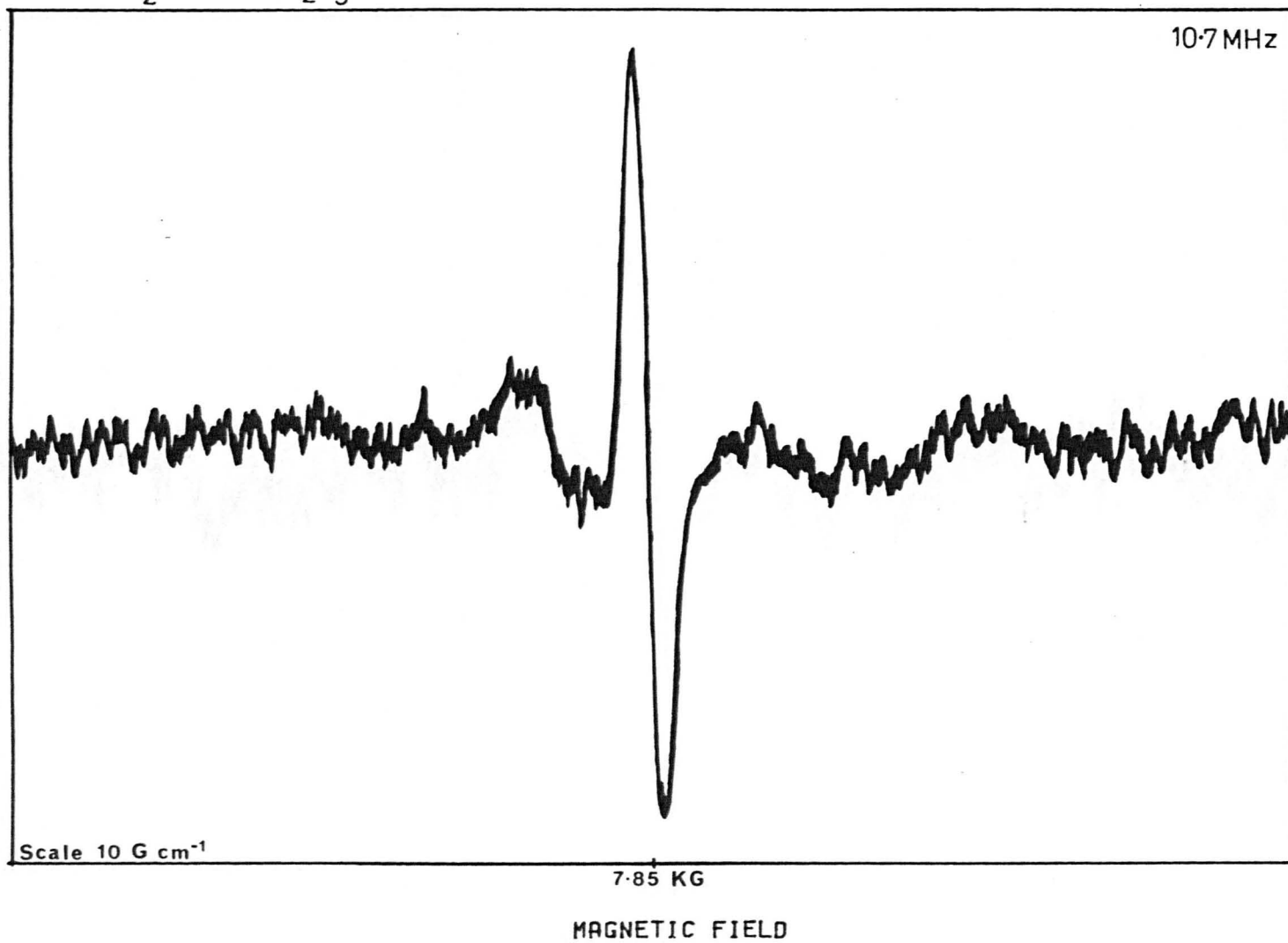


FIGURE 6.44

BORON NUCLEAR RESONANCE

10% NaCl + 18% Na₂O + 72% B₂O₃ (HEAT TREATED)

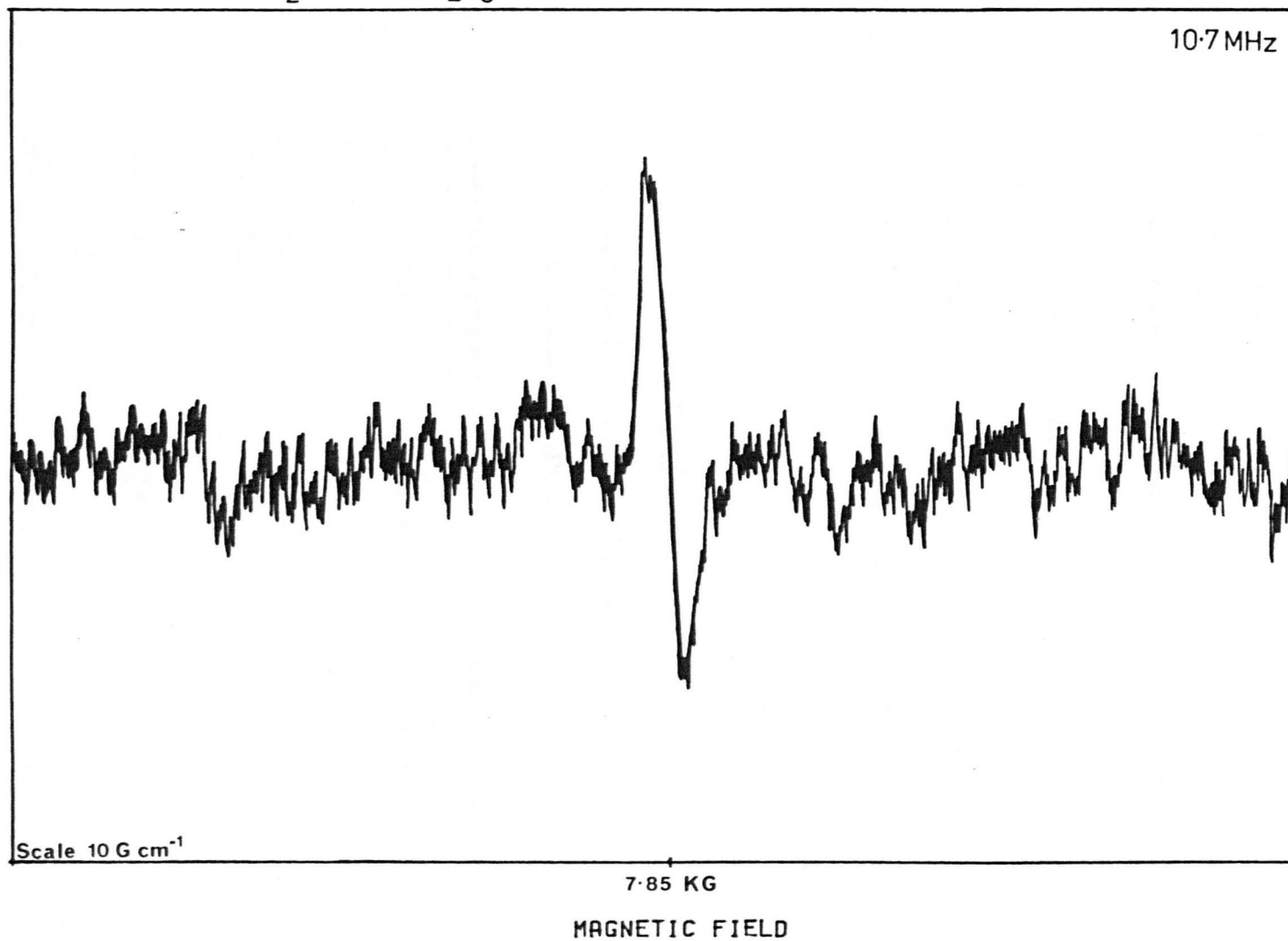


FIGURE 6.45

Table 6.6Boron Co-ordination in Borax-based Materials.

<u>Content</u>	<u>Effective Content</u>	<u>Type</u>	<u>N₄ (Peak Height Ratio)</u>
100% borax	33.3% modifier 66.7% B ₂ O ₃	Glass	18.4 ± 0.5
70% borax 30% NaCl	41.7% modifier 58.3% B ₂ O ₃	Glass	18.4 ± 0.6
100% borax	33.3% modifier 66.7% B ₂ O ₃	Cryst.	18.0 ± 0.7
70% borax 30% NaCl	41.7% modifier 58.3% B ₂ O ₃	Cryst.	17.9 ± 0.7

Table 6.7Boron Co-ordination in Materials having
Lower Modifier Content.

<u>Content</u>	<u>Effective Content</u>	<u>Type</u>	<u>N₄ (Peak Height Ratio)</u>
20% Na ₂ O 80% B ₂ O ₃	20% modifier 80% B ₂ O ₃	Glass	17.4 ± 0.6
18% Na ₂ O 72% B ₂ O ₃ 10% NaCl	28% modifier 72% B ₂ O ₃	Glass	17.8 ± 0.3
20% Na ₂ O 80% B ₂ O ₃	20% modifier 80% B ₂ O ₃	Cryst.	16.3 ± 0.7
18% Na ₂ O 72% B ₂ O ₃ 10% NaCl	28% modifier 72% B ₂ O ₃	Cryst.	16.7 ± 0.5

degree, addition of NaCl to the sodium borate materials results in an increase in the fraction of boron atoms that are four co-ordinated. However, it is not believed that there is a one-to-one correlation between the addition of a unit of NaCl and one further boron atom becoming four co-ordinated. The results firmly indicate otherwise. For example, a glass of 33% modifier has an N_4 value 18.4 (Table 6.6), while a glass with only 20% modifier has a corresponding value of 17.4 (Table 6.7). Consequently, if a linear change is presumed, a glass with 28% modifier would have an N_4 value of 18.15. However, the doped specimen with this percentage of modifier has an N_4 value of only 17.8 (Table 6.7). Actually, this face value discrepancy should be increased further because the assumed linear change in N_4 is not correct. The rate of increase in N_4 starts to become less steep above approximately 25% modifier (221), thus the N_4 value for 28% modifier should be above 18.15.

In summary, the N.M.R. results have shown that the fraction of boron atoms in four co-ordination increases on the addition of a halide, but to a far less extent than would be expected for a direct relationship. There is no apparent reason why the halide should indirectly affect the boron-oxygen co-ordination, consequently the increase in four co-ordination is presumed due to the presence of some BO_3Cl units. It should be emphasised once again that only a relatively small fraction of the added halide ions are thought to bond in this way. Results for the re-crystallised materials are very similar to those of the glasses.

6.4.2 Studies on the Sodium Nucleus.

Details of the experimental parameters used in these observations were given in section 4.7.4.

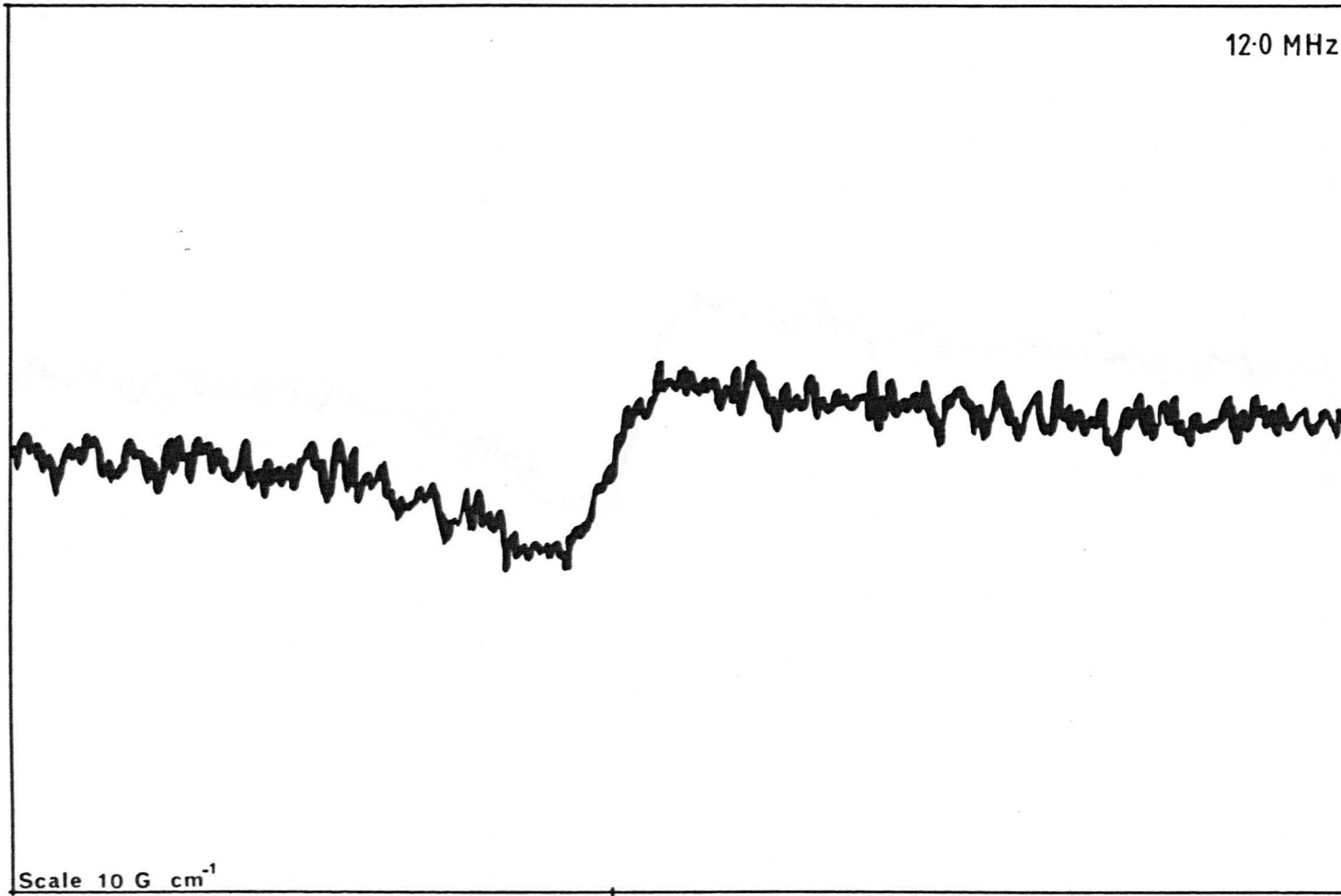
The difficulty in observing the sodium resonance makes accurate quantitative analysis impossible so only qualitative comparisons of the resonance for various specimens will be made. This section of work, unlike the study on the boron nucleus, does not suffer from any drawbacks regarding the use of the borax composition and will therefore use borax as its standard. The observed sodium resonance for a specimen of borax glass is shown in Fig. 6.46. The signal, though weak, is just observable and should be compared to that reported by Bray and Silver (217). The resonance appears as a single line; any satellite lines that are present being too broad to be observed. In this situation the line has a width of 25 ± 3 KHz. If quadrupolar broadening is assumed then this width corresponds to a coupling constant of 1.5 ± 0.3 MHz. Previously reported results are 1.9 MHz (221) and 1.85 MHz (217). The observed coupling constant is slightly lower than these values, but given the unavoidable poor quality of the resonance it is not surprising that some discrepancy occurs. Also, the observed sodium resonance does not have the double peaked character of a typical second order quadrupole broadened line (215, 220). Hence, as such effects may not be the primary cause of broadening, the value of the coupling constant quoted above represents a maximum value rather than an absolute value.

The next sample investigated was the doped glass of composition 30% NaCl + 70% borax. The observed sodium resonance is shown in Fig. 6.47. It is very like that of the pure borax glass. Hence, the environment of the sodium ions in each of the

SODIUM NUCLEAR RESONANCE

100 % BORAX (GLASS)

12.0 MHz



10.7 KG

MAGNETIC FIELD

FIGURE 6.46

SODIUM NUCLEAR RESONANCE

30% NaCl + 70% BORAX (GLASS)

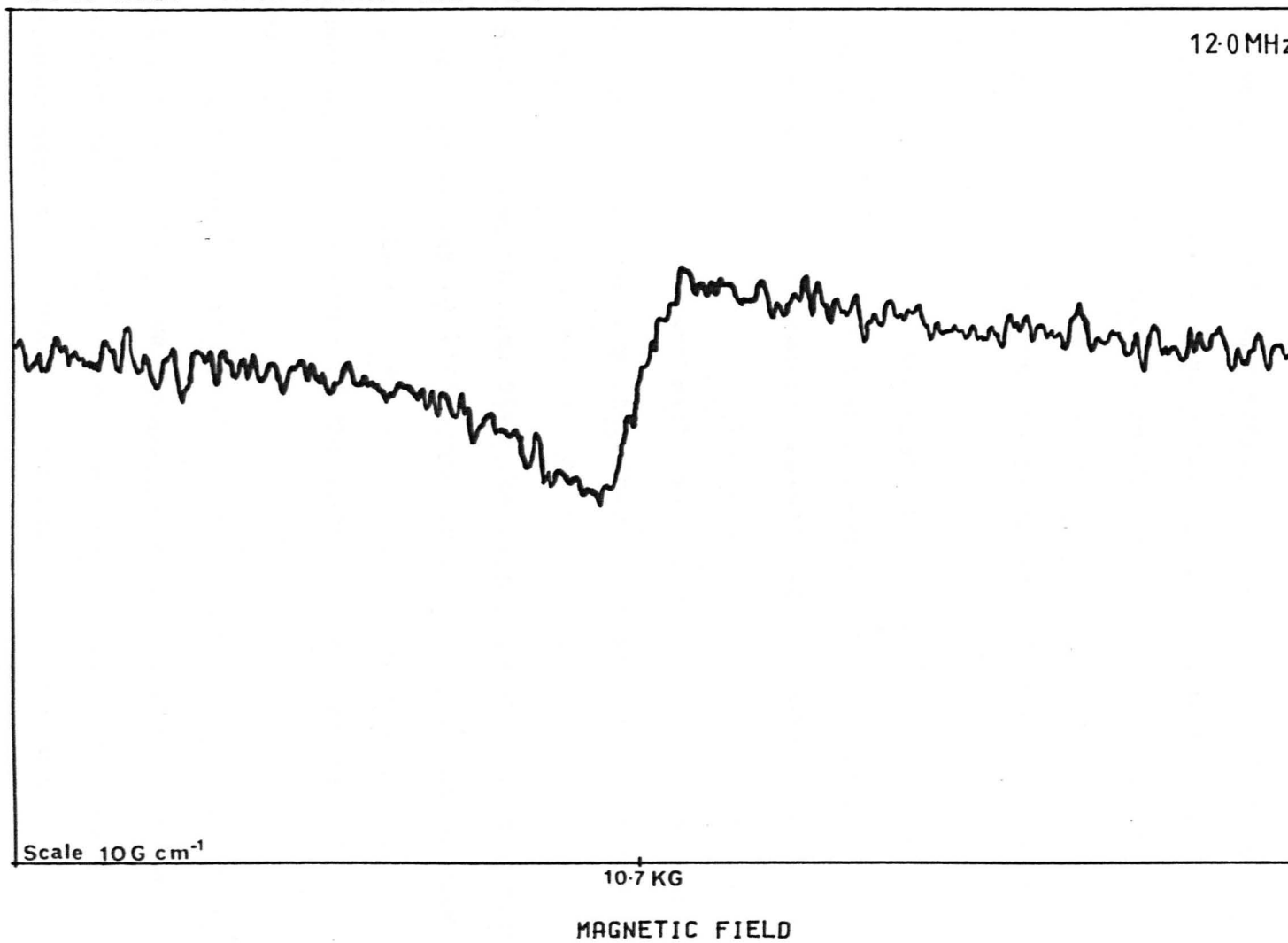


FIGURE 6.47

two cases is quite similar.

Attention was then paid to the re-crystallised materials. The sodium resonance for a specimen of re-crystallised pure borax can be seen in Fig. 6.48. In obtaining this result it was found that the signal saturated very easily, consequently the R.F. power input had to be reduced to a very low level indeed, with a corresponding loss in signal to noise ratio. Despite the resulting poor quality of the resonance, it can be seen that once again no new features are present, with the trace resembling those of the glasses reported above.

In the three materials discussed above the sodium ions appear to exist in not very different environments. It should be remembered that there is also no dramatic difference in the electrical conductivity, so the two sets of experimental results are inter-supportive. It was with re-crystallised doped specimens that conductivity was greatly increased. The sodium resonance for a re-crystallised specimen of 30% NaCl + 70% borax is displayed in Fig. 6.49. It can be seen that the signal is very much larger than in the case of the earlier reported results, and it is also asymmetric to a certain degree. It is quite obvious that the environment of at least some of the sodium ions has changed considerably.

The signal-to-noise ratio and general clarity of the curve are still not very high; so interpretation must therefore be rather tentative. However, the width and overall appearance of the line does seem to resemble a combination of a resonance similar to that observed in the previous three occasions, plus a second, narrower resonance superimposed on it, with this second resonance being offset to the left of centre as drawn. If this

SODIUM NUCLEAR RESONANCE

100 % BORAX (HEAT TREATED)

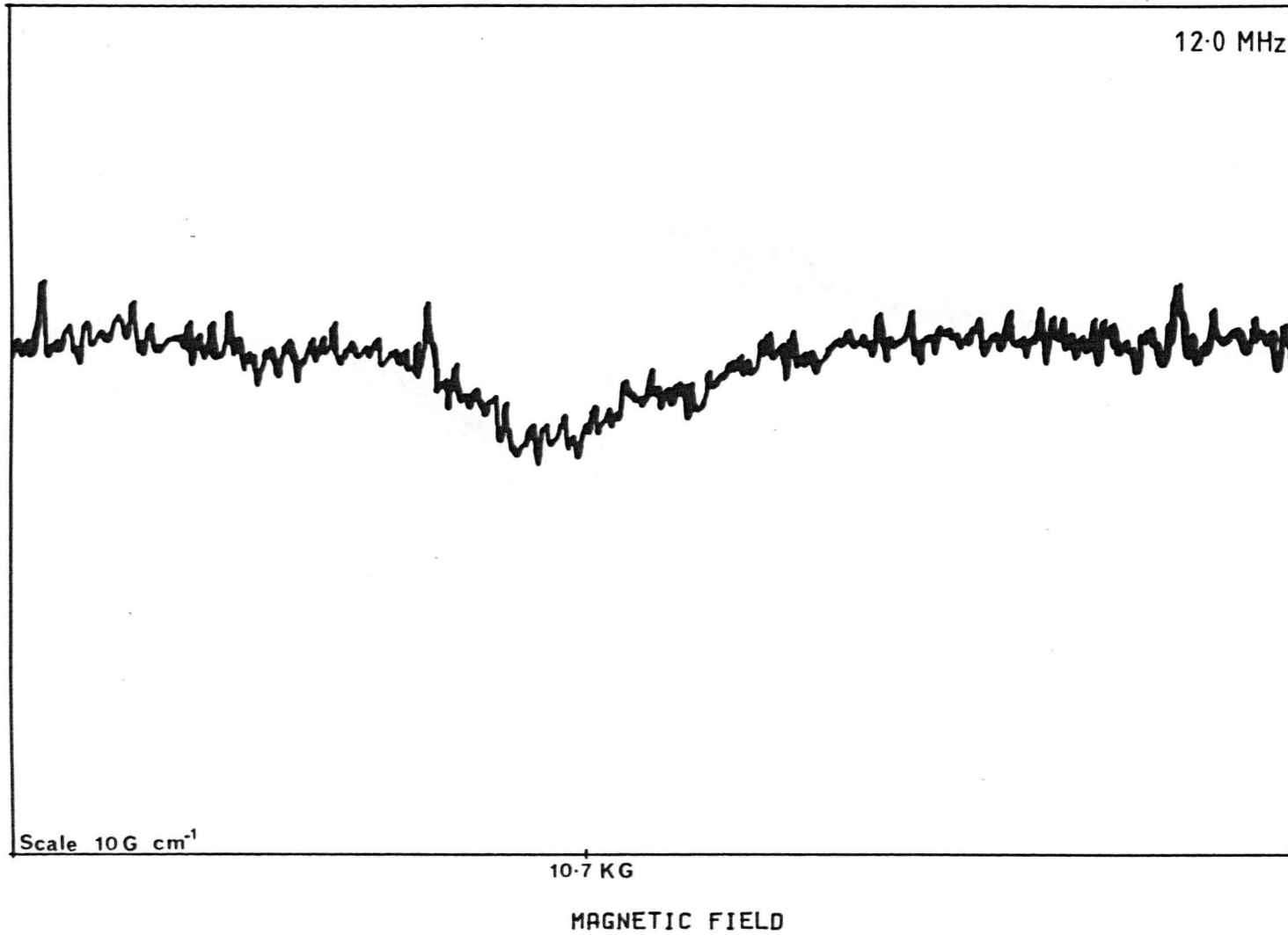


FIGURE 6.48

SODIUM NUCLEAR RESONANCE

30% NaCl + 70% BORAX (HEAT TREATED)

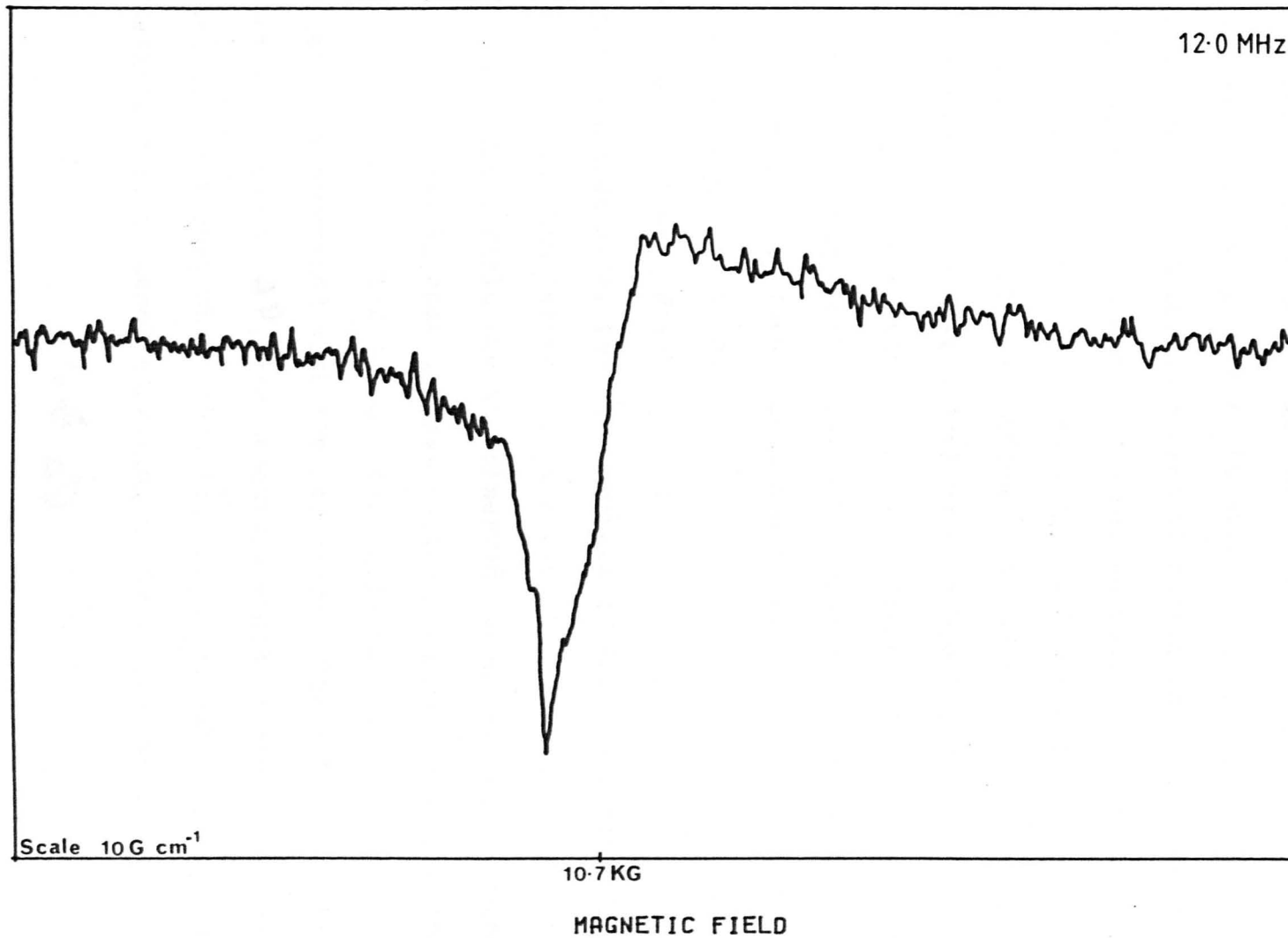


FIGURE 6.49

is true then it can be argued that the 'usual' broad resonance line is due to immobile sodium ions in certain sites within the crystal lattice or in the residual glassy phase, and that the narrow resonance is due to sodium ions in alternative sites within the crystal that give rise to high mobility. The fact that highly mobile ions can give rise to narrow resonance lines is well known, and the phenomenon is called motional narrowing. It is therefore necessary to discuss motional narrowing and to calculate whether it could be applicable in this type of material.

The magnetic field that a nucleus is subjected to in an N.M.R. experiment is not only the applied field; there is also a contribution resulting from neighbouring nuclei. This second component is called the local field and it will vary in magnitude and direction from site to site and thus contributes to the width of the resonance line. However, if the nuclei are in rapid motion, constantly changing site, the time average of the local field will fall to zero. In this latter case the effective field in operation is only the applied field and the observed resonance becomes much narrower. The general case is that motional narrowing will occur if the time average of the local field falls to zero within the relaxation time concerned with the resonance. The relaxation time is directly related to $\Delta\nu$, the frequency width of the un-narrowed line, and simple theory shows that the following relationship has to be satisfied if motional narrowing is to be observed:

$$T_c \ll \frac{1}{\Delta\nu}$$

where T_c is the dwell time of the relevant ion at a particular site (usually known as the correlation time). A full description of motional narrowing can be found in most of the publications

referred to for general theory (see section 4.7), in many of the other references mentioned in course of this discussion and in texts concerned with ion transport (e.g. 337).

T_c can be found, at least approximately, from knowledge of the activation energy found in electrical conductivity experiments. The inter-site jumping frequency of an ion, f , is given by (see section 2.1.4):

$$f = f_0 \cdot \exp\left(\frac{-u}{kT}\right)$$

where f_0 is the thermal vibration frequency of the ion and u is the activation energy for motion. Typically f_0 is of the order of 10^{13} Hz and it has been found that u is approximately 0.3 eV. Now $T_c = 1/f$, therefore it follows that T_c is of the order of 5×10^{-8} secs. The observed value for $\Delta\nu$ was 25 KHz, therefore $1/\Delta\nu \approx 4 \times 10^{-5}$ secs. Thus T_c is indeed less than $1/\Delta\nu$ and the condition for motional narrowing is easily satisfied. It is therefore perfectly plausible that the narrow line observed in this resonance is caused by sodium ions capable of a high degree of mobility.

It will be noticed that the superimposed narrow line is quite strong, yet the original broad line has shown no loss of intensity in comparison to that observed in the previous three occasions. The number of sodium ions has remained approximately constant, therefore a boost in overall signal strength seems to have occurred. In order to understand why this has happened the concept of motional narrowing has to be taken a stage further. It should be remembered that the theoretical sodium resonance has a pair of satellite lines as well as the central line (see section 4.7.2), but because of broadening (see section 4.7.4) these satellite

lines are not frequently observed in polycrystalline or glassy materials. It can be shown that (see previous references), if ionic motion is sufficiently fast, the satellites can be narrowed to the extent where they are contained within the central line and consequently boost its intensity considerably. This requires much faster motion than the more usually observed motional narrowing effect discussed earlier. It is necessary that:

$$T_c \ll \frac{\Delta\nu_f}{\Delta\nu_s^2}$$

where $\Delta\nu_f$ is the frequency width of the final line and $\Delta\nu_s$ is the typical frequency separation of the original central and satellite lines. The work of Cuthbert and Petch (319) yields a value for $\Delta\nu_s$ of approximately 225 KHz, while $\Delta\nu_f$ is about 15 KHz. Thus, in order to observe this effect, T_c needs to be less than 3×10^{-7} secs. Again the result is satisfied, thus the extra signal strength could be due to this effect.

In summary, the overall shape and magnitude of this final resonance is well described by the situation where some of the sodium ions are mobile to the extent illustrated by the resistivity results. The remainder of the sodium ions exist in sites not very different to those that they occupy in the glassy or undoped product.

6.5 Density Measurements.

The results of density measurements on a range of the glassy materials will be used in the discussion on the relationship between structure and resistivity that will follow in the next chapter. The general technique and methods used were explained in section 4.8. Also in this section it was illustrated how the density measurements can lead to an approximate value for the

Table 6.8

Results of Density Measurements on various
of the Glassy Materials.

<u>Glass Composition</u>	<u>Density (gm/cm³)</u>	<u>Boron-Boron Separation (Å)</u>
100% borax	2.37	3.27
90% borax + 10% NaCl	2.37	3.32
90% borax + 10% CaCl ₂	2.36	3.35
85% borax + 15% CaCl ₂	2.36	3.39
80% borax + 20% CaCl ₂	2.35	3.43
90% borax + 10% CaBr ₂	2.42	3.37
90% borax + 10% CaF ₂	2.41	3.31
90% borax + 10% MgCl ₂	2.33	3.35
90% borax + 10% CaO	2.40	3.30
90% borax + 10% MgO	2.38	3.30
83.34% borax + 8.77% NaCl + 7.89% B ₂ O ₃	2.36	3.30

boron-boron separation distance, S.

While it was thought that, in the case of the glassy materials, density measurements could help explain the dependency of resistivity and structure on the doping involved, it was not believed that such results would be as helpful in the case of the re-crystallised materials. For this reason the work was confined to glassy specimens.

The results are given in Table 6.8. A possible error of $\pm 0.01 \text{ gm/cm}^3$ should be allowed for in the quoted density

values, this converts to $\pm 0.01 \text{ \AA}$ for the boron separation results. The observed density for pure borax glass is in excellent agreement with the value of 2.377 gm/cm^3 quoted elsewhere (338). No published data on the density of halide doped borate glasses has been discovered.

Further discussion of these observations is delayed until the following chapter.

CHAPTER 7

Discussion of the Results and of Possible Explanations.

7.1 Initial Comment.

Several of the investigatory techniques that have been used have yielded rather similar types of results for glassy and re-crystallised materials. However, the main topic of concern in this thesis is electrical conductivity, and in these investigations the two types of specimen show very different behaviour when subjected to doping. Consequently this Chapter is most conveniently divided into two main sections. The first of these sections will be concerned with glassy materials, and the second will concern re-crystallised specimens.

The form of each section will be rather similar. Firstly there will be a review of the points to arise from the conductivity results, secondly a summary of information resulting from various structural investigatory techniques, thirdly an attempt to interpret these findings in terms of a possible explanation and fourthly, where possible, a discussion to compare and contrast any previously published work on the same general topic.

7.2 Glassy Materials.

It has been shown that, by suitable halide doping, it is possible to reduce the resistivity of a glass with a basic borax composition by over two orders of magnitude. An overall room temperature resistivity in the region of $10^9 \Omega \cdot \text{cm}$. can be achieved. A wide range of halide dopants can be used, though some are not as effective as others in reducing resistivity. In pure borax glass the conduction mechanism is primarily due to the mobility of the sodium ions. It is not believed that any other mechanism replaces this when doping occurs, i.e. the halide ions indirectly

increase the mobility of the sodium ions rather than themselves taking part in charge transfer. It has also been shown that increasing the level of doping results in a steady decrease in resistivity right up until the limit of glass formation is reached.

The above paragraph effectively lists the most important points to emerge from the resistivity investigations, however some of the findings require a more detailed comment before a realistic explanatory discussion can be attempted.

The relative effects of the various halide ions on resistivity is one such point in question. For several types of dopant cation the use of either chlorides or bromides results in a rather similar reduction in resistivity. Thus, it is thought that chloride and bromide ions play similar roles on their addition to sodium borate glass. In contrast, it was found that CaF_2 actually increases the resistivity of borax glass. Thus, fluoride ions are not capable of acting in the same way as chloride or bromide ions. It may, at first thought, be believed that some inconsistency is present due to the fact that the addition of NaF to borax results in a small resistivity decrease. However, it should be remembered that the addition of NaF also increases the number of sodium ions in the glass. It is presumed that it is the presence of these extra sodium ions that causes the decreased resistivity.

It has proved impossible to investigate the effect of adding iodide ions because of the high volatility of the associated halides.

As discussed in Chapter 2, incorporating ions such as those of calcium or magnesium into a sodium borate glass would normally

result in an increased resistivity. Consequently, the decreased resistivity effect caused by adding the chloride or bromide ions is large enough to overcome the converse detrimental effect of adding the calcium or magnesium ions.

The resistivity reduction that occurs is also dependent on the nature of the cation involved in the halide. It is perhaps not surprising that the addition of 20% NaCl to borax decreases the resistivity by considerably more than does the addition of 10% CaCl₂ (see Figs. 5.1 and 5.7) despite the fact that similar numbers of chloride ions are involved; the added alkali ions will also serve to increase conduction. Of further interest are the resistivity results for a series of dopants where the cations are from a particular group. The alkaline-earth chlorides have been thoroughly investigated and it has been found that the presence of a large cation (e.g. barium) tends to reduce the magnitude of the resistivity reduction. The greatest conductivity increase for this series of halides was brought about by the use of magnesium chloride.

The theoretical treatment in Chapter 2 demonstrated that the resistivity equation could be written in the form:

$$\log \rho = \log \rho_0 + \frac{U}{kT}$$

The question must be answered as to whether the resistivity decrease has been brought about by a change in activation energy, U , i.e. a change in slope of the drawn curves, or by a change in ρ_0 , i.e. a change in intercept. In many of the observed results this answer is difficult to ascertain. The measured reduction could apparently be caused by small changes in either of the quantities. It is most useful to look at the

curves corresponding to higher levels of doping, e.g. that observed for the glass containing 30% NaCl (Fig. 5.7). The activation energy for pure borax is 73 ± 4 kJ/mole (section 4.1.4) while that for the doped glass is 63 ± 3 kJ/mole. There has been an obvious reduction in this case. Indeed, a steady activation energy decrease is observed, with increasing doping level, for other members of the series of specimens doped with NaCl. The value of $\log \rho_0$ for pure borax, calculated from the observed resistivity graph, is $-2.25 \pm 0.07 \Omega \cdot \text{cm.}$, while the corresponding quantity for the glass containing 30% NaCl is $-2.31 \pm 0.09 \Omega \cdot \text{cm.}$ These values are remarkably similar, so consequently it can be stated that the reduction in resistivity caused by doping is primarily due to a decrease in activation energy rather than a change in the ρ_0 term.

In the case of the alkali-free borate glasses the effect of the addition of halides was to slightly increase the resistivity of the material. This increase was small, but is nevertheless the opposite to that observed with sodium borate glasses. Any theory regarding these effects would have to explain this opposing trend, though it should be remembered (see section 2.7.6) that the conductivity mechanism involved with alkali-free borate glasses remains under some debate, and is said by certain authors (165, 166) to be due to oxygen ion migration. If this latter comment is true then it is hardly surprising that the effect of doping is considerably different in the cases of sodium borate glasses and alkali-free borate glasses.

One further point to arise from the resistivity results is that the nature of the environment in the melting furnace has no apparent bearing on the observed resistivity. Glasses melted in

nitrogen or melted in air exhibit a similar electrical resistivity.

Knowledge of the relative distribution of the various ions through the glassy network is the obvious base from which to discuss the observed effects on resistivity. X-ray diffraction was used only to confirm the glassy nature of the materials and thus to indicate that the crystalline halide additives had been completely assimilated. Infra-red absorption was perhaps the technique that was best suited to the investigations. Several points arising from this work are worth summarising.

Firstly, only slight absorption was noted at the fundamental vibrational frequency of the added halide; this confirms that the additive is virtually completely disassociated. Secondly, no vibrational absorption has been assigned to a B-Cl linkage. However, this statement should be discussed further because no published data on such vibrations in glass exists. As mentioned in the previous Chapter, the only data that may be remotely relevant is that for crystalline boron trihalides, though even in this case any comparison is rather tenuous.

The vibrational frequencies of BCl_3 are observed to be at approximately 250 cm^{-1} , 460 cm^{-1} , 470 cm^{-1} and 960 cm^{-1} (339 - 341). In the materials under investigation the first and last of these values lie in regions of strong absorption, consequently it is not surprising that no effect is noted. It is only in the case of the second and third frequencies that observation of extra absorption lines may have been expected. A theoretical approach assigns a value of 839 cm^{-1} to the vibrational frequency of a 'B-Cl diatomic molecule' (334). It may be thought that this is a possible comparison with the glassy situation. No extra absorption is observed at this value, but once again the situation is that in

this wavenumber region there is already quite strong absorption. Overall it must be acknowledged that this direct approach is rather inconclusive; no definite B-Cl vibrations have been identified, but comparisons with established data are so weak that the presence of such bonds can not definitely be ruled out.

An interesting point arising from the infra-red measurements is that at least some of the halide ions replace residual hydroxyl ions in the glass. This was evident from the reduced strength of the 3500 cm^{-1} water absorption at higher doping levels.

However, the most emphatic result to emerge from the infra-red work is the great degree of similarity between the absorption curves for the pure and doped glasses. Even when the doping level reaches 30 mol.% the differences are relatively minor. It is quite remarkable that so much halide can be assimilated into the glass yet the basic network remains relatively unchanged. This clearly indicates that the decreased electrical resistivity brought about by doping is a result of subtle network manipulation rather than by structural rearrangement.

It was stated earlier that no vibration due to a boron-halide ion bond in a glass has yet been identified and that perhaps the best comparative data comes from work on boron trihalides. This is believed true, but it should be mentioned that some other infra-red work on the addition of halides to borate glasses has been reported. For example, Minami et al (80) have investigated the system $\text{AgX-Ag}_2\text{O-B}_2\text{O}_3$ (X=I,Br) and Irion et al (342) have investigated the system $\text{LiCl-Li}_2\text{O-B}_2\text{O}_3$. Both are analogues of the sodium system discussed here. In the former of these cases it is stated that "no new bands were observed on the addition of AgI to $\text{Ag}_2\text{O-B}_2\text{O}_3$ glasses". Similarly in the second case, when

considering the general formula $B_2O_3-xLi_2O-yLiCl$, it was found that "no new features are detected compared with the spectra of the $B_2O_3-xLi_2O$ glasses; for a given x the spectra of the binary and ternary compounds are nearly identical". It is further concluded that "in the boron-oxygen 'lattice' $LiCl$ is apparently 'diluted' without producing strong interactions". The general results from these two investigations are clearly very similar to those reported in this work.

The third structural investigatory technique that was employed was N.M.R. The study on the boron nucleus revealed that on adding a halide there was a slight increase in the fraction of four co-ordinated boron atoms. This was not to the extent that would be expected if an equivalent further amount of alkali-oxide modifier was introduced. This increase in four co-ordination could be accounted for either by extra BO_4 units or by the appearance of BO_3X units ($X =$ a halide ion). Consequently, the presence of a small number of B-X bonds could not be ruled out.

The study on the sodium nucleus demonstrated that, in the case of the glassy materials, no dramatic change had occurred in the environment of the sodium ions on adding the halide dopant. Only minor changes could have taken place.

It is not believed that any published work exists on the relationship between the N.M.R. spectra of borate glasses and halide doping.

Perhaps the best starting point in trying to relate the observed structural effects to the resistivity results is to comment on how the halide ions could physically fit into the glassy network. The radius of a fluoride ion is 1.33 \AA , that of a chloride ion is 1.81 \AA and that of a bromide ion is 1.95 \AA .

It is also important to note that the radius of an oxygen ion is 1.32 \AA , which is very similar to the fluoride ion value. Compared to this the chloride and bromide ion radii are much larger and relatively equivalent. Consequently, from a simplistic argument, the fluoride ions could be assimilated into the network quite easily, whereas the structure would have to be considerably stretched in order to accommodate either chloride or bromide ions.

Evidence for this statement is supplied by the boron-boron separation distances, S , extrapolated from the density measurements of the previous Chapter (see section 6.5). It can be seen that the presence of CaCl_2 or CaBr_2 substantially increases S . However, the addition of CaF_2 only increases S by an amount comparable to that resulting from the inclusion of CaO . This is best observed by comparing S values for the addition of 10% of each of CaBr_2 , CaCl_2 , CaF_2 and CaO .

It appears that S is rather independent of the exact nature of the alkaline-earth ion. The value of S for the addition of 10% MgCl_2 equals that for the glass containing 10% CaCl_2 . A similar result occurs for the glasses doped with 10% MgO and 10% CaO . The alkaline-earth metal ions, being doubly charged, are quite small; presumably they therefore fit into the glassy network quite easily,

As was discussed in section 2.1.6, Anderson and Stuart (112) have put forward a model which describes the activation energy for electrical conduction as being made up of an electrostatic attraction contribution plus an elastic strain deformation contribution. It is illuminating to consider how the presence of halide ions could affect either of these quantities.

Firstly, halide ions are, of course, singly charged, and this single charge is distributed over a large volume. This is in comparison to the double charge on the smaller oxygen ion. Consequently, any sodium ions moving in the vicinity of the halide ions would experience a much reduced electrostatic field and would therefore be more mobile.

Secondly, the halide ions, because of their size, have been shown to stretch the boron-oxygen network. Thus, when a sodium ion attempts to pass through the structure, part of the expansion necessary for its passage has already taken place. Here again, high mobility of the sodium ions is favoured.

Neither of these favourable effects relies on any particular bonding of the halide ion within the network. Its volume alone is sufficient to decrease resistivity. The fact that only a few, if any, direct B-Cl bonds occur has no effect on the interpretation. These ideas are also in good agreement with other observations that have been made. For example, this behaviour would not give rise to any sudden or dramatic drop in resistivity. The effect would be of a gradual nature; which is exactly what was found experimentally. Furthermore, this explanation would indicate that the reduction in resistivity had been caused by a decrease in the potential barrier to motion, i.e. activation energy. Again this is what was found in practice; the pre-exponential factor remains almost unchanged.

The results for the alkali-free glasses (i.e. that halide doping led only to a small change in resistivity, generally an increase) would also not be surprising according to this scheme. It must be remembered that there are two schools of thought regarding the conductivity mechanism for alkaline-earth borate

glasses, see section 2.7.6. The first, led by Owen (165, 166), believes that the mobile ions are the oxygen ions. If this is the case it is not difficult to see why doping with a halide results in a slight rise in resistivity. First of all, the atomic percentage of oxygen would be reduced, and secondly regions of the network through which the oxygen ions may have passed are now blocked by negative halide ions. Indeed, it is possible that the halide ions occupy sites similar to those preferred by oxygen ions, effectively reducing the number of sites for the oxygen ions to move into. Overall these results could be taken as good circumstantial support for Owen's theory, though this argument assumes that the halide ions are immobile, which may be an oversimplification.

The second, more conventional, view regarding the main conductivity mechanism is that the primary mobile ion is the alkaline-earth ion. The reason that the resistivity of these base glasses is so high is mainly because the double charge on the alkaline-earth ion results in it being very strongly bound in the network. The subtle changes in the structure brought about by the addition of a halide are going to have a very negligible effect in comparison. Consequently, if this second view is taken it is easy to see why only a small change in resistivity is observed on doping, though admittedly this does not explain why the trend is towards a slight increase.

It is informative to expand slightly at this point and to consider in terms of the results obtained in this study, some of the 'standard' conductivity theories. For example, the weak electrolyte theory which has been discussed by several authors, including Ravaine and Souquet (109). The main ideas in this theory

are that only a relatively small number of the mobile-type ions are actually mobile. The remainder of these ions being relatively strongly bound in molecular complexes. In attempting to explain the observed effects in terms of this theory it could be argued that there would be a reduced dissociation energy concerned with the added halide and hence there would be an increase in the equilibrium number of cations actually mobile. However, this set of ideas does not agree with the experimental findings. An increase in the number of mobile cations would result in a change in the pre-exponential factor and not the activation energy. This has been shown not to be the case. Overall it can be stated that these experimental results do not support the ideas of the weak electrolyte theory.

A second conductivity theory is the random site model. This has been discussed by Glass and Nassau (111) amongst others. In this model it is deemed that due to the random nature of the glassy structure there must be a wide range of sodium sites with differing energies. Consequently, it is thought that a true distinction between a 'mobile' alkali ion and an 'immobile' alkali ion is unjustified. A theoretical treatment shows a direct relationship between ion mobility and the extent of the site energy distribution. The addition of a halide to the glass is bound to lead to the appearance of some new types of sodium sites and consequently there is an increase in the site energy distribution and therefore ion mobility. In summary, the random site model does not disagree with the experimental findings reported here.

While it is not believed that any work has previously been reported on halide doped sodium borate glasses (or halide doped alkaline-earth borate glasses) some results have been published

for rather analogous systems. Most of these results were mentioned in section 2.7.4, (and source references quoted), and it is interesting to consider the explanations for the observed effects put forward by the various authors.

Perhaps the most similar system to that investigated in this work was the study of the $B_2O_3 + Li_2O + LiX$ ($X =$ a halogen) series of glasses carried out by Levasseur and co-workers (73, 74, 153, 154). They too found that the addition of the halide could reduce resistivity, with the effect of chlorides and bromides being considerably greater than that of fluorides. Only small amounts of iodides could be incorporated into the glasses. Overall these results show a great qualitative similarity to those reported here. The explanation did not contain any theoretical model but it was supposed that (73) "this phenomenon may be the consequence either of a dilation of the boron-oxygen matrix or of the higher polarisability of the halogen". Such views are not unlike those proposed earlier in this Chapter in explanation of the results obtained in the present study.

The work of Button et al concentrates on the chloride version of the above lithium ternary glasses. A reduced resistivity was achieved on the addition of the halide, which was brought about by a reduction in activation energy. Several suggestions are put forward in an attempt to explain the effect such as (155) "Cl additions can dramatically affect the total number of (lithium) sites and thus the effective Li^+ ion jump distance" (a result which would reduce resistivity, see section 2.4), "chlorine additions ... lower the strain energy barriers to ion motion" and "the coulombic potential ... must be affected by halide additions". It was also acknowledged that their observed results

tend to favour the random site model in comparison to the weak electrolyte model, which is a result in agreement with this study.

The analagous fluoride doped lithium ternary system was investigated by Smedley, Angell and co-workers, the addition of the fluoride caused a reduced resistivity. However, no theory stating that the reduction was directly related to the presence of the fluoride ion was put forward. Instead, the authors appear to believe that (76) the high conductivity is caused simply by being able to incorporate more lithium ions into the glass than would have been possible just by the addition of the oxide. Indeed, they find that the replacement of Li_2O by LiF decreases the conductivity. At first this may seem contrary to the results of this study where it has been observed that the addition of a chloride increases conductivity even when the overall sodium content is reduced. However, it should be remembered that the additive under discussion is the fluoride. It was the case that in this work the addition of CaF_2 to borax indeed increased resistivity. It was only the addition of NaF (i.e. an effective increase in sodium content) that brought about a reduction, i.e. there is no general disagreement.

Moving slightly away from alkali borate materials, Minami and co-workers (78 - 81) have studied the effects of adding silver halides to various silver based glasses; silver phosphate, silver molybdate and silver borates. Most of their work is concentrated on the addition of silver iodide and once again a reduction in resistivity is reported (sections 1.3 and 2.7.4). In the case of the most relevant materials, the doped silver borate glasses, it is generally concluded that not all silver ions contribute to conduction; the silver ions interacting mainly

with the halide ions being especially mobile. A significant contribution from silver ions interacting with a BO_4^- group is suspected and the dominant conduction mechanism is thought to be dependent on composition. The third type of silver ion site, where the ions form partially covalent bonds with non-bridging oxygen ions, is not thought to give rise to high ion mobility. These views are not entirely in agreement with those expressed in this study but nevertheless the most important idea, that regions near the added halide ions are areas of high mobility, is again put forward.

One final interesting point also arises from the work of Minami et al. When investigating the system $\text{AgI-Ag}_2\text{O-MoO}_3$ (79) (for which the addition of the AgI increases conductivity) a comparison is made to the conductivity of the equivalent crystallised material. Invariably the crystallised material is found to be more resistive. This is the opposite effect to that found in this study. For all the halide doped glasses mentioned above this is the only occasion on which the crystallised product is mentioned. It is not known whether measurements have been performed on such materials and the results found to be inferior and therefore not reported, or if the crystallised materials simply have not been investigated.

In summary, it is believed that the reduced resistivity values for the doped glasses are the result of the halide ion improving sodium ion mobility by two means. Firstly, the electric field around the halide ion is reduced in respect to that around an oxygen ion. This is because of its large size and single valency. Secondly, the network around the halide ion has become distorted in order to accommodate the dopant ion and is consequently

more 'open'. Both these situations would afford easier transport of the sodium ions.

It should be made clear that the dramatic effect noticed on the resistivity of re-crystallised material is not thought to be due to a similar explanation. The resistivity decrease is altogether too abrupt for it to be directly caused by a subtle change in lattice structure.

7.3 Glass-Ceramics.

The room temperature resistivity of the re-crystallised products can be over four orders of magnitude below that of the parent glass. In contrast to the situation with glassy materials (where there is a gradual reduction in resistivity with increased doping level) light doping of the glass-ceramics leads to a very dramatic decrease in resistivity, but on further doping the rate of reduction in resistivity is much smaller. Indeed, it has been found in one case, where the doping level was particularly high, that the resistivity reached a minimum at a certain amount of additive and that a higher doping fraction resulted in a slight resistivity increase.

The resistivity is relatively independent of heat treatment temperature provided that the specimen is well crystallised through its volume. Scanning electron microscopy was used to observe the crystallites. Typically, at the high end of the crystallisation temperature range (a limit set by deformation of the specimen) the dimensions of the crystallites were of the order of 10 - 50 μm , while at lower crystallisation temperatures the crystallite dimensions were below 1 μm . The nucleating effect of the halides should also be considered; the crystallites formed on heat treating pure borax were very large indeed.

Overall it appears that the resistivity does not depend greatly on crystallite size for a given volume fraction of crystal phase. The reduction in resistivity brought about by crystallisation is therefore a bulk effect and is not concerned with sodium ion motion along the glass/crystal interface; a situation which would be highly dependent on crystallite size.

For any given composition the decrease of the observed electrical resistivity occurs very abruptly as the heat treatment dwell temperature increases, and therefore as the crystal volume fraction reaches a certain proportion. Simplistically, this fact can be associated with the cross-linking of crystalline regions. However, this does not necessarily mean that the 'light' crystalline regions have to overlap. A considerable percentage of 'the residual dark area' may be crystalline, and, as these regions contain at least some halide ions, the crystallites will be reasonably conducting. The presence of such secondary crystallites could therefore facilitate the linking of conducting regions.

The lowest obtainable room temperature resistivity is dependent on the type of added halide, but a value of $10^6 \Omega \cdot \text{cm}$. is approachable with most of the chlorides and bromides that have been investigated. It should be remembered that crystallisation of a pure borax glass resulted in an increased resistivity, as generally expected.

Before any further discussion of the resistivity results it is beneficial to emphasise certain points. Firstly, the 'charging-up' experiments using an electron microscope have proved without doubt that it is the crystalline phase formed during heat treatment that is the highly conducting region. The residual glassy phase is of minor importance, especially at low temperatures

(see later discussion). The abrupt change of resistivity on doping is so marked that it may be believed that some mechanism other than sodium ion transport is responsible. However, the 'triple-disc' experiments and the thermopower work have shown that this is not the case. The major electrical conductivity mechanism is still sodium ion transport.

As with the glassy specimens one of the most important queries regards the effect of the addition of the various types of halide ion. This is best answered by considering the series of glass-ceramics where NaX (X = a halogen) is the dopant. It was clearly shown that in the case of Cl^- and Br^- a very large increase in conductivity was observed, with Cl^- ions providing a slightly greater resistivity reduction. However, F^- did not reduce the resistivity, its presence actually increased resistivity over most of the temperature range (that is with respect to pure borax glass).

The nature of the added cation appears to be of less importance. For example, there is little difference in resistivity between the glass-ceramic containing 10% ZnCl_2 and that containing 10% CaCl_2 . Both show a resistivity of approximately $10^6 \Omega \cdot \text{cm}$. at room temperature. Indeed, even when the cation is the large barium ion the resistivity only increases to $7 \times 10^6 \Omega \cdot \text{cm}$. When the additive is simply NaCl, once again a resistivity value of $10^6 \Omega \cdot \text{cm}$. is achieved; this figure is the approximate result over quite a large range of dopant concentrations.

The resistivity-temperature graphs all show a consistent pattern. Obviously, the activation energy has changed dramatically on crystallising the glass, which results in the observed reduced resistivity. However, because of the low gradient, at high

temperatures the magnitude of the resistivity reduction with respect to the parent glass becomes smaller. Usually in the temperature region where the two respective curves begin to converge there is quite a sharp change in the activation energy for the glass-ceramic. Above this 'transition temperature' the activation energy is similar to that shown by the glassy product, though the overall resistivity usually still maintains a slightly reduced value.

A further point of note is that in general the surface conductivity of the specimens was found to be negligible in comparison to the bulk conductivity. Surface conduction was only found to be a problem in one isolated case, where the dopant was 10% ZnCl_2 and the heat treatment temperature used was not high enough to fully crystallise the glass.

One of the most interesting sets of results were those obtained for alkali-free glass-ceramics. The reduced resistivity effect was still present, at least to some extent, in all three doped compositions investigated. The added halide ions seem to affect this type of material in a similar manner to that in which they affect the sodium borate specimens. In the sodium borate glass-ceramics the mobile ion is the sodium cation, consequently it seems only reasonable that the mobile ions in the alkali-free glass-ceramics are the alkaline-earth cations. This is true whatever the conductivity mechanism in the parent glass (see earlier discussion on alkali-free glasses). The confirmation, or otherwise, of this statement is a possible area of future work.

Having discovered such a dramatic effect on the observed resistivity when the specimen is crystallised, the prime concern was then the identification of the crystalline species, mainly

by X-ray diffraction. The most important feature of the X-ray patterns was that all the observed lines could be assigned to well-characterised sodium (or dopant metal) borates with no unidentified lines which might indicate some unknown and possibly highly conducting phase. The low resistivity phenomena must therefore arise from subtle modification of the structure of simple metal borates.

The actual crystal phases formed depend on dopant concentration e.g. as increased amounts of NaCl are added, $\text{Na}_4\text{B}_2\text{O}_5$ is formed in preference to $\text{Na}_2\text{B}_4\text{O}_7$. However, these trends have little influence on the observed conductivity.

Furthermore, the X-ray diffraction data indicates that the atomic fraction of sodium in the crystalline borate phase that is produced on heat treatment is always increased relatively to that in the parent glass composition. Thus, the residual glassy phase is left comparatively depleted in sodium and therefore it would be expected to have a higher resistivity than the original composition. This inference, that the highly conducting phase must be the crystalline phase and not the residual glass, is supported experimentally by the findings of the 'charging-up' experiments utilising electron microscopy.

Finally, none of the diffraction patterns showed any trace of a halide phase. This is quite remarkable given the high dopant concentrations occasionally used, and shows how easily the halides can be incorporated into the sodium borate structure.

Most of the above statements regarding X-ray diffraction results have been directed at the sodium borate based materials. However, rather similar results were obtained with the alkali-free materials and the same general conclusions apply.

The X-ray diffraction work is in excellent agreement with the electron microscopical studies and with the associated E.D.A.X. analysis. The number of phases revealed in the micrographs always corresponds to the number found using X-rays, and the distribution of the dopant cations and sodium ions as shown via E.D.A.X. again also correlates with the X-ray analysis. The E.D.A.X. work also showed that the halide ions remain well distributed through both types of phase, though the crystalline phase is favoured slightly on some occasions. This is the first positive indication of the placement of these ions within the formed glass-ceramic and is of considerable importance.

The first section of the N.M.R. study, the investigation of the boron nucleus, showed similar trends for the glass-ceramic materials as it did for the glassy specimens. Dependent on overall composition, the fraction of four co-ordinated boron atoms appeared to increase slightly with doping. However, the observed changes are only of the order of the inherent experimental error and it is therefore acknowledged that such a claim is rather tentative. However, it is quite clear that there is no dramatic change in the environment of the boron nucleus within the glass-ceramic specimens on the addition of a halide dopant. This supports the results of X-ray diffraction and of other studies.

The latter part of the N.M.R. study, those experiments concerning the sodium nucleus within the glass-ceramics, does, however, illustrate a marked environmental change. In the case of a doped specimen a significant, large resonance peak has appeared which is perhaps superimposed on a trace similar to that occurring for an undoped sample. It has been concluded that this sharp resonance is indicative of some sodium nuclei present in new,

highly mobile sites, while the broad peak is formed by some sodium ions remaining in more traditional environments. Furthermore it has been shown, in a quantitative theoretical treatment using observed activation energies, that this sharp peak is capable of being caused by the situation known as motional narrowing. This phenomenon is a direct result of the presence of highly mobile ions. Comparison of the N.M.R. spectra of the doped and pure samples provides a unique and clear demonstration of the change in environmental situation and of the mobility of the sodium ions within the doped glass-ceramics.

The infra-red absorption work has already been thoroughly discussed both in the previous Chapter and in the comment on glassy materials earlier in the present Chapter; only the very broad conclusions will be mentioned here. Firstly, there is very little difference between the absorption spectra of the pure and doped glass-ceramics. This is true even when the doping level is quite high and is the case for both sodium borate based specimens and alkali-free specimens. Clearly the situation is that the large reduction in resistivity is achieved despite only minor changes in the boron-oxygen lattice structure. This comment has been made in almost all of the individual discussions on each experimental technique and is a common theme throughout this study. A second observation made in this work is that occasionally a trace, but only a trace, of the dopant halide may remain un-dissociated. It appears that infra-red absorption is a more sensitive tool for the identification of trace materials than is X-ray diffraction analysis. Presumably in this latter technique the peaks from the trace compound are totally swamped in the plethora of other, larger, peaks. It is not thought that these

trace compositional remnants are important in the interpretation of the resistivity phenomenon.

In attempting any explanation of the observed resistivity reduction it is best to consider firstly which situations already give rise to high ionic conduction. The obvious first choice material is β -alumina. In this case, as was discussed in section 2.9.1, layers of loosely bound sodium ions exist within the structure. It is not thought that any similar arrangement occurs in the materials under study here. A second structural arrangement giving rise to high ionic mobility is the tunnel formation found in ReO_3 and TiO_2 type compounds (e.g. 343). The base unit that gives rise to the tunnels, when configured suitably, is the octahedral arrangement of oxygens around a central cation. It is not believed that the presence of a halogen in the materials under consideration in this study could in any way influence the formation of similar units. In any case, such a major lattice rearrangement would surely be observed in one of the structural techniques used.

The complex materials proposed by Goodenough et al (175) for fast sodium ion transportation, which also were mentioned in section 2.9.1, again rely on a skeletal tunnel arrangement. However, in this work it is also emphasised that high mobility would not be achieved without the presence of partially occupied lattice sites of approximately equivalent energy, i.e. there must be vacancies for the mobile ions to move into. This idea of vacancies being necessary is found in the work of many other authors for a wide range of materials. For example, the fast motion of silver ions through compounds based on silver iodide is alleged to be the result of the two silver ions within the unit

cell being mathematically distributed over a great number of equivalent sites (see section 2.9.2). In the present work the 'available vacancy' theory seems to be a suitable starting point. If the presence of the halide ions could somehow introduce sodium ion vacancies into the normal lattice structure then the resistivity would be greatly reduced. This would be achieved without major structural upheavals which could be observed by the standard techniques used. Certainly, further consideration is merited.

The simplest case to consider is the addition of NaCl to borax. X-ray analysis has shown (section 6.1.2) that in this case relatively larger amounts of the crystal phase $\text{Na}_4\text{B}_2\text{O}_5$ are present at higher doping levels than at low doping levels, while the reverse trend is shown for $\text{Na}_2\text{B}_4\text{O}_7$. The situation is as if further Na_2O has been added to borax rather than NaCl. It is not claimed that the addition of NaCl exactly mimics the addition of Na_2O but certainly from an X-ray analysis point of view there is a similar trend. From this evidence the conclusion to be drawn is that the halide ions occupy sites that would normally be occupied by oxygen ions and that in some respects there is little difference between the two situations. It is not believed that the halide ions bond in precisely the same manner as the oxygen ions which they replace, the difference in valency will obviously not allow this. A point worth emphasising is that the X-ray diffraction pattern depends much more on the position of the scattering centres than on the interatomic bonding.

Assuming the situation is as described above, if the additive had been Na_2O then two sodium ions would be included for each added anion. However, when the additive is NaCl only one sodium

ion is added for each anion. Consequently, as similar crystal lattices result in the two situations, there must be unfilled sodium ion sites in the latter case. It is believed that it is these vacancies that are responsible for the observed reduced resistivity.

The production of halide ion interstitials is a competing process against the formation of sodium ion vacancies. The governing factor will be the energy involved with each process, which may be dependent on the type of halide ion concerned, and on dopant concentration. It is generally found that vacancy production requires less energy than interstitial formation, though at higher dopant levels the reverse may well be true because the lattice would find it increasingly more difficult to accommodate halide ions. Notably, fluoride ions tend to form interstitials very easily, for example in $\text{CaF}_2 + \text{CaYF}_2$ (344), which has a high conductivity due to fluoride ion motion. It is believed that the production of halide ion interstitials would not be remotely as beneficial for conductivity purposes as would be the production of sodium ions vacancies; the ions would certainly not contribute directly because of their relatively large size. In the case of glassy materials it was found that the presence of the halide ions did increase conductivity to a certain degree due to expansion of the network and electrostatic effects. However, in the case of a crystal the lattice is much more rigid and therefore these effects would be less pronounced and the halides might even prove to be a hindrance to sodium ion motion by blocking tunnel paths etc. At best, the formation of interstitials in preference to sodium vacancies at higher doping levels would decrease the rate of resistivity reduction with dopant

concentration and perhaps stop it altogether.

This vacancy/interstitial theory now has to be tested against some of the experimental results. The question is raised as to why the dramatic effect is not also seen in the glassy materials. It is believed that the answer to this lies in the differing nature of the two structures. For the effect to occur there must be particular vacant sites concerned with the sodium ions and particular oxygen-type sites for the halide ions to occupy. This simply does not occur in a random glassy network. In such a network there can be no precise identification of a site or of a vacant site; the situation becomes too vague a concept. What is needed for the resistivity reduction effect to be observed is a regular situation in which occupation or vacancy of a particular site is well defined.

It is easy to see that the introduction of a halide will give rise to a very abrupt reduction in resistivity; each vacancy will contribute to improved conduction. This is a direct effect and it is not surprising that the reduction in resistivity is much more dramatic than in the case of glassy materials in which the reduction is due to subtle changes in the network, as discussed earlier.

It was observed that high doping levels do not greatly further reduce resistivity in comparison to low doping levels. This is exactly as was predicted would occur if interstitial halide ions started to form in preference to sodium ion vacancies, and is therefore good evidence in support of the theory. At low doping levels sodium ion vacancy production occurs and the resistivity is drastically reduced, at higher levels halide interstitials occur and the rate of resistivity reduction is not maintained.

Another aspect of the resistivity results that needs discussion is the sharp increase in activation energy that usually occurs at high temperatures. Two explanations at first appear plausible. Consider first the two activation energy terms, U and $\frac{1}{2}W$, that occur in the resistivity equation mentioned in section 2.1.4. In that section it was explained that if sufficient defect states already exist then the energy term for their production, $\frac{1}{2}W$, becomes irrelevant and may be dropped from the equation. The resulting lower activation energy could then be deemed to describe the low temperature regions where there would be ample vacancies for the sodium ions to move into because of doping. At elevated temperatures a higher activation energy results as the $\frac{1}{2}W$ term has to be included because the thermal production of vacancies can no longer be ignored. However, this explanation ultimately has to be rejected because the high doping levels involved would always lead to numbers of vacancies far in excess of whatever may be produced thermally.

A second, and more likely, explanation arises because of the observation that the high temperature activation energy is invariably similar to that of the parent glass. It seems quite probable that at these temperatures most conduction is taking place in the residual glassy phase. One experiment that would confirm the situation is a variation of the 'charging up' experiments using an electron microscope that have been described elsewhere in this thesis. On this occasion the specimen would be heated to above the

activation energy transition temperature. The phase that charges up would again be the more resistive phase. The experimental parameters would have to be considerably adjusted in order to compensate for the lower specimen resistivity at these temperatures.

The above arguments have been directed at the system where NaCl is the additive in sodium borate. However, it makes little difference whether another type of dopant is considered. The added halide ions could still occupy oxygen-type sites, causing vacancies in the existing sodium arrangement. The role of the added cation would be a secondary effect. This ion could sit at a sodium-like site or at any other interstitial site; the fact that sodium vacancies are being formed is unaffected.

Furthermore, there is no reason why the resistivity reduction effect should not be noticed in other borate systems, e.g. the alkali-free borates used in this study. The above discussion can be virtually repeated without modification for the alkaline-earth borate + alkaline-earth halide materials. The addition of a dopant halide would cause alkaline-earth ion vacancies to be formed, which would result in reduced resistivity. Whatever the mobile species in the glassy materials (see earlier discussion), it is proposed that in the more conducting, doped, re-crystallised specimens it is the alkaline-earth ion that is primarily responsible for conduction.

This theory appears to fit the resistivity and other transport measurements very well indeed, and it is now necessary to consider briefly whether it is compatible with other physical property measurements. The X-ray diffraction work has already been discussed, indeed the theory was initially put forward because it satisfied these findings, so no problem is encountered from this aspect.

The N.M.R. study on the boron nucleus showed that on doping there is no great change in the boron environment except, perhaps, some bonding of the chloride ion into the basic unit. There is no conflict between this and the conductivity theory. Work on the sodium nucleus demonstrated that, on crystallising the doped specimen, some of the sodium ions are in new, highly mobile sites while the environment of the remainder is unchanged. These two observations can now be related to sodium ions close to a vacancy and to sodium ions adjacent to filled sites.

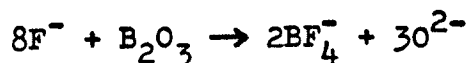
The main conclusions of the infra-red absorption study were that the dopant halide caused no great change in the overall borate network and that the halide was completely dissociated in the product (except for a trace at very high dopant concentrations). These conform to the requirements of the resistivity theory. Also, no particular identification was made of a bond involving a halide ion. The resistivity theory only demands that these ions occupy oxygen-ion type sites and does not demand a particular bond. Consequently there is no evidence to conflict with the theory.

The E.D.A.X. work, utilising electron microscopy, showed that in general the halide ions show some preference for the crystal phase rather than the residual glassy phase. From the resistivity theory point of view this should aid resistivity reduction, though admittedly the effect is not of prime importance because even relatively few halide ions in the crystal phase would cause a considerable resistivity decrease. Another result of this study was that the dopant cations, be they ions of zinc, calcium or sodium itself, also tended to preferentially congregate in the crystal phase. Again it can be argued that the consequence of this is that conductivity will be increased. If the doubly valent

cations occupy the same type of site as sodium ions then effectively one sodium ion vacancy is produced for each dopant ion.

There is one point which has not yet been mentioned but is one of the most surprising results of the resistivity measurements. This is the failure of the fluoride dopants to cause a resistivity reduction as was found with chlorides and bromides. This is despite the fact that the fluoride ion is very similar in size to the oxygen ion and would therefore seem an ideal candidate for occupation of an oxygen-ion-type site. The chloride and bromide ions are very much bigger than the oxygen ion and it is therefore more difficult to envisage them entering the lattice in place of an oxygen ion, yet they seem quite able to do so. However, this ignores the tendency of fluoride ions to easily become interstitials as has been observed by other workers (see earlier discussion). It has been argued that interstitial halide ions do not encourage high conductivity. It is therefore believed that the fluoride doped materials do not show improved resistivities because of a tendency to form fluoride ion interstitials.

There is also another explanation that merits consideration. It is a fact that fluoride ions can react with borates to form fluoborates (345) according to the reaction:



It could be that the formation of such units is not conducive to the resistivity reducing effect. It may be thought that the presence of these units would have been noted in the course of the infra-red absorption study. However, the absorption frequencies of sodium borofluoride are at 1036 cm^{-1} , 1076 cm^{-1} and several around 530 cm^{-1} (346). The first two of these values lie in

regions of strong absorption due to the usual borate structure and the latter group is also in a region of several absorption lines. These results coupled with the fact that this study has necessarily concentrated on chloride and bromide dopants because of favourable resistivity measurements, suggests that a more detailed investigation should be undertaken as a future project.

As mentioned previously, it is not believed that other work on re-crystallised sodium halo-borates has been reported. It is therefore impossible to directly compare the results and theory contained in this study with that of other authors. However, perhaps the most closely related work is that of Levasseur and co-workers (178, 179) who studied the lithium boracite $\text{Li}_4\text{B}_7\text{O}_{12}\text{Cl}$ (equivalent to $3\text{Li}_2\text{O} + 7\text{B}_2\text{O}_3 + 2\text{LiCl}$). As was discussed in section 2.9.1 this material is reported to have a reasonably high conductivity. The reason for this is thought to be due to its structure, which is said to consist of a borate framework of tetrahedral BO_4 and trigonal BO_3 units with an interpenetrating sublattice containing only Li and Cl ions. This sublattice is said to contain a lithium ion site which has only 0.25 probability of being filled. It is not suggested that Levasseur's work and the work reported here are entirely analogous, but there do seem to be distinct similarities. The necessity for vacancies is a common theme, as is the absence of discrete halide units. The fact that the halide ion does not necessarily form a strong bond with the borate structure is also a point made in both studies.

The vacancy mechanism, and other associated theory mentioned in the above discussion, is put forward with a considerable degree of confidence as an explanation of the

observed resistivity phenomena and of other physical property and structural variations.

CHAPTER 8Final Overview.8.1 Achievements and Conclusions.

The aims and aspirations of this study were set out at the start of this thesis, (see sections 1.3 and 1.4) and it is interesting to look back to see if all, or indeed any, of these aims have been achieved.

Initial work involved confirming that reduced electrical resistivity resulted when a borate material was doped with a suitable halide. This turned out not to be the simple task that it appeared to be because it was not realised for some time that re-crystallisation was all-important. In most other known cases it is the glassy material, not the re-crystallised form, that is more conducting. The work on glasses proved very worthwhile and a descriptive theory explaining the observed effects on resistivity and other physical properties has been put forward. However, the resistivity reduction occurring in these materials is not really sufficient for them to be considered as, say, battery electrolytes, or for them to be known as fast ion conductors. Nevertheless, this class of specimen is very interesting from a more 'academic' viewpoint, and it is believed that the reasons behind the reduced resistivity are well understood.

It is with the re-crystallised products that by far the greatest resistivity reduction can be achieved and it is for this reason that most of the later work in this thesis has concentrated on them. A fairly wide range of dopants and of base borate materials have been tried and tested, with a high degree of success. It is believed that numerous other types of dopants would be suitable for use in improving the conductivity, however further

diverse exploration was not made as this would have meant cutting back on other fundamental studies. It is believed that the compositions investigated here give a solid experimental base from which to expand.

The lowest resistivity achieved, of between 10^5 and $10^6 \Omega \cdot \text{cm}$. at room temperature, is still rather high in comparison to β -alumina and other well-known conductors, and therefore these halo-borate products would have to be heated before their conduction can be truly 'fast'. However, it should be remembered that the minimising of the resistivity was never the prime aim of this work; such a task fell to the collaborating industry. Consequently, the figures quoted above represent the minimum achieved through using, from this point of view, materials not chosen for the purpose. Lower values than this are to be expected and indeed have been reported in private communications with B.R.L. The advantages of these new materials over their competitors are their ease of manufacture, their low raw material cost and the fact that common, non-toxic chemicals are involved. Indeed, it has been shown that even the heat treatment re-crystallisation process does not have strict limits.

Many considerable strides forward have been made in the characterisation of the conductivity mechanism. Basic facts such as the nature of the mobile ion, the relative resistivity of the glassy and crystalline regions and the identification of the crystalline phases have all been established. It is also now known that virtually all the dopant dissociates and that no unexpected crystal species is present. All these findings have been assimilated into a coherent theory that seems able to explain the majority of the observed effects.

It is believed that this work has introduced a new breed of highly ionically conducting materials which could have a number of practical uses. Because these materials are so novel, all this project could hope to cover was a broad base of resistivity measurements, physical property and structural investigations, and the proposal of a theory. Any detailed study of a particular aspect of a branch of any of these topics simply could not be entertained because of constraints of time etc., and must therefore be left to future workers. From time to time throughout this thesis attention has been drawn to suggested avenues down which such work might progress. These, and several other ideas are mentioned in the final section.

8.2 Suggestions for Future Work.

It is perhaps a measure of how new these materials are, and of how interesting the observed results, that so many lines of further study have appeared during the course of the experiments. What follows is basically a list of investigations which, if performed, would yield useful information. The justification of each suggested action should be evident from the text of this thesis. The order in which they appear is not meant to indicate any degree of importance, this is left to the discerning reader.

1. Resistivity results for doped alkali borates other than sodium borate.
2. Review of the melting procedure to somehow allow iodides to be retained in the parent material.
3. Investigation of the effect on resistivity of low doping levels ($<5\%$).
4. The vacancy formation could possibly 'relax' in some way, either simply through time or through further heat

treatment when in use. This could effect the resistivity and should therefore be considered closely.

5. The nature of the mobile ion in doped alkaline-earth re-crystallised specimens needs definite confirmation; perhaps by employing a more severe version of the 'triple-disc' experiments (using higher temperatures, greater polarising voltages and a longer time scale).
6. Determination of the relative conductivity of the crystalline and residual glassy phases at temperatures above that at which the activation energy increases (as is usually found). This could probably be achieved by a high temperature version of the 'charging-up' experiments using electron microscopy.
7. A detailed X-ray diffraction study on the relation between line widths and doping levels. Any increase in width could indicate an increase in the degree of disorder in the crystal.
8. Further investigation of the 530 cm^{-1} band in the infra-red absorption spectrum.
9. The N.M.R. investigations on the sodium nucleus could be improved upon by incorporating trace amounts of paramagnetic salts, e.g. Mn^{2+} , into the material. This would drastically reduce the relaxation time of the magnetic excitations which would mean that increased R.F. power input could be used without saturation, consequently increasing the signal to noise ratio.
10. Further general tests on materials with fluoride dopants to see if reasons for their inconsistent behaviour can be confirmed. Specifically, the presence, or otherwise, of the fluoroborate ion should be ascertained.

11. A systematic set of experiments using electron microscopy to plot the dependence between resistivity and crystal phase volume fraction. As well as being of general interest this would reveal if the abrupt reduction in resistivity does occur when the crystals become cross-linked.

References.

1. G. Tammann. "Kristallisieren und Schmelzen", 1905; "Aggregatzustände", 1922; "Der Glaszustand", 1933. Leonard Voss, Leipzig.
2. L. D. Pye reviewed in "Introduction to Glass Science", ed. Pye, Stevens and LaCourse, Plenum Press, New York, 1972.
3. G. W. Morey. "The Properties of Glass", Reinhold Publishing Corp., New York, 1938.
4. K. H. Sun. J. Am. Ceram. Soc., 30, 277, 1947.
5. G. O. Jones. "Glass", Methuen, London, 1956.
6. J. D. Mackenzie in "Modern Aspects of the Vitreous State", ed. J. D. Mackenzie, Butterworths, London, 1960.
7. A. A. Lebedev. Tr. GOI, 2, Part 10, 1921; 3, Part 24, 1921; Izd. AN. SSSR., ser. phys., N3, 381, 1937; Izd. AN. SSSR., N4, 584, 1940.
8. J. T. Randall, H. P. Rooksby and B. S. Cooper. Z. Krist, 75, 196, 1930; J. Soc. Glass Technol., 15, 54, 1931.
9. W. H. Zachariasen. J. Am. Chem. Soc., 54, 3841, 1932.
10. V. M. Goldschmidt in "Geochemical Distribution Laws No. 8", p137, Skiffer Norske Videnskaps. Akad. Mat. Naturv., K1, 1926, and Trans. Far. Soc., 25, 253, 1929.
11. B. E. Warren. Z. Krist, 86, 349, 1933.
12. B. E. Warren. J. Am. Ceram. Soc., 17, 249, 1934.
13. B. E. Warren and C. F. Hill. Z. Krist, 89, 481, 1934
14. B. E. Warren and A. D. Loring. J. Am. Ceram. Soc., 18, 269, 1935.
15. B. E. Warren, H. Krutter and O. Morningstar. J. Am. Ceram. Soc., 19, 202, 1936.
16. B. E. Warren. J. App. Phys., 8, 645, 1937.
17. B. E. Warren and J. Biscoe. J. Am. Ceram. Soc., 21, 29, 1938.
18. J. Biscoe and B. E. Warren. J. Am. Ceram. Soc., 21, 287, 1938.

19. B. E. Warren. J. App. Phys., 13, 602, 1942.
20. G. Hagg. J. Chem. Phys., 3, 42, 1935.
21. N. V. Solomin. Zh. F. Ch., 14, 235, 1940, Scientific-technical compendium NIIES, Part 14, 1959, p3.
22. V. V. Tarasov. DAN. SSSR., 46, 122, 1945; 58, 574, 1947.
23. V. V. Tarasov. "New Problems on the Physics of Glass", Gosstrolizdat, Moscow, 1959, Translation from Russian, Israel Program for Scientific Translations, Jerusalem, 1963.
24. H. Richter, G. Breitling and F. Herre. Naturwiss, 40, 621, 1953.
25. J. M. Stevels. Glass Ind., 35, 69, 135, 657, 1954; Verres et Refract., Nr. 2, 91, 1953.
26. R. Bruckner. Glastech. Ber., 37, 500, 1964.
27. M. L. Huggins, K. H. Sun and A. Silverman. J. Am. Ceram. Soc., 26, 393, 1943.
28. J. R. Van Wazer. "Phosphorus and its Compounds" Vol. 1, Interscience, New York, 1958.
29. J. O'm. Bockris, J. D. Mackenzie and J. A. Kitchener. Trans. Faraday. Soc., 51, 1734, 1955.
30. J. O'm. Bockris, J. W. Tomlinson and J. L. White. Trans. Faraday. Soc., 52, 299, 1956.
31. K. Fajans and S. W. Earber. J. Am. Chem. Soc., 74, 2761, 1952.
32. P. P. Kobeko. The Structure of Glass, Izd. AN. SSSR, 1955.
33. N. Valenkov and E. A. Porai-Koschitz. Z. Krist, 95, 195, 1936; Nature, 137, 273, 1936.
34. E. A. Porai-Koschitz. DAN. SSSR, 40, 1943; "Uspekhi Khimii", 13, 115, 1944; The Structure of Glass, Izd. AN. SSSR, 1955; The Glass Like State, Izd. AN. SSSR, 1960; The Structure of Glass Consultant Bureau Inc., New York, 1958.
35. E. A. Porai-Koschitz and N. S. Andreev. Nature, 182, Nr. 4631, 336, 1958; DAN. SSSR, 118, 735, 1958.
36. A. Smekal. J. Soc. Glass. Technol., 35, 411T, 1951.

37. J. E. Stanworth. J. Soc. Glass. Technol., 30, 54T, 1946; 32, 154T, 1948; 36, 217T, 1952.
38. R. S. Bradley. Quart. Rev. Chem. Soc. Lond., 5, 315, 1951.
39. D. G. Thomas and L. A. K. Stavely. J. Chem. Soc., p4569, 1952.
40. L. A. K. Stavely in "The Vitreous State", p85, Glass Delegacy of the University of Sheffield, 1955.
41. W. J. Dunning in "Chemistry of the Solid State", ed. ed. W. E. Gardner, Academic Press, New York, 1955.
42. J. H. Holloman and D. Turnbull. "Progress in Metal Physics" Vol. 4, 333, Pergammon Press, London, 1953.
43. D. Turnbull. "Solid State Physics" Vol. 3, Acedemic Press, New York, 1956.
44. D. Turnbull and M. H. Cohen. J. Chem. Phys., 29, 1094, 1958; Nature, 189, 131, 1961, and in "Modern Aspects of the Vitreous State", ed. J. D. Mackenzie, Butterworths, London, 1960.
45. P. W. McMillan. "Glass Ceramics" 2nd. Ed., Academic Press, London, 1979.
46. R. Becker and W. Doering. Ann. Phys., 24, 719, 1935.
47. R. Becker. Ann. Phys., 32, 128, 1938.
48. J. Frenkel. "The Kinetic Theory of Liquids", Clarendon Press, Oxford, 1946.
49. J. E. Stanworth. "Physical Properties of Glass", Clarendon Press, Oxford, 1950.
50. A. B. Pippard. "The Elements of Classical Thermodynamics", C.U.P., 1966.
51. R. H. Doremus. "Glass Science", John Wiley and Sons, New York, 1973.
52. C. G. Bergeron in "Introduction to Glass Science", ed. L. D. Pye, H. J. Stevens and W. C. LaCourse, Plenum Press, New York, 1972.
53. S. Badzioch, Borax Research Ltd., Chessington, Surrey, private communication.

54. Anon. Chem. Int., 1982, p14-19, part 3.
55. H. V. K. Udupa et al. Trans. SAEST, 16, 179, 1981.
56. J. Jensen and B. C. Tofield. Energy Storage, Pap. Int. Conf., 1, 205, 1981, ed. H. S. Stephens and B. Jarvis.
57. P. Schell et al. DECHEMA-monogr, 92, 89, 1982.
58. R. M. Meighan, D. R. Green and C. W. Fleischmann. Prog. Batteries Sol. Cells, 4, 161, 1982.
59. G. May and I. Wynn Jones. The Metallurgist and Materials Technologist, Aug. 1976, p427.
60. N. Weber and J. T. Kummer. Adv. Energy Conv. Eng. ASME Conf., Florida, 1967, p913.
61. J. L. Sudworth and M. D. Hames. "Power Sources 3", ed. D. H. Collins, Oriel Press, 1970, p327; L. J. Miles and I. W. Jones, *ibid*, p245.
62. J. Falley et al. J. Electrochem. Soc., 120, 1292, 1973.
63. R. J. Bones, R. J. Brook and T. L. Markin. "Power Sources 5", ed. D. H. Collins, Oriel Press, 1974, p539.
64. W. Fischer. Solid State Ionics, 3-4, 413, 1981.
65. Y. Jiho. C. A. 9373P, Jan-Jun 1982.
66. R. W. Minck and C. R. Halbach. Proc. Inter. Soc. Energy Convers. Eng. Conf. (17th) vol. 2, 557, 1982.
67. W. Fischer. DECHEMA-Monogr., 92, 103, 1982.
68. R. M. Dell and R. J. Bones in "Fast Ion Transport in Solids", ed. P. Vashita, J. N. Mundy and G. K. Shenoy, North Holland, 1979.
69. R. A. Huggins in "Fast Ion Transport in Solids", ed. P. Vashita, J. N. Mundy and G. K. Shenoy, North Holland, 1979.
70. D. Ravaine. J. Non-cryst. Solids, 38 + 39, 353, North Holland, 1980.
71. K. K. Evstop'ev. Doklady Akad. Nauk SSSR, 215, 902, 1974.
72. S. I. Smedley and C. A. Angell. Sol. Stat. Comm., 27, 21, 1978.

73. P. Hagenmuller et al. in "Fast Ion Transport in Solids", p637, ed. P. Vashita, J. N. Mundy and G. K. Shenoy, North Holland, 1979.
74. A. Levasseur et al. Mat. Res. Bull., 14, 921, 1979.
75. D. P. Button et al. J. Non-cryst. Solids, 42, 297, 1980.
76. S. I. Smedley and C. A. Angell. Mat. Res. Bull., 15, 421, 1980.
77. L. Boehm and C. A. Angell in "Fast Ion Transport in Solids", ed. P. Vashita, J. N. Mundy and G. K. Shenoy, North Holland, 1979.
78. T. Minami and M. Tanaka. Rev. de Chimie. Minerale, 16, 283, 1979.
79. T. Minami, H. Nambu and M. Tanaka. J. Am. Ceram. Soc., 60, 467, 1977.
80. T. Minami, Y. Ikeda and M. Tanaka. J. Non-cryst. Sol., 52, 159, 1982.
81. G. Baud and J. P. Besse. J. Am. Ceram. Soc., 64, 242, 1981.
82. D. Leroy et al. Mat. Res. Bull., 13, 1125, 1978.
83. A. M. Glass, K. Nassau and D. H. Olsen in "Fast Ion Transport in Solids", ed. P. Vashita, J. N. Mundy and G. K. Shenoy, North Holland, 1979.
84. A. E. Owen. J. Non-cryst. Sol., 25, p370, 1977.
85. N. F. Mott and E. A. Davis. "Electronic Processes in Non-crystalline Materials", 2nd. edition, Clarendon Press, Oxford, 1979.
86. C. Kittel. "Introduction to Solid State Physics", 5th. edition, J. Wiley & Son, New York, 1976.
87. R. E. Peierls. "Quantum Theory of Solids", Clarendon Press, Oxford, 1955.
88. H. M. Rosenberg. "The Solid State", 2nd. edition, Clarendon Press, Oxford, 1978.
89. D. A. Fraser. "The Physics of Semiconductor Devices", 2nd. edition, Clarendon Press, Oxford, 1979.

90. A. I. Gubanov. "Quantum Electron Theory of Amorphous Conductors", Consultants Bureau, New York, 1963.
91. L. Banyai in "Physique des Semiconducteurs", ed. M. Hulin, Dunod, Paris, 1964.
92. B. T. Kolomeits. Phys. Stat. Sol., 7, 359, 1964.
93. N. F. Mott. Adv. Phys., 16, 49, 1967.
94. R. W. Haisty and H. Krebs. J. Non-cryst. Sol., 1, p399 and p427, 1969.
95. J. L. Hartke. Phys. Rev., 125, 1177, 1962.
96. P. L. Baynton et al. J. Electrochem. Soc., 104, 237, 1957.
97. J. D. Mackenzie in "Electrical Conductivity in Ceramics and Glass, Part B", ed. N. M. Tallan, M. Dekker Inc., New York, 1974.
98. K. W. Hansen. J. Electrochem. Soc., 112, 994, 1965.
99. E. Rasch and F. Hinrichsen. Z. Elektrochem., 14, 41, 1908.
100. A. Jaffe. "The Physics of Crystals", 1931.
101. J. Frenkel. "Kinetic Theory of Liquids", Clarendon Press, Oxford, 1946.
102. J. M. Stevels. a. "Progress in the Theory of the Physical Properties of Glass", Elsevier, Amsterdam, 1948; b. "The Electrical Properties of Glass" in "Encyclopaedia of Physics - Vol. 20", Springer-Verlag, Berlin, 1957.
103. A. E. Owen in "Progress in Ceramic Science - Vol. 3", ed. J. E. Burke, Pergamon Press, New York, 1963.
104. L. L. Hench and H. F. Schaake in "Introduction to Glass Science", ed. L. D. Pye, H. J. Stevens and W. C. LaCourse, Plenum Press, New York, 1972.
105. O. V. Mazurin in "Electrical Properties and Structure of Glass", ed. O. V. Mazurin, Consultant Bureau, New York, 1965.
106. G. I. Skanavi. "The Physics of Dielectrics", Gostekhteorizdat, 1949.
107. W. D. Kingery, H. K. Bowen and D. R. Uhlmann. "Introduction to Ceramics", 2nd. edition, Wiley, New York, 1960.

108. E. Seddon et al. J. Soc. Glass Technol., 16, 450T, 1932.
109. D. Ravaine and J. L. Souquet. Phys. Chem. Glasses, 18, 27, 1977.
110. M. D. Ingram et al. J. Non-cryst. Sol., 38 + 39, 376, 1980.
111. A. M. Glass and K. Nassau. J. App. Phys., 51, 3756, 1980.
112. O. L. Anderson and D. A. Stuart. J. Am. Ceram. Soc., 37, 573, 1954.
113. C. P. Bean et al. Phys. Rev., 101, 551, 1956.
114. R. L. Myuller. Soviet Phys. Sol. Stat., 2, 1213, 1960.
115. C. Hirayama and D. Berg. Phys. Chem Glasses, 2, 145, 1961.
116. R. M. Hakim and D. R. Uhlmann. Phys. Chem. Glasses, 12, 132, 1971.
117. A. E. Owen and R. W. Douglas. J. Soc. Glass Technol., 43, 159T, 1959.
118. R. H. Doremus. J. Electrochem. Soc., 115, 181, 1968.
119. E. Seddon et al. J. Soc. Glass Technol., 16, 450, 1932.
120. J. Verhoogen. Amer. Minerals, 37, 637, 1952.
121. B. Laurent. Verres et Refra., 7, 167, 1983.
122. H. E. Taylor. Trans. Farad. Soc., 52, 873, 1956.
123. O. V. Mazurin and E. S. Borisovskii. Russ. Phys.-Tech. Phys., 2, 243, 1957.
124. A. Y. Kuznetsov. Russ. J. Phys. Chem., 33, 20, 1959.
125. Y. Haven and B. Verkerk. Phys. Chem. Glasses, 6, 38, 1965.
126. R. J. Charles. J. Am. Ceram. Soc., 49, 55, 1966.
127. Y. Gupta and U. Mishra. J. Physics Chem. Solids, 30, 1327, 1967.
128. K. Otto and M. E. Milberg. J. Am. Ceram. Soc., 50, 513, 1967.
129. R. H. Redwine and M. B. Field. J. Mat. Sci., 4, 713, 1969.
130. J. D. Mackenzie. Trans. Farad. Soc., 52, 1564, 1956.
131. Arndt and Gessler. A. Elektrochem., 14, 664, 1908.

132. S. A. Schtschukarew and R. L. Muller. Z. Physik. Chem., Abt. A, 150, 439, 1930.
133. S. B. Thomas. J. Phys. Chem., 35, 2103, 1931.
134. M. E. Spaght and J. D. Clark. J. Phys. Chem., 38, 833, 1934.
135. L. Shartsis, W. Capps and S. Spinner. J. Am. Ceram. Soc., 36, 319, 1953.
136. P.-C. Li, A. C. Ghose and G.-J. Su. Phys. Chem. Glasses, 1, 200, 1960.
137. H. Namikawa. J. Non-cryst. Sol., 18, 173, 1975.
138. S. Oka. J. Soc. Chem. Ind. (Japan), 30, 625, 1927.
139. K. Hughes and J. O. Isard. Phys. Chem. Glasses, 9, 37, 1968.
140. A. I. Parfenov et al. Vestn. Leningr. Gos. Univ., 10, 129, 1959.
141. B. Lengyel and Z. Boksay. Z. Phys. Chem. (Frankfurt), 204, 157, 1955.
142. R. J. Charles. J. Am. Ceram. Soc., 48, 432, 1965.
143. B. I. Markin. Struct. Glass, 1, 209, 1958.
144. W. A. Weyl and E. C. Marboe. "The constitution of Glass - Vol. 2", p504, 1964, John Wiley and Sons.
145. G. L. McVay and D. E. Day. J. Am. Ceram. Soc., 53, 508, 1970.
146. D. W. Fleming and D. E. Day. J. Am. Ceram. Soc., 55, 186, 1972.
147. D. E. Day. J. Non-cryst. Sol., 21, 343, 1976.
148. J. R. Hendrickson and P. J. Bray. Phys. Chem. Glasses, 18, 43 and 107, 1971.
149. R. Hayami and R. Terni. Phys. Chem. Glasses, 13, 102, 1972.
150. S. Sakka et al. Res. Rep. Fac. Eng. Mie. Univ., 3, 79, 1978.

151. K. Matusita et al. J. Non-cryst. Solids, 40, 149, 1980.
152. J. O. Isard. J. Non-cryst. Solids, 1, 235, 1969.
153. A. Lavasseur et al. Mat. Res. Bull., 13, 205, 1978.
154. A. Lavasseur et al. Sol. Stat. Ionics, 5, 687, 1981.
155. D. P. Button et al. Sol. Stat. Ionics, 5, 655, 1981.
156. B. Stalhane. Z. Electrochem., 36, 404, 1930.
157. M. Doreau et al. Mat. Res. Bull., 15, 285, 1980.
158. J. Kuwano and M. Kato. Denki-Kagaku, 43, 734, 1975.
159. T. Minami and M. Tanaka. J. Sol. State Chem., 32, 51, 1980.
160. D. Ravaine and D. Leroy. J. Non-cryst. Sol., 38 + 39, 575, 1980.
161. C. Hirayama. J. Am. Ceram. Soc., 45, 288, 1962.
162. M. Schwartz and J. D. Mackenzie. J. Am. Ceram. Soc., 49, 582, 1966.
163. W. C. Hagel and J. D. Mackenzie. Phys. Chem. Glasses, 5, 113, 1964.
164. L. Shartsis and H. F. Shermer. J. Am. Ceram. Soc., 37, 544, 1954.
165. A. E. Owen. Phys. Chem. Glasses, 2, 87, 1961.
166. A. E. Owen. Phys. Chem. Glasses, 6, 253, 1965.
167. K. S. Evstrop'ev and V. A. Khar'yuzov. Doklady Akad. Nauk. SSSR, 136, 140, 1961.
168. Y. F. Yao and J. T. Kummer. J. Inorg. Nucl. Chem., 29, 2453, 1967.
169. M. S. Whittingham and R. A. Huggins. J. Chem. Phys., 54, 414, 1971.
170. A. Virkar, G. J. Tennenhouse and R. S. Gordon. J. Am. Ceram. Soc., 57, 508, 1974.
171. R. W. G. Wyckoff. "Crystal Structures - Vol. 3", 2nd. edition, Interscience Publishers inc., New York, 1951.
172. P. McGeehin and A. Hooper. J. Mat. Sci., 12, 1, 1977.

173. G. C. Farrington and W. L. Roth. *Electrochim. Acta.*, 22, 767, 1977.
174. M. S. Whittingham and R. A. Huggins in "Solid State Chemistry", ed. R. S. Roth and S. J. Schneider, Nat. Bur. Standards Pub., 364, 139, 1972.
175. J. B. Goodenough, H. Y.-P. Hong and J. A. Kafalas. *Mat. Res. Bull.*, 11, 203, 1976.
176. H. Y.-P. Hong. *Mat. Res. Bull.*, 11, 173, 1976.
177. H. Y.-P. Hong. *Mat. Res. Bull.*, 13, 117, 1978.
178. B. Cales et al. *Sol. Stat. Comm.*, 24, 323, 1977.
179. A. Levasseur et al. *J. Sol. State Chem.*, 8, 318, 1973.
180. L. Trichet and J. Rouxel. *Mat. Res. Bull.*, 12, 345, 1977.
181. U. Von-Alpen, A. Rabenau and G. H. Talat. *App. Phys. Lett.*, 30, 621, 1977.
182. B. E. Taylor, A. D. English and T. Berzins. *Mat. Res. Bull.*, 12, 171, 1977.
183. D. M. Adams. "Inorganic Solids", J. Wiley and Sons, London, 1974.
184. R. D. Armstrong, R. S. Bulmer and T. Dickinson in "Fast Ion Transport in Solids", ed. W. Van Gool, Plenum Press, New York, 1973.
185. C. C. Liang in "Fast Ion Transport in Solids", ed. W. Van Gool, Plenum Press, New York, 1973.
186. B. B. Owens in "Fast Ion Transport in Solids", ed. W. Van Gool, Plenum Press, New York, 1973.
187. C. Lucat et al. *Mat. Res. Bull.*, 12, 145, 1977.
188. T. H. Estell and S. N. Flengass. *Chem. Rev.*, 70, 339, 1970.
189. T. Takahashi et al. *J. Appl. Electrochem.*, 2, 97, 1972; 3, 65, 1973; 5, 197, 1975.
190. B. L. Dunicz and R. C. Scheidt. Rept. No. USNRDL-TR-752, Naval Radiol. Defense Lab., San Francisco, Calif., 1964.
191. M. H. Rowell. *Inorg. Chem.*, 4, 1802, 1965.

192. C. Hirayama. J. Am. Ceram. Soc., 44, 602, 1961.
193. H. Moore and P. W. McMillan. J. Soc. Glass Technol., 40, 66T, 1956.
194. H. Rawson. "Inorganic Glass-Forming Systems", Academic Press, London, 1967.
195. R. N. Blumenthal and M. A. Seitz in "Electrical Conductivity in Ceramics and Glass - Part A", ed. N. M. Tallan, M. Dekker Inc., New York, 1974.
196. M. H. Jones. "A Practical Introduction to Electronic Circuits", Cambridge University Press, 1977.
197. M. M. Woolfson. "An Introduction to X-ray Crystallography", Cambridge University Press, 1970.
198. A. J. C. Wilson. "Elements of X-ray Crystallography", Addison-Wesley, Massachusetts, 1970.
199. L. Patrick and A. W. Lawson. J. Chem. Phys., 22, 1492, 1954.
200. R. W. Christy, E. Fukushima and H. T. Li. J. Chem. Phys., 30, 136, 1958.
201. R. W. Christy. J. Chem. Phys., 34, 1148, 1960.
202. L. B. Coleman in "Fast Ion Transport in Solids", p601, ed. P. Vashita, J. N. Mundy and G. K. Shenoy, North Holland, 1979.
203. I. Simon in "Modern Aspects of the Vitreous State", ed. J. D. Mackenzie, Butterworths, London, 1960.
204. J. L. Parsons and M. E. Milberg. J. Am. Ceram. Soc., 43, 326, 1960.
205. S. Anderson, R. L. Bohon and D. D. Kimpton. J. Am. Ceram. Soc., 38, 370, 1955.
206. N. F. Borrelli, B. D. McSwain and G.-J. Su. Phys. Chem. Glasses, 4, 11, 1963.
207. E. R. Andrew. "Nuclear Magnetic Resonance", Cambridge University Press, 1958.
208. A. Abragam. "The Principles of Nuclear Magnetism", Clarendon Press, 1961.

209. G. E. Pake in "Solid State Physics - Vol. 2", Academic Press, New York, 1956.
210. G. E. Pake. Am. J. Phys., 18, 438-473, 1950.
211. T. P. Das and E. L. Hahn. "Solid State Physics - Supplement 1", Academic Press, 1958.
212. R. V. Pound. Phys. Rev., 79, 685, 1950.
213. R. Bersohn. J. Chem. Phys., 20, 1505, 1952.
214. G. M. Volkoff. Canad. J. Phys., 31, 820, 1953.
215. M. Cohen and F. Reif. "Solid State Physics - Vol. 5", Academic Press, New York, 1957.
216. D. J. E. Ingram. "Spectroscopy at Radio and Microwave Frequencies", Butterworths, 1967.
217. P. J. Bray and A. H. Silver in "Modern Aspects of the Vitreous State", ed. J. D. Mackenzie, Butterworths, London, 1960.
218. C. P. Slichter. "Principles of Magnetic Resonance", Harper and Row, New York, 1963.
219. P. J. Bray in "Magnetic Resonance", ed. C. K. Coogan et al, Plenum Press, New York, 1970.
220. N. Bloembergen in "Report of Conference of Defects in Crystalline Solids - Bristol 1954", The Physical Society, London, 1955.
221. A. H. Silver and P. J. Bray. J. Chem. Phys., 29, 984, 1958.
222. A. H. Silver, J. G. O'Keefe and P. J. Bray. Bull. Am. Phys. Soc. Ser. II, 2, 225, 1957.
223. A. H. Silver, J. G. O'Keefe and P. J. Bray. Bull. Am. Phys. Soc. Ser. II, 3, 21, 1958.
224. J. G. O'Keefe and P. J. Bray. Bull. Am. Phys. Soc. Ser. II, 4, 250, 1959.
225. J. Krogh-Moe. Phys. Chem. Glasses, 3, 1, 1962.
226. S. E. Svenson, E. Forslind and J. Krogh-Moe. J. Phys. Chem., 66, 174, 1962.

227. P. J. Bray and J. G. O'Keefe. *Phys. Chem. Glasses*, 4, 37, 1963.
228. P. J. Bray, M. Leventhal and M. O. Hooper. *Phys. Chem. Glasses*, 4, 47, 1963.
229. M. Leventhal and P. J. Bray. *Phys. Chem. Glasses*, 6, 113, 1965.
230. D. Kline, P. J. Bray and H. M. Kriz. *J. Chem. Phys.*, 48, 5277, 1968.
231. J. F. Baugher and P. J. Bray. *Phys. Chem. Glasses*, 10, 77, 1969.
232. C. Rhee and P. J. Bray. *Phys. Chem. Glasses*, 12, 165, 1971.
233. C. Rhee. *J. Korean Phys. Soc.*, 4, 51, 1971.
234. S. Greenblatt and P. J. Bray. *Phys. Chem. Glasses*, 8, 190, 1967.
235. S. Greenblatt and P. J. Bray. *Phys. Chem. Glasses*, 8, 213, 1967.
236. H. M. Kriz and P. J. Bray. *J. Non-cryst. Solids*, 6, 27, 1971.
237. M. J. Park and P. J. Bray. *Phys. Chem. Glasses*, 13, 50, 1972.
238. K. S. Kim and P. J. Bray. *J. Non-Metal*, 2, 95, 1974.
239. D. Kline and P. J. Bray. *Phys. Chem. Glasses*, 7, 41, 1966.
240. S. G. Bishop and P. J. Bray. *Phys. Chem. Glasses*, 7, 73, 1966.
241. P. J. Bray, D. Kline and W. Poch. *Glastech. Ber.*, 39, 175, 1966.
242. W. Muller-Warmuth, W. Poch and G. Sielaff. *Glastech. Ber.*, 43, 5, 1970.
243. P. Beekenkamp and G. E. G. Hardeman. *Verres et Refract.*, 20, 419, 1966.
244. P. Beekenkamp. *Phys. Chem. Glasses*, 9, 14, 1968.

245. F. R. Landsberger and P. J. Bray. *J. Chem. Phys.*, 53, 2757, 1970.
246. J. R. Hendrickson and P. J. Bray. *J. Chem. Phys.*, 61, 2754, 1974.
247. K. S. Kim and P. J. Bray. *Phys. Chem. Glasses*, 15, 47, 1974.
248. K. S. Kim, P. J. Bray and S. Merrin. *J. Chem. Phys.*, 64, 4459, 1976.
249. G. E. Jellison, L. W. Panek and P. J. Bray. *J. Chem. Phys.*, 66, 802, 1977.
250. M. E. Milburg et al. *Phys. Chem. Glasses*, 13, 79, 1972.
251. J. Scheerer et al. *Glastech. Ber.*, 46, 109, 1973.
252. S. P. Zhdanov, L. Kerger and E. V. Koromal'di. *Dokl. Akad. Nank. SSR*, 204, 622, 1974.
253. M. P. Brung and E. R. McCartney. *Phys. Chem. Glasses*, 16, 49, 1975.
254. S. P. Zhdanov in "Proc. 10th Inter. Congr. Glass. - Kyoto, Japan", *Ceram. Soc. Japan*, 1974.
255. S. P. Zhdanov and G. Shmigel. *Fizika i Khim. Stekla*, 1, 452, 1975.
256. Y. H. Yun and P. J. Bray. *J. Non-Cryst. Sols*, 27, 363, 1978.
257. Y. H. Yun, S. A. Feller and P. J. Bray. *J. Non-Cryst. Sol.*, 33, 273, 1979.
258. H. L. Blood and W. G. Procter. *Phys. Rev.*, 96, 861, 1954.
259. H. Waterman. *Phys. Rev.*, 96, 862, 1954.
260. V. Ross and J. O. Edwards. *Am. Mineralogist*, 44, 875, 1959.
261. F. Holuj and H. E. Petch. *Can. J. Phys.*, 36, 145, 1958.
262. P. J. Bray, J. O. Edwards and V. Ross. Abstract, *Am. Cryst. Assn. Annual Meeting, Cornell Uni., New York*, 1959.
263. P. J. Bray et al. *J. Chem. Phys.*, 35, 435, 1961.

264. D. Kline, H. O. Hooper and P. J. Bray. Bull. Am. Phys. Soc., 2, 144, 1963.
265. H. M. Kriz and P. J. Bray. J. Mag. Res., 4, 69, 1971.
266. H. H. Waterman and G. M. Volkoff. Can. J. Phys., 33, 156, 1955.
267. A. H. Silver. J. Chem. Phys., 32, 959, 1960.
268. A. H. Silver and P. J. Bray. J. Chem. Phys., 32, 288, 1960.
269. H. E. Petch. J. Chem. Phys., 36, 2151, 1962.
270. J. D. Cuthbert and H. E. Petch. J. Chem. Phys., 38, 1912, 1963.
271. K. C. Lal and H. E. Petch. J. Chem. Phys., 43, 178, 1965.
272. P. J. Bray in "Materials Science Research - Vol. 12", p321 ed. L. D. Pye, V. D. Frechette and N. J. Kreidl, Plenum Press, New York, 1978.
273. G. E. Jellison and P. J. Bray. Sol. State Communications, 19, 517, 1976.
274. G. E. Jellison and P. J. Bray. J. Non-Cryst. Sol., 29, 187, 1978.
275. G. E. Jellison and P. J. Bray in "Materials Science Research - Vol. 12", p353, ed. L. D. Pyke, V. D. Frechette and N. J. Kreidl, Plenum Press, New York, 1978.
276. P. J. Bray. J. Non-Cryst. Sol., 38, 321, 1980.
277. P. J. Bray et al. J. Non-Cryst. Sol., 38, 93, 1980.
278. C. H. Townes and B. P. Dailey. J. Chem. Phys., 17, 782, 1949.
279. H. M. Kriz, S. G. Bishop and P. J. Bray. J. Chem. Phys., 49, 557, 1968.
280. J. F. Baugher, P. C. Taylor, T. Oja and P. J. Bray. J. Chem. Phys., 50, 4914, 1969.
281. G. H. Stauss. J. Chem. Phys., 40, 1988, 1964.
282. K. Narita et al. J. Chem. Phys., 44, 2719, 1966.
283. P. C. Taylor and P. J. Bray. J. Magn. Res., 2, 305, 1970.

284. J. F. Baugher, H. M. Kriz, P. C. Taylor and P. J. Bray. *J. Magn. Res.*, 3, 415, 1970.
285. H. M. Kriz and P. J. Bray. *J. Magn. Res.*, 4, 76, 1971.
286. H. M. Kriz, M. J. Park and P. J. Bray. *Phys. Chem. Glasses*, 12, 45, 1971.
287. P. C. Taylor and P. J. Bray. *J. Am. Ceram. Soc. Bull.*, 51, 234, 1972.
288. G. E. Peterson, C. R. Kurkjian and A. Carnevale. *Phys. Chem. Glasses*, 15, 52, 1974.
289. G. E. Peterson, C. R. Kurkjian and A. Carnevale. *Phys. Chem. Glasses*, 15, 59, 1974.
290. G. E. Peterson, C. R. Kurkjian and A. Carnevale. *Phys. Chem. Glasses*, 16, 63, 1975.
291. P. C. Taylor and E. J. Friebele. *J. Non-Cryst. Sol.*, 16, 375, 1974.
292. L. C. Snyder, G. E. Peterson and C. R. Kurkjian. *J. Chem. Phys.*, 64, 1569, 1976.
293. G. E. Jellison, P. J. Bray and P. C. Taylor. *Phys. Chem. Glasses*, 17, 35, 1976.
294. B. E. Warren, H. Krutter and O. Morningstar. *J. Am. Ceram. Soc.*, 19, 202, 1936.
295. J. Bischoe and B. E. Warren. *J. Am. Ceram. Soc.*, 21, 287, 1938.
296. K. Fajans and S. W. Barber. *J. Am. Chem. Soc.*, 74, 2761, 1952.
297. J. Goubeau and H. Keller. *Z. Anorg. Chem.*, 272, 303, 1953.
298. A. Richter, G. Breitling and F. Herre. *Z. Naturforsch.* 9A, 390, 1954.
299. J. Zarzycki. IV Congres. Inter. du Verre, Paris. 1956.
300. K. Grjotheim. *Glass Ind.*, 39, 201, 1958.
301. J. Despujols. *J. Phys. Radium*, 19, 612, 1958.
302. M. E. Milberg and F. Meller. *J. Chem. Phys.*, 31, 126, 1959.

303. S. L. Strong and R. Kaplow. Acta Cryst., B24, 1032, 1968.
304. G. E. Gurr et al. Acta Cryst., B26, 906, 1970.
305. M. Imaoka in "Advances in Glass Technology - part 1",
pl49, Plenum Press, New York, 1962.
306. M. P. Tabbey and J. R. Hendrickson. J. Non-Cryst. Solids,
38, 51, 1980.
307. S. G. Bishop and P. J. Bray. J. Chem. Phys., 48, 1709, 1968.
308. C. Rhee and P. J. Bray. J. Am. Ceram. Soc. Bull., 46, 389,
1967.
309. C. Rhee and P. J. Bray. Phys. Chem. Glasses, 12, 156, 1971.
310. D. Kline, H. S. Storey and W. L. Roth. J. Chem. Phys., 57,
5180, 1972.
311. D. Jerome and J. P. Boilot. J. Phys. Lett., 35, L-129, 1974.
312. I. Cheung et al. J. Chem. Phys., 63, 4903, 1975.
313. J. P. Boilot et al. Phil. Mag., 32, 343, 1975.
314. H. S. Storey et al. in "Superionic Conductors", ed.
G. D. Mahan and W. L. Roth, Plenum Press, 1976.
315. W. Bailey et al. J. Chem. Phys., 64, 4126, 1976.
316. R. E. Walstedt et al. Phys. Rev., B15, 3442, 1977.
317. M. S. Whittingham and B. G. Silbernagel in "Solid
Electrolytes", Academic Press, 1978.
318. L. C. West, T. Cole and R. W. Vaughan. J. Chem. Phys., 68,
2710, 1978.
319. J. D. Cuthbert and H. E. Petch. J. Chem. Phys., 39, 1247,
1963.
320. S. D. Dharmatti et al. J. Phys. Soc. Japan, 17, 1736, 1962.
321. B. G. Silbernagel and M. S. Whittingham. Mater. Res. Bull.,
11, 29, 1970.
322. J. Itoh, R. Kusaka and Y. Yamagata. J. Phys. Soc. Japan,
9, 289, 1954.
323. A. Weiss. Z. Naturforsch, 15A, 536, 1960.

324. H. E. Petch and K. S. Pennington. J. Chem. Phys., 36, 1216, 1962.
325. C. Berthier et al. S.F.P. Congress, Poitiers, 1977.
326. L. Trichet and J. Rouxel. Mat. Res. Bull., 12, 345, 1977.
327. W. Weltner and J. R. Warn. J. Chem. Phys., 37, 292, 1962.
328. H. Moore and P. W. McMillan. J. Soc. Glass Technol., 40, 97T, 1956.
329. J. Krogh-Moe. Phys. Chem. Glasses, 6, 46, 1965.
330. P. E. Jellyman and J. P. Proctor. Trans. Soc. Glass Tech., 39, 173T, 1955.
331. C. Duval and J. Lecomte. Bull. Soc. Chim. France, 101, 1952; J. Opt. Soc. Amer., 44, 261, 1954.
332. J. T. Quan and C. E. Adams. J. Phys. Chem., 70, 340, 1966.
333. S. A. Rice and W. Klemperer. J. Chem. Phys., 27, 573, 1957.
334. K. P. Huber and G. Herzberg in "Constants of Diatomic Molecules", Van Nostrand, 1979.
335. P. Tarte in "Physics of Non-Crystalline Solids", ed. J. A. Prins, North Holland, Amsterdam, 1965.
336. A. J. Harrison. J. Am. Ceram. Soc., 30, 362, 1947.
337. C. Berthier in "Fast Ion Transport in Solids", ed. P. Vashita et al., North Holland, 1979.
338. F. C. Eversteijn, J. M. Stevels and H. I. Waterman. Phys. Chem. Glasses, 1, 123, 1960.
339. R. J. H. Clark and P. D. Mitchell. J. Chem. Phys., 56, 2225, 1972.
340. D. A. Dows and G. Bottger. J. Chem. Phys., 34, 689, 1961.
341. Anderson, Lassetre and Yost. J. Chem. Phys., 4, 703, 1936.
342. M. Irion et al. J. Sol. State Chem., 31, 285, 1980.
343. P. G. Dickens and P. J. Wiseman in "International Review of Science - Inorganic Chemistry, Series 2", "Vol. 10, Solid State Chemistry", ed. L. E. J. Roberts, Butterworths, London 1975.

344. W. Baukel in "From Electrocatalysis to Fuel Cells",
ed. G. Stansted, Univ. of Washington Press, 1971, p345.
345. R. H. Biddulph. Borax Research Ltd., Chessington, Surrey,
private communication.
346. G. L. Cote and H. W. Thompson. Proc. Roy. Soc. (London),
A210, 217, 1951.